Ultrafast Control and Dynamics of Chemical Reactions

Thesis by

Earl Douglas Potter

In Partial Fulfillment of the Requirements

for the Degree of

Doctor of Philosophy

California Institute of Technology

Pasadena, California

1993

(Submitted March 10, 1993)

Acknowledgements

There are a great many people who deserve to be acknowledged for their help during my graduate education. To all of those, not included here specifically, you have my deepest gratitude for your efforts. There are, however, a number of people who I would like to name here for the sake of posterity.

First and foremost, I would like to thank my parents for supporting me through the many years of school. Without your help I could not have gotten as far as I have; you should be proud of your parenting skills. I know it was not easy to have a professional student for a son, but now at least, when someone asks, you can say "my son the doctor...."

I also wish to thank my advisor, Ahmed Zewail, for his financial support and his seemingly endless enthusiasm. In fact, his infectious enthusiasm for ultrafast chemical dynamics is what convinced me to travel this path. Also, that same enthusiasm buoyed my spirits when experimental obstacles loomed large before me.

Dean Willberg and Jennifer Herek deserve special attention for their friendship we've shared through the years. Dean and Jennifer have always been there, whenever I've needed to talk. Having such friends has meant a great deal to me.

I would like to thank all of the graduate students with whom I've worked through the years. From Norbert Scherer, for taking me under his wing, to Søren Pedersen and Jennifer Herek, for putting up with my intrusion into their laboratory, to Qianli Liu, for providing the expert assistance needed to collect the data required for my graduation, I thank you all and wish you the best in your future endeavors.

Finally, I owe my gratitude to all of the postdocs who are primarily responsible for my education through the years. Without their expertise I could not have arrived at this point. In particular, Jack Breen, Bob Bowman, and Martin Gruebele are responsible for much of what I know of chemical dynamics.

Abstract

This thesis presents four distinct applications of ultrafast laser spectroscopy. Unimolecular photodissociation was one of the early applications of this technique and proved to be invaluable in furthering the understanding of unimolecular dissociation mechanisms. As such, the photodissociation of ketene represents one of the two systems where micro-canonical, state-to-state reaction rates, have been measured. Clocking of bimolecular reactions, while still in its infancy, provides a means of measuring the rate at which an elementary reaction actually occurs--isolated from other molecules. The rate at which the bimolecular reaction of bromine atoms with molecular iodine to form iodine monobromide has been measured at two collision energies. An area where ultrafast techniques are just now seeing application, is control of chemical reactions. This thesis illustrates an initial study, albeit limited, of how ultrashort light pulses can be used to "control" the outcome of a chemical reaction. The experiments here show how the natural wave-packet motion of the initially prepared B state iodine can be used to "control" whether or not xenon iodide is formed even when the necessary photons are available. Finally, cluster science is becoming a mature field within physical chemistry, but one of the goals of such work has been to make a connection between gas-phase studies and condensed-phase work. Small clusters, those not large enough to bridge this gap, have proven sufficiently interesting to monopolize the efforts of many groups. Again in a limited way, we have begun to study large clusters in the hope that these systems will truly show characteristics that are somehow intermediate to the gas-phase and condensed-phase characteristics. A dissociating iodine molecule surrounded by many argon atoms encounters an environment that significantly alters the time scales and overall mechanism for separation of the two iodine atoms.

Work done under the direction of Professor Ahmed H. Zewail.

Table of Contents

Chapter 1

Introduction

Ultrafast laser spectroscopy has been applied to many systems thus far and will surely find continued utility well into the future. Early efforts employing picosecond lasers involved studies of unimolecular photodissociation.[1] These experiments were aimed at systems which dissociate via a "complex" mechanism, *e.g.*, vibrational predissociation, electronic predissociation, *etc.*, thereby matching the response time of the experimental apparatus to the time scales of the reaction of interest. The experimental results have highlighted the strengths and weaknesses of the various unimolecular statistical photodissociation theories. This work and some of the subsequent femtosecond experiments were reviewed by Khundkar and Zewail in 1990 [Ref. 2], and also by Reisler *et al.* and Green *et al.*[3]

With the advent of femtosecond lasers, a new class of experiments opened up. Wave-packet motion, or, in other words, coherent dissociation could be studied in real-time. The first example of this type of experiment was the photodissociaton of ICN, where the reaction proceeds along a repulsive coordinate and therefore the reaction is complete in less than 1ps [Ref. 4]. These experiments were quickly followed by studies of the vibrational motion of NaI in its first excited state [Ref. 5] and the prompt dissociation of HgI_2 [Ref. 6]. These systems provided an added level of complexity in that a second "degree of freedom" was introduced: in NaI, the dynamics are governed by the avoided crossing of two potential energy surfaces, and in HgI_2, the molecule has two channels by which it may dissociate.

As the broad utility of this technique became apparent, efforts have been extended into several distinct areas of application. One particularly fruitful area of research is the study of small cluster dynamics. In a beautiful study of the rate of excited-state proton transfer in napthol/ammonia clusters, Breen *et al.* showed a dependence on the cluster size, indicating the unique nature of these small clusters.[7] This work was followed by work on $I_2 \cdot (Rg)_n$ clusters, where the rare gas atom (Rg) was changed from helium to neon to argon.[8] In these experiments, the rate of vibrational predissociation (VP) was

measured and found to qualitatively agree with the energy-gap law. Willberg *et al.* found that as the I_2·Rg bond energy was increased, in the order He, Ne, Ar, the rate of VP increased, indicating the effect of stronger coupling of the two coordinates.[8] Likewise, as the excitation energy was increased, the vibrational energy lost to dissociation actually decreased (because the I_2 B-state is anharmonic), but the match between this vibrational energy and the I_2·Rg bond energy improved, thereby increasing the rate of reaction.

Taking advantage of the work of Soep *et al.*[9] and Wittig *et al.*,[10] ultrafast rate measurements were extended to bimolecular reactions. A crossed-beam collision of two reactants cannot be time resolved due to a long and random delay associated with the collision; however, van der Waals clusters offer the opportunity to initiate the bimolecular reaction with a well-defined impact parameter and a short, constant collision time. The work of Scherer *et al.*[11] and Wittig and coworkers[12] illustrates the utility of this approach for the reaction $H + CO_2 \rightarrow [HOCO]^{\ddagger} \rightarrow OH + CO$. The lifetime of the collision complex has been measured and found to be relatively stable.

Most recently, the work done thus far forms the basis for a novel technique, namely femtosecond electron diffraction.[13] In this method, an ultrashort electron pulse is used as a diffraction probe, thus indicating the actual structure of the transient species. This experiment has posed many experimental difficulties, but holds promise for exciting results in the future.

Along the theme of diverse applications of ultrafast techniques, this thesis presents results on four distinct experiments with ramifications in the fields of statistical unimolecular photodissociation, bimolecular collision and scattering potentials, control of chemical reactions, and cluster dynamics. All of this work has been performed in collaboration with several coworkers; my contribution to each project is detailed below. The chapters are arranged in reverse chronological order, beginning with the most recent experiments.

Chapter two presents a detailed summary of the experimental apparatus. The work on ketene dissociation was done using a picosecond laser system (described in detail in Ref. 1) but all other experiments were performed on the newly built femtosecond laser system described here. In addition to the lasers, there have been many changes in the apparatus which have not been described in detail previously. The data acquisition routine, for example, has been completely changed to an IBM-AT based system and the acquisition program can be found in the appendix of this thesis. Likewise, interlock circuits, molecular beam valve circuits, and electron impact circuits are discussed and diagrammed in detail.

Chapter three presents the preliminary results of our work on molecular iodine in large argon clusters. Much of the text of this chapter has been taken directly from a recently published paper.[14] In addition to his help in collecting the data, Q. Liu is responsible for the implementation of the molecular dynamics simulations. This system is being currently investigated further by Q. Liu and J. Wang.

Iodine in large argon clusters is a prototypical system for studying the effects of environment on reaction dynamics. Extensive work in this group and others has been performed using the I_2 (A'←D') emission as a signature upon which to study molecular iodine dynamics.[15] Fortunately, this emission is red-shifted significantly upon solvation within large argon clusters.[16] This effect has allowed us to contrast the dynamics of bare I_2 with I_2 in large clusters. The differences are striking and may represent an important step toward bridging the gap between gas phase and condensed phase experiments.

Chapter four is also preliminary in nature; it presents a demonstration of how the natural motion of a wave-packet can act as a very fast switch. A limited version of this work has been published in *Nature*,[17] but the account here is the most complete to date. J. Herek, S. Pedersen, and Q. Liu are the collaborators in this experiment. Our work on this experiment closely parallels the proposed experiment of Rice *et al.*,[18] demonstrating the simplest form of "control" of a chemical reaction. Other approaches to chemical

control are being investigated theoretically using complex pulse shapes, durations and spectra but the work here is meant merely to illustrate the feasibility of this method. The basis for these experiments stems from the nanosecond studies by Setser *et al.*[19]

Iodine, excited to the B electronic state with an ultrashort laser pulse, exhibits a wave-packet motion which can be preferentially transferred to an upper ion-pair state at one of the turning points within the B state.[15] The upper ion-pair state reacts rapidly with xenon to form the excimer XeI*.[19] The production of XeI is thus modulated by the natural I_2 B-state wave-packet "switch." Admittedly, we are not altering the way this reaction would proceed naturally, but rather are demonstrating the importance of wave-packet dynamics to the general field of chemical control (this concept is discussed in greater detail within the chapter).

Chapter five is the result of a painstaking effort to study the dynamics of a bimolecular collision unperturbed by external forces and at a sufficiently low collision energy to be sensitive to the underlying potential energy surface. The text is taken directly from a paper in the *Journal of Chemical Physics*, under the authorship of I. Sims, M. Gruebele, E. Potter, and A. Zewail.[20] The extensive experimental section of this paper has been pared down to include only those details unique to this particular experiment, since the experimental section of this thesis is quite detailed. The theoretical treatment of this work was primarily the work of M. Gruebele; building the femtosecond apparatus and collecting the data was a group effort.

The reaction is initiated from the van der Waals complex $HBr \cdot I_2$, which, when excited at 215nm, dissociates the HBr, sending the Br atom into the I_2 molecule. This approach allows us, as in the work on $[HOCO]^{\ddagger}$, to measure the rate of a bimolecular reaction, but unlike $[HOCO]^{\ddagger}$, has the added feature that the non-reacting atom is far afield during the actual reactive event. As such, the reaction $Br + I_2 \rightarrow IBr + I$ can be studied in detail without external interactions. Likewise, since the hydrogen atom takes most of the excess energy away as translational energy, the collision energy is quite low,

yielding results which are a direct consequence of the subtle details of the underlying potential energy surface.

Chapter six is a copy of a publication on the microcanonical state-to-state rates of unimolecular photodissociation of ketene.[21] This experiment was performed on the picosecond instrument which was later dismantled in order to build the femtosecond apparatus used for the work discussed above. The experiments were started in 1987 by L. Khundkar and A. Hoffman and were completed by myself and M. Gruebele, including full analysis of the results. More work on this system has since been performed by the Moore group, specifically, rate measurements close to threshold and other interesting facets of the overall mechanism.[3,22]

Ketene photodissociation is an ideal system for testing unimolecular statistical photodissociation theories because the internal conversion step is rapid and therefore the reaction essentially proceeds on a single potential energy surface. The pump photon excites the molecule to the S_1 surface where it quickly (<1ps probably) internally converts to the S_0 surface. At this energy, the system is above the dissociation limit of the S_0 surface and as such, the ketene fragments into carbon monoxide and methylene. The methylene fragment is easily detected via LIF such that, with picosecond lasers, the system can be studied at the state-to-state level. It has been found as a result of this work that the "classical" theories, which utilize a single transition state, cannot account for the rate of dissociation over the entire range of excess energies. The variation RRKM theory, developed by Marcus *et al.*,[23] reproduced the experimental results well by involving a transition state which moves inward as the energy is increased.

As evidenced by the variety of brief summaries presented above, the only unifying theme of this thesis is perhaps the diverse applications of ultrafast technology to chemical systems. Not surprisingly, this technique is being applied to an even broader class of experiments now and will probably see continued application in the years to come.

1.1 References

1. a) L. R. Khundkar, J. L. Knee, and A. H. Zewail, *J. Chem. Phys.*, **87**, 77 (1987); b) S. J. Klippenstein, L. R. Khundkar, A. H. Zewail, and R. A. Marcus, *J. Chem. Phys.*, **89**, 4761 (1988); c) N. F. Scherer, F. E. Doany, A. H. Zewail, and J. W. Perry, *J. Chem. Phys.*, **84**, 1932 (1986); d) N. F. Scherer, and A. H. Zewail, *J. Chem. Phys.*, **87**, 97 (1987); e) J. L. Knee, L. R. Khundkar, and A. H. Zewail, *J. Chem. Phys.*, **87**, 115 (1987); f) L. R. Khundkar and A. H. Zewail, *J. Chem. Phys.*, **92**, 231 (1990).
2. L. R. Khundkar, and A. H. Zewail, *Ann. Rev. Phys. Chem.*, **41**, 15 (1990).
3. a) H. Reisler, and C. Wittig, *Ann. Rev. Phys. Chem.*, **37**, 307 (1986); b) W. H. Green, C. B. Moore, and W. F. Polik, *Ann. Rev. Phys. Chem.*, **43**, 591 (1992).
4. a) N. F. Scherer, J. L. Knee, D. D. Smith, and A. H. Zewail, *J. Phys. Chem.*, **89**, 5141 (1985); b) M. Dantus, M. J. Rosker, and A. H. Zewail, *J. Chem. Phys.*, **87**, 2395 (1987).
5. T. S. Rose, M. J. Rosker, and A. H. Zewail, *J. Chem. Phys.*, **88**, 6672 (1988).
6. M. Dantus, and R. M. Bowman, and A. H. Zewail, *J. Chem. Phys.*, **91**, 7437 (1989).
7. J. J. Breen, L. W. Peng, D. M. Willberg, A. Heikal, P. Cong, and A. H. Zewail, *J. Chem. Phys.*, **92**, 805 (1990).
8. D. M. Willberg, M. Gutmann, J. J. Breen, A. H. Zewail, *J. Chem. Phys.*, **96**, 198 (1992).
9. C. Jouvet, and B. Soep, *Chem. Phys. Lett.*, **96**, 426 (1983).
10. S. Buelow, G. Radhakrishnan, J. Catanzarite, and C. Wittig, *J. Chem. Phys.*, **83**, 444 (1985).
11. a) N. F. Scherer, L. R. Khundkar, R. B. Bernstein, and A. H. Zewail, *J. Chem. Phys.*, **87**, 1451 (1987); b) N. F. Scherer, C. Sipes, R. B. Bernstein, and A. H. Zewail, *J. Chem. Phys.*, **92**, 5239 (1990).

12. a) S. K. Shin, C. Wittig, and W. A. Goddard, *J. Phys. Chem.*, **95**, 8048 (1991); b) S. L. Nickolaisen, H. E. Cartland, and C. Wittig, *J. Chem. Phys.*, **96**, 4378 (1992); c) Y. P. Zeng, S. W. Sharpe, S. K. Shin, C. Wittig, and R. A. Beaudet, *J. Chem. Phys.*, **97**, 5392 (1992); d) S. I. Ionov, G. A. Brucker, C. Jaques, L. valachovic, and C. Wittig, *J. Chem. Phys.*, **97**, 9486 (1992).

13. a) J. C. Williamson, and A. H. Zewail, *Proc. Natl. Acad. Sci.*, **88**, 5021 (1991); b) J. C. Williamson, M. Dantus, S. B. Kim, and A. H. Zewail, *Chem. Phys. Lett.*, **196**, 529 (1992).

14. E. D. Potter, Q. Liu, and A. H. Zewail, *Chem. Phys. Lett.*, **200**, 605 (1992).

15. a) R. M. Bowman, M. Dantus, and A. H. Zewail, *Chem. Phys. Lett.*, **161**, 297 (1989); b) M. Dantus, M. H. M. Janssen, and A. H. Zewail, *Chem. Phys. Lett.*, **181**, 281 (1991); c) M. Gruebele, and A. H. Zewail, *J. Chem. Phys.*, in print.

16. X. Zheng, S. Fei, M. C. Heaven, and J. Tellinghuisen, *J. Chem. Phys.*, **96**, 4877 (1992).

17. E. D. Potter, J. Herek, S. Pedersen, Q. Liu, and A. H. Zewail, *Nature*, **355**, 66 (1991).

18. B. Amstrup, R. J. Carlson, A. Matro, and S. A. Rice, *J. Phys. Chem.*, **95**, 8019 (1991).

19. a) J. Qin, T. O. Nelson, and D. W. Setser, *J. Phys. Chem.*, **95**, 5374 (1991); b) J. Qin, and D. W. Setser, *Chem. Phys. Lett.*, **184**, 121 (1991).

20. I. R. Sims, M. Gruebele, E. D. Potter, and A. H. Zewail, *J. Chem. Phys.*, **97**, 4127 (1992).

21. E. D. Potter, M. Gruebele, L. R. Khundkar, and A. H. Zewail, *Chem. Phys. Lett.*, **164**, 463 (1989).

22. a) I. Chen, and C. B. Moore, *J. Phys. Chem.*, **94**, 263 (1990); b) I. Chen, and C. B. Moore, *J. Phys. Chem.*, **94**, 269 (1990); c) S. K. Kim. Y. S. Choi, C. D. Pibel, Q. Zheng, and C. B. Moore, *J. Chem. Phys.*, **94**, 1954 (1991).

23. a) D. M. Wardlaw, and R. A. Marcus, *Adv. Chem. Phys.*, **70**, 231 (1988); b) S. J. Klippenstein, and R. A. Marcus, *J. Chem. Phys.*, **91**, 2280 (1989); c) S. J. Klippenstein, and R. A. Marcus, *J. Chem. Phys.*, **93**, 2418 (1990).

Chapter 2

Experimental Apparatus

The essential elements of the experimental arrangement can be classified into four main areas: generation of the ultrafast pump and probe laser pulses; characterization of the laser pulses; formation and characterization of cold molecules in the molecular beam; and signal processing.

2.1 Generation of the Ultrafast Pump and Probe Laser Pulses

The scheme for the generation of μJ level fs pump and probe laser pulses is shown in Figure 1. A mode-locked Nd:YAG laser (Coherent Antares 76S) was used as the primary ultrafast pump source. It generated ~50 ps, 30 nJ pulses of 532 nm light after second harmonic generation, at a repetition rate of 76 MHz, and a continuous-wave power of at least 2 W (the 3 Watt option has been installed, which is merely a heater used to equilibrate the temperature of the KTP crystal at ~180° C). There are several properties of this laser which were determined empircally and may prove to be useful information for future users.

1) Occasionally during warm-up, the remote control module will reset itself. The outcome of this event is that the lamp hours counter is set to zero, and more importantly, the lamp currents are set to ~27 amps. If the user is not cognizant of this event, he/she may spend an inordinate amount of time trying to tweak the laser in order to reestablish lasing. In reality, however, 27 amps is simply not enough current for this laser to lase. Should this occur, the user should simply ramp the current back up to the level at which it was running prior to this reset.
2) While the power output of this laser decreases during the lifetime of the lamps, it will at times be difficult to bring the power above the 2.3 watts required to pump the dye laser by merely adjusting the lamp currents, output coupler and doubling crystal. In this event, one of the following possibilities should be considered:
    a) Due to the continous adjustments of the output coupler over the lifetime of the lamps, the beam will walk off the center of the optics such that the beam no

longer effectively fills the YAG crystal. In this situation it is relatively simple to adjust the rear high reflector such that the power returns to a more acceptable level. This should be done with caution so that, in the event this action does not improve the performance, the high reflector can be returned to its prior position (full alignment of the cavity is a time-consuming task).

b) Every couple of months the beam splitter after the output coupler, used to monitor the IR power, gets dirty on the side closest to the output coupler. This has always been a baffling phenomenon since this optic is well protected from any dust; but, nonetheless, cleaning the back side of this optic has caused dramatic improvements in output power on several occasions.

3) The manual recommends that one be careful not to translate the doubling crystal too close to the focus of the optic just before the crystal. It is apparently possible to burn the crystal if the focus impinges upon the face of the crystal. However, since the 3 watt option has been installed, we have not seen any noticeable damage regardless of the position of the crystal. Perhaps extra care is not warranted.

The Antares has been equipped with the option of computer control. At first, this option appeared superfluous but two uses presented themselves as experiments were carried out. The first use is rather trivial but does save some time. Since the laser requires approximately 1 hour to fully warm-up, one can initiate the lamps one hour prior to anyone arriving at work. When one is ready to begin work in the morning, the laser is ready as well. The second use for computer control is more critical. If the Antares begins to self Q-switch, which can be caused by small temperature changes in the room, the system is designed to close the external shutter, thus avoiding possible damage to the KTP crystal. While this is a valuable interlock for the laser, it causes problems when one is trying to collect data over long periods of time. Computer control allows the data acquisition program to check that this shutter is open between scans. If the shutter is

closed, the scan terminates (if the scan is allowed to run, background noise will be averaged into the data). The computer code designed to carry out these tasks is shown below.

```
SUB LASER (OUT$, IN$)
'*************************************************************************
'*  This routine allows communication with the antares laser.  OUT$ contains the   *
'*   command sent to the laser, and IN$ contains the response if one is 'expected.   *
'*************************************************************************
PORT% = 3: BAUD% = 9600   'Laser is hooked up to com3 and communicates
                          'at 9600 baud--controlled by the remote module.
CALL QCINIT(4, 3, 0, 1, PORTSTATUS%, QCERROR%)      'Initialize the port.
CALL COPEN(PORT%, BAUD%, 1, 0, 8, 0, 20, 20, TXBUF3(), RXBUF3(), QCERROR%)
                                                    'Open the port.
CALL CBUFCLR(2, 3, QCERROR%)                        'Clear buffers.
OUT$ = OUT$ + CHR$(13)                              'Add return to OUT$.
CALL CPRINT(PORT%, OUT$, QCERROR%)                  'Send OUT$.
DO              'Wait until transmit buffer is empty.
     CALL CBUFFER(PORT%, RECV%, XMIT%, QCERROR%)
LOOP UNTIL XMIT% = 20             'Size of buffer is set to 20.
RELPOS% = 0: KB% = 0: FLAG% = 0
IN$ = SPACE$(20)              'Need to set aside an empty character string to get response.
CALL CINPUT(PORT%, IN$, RELPOS%, 0, "", "", KB%, FLAG%)    'Get response.
CALL CCLOSE(PORT%, QCERROR%)                        'Close port.
CALL QCEXIT                                         'Reset port.

END SUB
```

The RS-232 call commands are described in the Quick Comm manual. These routines are written in assembly and are included in the Quick Basic library INTRFC. Quick Basic should be started with the command QB /L INTRFC, so that this library is available. In order to use the above routine, the command "TEXT OFF" should be sent first so that only numbers are returned rather than text. This mode makes code generation easier. Likewise, "ECHO OFF" should also be sent (so that the laser will not echo the string sent). Regardless of the command sent, the laser will return at least a carriage return and a line feed. To check the status of the shutter, send "PRINT SHUTTER." A one will be returned if the shutter is open, and a zero will be returned if the shutter is closed. Since the communication with the laser is not without glitches, it is probably

advisable to check the status of the shutter several times should a zero be returned before terminating a potentially valuable transient. See the Antares manual for other available commands.

```
DECLARE SUB LASER (OUT$, IN$)
'************************************************************************
'* This routine is designed to start the Antares at a previously specified time. This allows *
'*       the user to warm-up the laser prior to arriving at work.
'************************************************************************
DIM SHARED TXBUF3(20), RXBUF3(20) AS INTEGER      'Dimension buffers.
INPUT "WHAT TIME TO TURN ON LASER (hh:mm:ss)"; T$ 'Get turn on time.
DO              'Loop until the proper time (this is not the best way to accomplish this).
LOOP UNTIL T$ = TIME$
        CALL LASER("ECHO OFF", REPLY$)          'Echo off.
        PRINT "ECHO OFF"; REPLY$
        CALL LASER("TEXT OFF", REPLY$)          'Text off.
        PRINT "TEXT OFF"; REPLY$
        CALL LASER("PUMP ON", REPLY$)           'Turn on cooling water pumps.
        PRINT "PUMP ON"; REPLY$
        FOR I = 1 TO 500000: NEXT I             'Delay long enough for resistivity to rise.
DO              'Wait until faults are all cleared.
     CALL LASER("PRINT FAULTS", REPLY$)
     PRINT "FAULTS"; REPLY$
LOOP UNTIL VAL(REPLY$) = 0
CALL LASER("LAMPS ON", REPLY$)                  'Turn on lamps.
PRINT "LAMPS ON"; REPLY$
END
```

The Antares is used to pump an ultrafast dye laser (Coherent Satori). This dye laser is a linear-cavity, synchronously-pumped, twin-jet (gain and saturable absorber) dispersion-compensated, design. Both directional and amplitude stabilization devices are employed on the pump beam and this, combined with active stabilization of the cavity length, ensure stable and uninterrupted operation over the long periods necessary for accumulation of experimental transients. These stabilization devices, at times, have not functioned properly. The position stabilizer has malfunctioned more than it has worked. The Satori can be run without this element, albeit with more instability. The cavity length stabilization on the Satori has also been inoperable for many months. The piezo-electric transducer on the output coupler ceases to operate on a regular basis, and unfortunately,

Coherent will only replace the entire assembly, costing hundreds of dollars. The Satori can also be run without this element; however, the stability suffers tremendously. The noise eater on the output of the Antares must be operational in order for the Satori to yield short pulses, and fortunately, this stabilization element has proven quite dependable.

The ouput of the Satori is tunable over the gain curves of the various dyes (see below) with an average power of 150-250 mW operating at 76 MHz (for an individual pulse energy of 2-3.2 nJ). The pulse duration is "tunable" in the range 90-500 fs. The peak power is then in the range 4-35 kW.

A single plate birefringent filter is employed to provide wavelength selection. One of the problems associated with this type of dye laser is the generation of satellite pulses. This problem has been partially alleviated in the Satori by cutting the birefringent filter on an axis with less than the maximum amount of birefringence; this requires the crystal to be significantly thicker. This thicker crystal separates the satellite pulse from the main pulse in time thereby discriminating against the satellite pulse since the gain has decayed.

We have used several different gain/saturable absorber dye combinations in order to generative a variety of wavelengths. The choice of dye not only influences the wavelength but also the shortest attainable pulse width. The laser was designed with the combination KR620/Malachite Green in ethylene glycol. This combination yields ~200 mW with a pulse duration of ~180 fs (auto-correlation width) tunable from ~608-645 nm. The combination LDS722/DDI (Exciton) in ethylene glycol has also been used. The laser was set to a wavelength of 716.5 nm, yielding 150-200 mW of light with a pulse autocorrelation of 350 fs. It was operated with this somewhat longer pulse to ensure stable operation, since with this dye combination proved more difficult to maintain a shorter pulse. We also used DCM as the gain dye for a brief amount of time; however, due to low solubility of this dye in almost any solvent, it was decided to discontinue the use of this dye. Coherent advised using instead, DCM Special from Lambda Physik, which contains a mixture of DCM and some Rhodamine dye. This option was never

actually tried. Finally, the combination R610/DODCI was tried. This combination turned out to be the best ever used. The ouput was ~250 mW with a pulse duration of ~100 fs (auto-correlation width). The laser operated with adequate stability without the use of the position or cavity length stabilization. For some reason R6G does not function well in this laser (according to Coherent, there is too much gain). As a result, wavelengths below ~610 nm have not been generated. Dyes to the blue of R6G have not been tested by Coherent but may yield wavelengths in the range 550-600 nm if appropriate saturable absorbers are found (it is not certain whether the current optic set will reflect adequately at these blue wavelengths).

The ~2 nJ, 76 MHz train of pulses are amplified in a four stage amplifier pumped by 532 nm (10 ns FWHM) light from a Q-switched Nd:YAG laser (Spectra Physics DCR-2A with filled-in beam option) operating at a 20 Hz repetition rate. The laser beam is introduced into the first stage after an optical delay of about three meters in order to eliminate ASE (amplified spontaneous emission) resulting from back reflection off the Satori's output coupler. A variety of dye combinations have been used to amplify the wavelengths used in this lab. The first three stages are side-pumped, and the final stage is end-pumped. The beam is focused through a 125 μm pinhole between the first and second stages. A saturable absorber jet is placed between the second and third stages. The polarization of the beam is vertical, and therefore, this jet should be horizontal, in order that the beam can impinge at Brewster's angle upon the jet, but this configuration is inconvenient and so the jet is actually vertical. Another pinhole is placed between the third and fourth stages (25 μm).

The beam is expanded between each of the stages, reaching a diameter of ~0.5 cm in the last stage. The 20 Hz amplified pulse energy is estimated to be in the range 60-500 μJ. This leads to an average power of 1.2-10 mW and a peak power of ~5 GW, depending upon the pulse width.

Due to group velocity dispersion, the output pulse of the amplifier is rarely as temporally short as the pulse sent into the amplifier. One way to alleviate this difficulty is to send a chirped pulse into the amplifier such that the dispersion introduced by the amplifier is offset by the initially prepared chirp. This can be accomplished with the Satori by taking glass out of the cavity and removing the romb prisms on the outside of the cavity. Unfortunately, this method has proven difficult to use, since any change in the amplifier will require a change in the amount of negative dispersion generated on the pulse leaving the Satori. It has been found easier to generate the shortest possible pulse from the dye laser, using the rhomb prisms to remove any residual chirp, followed by pulse recompression after the dye laser amplifier. This method appears to be less sensitive to the subtleties of the amplifier.

During the initial setup of this laboratory a choice was made to use SF-11 equilateral prisms for recompression. The Brewster's angle for a given wavelength is given by $\tan \phi = n_2 / n_1$, where ϕ is the angle at which the least reflection will occur, n_2 is the index of refraction for the material the pulse is entering, and n_1 is the index for the material the pulse is leaving (see table I for indices of refraction for a variety of materials at wavelengths throughout the uv and visible regions). For SF-11 at 620 nm, this angle is 60.68°; therefore, equilateral prisms are adequate. However, the SF-11 prisms absorbed a significant portion of the beam. The cause of this absorption is unknown but the assumption has been that the flint glass is of poor quality. BK7 with magnesium fluoride coating replaced the SF-11 prisms (the Brewster's angle for BK7 is 56.58°, but due to cost considerations, equilateral prisms were still used). Other materials were considered based on the following equations from Ref. 1.

The time required for the pulse to traverse the standard four prism sequence is given by:

$$T = \frac{d}{d\omega}\left(\frac{\omega P}{c}\right) \tag{2.1}$$

where P is the optical path length, ω is the pulse angular frequency, and c is the speed of light in vacuum. In general, the time delay for pulse propagation is simply the path length divided by the group velocity, however, in this treatment the path length is frequency dependent giving the above equation. The dispersion constant is the variation in this quantity with wavelength:

$$D = \frac{-1}{l}\frac{dT}{d\lambda} = \left(\frac{\lambda}{cl}\right)\frac{d^2P}{d\lambda^2} \tag{2.2}$$

where l is the physical path length. Therefore, the quantity of interest is $d^2P/d\lambda^2$. In a normal medium, such as a block of quartz:

$$\frac{d^2P}{d\lambda^2} = l\frac{d^2n}{d\lambda^2}. \tag{2.3}$$

However, the prism sequence yields the following equation:

$$\frac{d^2P}{d\lambda^2} = 4l\left\{\left[\frac{d^2n}{d\lambda^2} + \left(2n - \frac{1}{n^3}\right)\left(\frac{dn}{d\lambda}\right)^2\right]\sin\beta - 2\left(\frac{dn}{d\lambda}\right)^2\cos\beta\right\}, \tag{2.4}$$

where β is the angle of divergence of the dispersed beam (see Ref. 1 for a diagram). Since β is small, $\cos\beta$ is approximately unity and $l\sin\beta$ is on the order of the beam spot size. The required indices and derivatives of the indices can be found in Table I for a variety of materials at wavelengths spanning the uv and visible regions. Using these equations and an assumption regarding the approximate amount of positive dispersion due to the amplifier, it is possible to estimate the required prism separation for the chosen material. BK7 and SF-11 yield prism separations which can be accommodated on an average laser table.

The amplified beam from the first amplifier, following pulse compression, is split using a pellicle beam splitter in order to generate independently tunable pump and probe beams. One of the beams passes across to a variable optical delay where it undergoes one or two retro-reflections (depending upon whether a longer delay is necessary) off

appropriate reflectors mounted on a computer controlled linear stage (Micro Kinetics, 25 mm excursion, 0.1 μm resolution). This in turn is mounted on a much longer, low-resolution, manually controlled stage (Micro-Controle) which facilitates location of time zero. This stage can be computer controlled via a standard stepper-motor interface, although this facility is not currently available. After this variable optical delay, which requires careful alignment to avoid problems of beam walk-off, the beam passes across to the molecular beam where it is focused directly into the reaction zone using a plcx (planoconvex) lens, or is doubled prior to entering the vacuum chamber using an appropriate crystal.

The other portion of the initially amplified beam is focused into a 1 cm path length cell containing D_2O (Aldrich). This provides a white light continuum, which is recollimated and directed through a 10 nm FWHM interference filter (Corion), which can be tilted so as to shift its center wavelength to the blue of the specified wavelength. The resulting low intensity beam (estimated pulse energy 50 nJ) is reamplified in a three stage amplifier side pumped by 355 nm laser light from the Q-switched Nd:YAG laser, unless the desired wavelength is red of 532 nm. In this case, the second amplifier is pumped by 50% of the 532 nm light from the Q-switched laser. This amplifier is similar in design to the first one, except that it lacks the final, end-pumped stage and the saturable absorber. The dye is frequently a coumarin dye in methanol. These dyes often have a short lifetime under 355 nm radiation. The radical scavenger diazabicyclo[2.2.2]octane (DABCO; Kodak) is usually added to prolong the dye lifetime. Even so, initial experiments were hindered due to a dye lifetime of one hour or less. Increasing the dye volume, purging the solutions with nitrogen and minimizing the 355 nm pump laser intensity together allow for continuous runs of twelve hours or more.

The pulse energy of the second amplifier is usually in the range 40-250 μJ of amplified light and ~20 μJ of ASE (the latter is essentially eliminated if the desired frequency is doubled). Again, pulse recompression is accomplished via a prism pair similar

to that which is done following the first amplifier. The blue wavelengths frequently used require that BK7 prisms be used since the absorption problem discussed above is even more problematic. The resulting beam passes over to the molecular beam apparatus, where the second harmonic can be generated. The recollimated and focused beam enter into the chamber via a 50 cm focal length plcx UV lens after reflection off an appropriate dichroic beam splitter, used to recombine the pump and probe beams.

2.2 Characterization of the Pulses

The pulse width of the unamplified beam is monitored by a real-time scanning autocorrelator of the rotating-mirror type, built in this lab and similar to that described by Yasa and Amer.[2] The first optical element in the autocorrelator-a beam splitter-was initially a pellicle from Melles Griot; however, the rotating mirrors caused the thin pellicle material to "flap in the wind." The pellicle was replaced by a 50% reflection coating on a 1 mm thick glass substrate. Of course, this substrate causes a small amount of dispersion (this can be calculated by the equations above) but this did not appear to be a significant problem. The rotating mirror assembly is placed atop a CD motor (C&H Surplus), which operates at 10 Hz with a 5 volt power supply. Early attempts were made with a motor revolving at a higher rate, since the oscilloscope trace would be refreshed more often. Unfortunately, the mirrors mounted on the motor flexed outward under rotation thereby making alignment nearly impossible. After the two arms are recombined they are focused via a 5 cm plcx glass lens into a $LiIO_3$ crystal. The crystal is approximately 1 mm thick. The amount of dispersion present in this autocorrelator sets a lower limit of ~100 fs on the shortest pulse measurable, assuming the beams travel through 10 mm of quartz (the crystal is more dispersive than quartz, admittedly, but the total distance is actually less than 10 mm, offsetting the difference). The sum frequency is detected by a 1P28 photomultiplier tube with a Schott filter mounted in front to block out the room light.

After amplification the pulse width is measured via a non-collinear autocorrelator utilizing a linear, computer-controlled stage. A real-time autocorrelator cannot be used after amplification owing to the low repetition rate (20 Hz). The design of this autocorrelator is conceptually identical to the real-time autocorrelator described above but requires several minutes for data collection. The lower limit for this autocorrelator is similar to that calculated above, although a 100 μm KD*P crystal is typically used for sum frequency generation thereby reducing the overall dispersion.

2.3 Formation and Characterization of Molecules in the Molecular Beam

The molecular beam apparatus used is shown in Fig. 2; only the differences to the setup described previously[3] will be reported in detail here. The beam is constructed of two main cylindrical chambers separated by a skimmer, and each pumped by a separate diffusion pump and cryobaffle, backed by a single high throughput rotary pump. The primary chamber, which is operated at a pressure of 10^{-4} torr or less during experiments, is arranged with the nozzle, laser entrance, and exit baffle arms/LIF collection optics on three mutually orthogonal axes. The skimmed molecular beam passes into the second chamber which containes the time-of-flight mass spectrometer (TOFMS), and is operated at a pressure of typically 10^{-6} torr.

A new addition to this molecular beam has been the D90 rotary-vane pump, manufactured by Leybold-Hereaus, used to back the diffusion pumps. This pump replaced the 160 cubic feet per minute (cfm) Stokes pump used previously. The new pump has a throughput of 60 cfm; this is at least several times the required throughput necessary for the VH-6 diffusion pumps. Due to the corrosive nature of the chemicals typically used in the laboratory, this pump has suffered a great deal. As the pump oil degrades it creates particulates within the oil (this could also be the condensed phase molecules initially sent through the molecular beam), these particulates score the inside of the pump. As a result,

the vanes no longer seal against the inside chamber, and the ultimate pressure of the system rises to an unacceptable level. This pump should undergo routine service (at least yearly) to avoid this problem. Addition of an external oil pump may also help to alleviate this difficulty.

The reactant gases, prior to entering the molecular beam, pass through a gas mixing manifold (see Fig. 3). This manifold with the three mass-flow meters was designed to be used for the $HBr/I_2/He$ mixture (see Chapter 5) but the corrosiveness of this mixture precluded the use of the mass-flow meters. After several hours use, the small needle valve inside the flow meters would corrode to the point where no gas would pass through. While this system has not yet been used to its fullest potential, should an experiment such as the $Xe/He/I_2$ mixture proposed in Chapter 4 be initiated, this manifold could prove invaluable. The mass-flow meters work exceptionally well with non-corrosive gases, and the controller can be operated in a mode assuring a constant ratio of one gas to another regardless of the backing pressure. This capability has never been used, but represents the best method for study of these mixed rare-gas systems.

The nozzle within the molecular beam has one of two designs. The first is a low-termperature design which utilizes the standard General Valve Series 9 valve (see Fig. 4). This design requires only the gas line, attached to the rear of the valve, and the electrical contacts, which are made behind the nozzle. While the voltage required to open the valve is ~28 volts, higher potentials will open the nozzle faster. As such, the controller described below is designed to initiate the gas pulse with a 300 volt potential. A potential of 10 volts is sufficent to keep the valve open once the initial potential is applied. Therefore, after the valve has been opened the potential of the valve is reduced to ~30 volts. This system allows the valve to open within tens of microseconds. It is typically held open for hundreds of microseconds. The time required to close is uncertain but is considerably slower than the opening time. In order to avoid corrosion inside the body of the valve, all parts have been coated with teflon. Eventually the corrosive gases get under

the teflon coating causing it to bubble. Under these circumstances, the only alternative is to remove the coating altogether. In general however, under normal conditions, operating at 20 Hz, this valve has not caused any serious difficulties (the only disposable part, the teflon poppet, needs to be replaced when the seal is inevitably compromised).

The heatable nozzle assembly (a modified General Valve Series 9) consists of a solenoid-actuated stainless steel piston which mates with an orifice in a Rulon polymer insert, which is screwed into a face plate. Figure 5 shows the diagram for the valve body and Figure 6 shows the dimensions of the various inserts made here at Caltech. A channel in the plate leads from an external chamber, used for solid chemical samples, to the gas stream just before the orifice. Two heating elements and a thermocouple mounted on this plate allow the whole assembly to be maintained at a temperature up to 200° C via an external temperature controller (Omega). This design requires additional access to the face plate from inside the vacuum chamber to accommodate the heating cartridges and the thermocouple wires. Also, since the solid sample holder is inside the chamber, refilling requires the chamber to be vented; however, this design is preferable to placing the solid sample behind the nozzle. When the sample requires heating and is entrained in the carrier gas centimeters behind the nozzle, clogging becomes a constant concern due to the significant amount of material which must be kept hot. In this design, only the face plate need be kept hot, thereby nearly eliminating the problem of clogging. In general, this design requires more attention than the room temperature valve due to the extra components and the difficulty associated with retaining an adequate seal when the valve is closed. The poppet is stainless steel with a machined tip; which, if not matched well to the Rulon insert, will not form a good seal (particularly at low temperatures, where the Rulon has not softened significantly). Several hours of operation at an elevated temperature often help to form an adequate seal.

The molecular beam valve controller is home built (see Fig. 7 for a schematic) and is based upon the controller built by General Valve. There are essentially three parts to

this design. The first includes a TTL cicuit which provides an internal trigger at 20 Hz, a method for delaying the external trigger in the range 1-3 ms, and a means of controlling the duration of the gas pulse. The internal trigger is generated from a 555 oscillator and the timing is controlled by a 74221 multi-vibrator chip. The second component is a high-voltage regulated power supply. This component turns out to be over-kill but at one point was considered necessary; a simple full bridge rectifier would have worked adequately. At any rate, this component delivers 300 volts dc with less than 1% ripple. The design was taken directly from Ref. 4, page 207. It is important to realize that with this design the two transistors float at ~300 volts, and, therefore, the cases are electrically "hot," representing a potential hazard for anyone trying to repair this system with the power on. The third component is the actual valve driver. Prior to the TTL pulse, the power supply has charged up capacitor C1. When the TTL pulse arrives the transistor (NTE 238) is opened and capacitor C1 discharges and quickly opens the valve with a potential of 300 volts. The charge is quickly dissipated from this capacitor and now the power supply voltage is divided over resistor R1 and the valve (~30 Ω) suppling a constant 3 volts dc to the valve -- enough to keep it open. When the TTL pulse goes to ground, the transistor closes, the capacitor is recharged, and the valve closes. See notebook EDP, page 78-79 for a mask used for generating the printed circuit board.

The laser beams, typically focused to an approximately 300 μm beam waist, intersect the molecular beam approximately 15 mm downstream of the nozzle, corresponding to an X/D of 30. Fluorescence is collected by a 5 cm diameter F/1.5 Suprasil plcx lens aided by a 4 cm diameter, 2.4 cm focal length concave parabolic mirror placed below the beams. The emission passes either through appropriate Schott filters to block scattered light or a newly installed 100 mm monochromator. With the filter arrangement, another plcx lens (5 cm diameter, f/1.5) focuses the fluorescence onto an adjustable slit to further discriminate against scattered light. Lastly, a f/1.5 lens recollimates the light and a final f/1.5 lens focuses it onto the photocathode of a GaAs

single photon counting PMT (Hamamatsu R943-02 for visible and near uv wavelengths, or Amperex XP2020Q for uv detection), mounted within a thermoelectrically cooled housing (Products For Research).

Under the monochromator arrangement, the emission, after collection with the F/1.5 lens, is reflected 90° (parallel to the incoming laser beams), focused via a F/3.5 lens onto the input slit of an ISA, H-10, 100 mm monochromator. The output is focused with an F/1 lens onto one of the two photomultipliers listed above. The single grating within the monochromator is suitable for wavelengths in the range 200-800 nm with a blaze at 250 nm. The bandpass is set by the interchangeable slit width; currently the slits available yield a bandpass of 2, 4, 8, 16, or 32 nm. This arrangement is preferable to the filter arrangement because it is easier to discriminate signal from scattered light. Shielding is required to completely eliminate stray light since the interface between the monochromator and PMT housing is not perfectly light tight.

The electron impact time-of-flight spectrometer (EI-TOFMS) arrangement has been described previously.[3] A microchannel plate (MCP) assembly constructed in this laboratory is used instead of the former electron multiplier, and the length of the flight tube has been increased from 1 to 1.2 meters in order to facilitate a gate-valve separating the chamber from the MCP. The MCP consists of two Varian plates held together by a Kimbel Physics construction. The signal is not efficiently collected with a cone as in the commercially available products but rather is taken directly from the back of the second plate. The high-voltage input is divided inside the chamber via a resistor chain and then distributed to the front and back of the first plate and the front of the second plate. A new switching circuit for the electron impact has also been constructed (see Fig. 8), designed to have ~1 ns risetimes for improved EI-TOF mass spectra.

An accident which caused the molecular beam to be filled with black soot and oil prompted the building of an all-inclusive interlock system. This system has been designed with the following objectives:

1. If the power to the laboratory should shut off unexpectedly, nothing on the molecular beam should come back on by itself after the power has been restored. The roughing pump is on an independent circuit breaker which does not reset automatically when the power is turned off and then back on. Therefore, when the power is restored, it is possible for the diffusion pumps to begin heating without maintenance of a satisfactory vacuum on the fore-line.

2. If the pressure in the fore-line rises above a predetermined level, several actions should be taken:
   a) The power to the diffusion pumps should be cut off.
   b) The gate-valves to the chamber should be closed, in order to avoid any deletrious effects as a result of residual overheating of the diffusion pump oil.
   c) Although the pressure may return to an acceptable level spontaneously, neither of the above conditions should be reversed.

3. If the pressure in the chamber rises above a predetermined level (although the pressure in the fore-line is acceptable), the power supplies used to control the mass spectrometer should be turned off. This interlock does not remain latched when the pressure is brought below the desired level.

4. If the cooling water to the diffusion pumps shuts off, then the power should be discontinued to the pumps.

The interlock shown in Fig. 9 has been designed to accomplish the tasks 1-3. Task 4 is accomplished by the Neslab heat exchanger used to cool the diffusion pumps. This unit has an internal flow switch which opens an external interlock when the flow is interupted. This external interlock is placed in series with the power switch of the diffusion pumps on the main interlock system. The diffusion pump power is routed through the interlock system and controlled by a single pole, quadruple throw relay. The pressure in the fore-line and in the vacuum chamber is monitored by the chart-recorder output of the ion-guage controller and compared to a preset internal voltage via two voltage comparator circuits within the interlock system. The high voltage power supplies can be shut off by plugging these units into the power strip output on the rear of the interlock system. This output shuts down when the chamber pressure is too high (it is worth noting that this part of the system should be changed -- the relay used to open and close this output is too small to handle the current required by the high voltage power supplies, therefore this

relay should be used to control a second, larger relay, capable of handling the necessary currents). The pneumatic gate valves are controlled by solenoids attached to the nitrogen tank used to open or close these valves. A normally open solenoid is attached directly on the nitrogen tank, in order that small leaks in the line from the tank to the gate valves does not empty the contents on a regular basis. The normally closed solenoids attached to the gate valves close the valves when power is discontinued. This overall system will force the gate valves closed in the event of a power outage or a rise in fore-line pressure.

2.4 Signal processing

The 50 Ω terminated output of the PMT is amplified in the same way as the TOFMS signal, through a Stanford Research fast preamplifier (SR445), and fed into either the Stanford Research gated photon counter or an EG&G boxcar. A fast photodiode mounted behind one of the 532 nm Q-switched Nd:YAG laser turning mirrors provides the trigger pulse for either instrument, although the photodiode signal is first sent through a pulse generator because the temporal pulse shape is multi-lobed and tends to trigger the photon counter multiple times per laser shot.

The boxcar integrator is typically used without any external control, except the trigger, to collect transients. The analog output of the boxcar is sent to an A/D converter (Metrabyte, DAS-8). The assembly routines used to control and read the A/D converter are compiled and placed in the Quick Basic library "INTRFC.Lib." These routines and their calling protocols are described in the Metrabyte manual. However, the following routine is used to read the voltage on the converter without using the compiled routines, where CHANNEL% is the channel connected to the device one wishes to measure (usually zero for the boxcar) and DIO% is the actual 12-bit conversion. The base address for this card is held in a file named "das8.adr." This file is read when the acquisition program is started and then the global variable BASADR% is defined.

```
'*****************************************************************
'*          Read A/D converter without using DAS8 command        *
'*****************************************************************
SUB DAS (CHANNEL%, DIO%)        'CHANNEL% is the number of the conversion
                                'channel.  DIO% is the data.

OUT BASADR% + 2, CHANNEL%       'Send out channel number to the control register.  The
      'lowest three bits are used for assigning which channel is being converted.  See the manual
      'for a description of how the remaining five bits are used.
OUT BASADR% + 1, 0              'Send out zero on secone byte, in order to initiate a 12-bit
                                'conversion.
DO
      STATUS = INP(BASADR% + 2)         'Wait until the status register bit 8 is set to zero.
LOOP UNTIL STATUS < 128
XL% = INP(BASADR%)                      'Low data byte is at base address (first byte)
XH% = INP(BASADR% + 1)            'High data byte is at base address plus one (second byte).
DIO% = 16 * XH% + XL% / 16 - 2048 'Form the data from the two bytes by multiplying the high
      'byte by sixteen and adding the low byte divided by 16 (subtract 2048 so that negative
      'voltages correspond to integers below zero).

END SUB
```

The boxcar can also be used to collect a temporal scan of the emission by scanning the boxcar gate through time. While it is possible to set up the boxcar to scan independently, it is easier to send a voltage ramp to the rear port to control the gate position. This method has been implemented via a D/A converter sent to this port. The following routine is used to send a voltage to the D/A converter. As above, CHANNEL% is the ouput channel of the D/A converter (0 or 1) and DIGITAL% is the 12-bit representation of the desired voltage. The D/A converter can be configured to deliver a voltage in the range of 0 to 5, -5 to 5, 0 to 10, or -10 to 10 volts by placing either -5 volts or -10 volts on the reference pin for the desired channel and then using either the unipolar or bipolar output. In any case, the full voltage range is divided up into 4096 parts (12-bits). The base address for this card has been set to Hex 330 (see Table II for an I/O map of the laboratory IBM-AT computer).

```
SUB DAC (CHANNEL%, DIGITAL%)    'taken out of DAC-02 manual p.3-4.

DH% = INT(DIGITAL% / 16)        'generate high byte
```

```
DL% = DIGITAL% - 16 * DH%       'get remainder to be put into low byte
DL% = 16 * DL%                  'shift over 4 places to the left (12 bit resolution instead of 16)
SELECT CASE CHANNEL%
    CASE 0                      'converter number for channel 0
        OUT &H330, DL%
        OUT &H331, DH%
    CASE 1                      'converter number for channel 1
        OUT &H332, DL%
        OUT &H333, DH%
END SELECT

END SUB
```

The photon counter can be used to take data in a similar manner to the boxcar as described above, i.e., collecting data with a fixed gate or a scanning gate. However, the photon counter has an RS-232 interface, which can be used to control every function of the device. A separate interface routine has not been written due to the ease with which this instrument accepts and returns information (see manual for details regarding acceptable commands and their functions). The acquisition program does send the instrument a set of default parameters every time the program is initiated and likewise, the user can set these default parameters with the photon counter and request the acquisition program to read these values and store them as defaults. The file used to store these values can be found under the name "default.dat" a copy of which can be found in Table III.

A transient involves a scan of the delay of one pulse with respect to the other. This is accomplished via a linear stage with at least 10 μm resolution. The work presented here has been almost exclusively collected with a 25 mm, 0.1 μm resolution stage from Microkinetics (the photodissociation of ketene exeperiments (Chapter 6) were done with a 25 cm, 10 μm resolution stage from Klinger). One of two gear boxes are used with the following calibrations:

261:1 0.1994 fs/encoder count
29.89 nm/encoder count

76:1 0.68595 fs/encoder count
102.82 nm/encoder count

The interface routine for this stage follows. COMM$ is the command sent to the stage and REPORT$ is the string sent back to the calling routine if one is expected.

```
SUB MOTION (COMM$, REPORT$)

CALL QCINIT(4, 3, 0, 1, PORTSTATUS%, QCERROR%)      'Initialize port.
CALL COPEN(2, 9600, 1, 0, 8, 0, 20, 20, TXBUF2(), RXBUF2(), QCERROR%)     'Open port.
CALL CBUFCLR(2, 3, QCERROR%)              'Clear the buffers.
CODE$ = MID$(COMM$, 2, 2)                 'Eliminate the channel designation.
SELECT CASE CODE$
        CASE "MR", "MA", "GH", "MN", "DH", "AB", "SV"    'These commands get no return.
                SEN$ = COMM$ + CHR$(13)           'Add a carriage return to the command.
                CALL CPRINT(2, SEN$, QCERROR%)          'Send command.
                FOR i = 1 TO 1000: NEXT i               'Pause.
                DO
                        CALL CBUFFER(2, RECV%, XMIT%, QCERROR%)
                LOOP UNTIL XMIT% = 20     'Wait until the transmit buffer is empty.
                REPORT$ = "NO RETURN VALUE"             'Nothing in return.
        CASE "TP", "TE", "TV"                   'These commands send back information.
                SEN$ = COMM$ + CHR$(13)
                CALL CPRINT(2, SEN$, QCERROR%)
                FOR i = 1 TO 1000: NEXT i
                DO
                        CALL CBUFFER(2, RECV%, XMIT%, QCERROR%)
                LOOP UNTIL XMIT% = 20
                REPORT$ = SPACE$(20)        'Set aside a string for return information.
                RELPOS% = 0: FLAG% = 1
                CALL CINPUT(2, REPORT$, RELPOS%, 0, "", "", KB%, FLAG%)  'Get data.
                REPORT$ = RIGHT$(REPORT$, LEN(REPORT$) - INSTR(REPORT$, " "))
                REPORT$ = LEFT$(REPORT$, 10)     'Eliminate channel designation.
END SELECT
CALL CCLOSE(2, QCERROR%)                  'Close port.
CALL QCEXIT                               'Exit communication protocol.

END SUB
```

This routine does not accommodate all of the commands which can be sent to this device (see manual for a complete listing); however, it is a simple matter to include these commands in the CASE lines above depending upon whether a response is anticipated or not.

The monochromator discussed above is controlled by a simple stepper motor which can be interfaced through an RS-232 port. The controller does not have externally accessible settings and therefore, in order to intiate communication with this device a series of commands must be sent to set the proper protocol (baud rate, etc.). The following routine was written for this purpose.

```
SUB INITMONO (MONOAVAILABLE%)                'Returns 1 if mono. is available

PORT% = 4              'Mono. is hooked up to com4.
CALL QCINIT(4, 3, 0, 1, PORTSTATUS%, QCERROR%)      'Initialize port.
CALL COPEN(PORT%, 9600, 1, 0, 8, 0, 40, 40, TXBUF6(), RXBUF6(), QCERROR%)  'Open
                                                                            'port.
NUMTRIES% = 0
DO                     'Call at least 10 times before returning 0.
     NUMTRIES% = NUMTRIES% + 1          '# of tries
     CALL CBUFCLR(PORT%, 3, QCERROR%)       'Clear buffers
     CALL CPUTCHAR(PORT%, 32, QCERROR%)     'Put a space on the output line.
     NOW! = TIMER
     DO                'Loop until an asterisk is returned.
          CALL CBUFREC(PORT%, STATUS%, QCERROR%)  'wait until buffer sees
                    'a character or until 5 seconds have elapsed.
          LATER! = TIMER
          IF LATER! - NOW! > 5 THEN EXIT DO
     LOOP UNTIL STATUS% = 1      'Something is in buffer.
     CHAR% = 0
     CALL CGETCHAR(PORT%, CHAR%, STATUS%)       'Get buffer contents.
     IF CHAR% = 70 THEN             'Mono. is available (* returned).
          MONOAVAILABLE% = 1
          CALL CCLOSE(PORT%, QCERROR%)      'Close buffers.
          CALL QCEXIT               'Exit communication protocol.
          EXIT SUB                  'Return to calling routine.
     END IF
     IF NUMTRIES% = 10 THEN         'Mono. is not available.
          CALL MCLEAR               'Clear menu line.
          INPUT "MONOCHROMETER NOT RESPONSING                    CONTINUE
(Hit n to end, else any key to continue)"; DUMMY$
          IF DUMMY$ = "N" OR DUMMY$ = "n" THEN
               CLS
               END          'If user wishes not to continue without the mono.--end.
          ELSE              'Continue without the use of the monochromator.
               MONOAVAILABLE% = 0
               CALL CCLOSE(PORT%, QCERROR%)         'Close port.
               CALL QCEXIT                  'Exit communication protocol.
               EXIT SUB                     'Return to calling routine.
```

```
        END IF
    END IF
LOOP UNTIL CHAR% = 42           'If mono. is already initialized, a 42 will be returned.
FOR I = 1 TO 500: NEXT I        'Pause.
CALL CBUFCLR(PORT%, 3, QCERROR%)  'clear the buffers.
    CALL CPUTCHAR(PORT%, 247, QCERROR%)        'Put a 247 out to mono.
    DO              'Wait until the receive buffer gets something in return.
        CALL CBUFREC(PORT%, STATUS%, QCERROR%)
    LOOP UNTIL STATUS% = 1
    CALL CGETCHAR(PORT%, CHAR%, STATUS%)       'Get the character
FOR I = 1 TO 500: NEXT I    'Pause.
CALL CBUFCLR(PORT%, 3, QCERROR%)  'clear buffers.
    STRNG$ = "O2000" + CHR$(&H0)            'Send O2000 + chr$(&h0).
    CALL CPRINT(PORT%, STRNG$, QCERROR%)
    DO              'Wait until something is returned.
        CALL CBUFREC(PORT%, STATUS%, QCERROR%)
    LOOP UNTIL STATUS% = 1
    CALL CGETCHAR(PORT%, CHAR%, STATUS%)       'Get character.
FOR I = 1 TO 500: NEXT I        'Pause.
CALL CBUFCLR(PORT%, 3, QCERROR%)  'Clear buffers.
    STRNG$ = "B14,300,450,2000" + CHR$(13)     'Initialize if mono has just been
                                                turned on.
    CALL CPRINT(PORT%, STRNG$, QCERROR%)       'Send to the port.
    DO              'Wait until mono sends something back.
        CALL CBUFREC(PORT%, STATUS%, QCERROR%)
    LOOP UNTIL STATUS% = 1
    CALL CGETCHAR(PORT%, CHAR%, STATUS%)       'Get character.
MONOAVAILABLE% = 1              'Mono is available.
CALL CCLOSE(PORT%, QCERROR%)      'close buffers.
CALL QCEXIT

END SUB
```

After the above routine has been executed, the following routine is a general interface routine used to communicate with the monochromator. INTO$ is the command to be sent, and OUTOF$ is the returned information if anything is expected.

```
SUB MN (INTO$, OUTOF$)

PORT% = 4
CALL QCINIT(4, 3, 0, 1, PORTSTATUS%, QCERROR%)
CALL COPEN(PORT%, 9600, 1, 0, 8, 0, 40, 40, TXBUF6(), RXBUF6(), QCERROR%)
CALL CBUFCLR(PORT%, 3, QCERROR%)
CALL CPRINT(PORT%, INTO$, QCERROR%)        'Send the command.
TIMEIN! = TIMER
DO
```

```
    CALL CBUFFER(PORT%, RECV%, XMIT%, QCERROR%)
LOOP UNTIL RECV% <> 0    'Loop until something is returned.
CMND$ = LEFT$(INTO$, 1)  'Eliminate all but the command.
SELECT CASE CMND$
    CASE "A", "B", "F", "G", "L", "p", "q", "v"          'These commands return only "o".
        CALL CGETCHAR(PORT%, CHAR%, STATUS%)
        OUTOF$ = CHR$(CHAR%)
    CASE "C", "H", "r", "s", "t"          'These commands return "o" followed by data and a CR.
        OUTOF$ = ""
        DO
            FOR I = 1 TO 200: NEXT I
            CALL CGETCHAR(PORT%, CHAR%, STATUS%)     'Get data one character
                                                                    at a time.
            IF CHAR% <> 32 OR CHAR% <> 13 THEN OUTOF$ = OUTOF$ +
                    CHR$(CHAR%)          'Generate the output string.
        LOOP UNTIL CHAR% = 13            'Stop when CR is returned.
    CASE "E", "K"              'These commands send two characters ("o" and something else).
        CALL CGETCHAR(PORT%, CHAR%, STATUS%)
        OUTOF$ = CHR$(CHAR%)
        CALL CGETCHAR(PORT%, CHAR%, STATUS%)
        OUTOF$ = OUTOF$ + CHR$(CHAR%)
END SELECT

CALL CCLOSE(PORT%, QCERROR%)
CALL QCEXIT

END SUB
```

The above routines represent the most substantive elements of the data acquisition program found in the Appendix. In addition to these routines, several other important points should be made about the operation of the acquisition program. First, this program is not portable, in that it cannot be run on another computer unless all of the same components are present. For example, if the DAS-8 board is missing the program will terminate immediately. Second, three files are necessary for this program to run properly,

a) "C:\QB45\PROGRAMS\DAS8.ADR" is used for defining the base address of the DAS-8 board,

b) "C:\QB45\DATA\DEFAULT.DAT" is used to set the default parameters for the program and the photon counter,

c) "C:\QB45\STATUS" is used to keep the running total of scans already taken (e.g., IBR**321**.dat).

Currently the serial ports are utilized as follows:

Com 1: Photon Counter
Com 2: Microkinetics Linear Stage
Com 3: Antares Laser
Com 4: Monochromator.

Note: the digiboard ports are labeled 1-8, but the ports are actually Com2-Com9 (Com1 is one of the original serial ports which were installed prior to the digiboard).

Table I. Indices of refraction for various optical materials. The first entry is the index of refraction, the second is the first derivative of the index with respect to wavelength, $dn/d\lambda$ (μm^{-1}), and the third is the second derivative with respect to wavelenth, $d^2n/d\lambda^2$ (μm^{-2}). The first three materials cannot be used below ~350 nm and therefore an index has not been calculated. The constants and formulae for these values can be found in ref. 5, pp. 3-1 to 3-20, and notebook EDP, p.107.

Wavelenth (nm)	BK7	SF-11	LaSF-9	UV-FS	Sapphire
200	-	-	-	1.55051	1.91194
	-	-	-	-1.35138	-2.07208
	-	-	-	30.3007	45.00985
210	-	-	-	1.53836	1.89326
	-	-	-	-1.09163	-1.68392
	-	-	-	22.21016	33.39013
220	-	-	-	1.52845	1.87795
	-	-	-	-0.89845	-1.39217
	-	-	-	16.76685	25.43479
230	-	-	-	1.52024	1.86519
	-	-	-	-0.75087	-1.16754
	-	-	-	12.96367	19.80217
240	-	-	-	1.51333	1.85443
	-	-	-	-0.63565	-0.99106
	-	-	-	10.22348	15.70144
250	-	-	-	1.50745	1.84525
	-	-	-	-0.54403	-0.85005
	-	-	-	8.19803	12.64531
260	-	-	-	1.50239	1.83734
	-	-	-	-0.47005	-0.73572
	-	-	-	6.66823	10.32174
270	-	-	-	1.498	1.83047
	-	-	-	-0.4095	-0.64186
	-	-	-	5.49122	8.52435
280	-	-	-	1.49416	1.82445
	-	-	-	-0.35937	-0.56395
	-	-	-	4.57105	7.11294
290	-	-	-	1.49079	1.81915
	-	-	-	-0.31745	-0.49865
	-	-	-	3.84149	5.98976
300	-	-	-	1.48779	1.81445
	-	-	-	-0.28206	-0.44343
	-	-	-	3.25592	5.0854

310	-	-	-	1.48513	1.81026
	-	-	-	-0.25196	-0.39638
	-	-	-	2.78067	4.3495
320	-	-	-	1.48274	1.8065
	-	-	-	-0.22616	-0.356
	-	-	-	2.39116	3.745
330	-	-	-	1.48059	1.80312
	-	-	-	-0.20391	-0.32113
	-	-	-	2.06905	3.24413
340	-	-	-	1.47865	1.80006
	-	-	-	-0.18461	-0.29085
	-	-	-	1.80053	2.82588
350	1.53916	1.89229	1.93739	1.47689	1.79729
	-0.41247	-2.6326	-1.98263	-0.16776	-0.26439
	2.32716	23.0149	15.77297	1.57503	2.47411
360	1.53719	1.88008	1.92813	1.47529	1.79476
	-0.37448	-2.26086	-1.72561	-0.15299	-0.24118
	2.03504	18.52637	12.85355	1.38438	2.17632
370	1.53539	1.86954	1.92003	1.47383	1.79245
	-0.3413	-1.96043	-1.51551	-0.13998	-0.22072
	1.79078	15.0924	10.60781	1.22218	1.92268
380	1.53374	1.86036	1.91288	1.47248	1.79034
	-0.31215	-1.7149	-1.34169	-0.12847	-0.20261
	1.58463	12.43556	8.85802	1.08342	1.70545
390	1.53223	1.8523	1.90654	1.47125	1.7884
	-0.28638	-1.51209	-1.19628	-0.11824	-0.18651
	1.40918	10.3571	7.47748	0.96405	1.51842
400	1.53085	1.84516	1.90086	1.47012	1.7866
	-0.26351	-1.34287	-1.07337	-0.10913	-0.17216
	1.25874	8.71347	6.37519	0.86087	1.35664
410	1.52957	1.8388	1.89574	1.46907	1.78495
	-0.24312	-1.20033	-0.9685	-0.10098	-0.15931
	1.12892	7.39989	5.48488	0.77127	1.21603
420	1.52839	1.8331	1.89112	1.46809	1.78341
	-0.22487	-1.07918	-0.87823	-0.09367	-0.14778
	1.01621	6.33935	4.75784	0.69314	1.09334
430	1.52729	1.82796	1.88691	1.46719	1.78199
	-0.20847	-0.97536	-0.79993	-0.08709	-0.13739
	0.91783	5.47469	4.15803	0.62472	0.98584
440	1.52627	1.82329	1.88307	1.46635	1.78066
	-0.1937	-0.8857	-0.73151	-0.08115	-0.12802
	0.83155	4.76313	3.65834	0.56459	0.89131

450	1.52532	1.81905	1.87955	1.46557	1.77942
	-0.18034	-0.80772	-0.67135	-0.07577	-0.11953
	0.75553	4.17228	3.2383	0.51155	0.80789
460	1.52443	1.81517	1.87631	1.46483	1.77827
	-0.16824	-0.73946	-0.61814	-0.0709	-0.11183
	0.6883	3.67753	2.88224	0.46461	0.73402
470	1.52361	1.81161	1.87332	1.46415	1.77719
	-0.15724	-0.67935	-0.57083	-0.06460	-0.10482
	0.62859	3.25995	2.57808	0.42293	0.66841
480	1.52283	1.80834	1.87056	1.4635	1.77617
	-0.14722	-0.62611	-0.52855	-0.06242	-0.09843
	0.57541	2.90485	2.31636	0.38582	0.60997
490	1.5221	1.80531	1.868	1.4629	1.77522
	-0.13807	-0.57874	-0.49062	-0.05873	-0.0926
	0.52788	2.60079	2.08971	0.35268	0.55777
500	1.52141	1.80251	1.86561	1.46233	1.77432
	-0.1297	-0.53639	-0.45645	-0.05536	-0.08726
	0.48527	2.33872	1.89223	0.32301	0.51101
510	1.52077	1.79991	1.86339	1.46179	1.77347
	-0.12202	-0.49836	-0.42555	-0.05226	-0.08236
	0.44697	2.11146	1.7192	0.29637	0.46902
520	1.52016	1.79749	1.86131	1.46128	1.77267
	-0.11497	-0.46409	-0.39752	-0.04942	-0.07787
	0.41245	1.91328	1.56684	0.2724	0.43122
530	1.51958	1.79523	1.85937	1.4608	1.77191
	-0.10849	-0.43309	-0.37202	-0.04681	-0.07373
	0.38127	1.73956	1.43204	0.25078	0.39712
540	1.51904	1.79312	1.85755	1.46034	1.77119
	-0.10251	-0.40496	-0.34875	-0.0444	-0.06991
	0.35303	1.58653	1.31227	0.23123	0.36628
550	1.51852	1.79114	1.85584	1.45991	1.77051
	-0.09699	-0.37935	-0.32747	-0.04218	-0.06639
	0.32741	1.45112	1.20544	0.21352	0.33834
560	1.51803	1.78928	1.85423	1.4595	1.76986
	-0.09188	-0.35598	-0.30796	-0.04012	-0.06314
	0.3041	1.3308	1.10981	0.19745	0.31297
570	1.51757	1.78754	1.85271	1.45911	1.76925
	-0.08716	-0.33459	-0.29004	-0.03822	-0.06013
	0.28287	1.22347	1.02391	0.18283	0.28989
580	1.51712	1.7859	1.85128	1.45873	1.76866
	-0.08278	-0.31496	-0.27353	-0.03646	-0.05733
	0.26348	1.12737	0.9465	0.1695	0.26886

590	1.5167	1.78435	1.84993	1.45838	1.7681
	-0.07871	-0.29692	-0.2583	-0.03483	-0.05474
	0.24575	1.04106	0.87656	0.15734	0.24966
600	1.51629	1.78289	1.84866	1.45804	1.76756
	-0.07492	-0.2803	-0.24423	-0.03331	-0.05233
	0.22951	0.96329	0.81319	0.14622	0.2321
610	1.51591	1.78151	1.84744	1.45771	1.76705
	-0.07140	-0.26495	-0.23121	-0.0319	-0.0501
	0.2146	0.893	0.75565	0.13603	0.216
620	1.51554	1.7802	1.8463	1.4574	1.76656
	-0.06812	-0.25076	-0.21913	-0.03059	-0.04801
	0.2009	0.82932	0.70324	0.12668	0.20124
630	1.51519	1.77896	1.84521	1.4571	1.76609
	-0.06505	-0.23761	-0.20791	-0.02936	-0.04607
	0.18829	0.77146	0.65544	0.11809	0.18768
640	1.51485	1.77778	1.84417	1.45681	1.76564
	-0.06219	-0.22541	-0.19748	-0.02822	-0.04425
	0.17666	0.71877	0.61173	0.11019	0.17519
650	1.51452	1.77666	1.84318	1.45653	1.76521
	-0.05952	-0.21406	-0.18777	-0.02716	-0.04256
	0.16593	0.67068	0.5717	0.10291	0.16368
660	1.51421	1.7756	1.84224	1.45627	1.76479
	-0.05702	-0.20351	-0.17872	-0.02616	-0.04098
	0.15602	0.6267	0.53497	0.09619	0.15307
670	1.51391	1.77458	1.84134	1.45601	1.76439
	-0.05467	-0.19367	-0.17026	-0.02523	-0.0395
	0.14683	0.5864	0.50119	0.08998	0.14325
680	1.51362	1.77361	1.84049	1.45576	1.764
	-0.05247	-0.18448	-0.16236	-0.02436	-0.03811
	0.13832	0.54939	0.47009	0.08423	0.13417
690	1.51334	1.77269	1.83967	1.45552	1.76362
	-0.05041	-0.1759	-0.15497	-0.02355	-0.03681
	0.13043	0.51535	0.44142	0.07891	0.12576
700	1.51307	1.77181	1.83888	1.45529	1.76326
	-0.04847	-0.16787	-0.14805	-0.02278	-0.03559
	0.12309	0.48398	0.41494	0.07397	0.11796
710	1.5128	1.77097	1.83813	1.45507	1.76291
	-0.04664	-0.16035	-0.14155	-0.02207	-0.03445
	0.11627	0.45504	0.39044	0.06939	0.11072
720	1.51255	1.77016	1.83741	1.45485	1.76257
	-0.04493	-0.1533	-0.13546	-0.02139	-0.03338
	0.10992	0.42829	0.36775	0.06513	0.10398

730	1.51231	1.76938	1.83672	1.45464	1.76224
	-0.04331	-0.14668	-0.12974	-0.02076	-0.03237
	0.104	0.40353	0.34672	0.06116	0.09772
740	1.51207	1.76864	1.83606	1.45444	1.76193
	-0.04179	-0.14046	-0.12435	-0.02017	-0.03142
	0.09848	0.38058	0.32718	0.05746	0.09188
750	1.51184	1.76793	1.83542	1.45424	1.76162
	-0.04036	-0.1346	-0.11929	-0.01961	-0.03053
	0.09332	0.35927	0.30903	0.05402	0.08643
760	1.51162	1.76725	1.83481	1.45404	1.76131
	-0.039	-0.1291	-0.11452	-0.01909	-0.02969
	0.0885	0.33948	0.29213	0.0508	0.08135
770	1.5114	1.76659	1.83422	1.45385	1.76102
	-0.03773	-0.12391	-0.11002	-0.0186	-0.0289
	0.08399	0.32106	0.27639	0.0478	0.0766
780	1.51119	1.76596	1.83365	1.45367	1.76074
	-0.03652	-0.11901	-0.10577	-0.01813	-0.02816
	0.07977	0.3039	0.2617	0.04498	0.07216
790	1.51098	1.76535	1.8331	1.45349	1.76046
	-0.03538	-0.11439	-0.10176	-0.0177	-0.02746
	0.07581	0.2879	0.24799	0.04235	0.068
800	1.51078	1.76476	1.83258	1.45332	1.76019
	-0.0343	-0.11003	-0.09798	-0.01728	-0.0268
	0.0721	0.27296	0.23518	0.03988	0.0641
810	1.51058	1.76419	1.83206	1.45315	1.75992
	-0.03328	-0.1059	-0.09439	-0.0169	-0.02617
	0.06861	0.259	0.22319	0.03757	0.06044
820	1.51039	1.76365	1.83157	1.45298	1.75966
	-0.03231	-0.102	-0.09101	-0.01653	-0.02559
	0.06533	0.24594	0.21197	0.0354	0.05701
830	1.51021	1.76312	1.83109	1.45282	1.75941
	-0.03139	-0.0983	-0.0878	-0.01619	-0.02503
	0.06225	0.2337	0.20145	0.03336	0.05379
840	1.51002	1.76261	1.83063	1.45266	1.75916
	-0.03052	-0.0948	-0.08475	-0.01586	-0.02451
	0.05935	0.22224	0.19158	0.03144	0.05076
850	1.50984	1.76212	1.83018	1.4525	1.75892
	-0.0297	-0.09148	-0.08187	-0.01556	-0.02402
	0.05662	0.21148	0.18232	0.02963	0.04791
860	1.50967	1.76164	1.82975	1.45234	1.75868
	-0.02892	-0.08834	-0.07914	-0.01527	-0.02355
	0.05405	0.20139	0.17361	0.02793	0.04523

870	1.5095	1.76118	1.82932	1.45219	1.75845
	-0.02817	-0.08535	-0.07654	-0.015	-0.02311
	0.05161	0.19189	0.16543	0.02633	0.0427
880	1.50933	1.76073	1.82891	1.45204	1.75822
	-0.02747	-0.08251	-0.07407	-0.01474	-0.0227
	0.04933	0.18296	0.15772	0.02482	0.04032
890	1.50916	1.76029	1.82852	1.4519	1.758
	-0.0268	-0.07981	-0.07173	-0.0145	-0.0223
	0.04716	0.17456	0.15047	0.0234	0.03807
900	1.509	1.75987	1.82813	1.45175	1.75777
	-0.02616	-0.07724	-0.06950	-0.01428	-0.02194
	0.04512	0.16663	0.14363	0.02205	0.03594
910	1.50884	1.75946	1.82775	1.45161	1.75756
	-0.02556	-0.07480	-0.06738	-0.01406	-0.02159
	0.04319	0.15917	0.13718	0.02078	0.03393
920	1.50869	1.75906	1.82739	1.45147	1.75734
	-0.02499	-0.07248	-0.06536	-0.01386	-0.02126
	0.04136	0.15213	0.13109	0.01957	0.03203
930	1.50853	1.75868	1.82703	1.45133	1.75713
	-0.02444	-0.07026	-0.06344	-0.01367	-0.02094
	0.03963	0.14547	0.12534	0.01843	0.03024
940	1.50838	1.7583	1.82668	1.4512	1.75692
	-0.02392	-0.06815	-0.06161	-0.01349	-0.02065
	0.03799	0.13919	0.11991	0.01735	0.02854
950	1.50823	1.75793	1.82634	1.45107	1.75672
	-0.02342	-0.06614	-0.05986	-0.01332	-0.02037
	0.03643	0.13324	0.11476	0.01633	0.02693
960	1.50808	1.75758	1.82601	1.45093	1.75652
	-0.02295	-0.06422	-0.0582	-0.01317	-0.02011
	0.03496	0.12762	0.1099	0.01536	0.0254
970	1.50793	1.75723	1.82569	1.4508	1.75632
	-0.0225	-0.06239	-0.05661	-0.01302	-0.01987
	0.03356	0.1223	0.10529	0.01444	0.02395
980	1.50779	1.75689	1.82537	1.45067	1.75612
	-0.02208	-0.06064	-0.05509	-0.01288	-0.01963
	0.03224	0.11726	0.10093	0.01357	0.02258
990	1.50765	1.75656	1.82506	1.45054	1.75592
	-0.02167	-0.05897	-0.05365	-0.01274	-0.01941
	0.03098	0.11248	0.09679	0.01274	0.02127
1000	1.50751	1.75623	1.82476	1.45042	1.75573
	-0.02128	-0.05738	-0.05226	-0.01262	-0.01921
	0.02978	0.10795	0.09286	0.01195	0.02003

Table II. I/O map of the IBM-AT laboratory computer. The information regarding common uses of these addresses came from the Digiboard Installation Guide and may include devices this particular computer does not possess. The addresses for the devices shown in bold represent cards placed in the computer by this author and therefore, can be assumed to be accurate.

Address (Hex)	Common Use of this Address	Address (Hex)	Common Use of this Address
000		200	Game Controller
008	DMA Controller	208	
010	8287A-5	210	
018		218	
020		220	**Transient**
028	Interrupt (master)	228	**Digitizer (not inst.)**
030	Controller 8259A	230	
038		238	
040		240	
048	Timer: 8254-2 (AT)	248	
050		250	
058		258	
060	Keyboard 8042 (AT)	260	
068		268	
070	Real Time Clock	270	
078		278	Parallel Port 2
080		280	
088	DMA Page	288	
090	Register (LS612 AT)	290	
098		298	
0A0		2A0	
0A8	Interrupt Controller	2A8	
0B0	2-8259A (AT)	2B0	
0B8		2B8	Alternate Enhanced
0C0		2C0	Graphics Adapter
0C8	DMA Controller	2C8	
0D0	2-8237A-5 (AT)	2D0	
0D8		2D8	
0E0		2E0	GPIB (adapter 0)
0E8		2E8	
0F0	Clear Math bus (AT)	2F0	
0F8	Math Co-processor (AT)	2F8	**Serial Port #2-disable**
100	**Com 2**	300	**DAS-8**
108	**Com3**	308	
110	**Com4**	310	
118	**Com5**	318	
120	**Com6**	320	

128	**Com7**	328	
130	**Com8**	330	**DAC-02**
138	**Com9**	338	
140	**Status Port**	340	
148		348	
150		350	
158		358	
160		360	Reserved (AT)
168		368	
170		370	
178		378	Parallel Port #1
180		380	SDLC Bisync #2
188		388	
190		390	
198		398	
1A0		3A0	Bisynchronous 1
1A8		3A8	
1B0		3B0	Monochrome Display
1B8		3B8	Printer Adapter
1C0		3C0	Reserved (AT)
1C8		3C8	
1D0		3D0	CGA Display
1D8		3D8	"
1E0		3E0	
1E8		3E8	
1F0	Fixed Disk (AT)	3F0	Diskette Controller
1F8		3F8	**Serial Port 1**

Table III. The following is an exact copy of the file "default.dat" used to initiate the acquisition program and reset the parameters governing the operation of the photon counter.

```
MODE = 1

MODE 1 PARAMETERS:
TOTAL # OF STEPS:  200
STEP TIME:         .2
INVERT:            1
TIME FACTOR:       .1

MODE 2 PARAMETERS:
# OF POINTS:       200
STEPSIZE:          60
STEP TIME:         1
INVERT:            1
FULL SCALE VOLTS:  2
START SCAN:        0

MODE 3 PARAMETERS:
# OF STEPS:        200
STEPSIZE:          5
STEP TIME:         1
START TIME:        .1
FULL SCALE:        100

MODE 4 PARAMETERS:
# OF POINTS:       200
STEPSIZE:          30
STEP TIME:         20
INVERT:            1
FULL SCALE:        350
START SCAN:        0

PHOTON COUNTER PARAMETERS:
MODE =             0
COUNTER A =        1
COUNTER B =        2
COUNTER T =        3
PRESET T =         20
# OF STEPS =       200
SCAN END MODE =    1
DWELL TIME =       0
D/A OUTPUT =       0
```

D/A SCALE = 7
DISPLAY MODE = 0
TRIGGER SLOPE = 0
TRIGGER LEVEL = 2
A DISC SLOPE = 1
B DISC SLOPE = 1
T DISC SLOPE = 1
A DISC MODE = 0
B DISC MODE = 0
T DISC MODE = 0
A DISC STEP = .01
B DISC STEP = .01
T DISC STEP = .01
A DISC LEVEL = -.005
B DISC LEVEL = -.0802
T DISC LEVEL = -.0032
A GATE MODE = 1
B GATE MODE = 1
A GATE SCAN = .0001
B GATE SCAN = .0001
A GATE DELAY = 0
B GATE DELAY = .0001
A GATE WIDTH = .0000015
B GATE WIDTH = 1.51E-06

2.5 References

1. (a) R. L. Fork, O. E. Martinez, and J. P. Gordon, *Optics Letters*, **9**, 150 (1984); (b) J. P. Gordon, and R. L. Fork, *Optics Letters,* **9**, 153 (1984); (c) F. Salin and A. Brun, *J. Appl. Phys.*, **61**, 4736 (1987); (d) R. L. Fork, C. H. Brito Cruz, P. C. Becker, and C. V. Shank, *Optics Letters,* **12**, 483 (1987).
2. Z. A. Yasa, and N. M. Amer, *Opt. Commun.*, **36**, 406 (1981).
3. N. F. Scherer, L. R. Khundkar, R. B. Berstein, and A. H. Zewail, *J. Chem. Phys.*, **87**, 1451 (1987).
4. P. Horowitz, and W. Hill, *The Art of Electronics,* 1st ed., Cambridge Univ. Press, New York (1980).
5. Melles Griot, *Optics Guide 5* (1990).

2.6 Figure Captions

1. Schematic overview of the experimental apparatus. Recompression prisms, while shown as dotted lines, were required for dispersion compensation in the I_2 experiments.
2. Exploded view of the molecular beam apparatus. The newly installed monochromator, used to disperse the fluorescence is not shown.
3. Gas mixing manifold, used for gas preparation prior to expansion through molecular beam nozzle.
4. Standard Series 9 molecular beam nozzle. Panel A illustrates the internal mechanism. Panel B diagrams the dimensions. Panel C is a drawing of the flange used to mount the valve onto the molecular beam.
5. Custom made molecular beam nozzle. This nozzle has the capability for heated samples. The front flange has three holes bored perpendicular to the gas flow. Two of these holes are used to hold cartridge heaters. The third hole has access to the gas flow and is equipped with a sample holder for solid samples. The maximum operating temperature is 200° C. The front of this flange is designed to accept an insert made of a soft material (either Teflon or Rulon).
6. Diagram of the insert used for the expansion into the molecular beam. The inserts fabricated here at Caltech were made of Rulon, while those made by General Valve were made of Teflon.
7. Electrical diagram of the molecular beam valve controller circuit.
8. Electrical diagram of the new electron impact time-of-flight mass spectrometer circuit.
9. Electrical diagram of the interlock circuit used to protect the molecular beam from accidental leaks in the vacuum.

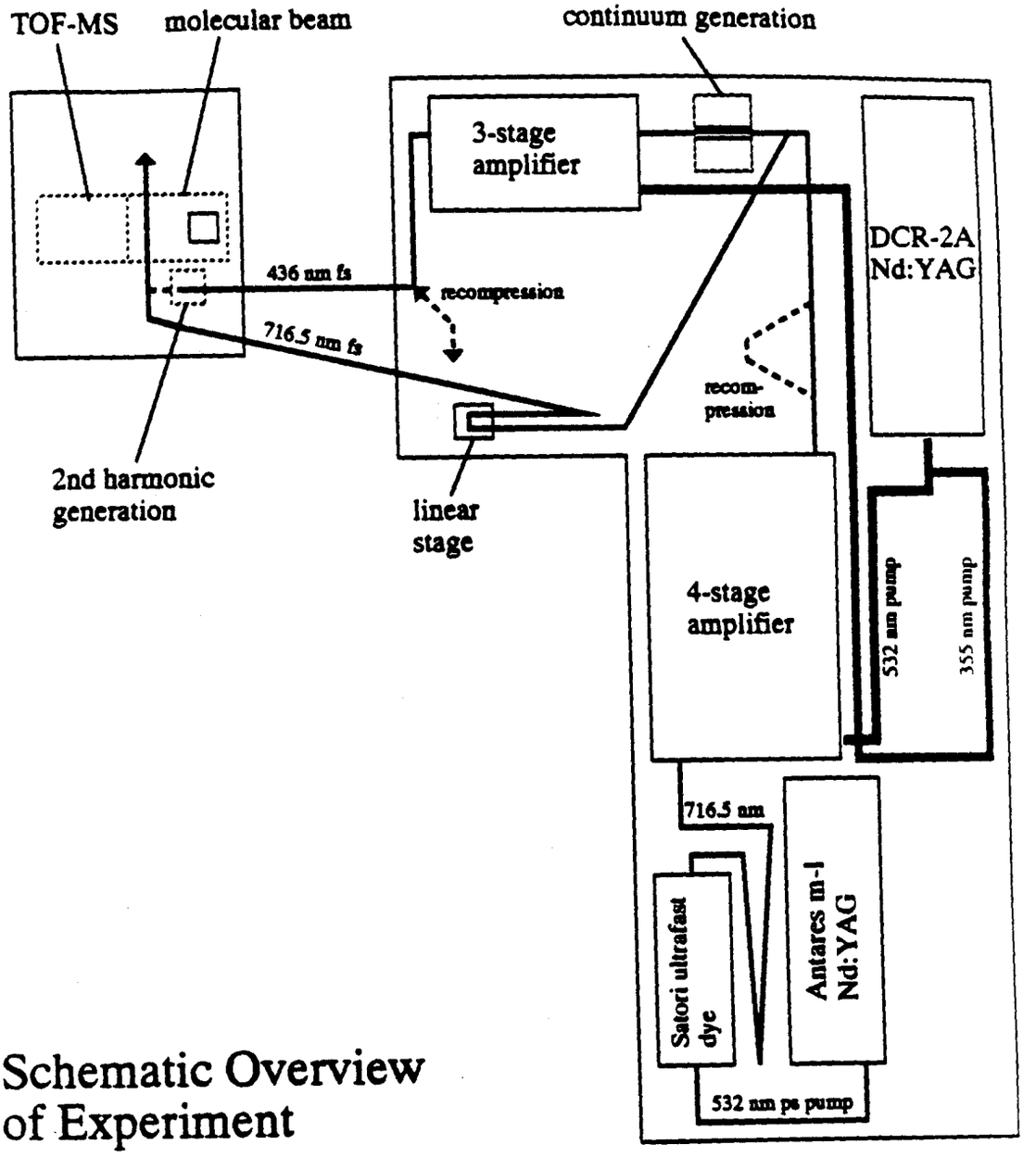

Schematic Overview of Experiment

Figure 1.

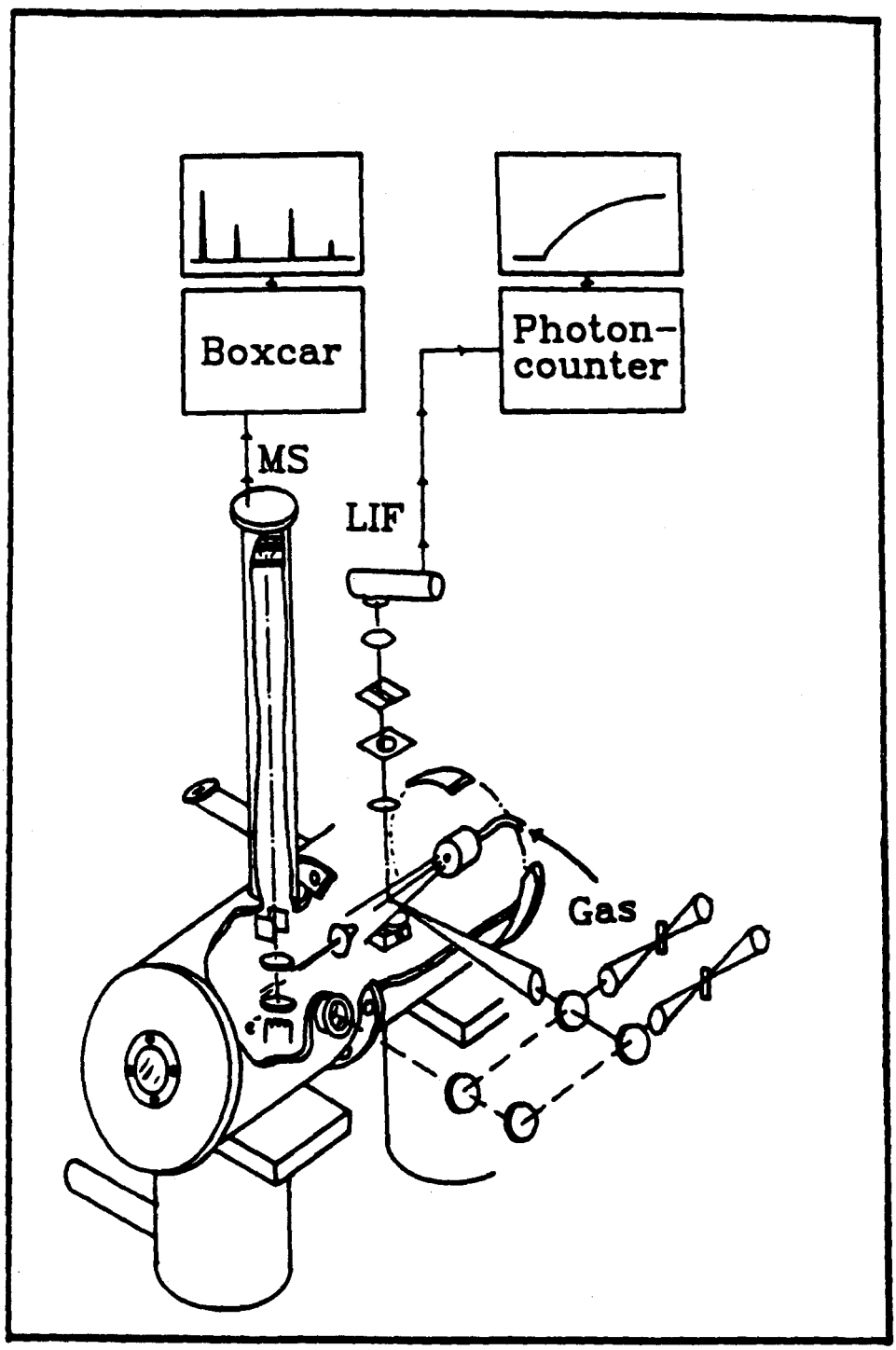

Figure 2.

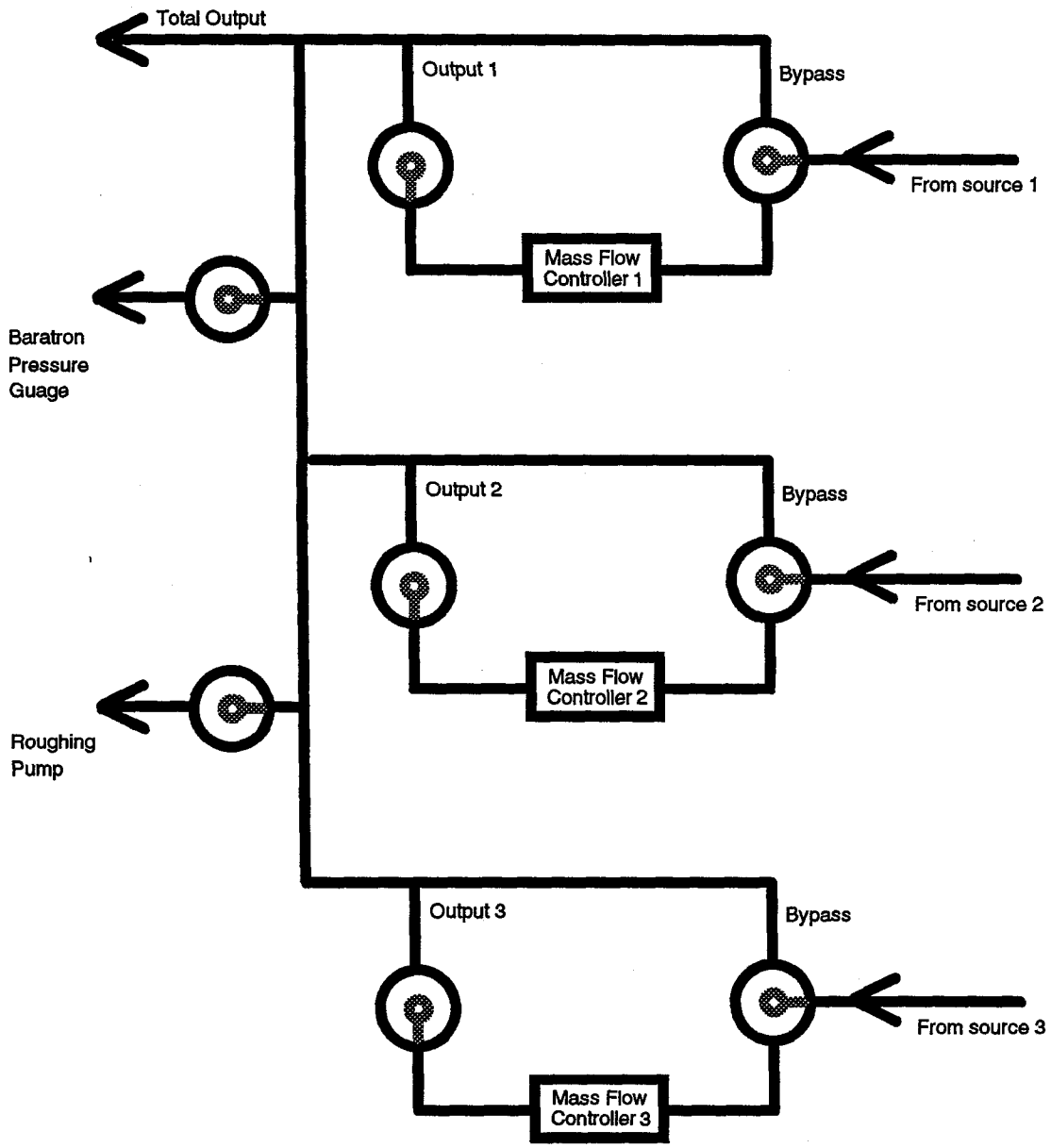
Total Output
Output 1
Bypass
From source 1
Mass Flow Controller 1
Baratron Pressure Guage
Output 2
Bypass
From source 2
Mass Flow Controller 2
Roughing Pump
Output 3
Bypass
From source 3
Mass Flow Controller 3

Figure 3.

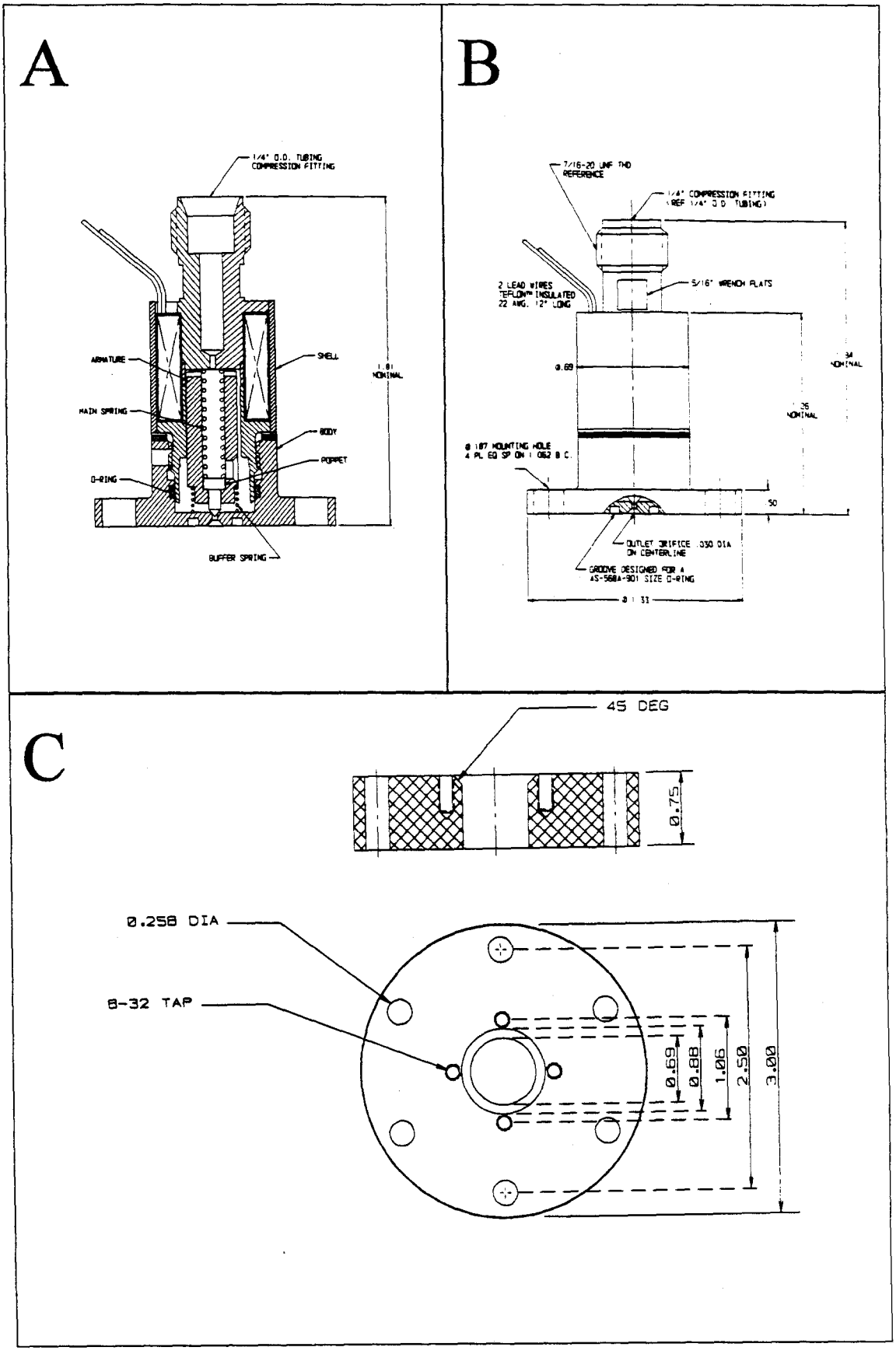
A
1/4" O.D. TUBING COMPRESSION FITTING
ARMATURE
SHELL
MAIN SPRING
BODY
POPPET
O-RING
BUFFER SPRING
B
7/16-20 UNF THD REFERENCE
1/4" COMPRESSION FITTING (REF 1/4" O.D. TUBING)
2 LEAD WIRES "TEFLON" INSULATED 22 AWG. 12" LONG
5/16" WRENCH FLATS
.69
.36 NOMINAL
.187 MOUNTING HOLE 4 PL EQ SP ON 1.062 B.C.
.50
OUTLET ORIFICE .030 DIA ON CENTERLINE
GROOVE DESIGNED FOR A AS-568A-901 SIZE O-RING
1.31
C
45 DEG
0.75
0.258 DIA
8-32 TAP
0.69
0.88
1.06
2.50
3.00

Figure 4.

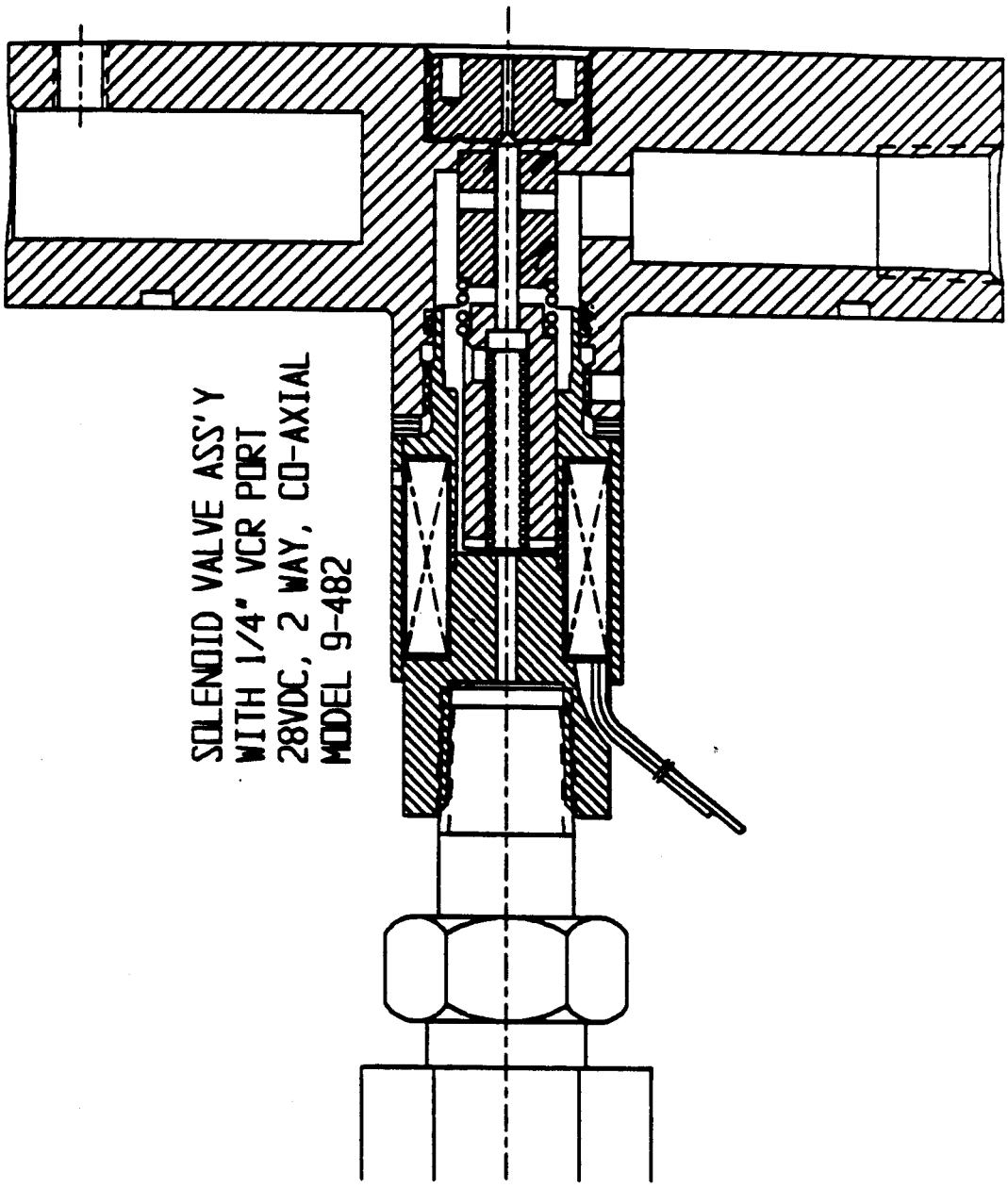
SOLENOID VALVE ASS'Y
WITH 1/4" VCR PORT
28VDC, 2 WAY, CO-AXIAL
MODEL 9-482

Figure 5.

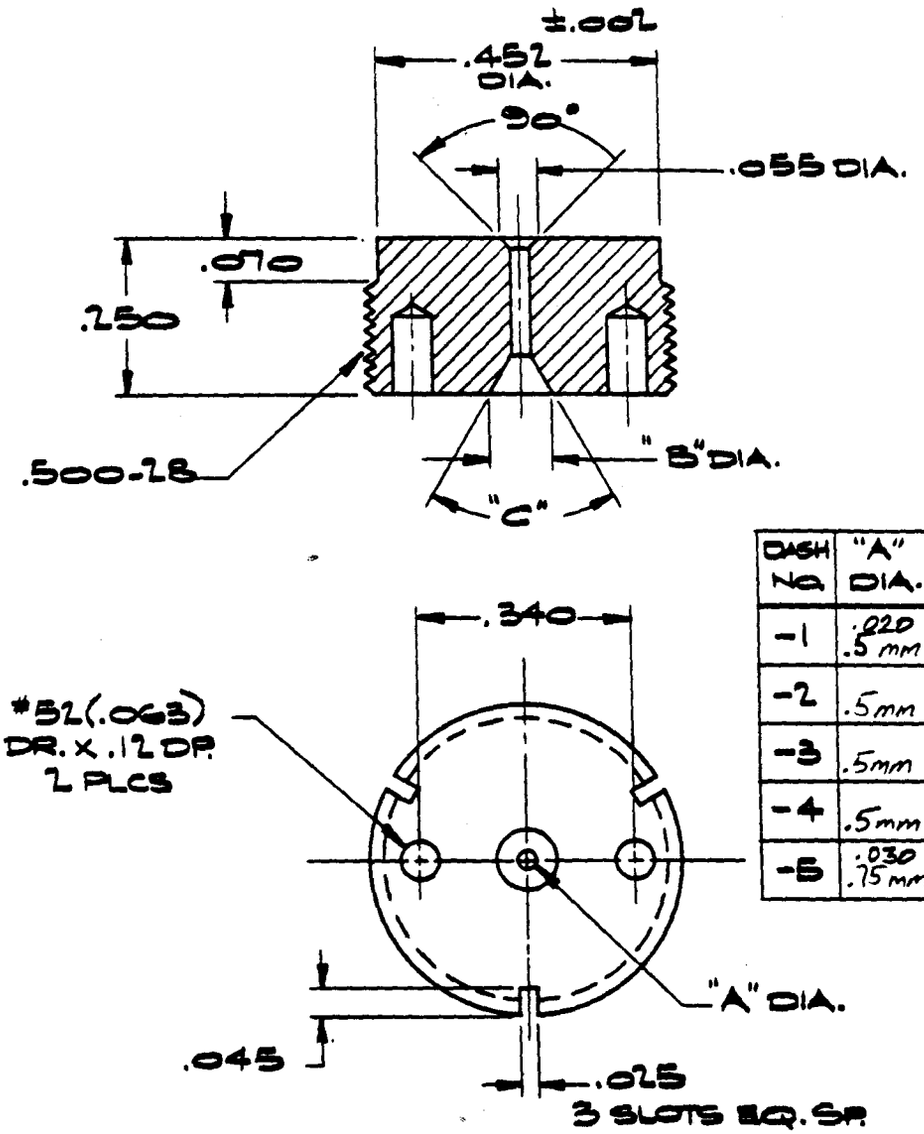

DASH NO.	"A" DIA.	"B" DIA.	"C" ∠
-1	.020 .5 mm	.100"	30°
-2	.5mm	.067"	30°
-3	.5mm	.033"	30°
-4	.5mm	.149"	60°
-5	.030 .75 mm	.75mm	—

Figure 6.

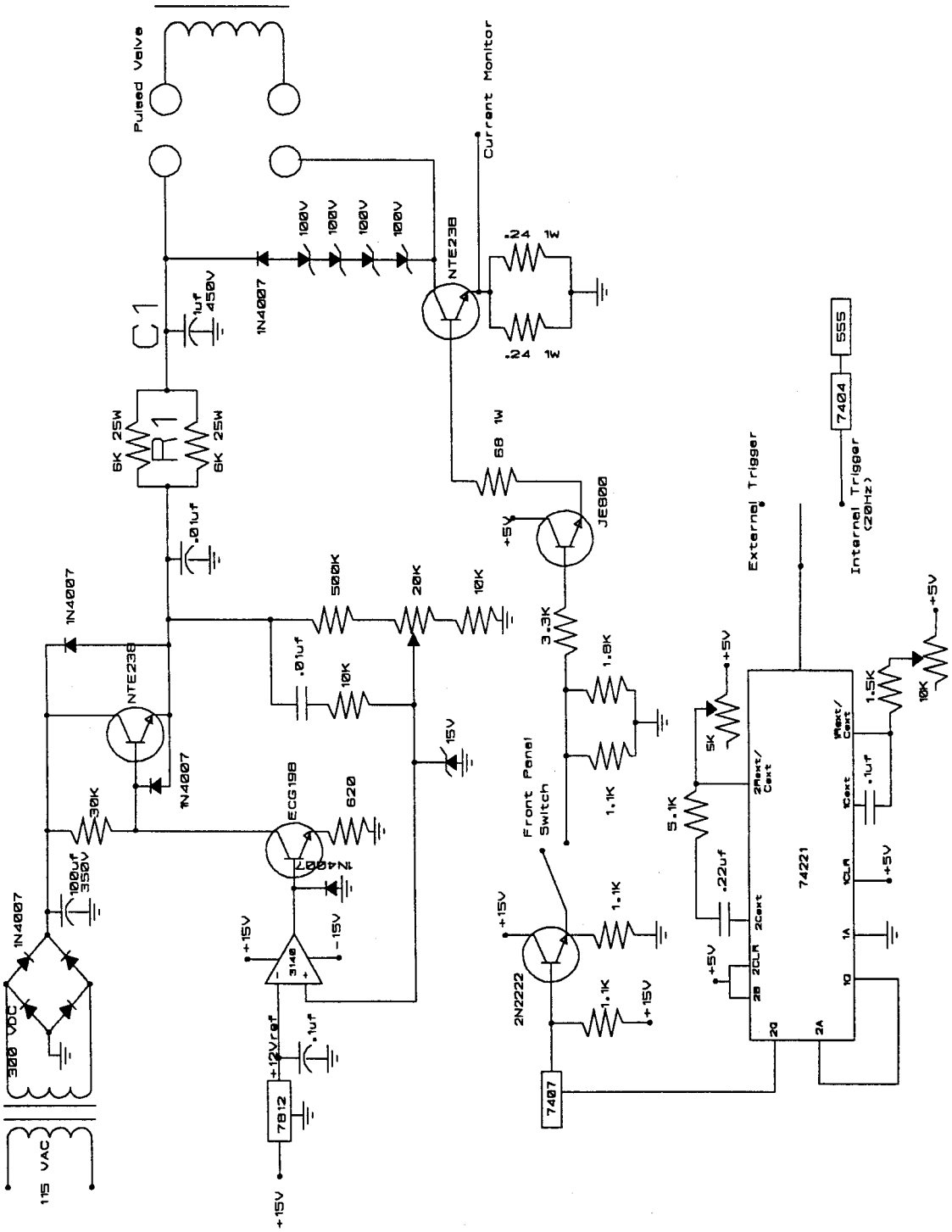
Pulsed Valve
Current Monitor
C1
1uf 450V
1N4007
100V
100V
100V
100V
NTE238
.24 1W
.24 1W
6K 25W
R1
6K 25W
.01uf
68 1W
JE800
+5V
500K
20K
10K
3.3K
1.8K
1.1K
.01uf
10K
15V
1N4007
NTE238
1N4007
30K
ECG198
620
Z4007
100uf 350V
1N4007
300 VDC
115 VAC
+15V
-15V
3140
+12Vref
.1uf
7812
+15V
Front Panel Switch
+15V
2N2222
1.1K
1.1K
+15V
External Trigger
7404
555
Internal Trigger (20Hz)
+5V
5K
5.1K
.22uf
+5V
+5V
2Next/Cent
2Cent
2CLR
2B
2Q
74221
1Q
1A
1CLR
1Cent
1Next/Cent
.1uf
+5V
1.5K
10K
+5V
7407

Figure 7.

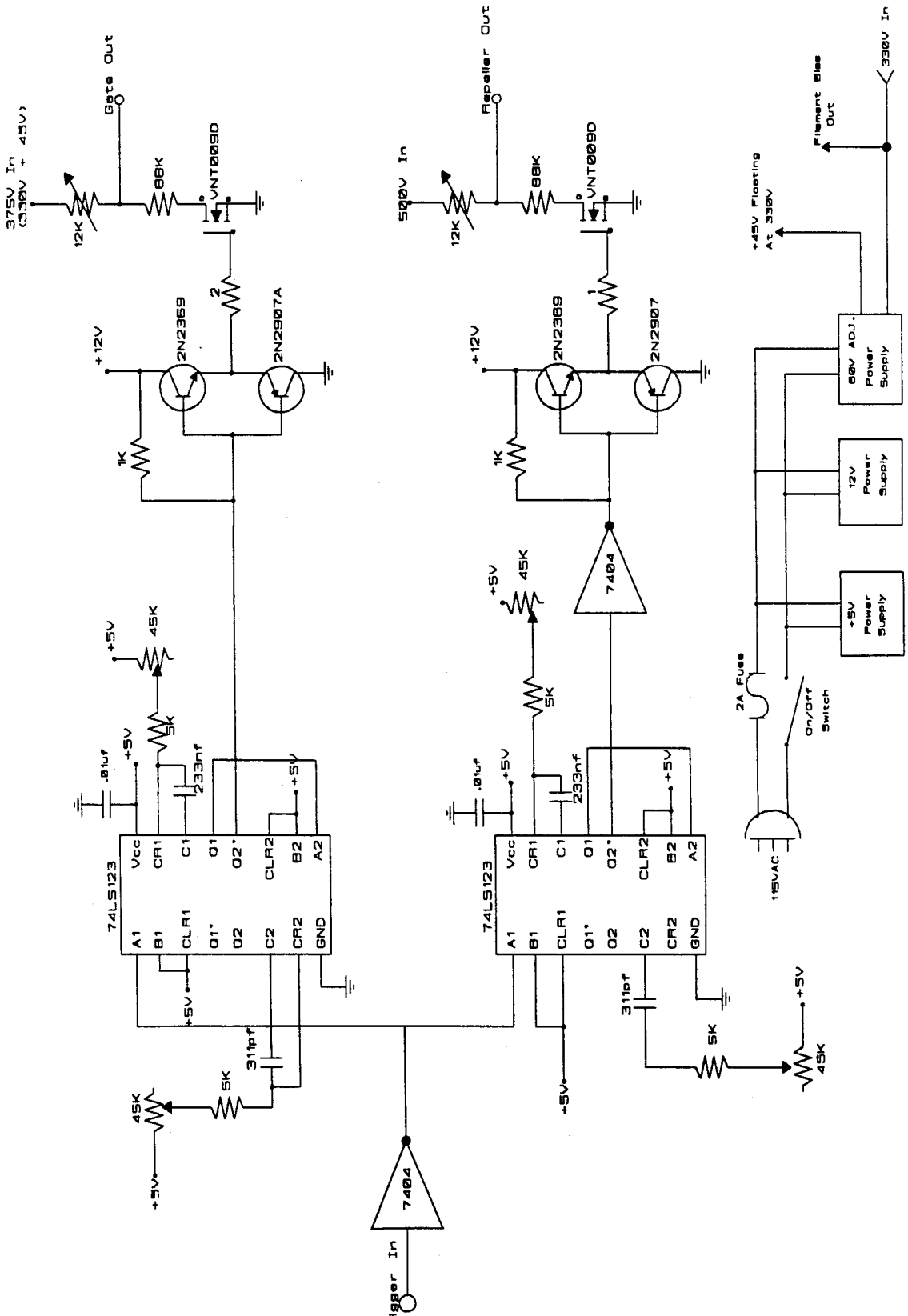
375V In
(330V + 45V)
Gate Out
12K
88K
VNT009D
2
+12V
2N2369
2N2907A
1K
+5V
45K
5K
.01uf
233nf
74LS123
Vcc
CR1
C1
Q1
Q2'
CLR2
B2
A2
A1
B1
CLR1
Q1'
Q2
C2
CR2
GND
311pf
7404
Trigger In
500V In
Repeller Out
1
2N2907
+45V Floating
At 330V
Filament Bias
Out
330V In
60V ADJ.
Power
Supply
12V
Power
Supply
+5V
Power
Supply
2A Fuse
On/Off
Switch
115VAC

Figure 8.

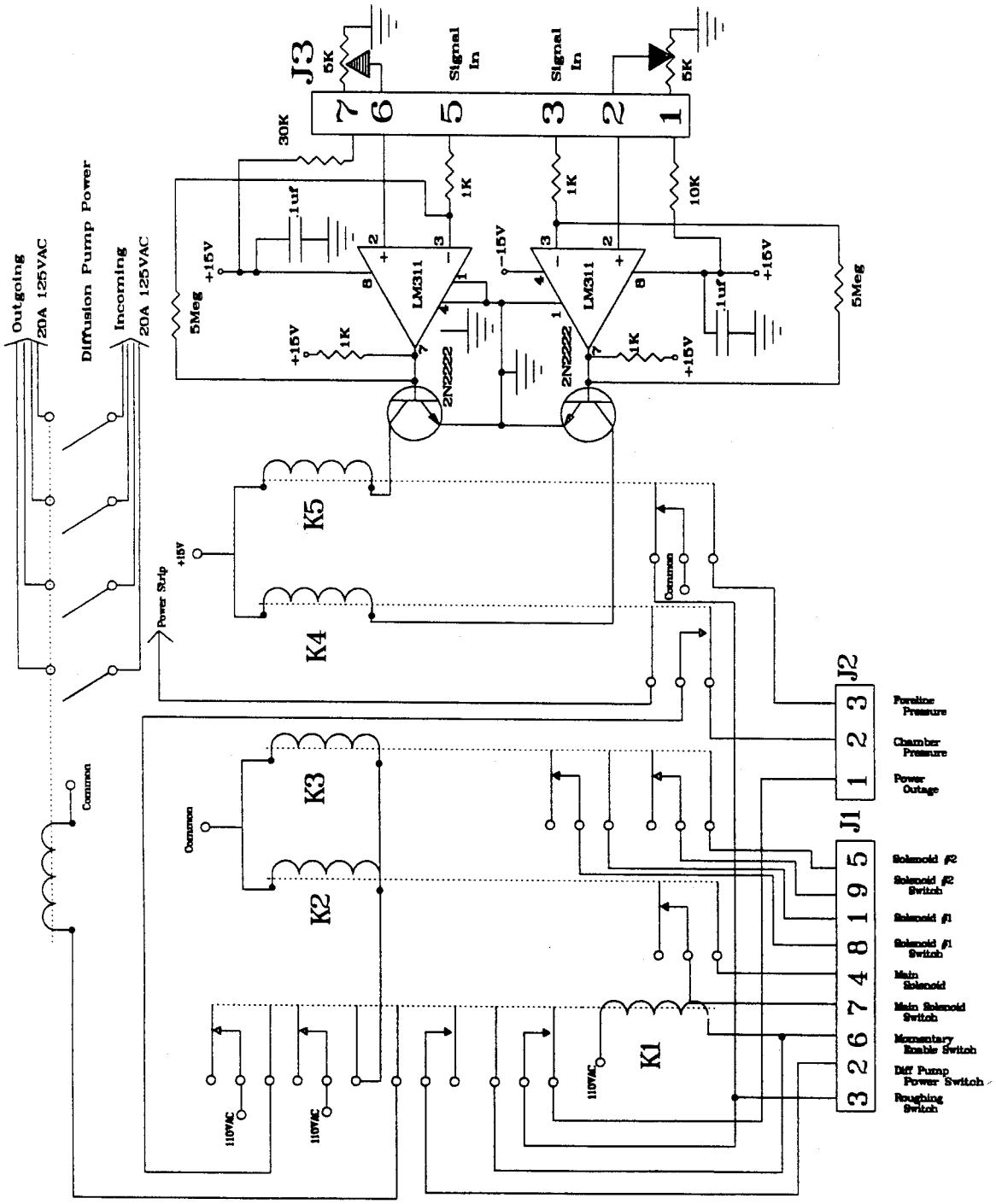
J3
5K
Signal In
Signal In
5K
7 6 5 3 2 1
30K
1K
1K
10K
1uf
+15V
-15V
LM311
LM311
5Meg
5Meg
1K
1K
2N2222
2N2222
1uf
+15V
+15V
Outgoing
20A 125VAC
Diffusion Pump Power
Incoming
20A 125VAC
K5
K4
K3
K2
K1
Power Strip
Common
Common
Common
110VAC
110VAC
110VAC
J2
3 2 1
Foreline Pressure
Chamber Pressure
Power Outage
J1
5 9 1 8 4 7 6 2 3
Solenoid #2
Solenoid #2 Switch
Solenoid #1
Solenoid #1 Switch
Main Solenoid
Main Solenoid Switch
Momentary Enable Switch
Diff Pump Power Switch
Roughing Switch

Figure 9.

Chapter 3

Femtosecond Reaction Dynamics in Macroclusters--
Effect of Solvation on Wavepacket Dynamics

3.1. Introduction

Reaction dynamics in macroclusters offer an opportunity to study solute-solvent interactions in a confined environment, potentially bridging the gap between isolated systems and the condensed phase. These types of clusters have both microscopic and macroscopic properties which have been studied as a function of size and composition [for review, see Ref.1]. On the femtosecond time scale it should be possible to examine the elementary motions of reactions [for a review, see Ref. 2] in these clusters and to elucidate the effect of the solvent shells and compositions on the wavepacket motion. As demonstrated by the Lineberger group[3] size-selected clusters of negative ions can be studied on the picosecond time scale to examine the caging phenomena. With femtosecond resolution, the early time behavior can be followed and contrasted with the dynamics of the reaction under collisionless conditions.

In this paper, we present our first study of the femtosecond dynamics of I_2 dissociation and recombination (caging) within macroclusters of argon. We present results for isolated I_2 wave packet motion and the dynamics in various sized clusters. Time scales for dissociation and subsequent caging are directly observed. Based on electron diffraction data of pure argon clusters, the average size of the clusters studied here is in the range of ten to seventy atoms, depending on the pressure[4] (this translates to a cluster diameter on the order of 20 Å). Extensive molecular dynamics simulations were performed for comparison with experimental results. These simulations, which are similar in nature to those of Berne, Amar, and Stace,[5] illustrate the changes in temperature, size, and energy of the clusters as well as the time scales for dissociation, caging, and vibrational relaxation. Fig. 1 presents a simulated cluster of I_2 surrounded by 44 argon atoms, together with the potential curves for isolated I_2.

Molecular iodine serves as a prototypical system in studies of ultrafast dynamics for a number of reasons. The femtosecond dynamics of I_2 have been studied in a gas cell, and in a molecular beam.[6] Also, the dynamics of the isolated molecules have been

contrasted with those of high-pressure gases,[7] and in clusters with one or few rare-gas atoms.[8] In addition, earlier studies have examined the process of caging, at very high pressures,[9] in liquids,[10] in matrices,[11] and more recently, of predissociation in liquids.[10e] The attractiveness of iodine as a solute lies in its "simplicity" as a diatomic molecule and in the characterization of its potential energy curves.[12]

In the present studies, I_2 is excited to either the B ($^3\Pi_{0^+u}$) state or the $^1\Pi_{1u}$ state and the dynamics are followed by LIF (see Fig. 1 for the pertinent potential energy curves). The fluorescence at 400 nm has been assigned as D' ($^3\Pi_{2g}$) $\rightarrow$ A' ($^3\Pi_{2u}$) by Heaven and Tellinghuisen[13] in their spectroscopic work on large $I_2 \cdot (Ar)_n$ clusters. In isolated I_2, this transition yields 340 nm emission; however, when I_2 is solvated by sufficient argon atoms, the ion-pair states are stabilized relative to the valence states such that the emission shifts toward 400 nm.[13] Thus, we are able to monitor the dynamics of large clusters by detecting fluorescence at 400 nm, and dynamics of smaller clusters by detecting fluorescence at 340 nm. This type of spectroscopic selection is in contrast to the mass selection used in the studies of $I_2^- \cdot (CO_2)_n$ (n = 1 to 17).[3] Since the clusters examined here are neutral, a method involving mass selection is not possible with conventional techniques.

Our goal here is to study the dynamics of I_2, particularly in the large cluster limit, in order to examine the processes of exiting the solvent cage and of recombination (caging) of the separated iodine atoms. Comparison with one atom predissociation[8] and one-atom caging[14] is of interest.

3.2 Experimental

The results presented here were taken under the following conditions: The pump pulse was centered at 510 nm or 490 nm (output of the continuum, subsequently amplified with the 355 nm light), the probe pulse at 308 nm. The pulse width of our initially generated femtosecond pulse is ~100 fs (using R610 in the Satori with DODCI as the

saturable absorber) and in these experiments, after amplification and continuum generation, the overall response function of the system was ~300 fs (FWHM). This was routinely measured by obtaining a transient of pure I_2 (see Fig. 2a for an example). The rise time and depth of modulation reflects the duration of the pulses. The expansion consisted of pure Ar held at 0.6-1.6 atm flowing through a room-temperature sample of I_2 (vapor pressure ~0.33 torr). The emission was monitored at 340 nm or 400 nm. The bandwidth of the monochromator was 32 nm for the transients shown. Narrowing the slits to improve the spectral resolution of the monochromator to 16 nm did not noticeably change the results presented, however the S/N ratio was adversely affected. All transients shown are the result of averaging at least 25 scans.

3.3 Results and Discussion

Two types of experiments were performed. In order to investigate the nature of the species found in the molecular beam, the cluster is excited via the pump beam, followed by the probe beam hundreds of femtoseconds later. The emission is then dispersed and the monochromator scanned. This dispersed fluorescence spectra allows one to measure the pump and probe wavelengths as a result of elastic scattering, as well as emission from the species of interest. The second type of experiment generally performed is a transient, where the time delay between the pump and probe beam is scanned while the monochromator is placed atop a single emission peak.

3.3.1 Dispersed Fluorescence Spectra

Figure 2 presents illustrative spectra under different expansion conditions. The conditions for the three traces are: a) 1.6 atm argon, b) 0.6 atm argon, c) 1 atm helium (the resolution of the monochromator was 16 nm for the argon scans and 8 nm for the helium scan). In general, there are three well-separated broad peaks in these spectra which are due to both the pump and probe and require the pump to proceed the probe (the peak at 308 nm is merely the scatter of the probe beam and is found in all scans). One of

these peaks, seen only in the helium scan, is centered around 280 nm; this emission can be assigned to ion-pair emission from isolated I_2. The other two peaks--at 340 nm and at 400 nm--are due to $D' \rightarrow A'$ emission of I_2 as discussed above. In helium and low pressure argon, only the 340 nm peak is observed. In higher pressure argon, the 400 nm emission intensity increases at the expense of the 340 nm emission. These effects support the assignment that the redder emission is due to I_2 in large argon clusters, and that the cluster size is increasing with increased backing pressure.

3.3.2 Exit-Channel: Dissociation and Evaporation

Shown in Fig. 3a is a transient of I_2 expanded in ~1 atm helium. Helium does not cluster effectively with I_2 under these conditions,[16] therefore these data represent the nuclear dynamics of isolated I_2.[6] A wavepacket is prepared on the B state of I_2 (see Fig. 1) with the 510 nm pump pulse. The excited state motion is subsequently detected via a probe pulse transferring the packet to an ion-pair state which undergoes relaxation to the lowest-lying ion-pair state, D'. The D' state emits to the A' state at ~340 nm. Due to the preferential absorption of the probe pulse at the inner turning point of the B state, the signal is modulated at the period of the specific vibrational state(s) initially excited.[6] The oscillations persist for >5 ps, indicating that the initially prepared wavepacket dephases slowly compared to the vibrational period. Furthermore, even after dephasing, the packet rephases and the system remains in the B state for times greater than 100 ps.

Shown in Fig. 3b is the same scan taken with ~1 atm of argon instead of helium. In contrast to helium, argon clusters very effectively under these conditions. In fact, as mentioned above, the average cluster size is estimated to be ~30 argon atoms at this pressure.[4] Thus, the dynamics observed are those of an I_2 molecule solvated by a significant number of argon atoms (Heaven *et al.* showed that large cluster fluorescence is not due to secondary collisions in the expansion but rather from clusters formed prior to excitation[13]). The difference between the two transients is striking. First, there is no

evidence of oscillation on the signal, this suggests that the argon solvation effectively dephases the system on a time scale shorter than our response function. The mechanism for such dephasing is the frequent "collisions" with the surrounding solvent, indeed similar to that which occurs at high pressures.[7]

Second, the signal decays on a ~12 ps time scale indicating that the excited-state I_2 is disappearing. The mechanism for this effect must be I_2 dissociation. It is possible that due to the interactions with the solvent, energy transfer might relax the I_2 molecule, thereby taking it out of our probe window. However, experiments on isolated I_2 with a range of pump energies (620 nm to 490 nm) show no significant change in signal intensity. Thus, with vibrational excitation in the *B* state, the probe pulse still effectively transfers population to the ion-pair states. This result is not surprising, since the probe pulse has a large bandwidth and there are a number of energetically-accessible ion-pair states. The separated iodine atoms, however, do not lead to LIF at these wavelengths.

As shown in Fig. 1, there is a crossing between the repulsive $^1\Pi_{1u}$ curve and the bound *B* state. With one argon atom in a van der Waals complex with I_2, electronic predissociation is significant with a rate of $(2 \times 77 \text{ ps})^{-1}$ (for $v' = 21$)[8] and a yield of 50%.[16,17] The breakage of the I_2 by electronic predissociation is described by a non-adiabatic coupling between the potentials. The presence of an argon atom lowers the effective symmetry and the coupling is estimated to be ~400 cm^{-1} [Ref. 8]. In an argon cluster, the coupling is a dynamical effect. Molecules with different energies on the *B* state experience different effective coupling to the $^1\Pi_{1u}$ state (proportional to $V^2/\Delta E$, where V is the non-adiabatic matrix element and ΔE is the energy separation of the two potential energy surfaces at a given internuclear distance[14b]). Hence, the solute-solvent interaction, which leads to vibrational relaxation on the *B* state, determines the rate of electronic predissociation. Molecules at the crossing region can break the bond very effectively as $\Delta E \rightarrow 0$.

The van der Waals bonds of the argon cluster are much weaker than the total energy that is released, so, in principle, evaporation of some argon atoms can take place.[5] This could be reflected in the initial decay, provided the "evaporated clusters" have enough spectral shift to take them out of the probe window. For large clusters, evaporation is rather slow, and the initial decay measures the exit channel rate for $I_2 \rightarrow 2I$ through vibrational relaxation/electronic predissociation. The same conclusions were reached in the studies of the femtosecond dynamics in dilute solution of argon[7] and are further supported by the dynamical calculations given below.

It should be noted that at 510 nm, ~20% of the molecules are excited directly to the dissociative $^1\Pi_{1u}$ state,[12] which of course would also lead to a decay in the signal. In the absence of solvent molecules, such a decay occurs in less than 1 ps.[6] In the presence of a solvent shell, however, even this process could take considerable time as pointed out by Alimi *et al.* in the work on the cage exit effect of Cl_2 in argon matrices.[18] One should note, however, that in a matrix there is an energy barrier in the exit channel (due to the repulsion between the solute and the blocking rare gas atoms) and the atomic yield depends crucially on the total energy available, as demonstrated for Cl_2/Ar by Chergui and Schwentner.[18]

For clusters the picture is different. As isolated iodine atoms separate, some of the energy is transferred into translational energy of the solvent shell. Because the cluster is finite in size and "flexible" (finite temperature) the hot atoms can escape and be replaced by solvent argon atoms. If they recombine again the motion must involve the solvent, and our transients should recover again as the I_2 bond is formed.

3.3.3 Recombination: Caging and Bond Formation

The transients taken at 400 nm show a recovery of signal as the time delay between pump and probe is increased beyond the time scale of the decay discussed above. Shown in Fig. 4 are three such transients with varying backing pressure. This rise in signal

must ultimately be attributed to the recombination of the iodine atoms to reform molecular iodine. As discussed above, because of the total energy, the recombination cannot lead to *B* state I_2. As the two iodine atoms release their translational energy, there are available states upon which the iodine atoms can recombine, namely the *A*, *A*' or *X* states (see Fig. 1). These states have allowed transitions into ion-pair states.[12] It is therefore consistent that *A* or *A*' state I_2 is within our probe window, leading to a recovery in the overall signal intensity. The issue, however, is why this recombination occurs so slowly (25 ps to 60 ps).

Our simulations, discussed below, suggest that the actual recombination occurs faster than the experimentally measured rise time. The slow rise indicates that in the process of recombination, vibrational relaxation may be involved on the *A*, *A*' or the *X*-state surface, in analogy to the case in liquids.[10b,c,d] Diffusion of the two iodine atoms within a large cluster until they encounter one another, cannot be ignored. If the initial dissociation of the iodine atoms leads to a large internuclear separation of the iodine atoms, then one or more argon atoms can intercalate.

The energy transferred to the van der Waals modes should make the cluster "molten," allowing not only the possibility of large internuclear separation of the iodine atoms but also facilitating the motion of the argon atoms into a position between the separated iodine atoms. Our simulations verify that indeed, from such a configuration, the time scale for recombination is commensurate with the experimentally observed rates. These two mechanisms are not exclusive of one another. It is possible that both mechanisms are responsible for the rise in signal. We have simulated the overall kinetics of these processes (i.e., dissociation with a time constant τ_1 and recombination with time constant τ_2 in a consecutive process). The kinetic model was not entirely appropriate for fitting the data and we noticed deviations, particularly at high pressures. In fact, better agreement (at higher pressures) could be obtained if we allow some delay (~10 ps) prior to the rising component of the signal. Such a mechanism would imply a coherent

propagation of the system up until recombination; given the number of degrees of freedom and the time scales involved, this interpretation appears unlikely. Rather, a kinetic model, involving numerous processes with many different rates would probably fit the data more adequately, but not improve the overall understanding of the experiment. Molecular dynamics simulations (section 3.3.4) deal with these points in detail and also discuss the non-adiabatic effects in the recombination process which can lead to slower recombination times.

The kinetic model used to fit these data, albeit simplified, does lead to the interpretation given here and is believed to illustrate the salient features of the overall reaction mechanism. The basis of the model is the reaction $A \xrightarrow{k_1} B \xrightarrow{k_2} C$, where the probe window includes both A and C. The appropriate differential equations and solutions follows:

$$\begin{aligned} \frac{d[A]}{dt} &= -k_1[A] \\ \frac{d[B]}{dt} &= k_1[A] - k_2[B] \\ \frac{d[C]}{dt} &= k_2[B]. \end{aligned} \tag{3.1}$$

The solutions of which, under the initial conditions $[A](0) = A_O$, $[B](0) = 0$, and $[C](0) = 0$, are:

$$\begin{aligned} A(t) &= A_o e^{-k_1 t} \\ B(t) &= A_o\left(\frac{k_1}{k_1 - k_2}e^{-k_2 t} + \frac{k_1}{k_2 - k_1}e^{-k_1 t}\right) \\ C(t) &= A_o\left(1 + \frac{k_2}{k_1 - k_2}e^{-k_1 t} + \frac{k_1}{k_2 - k_1}e^{-k_2 t}\right). \end{aligned} \tag{3.2}$$

Assuming that both A and C are within the probe window--allowing for different absorptivities--the observed signal is:

$$S(t) = c_1 A(t) + c_2 C(t). \tag{3.3}$$

This is the equation to which the data was fit using a non-linear least squares fitting routine.

Fig. 4 also illustrates the effect backing pressure has on the measured time constants. As the pressure is increased, τ_1 does not significantly change, however, τ_2 becomes faster. The increased pressure should have two effects on the expansion. First, the average cluster size should increase. Second, the cooling within the cluster should be enhanced at higher pressures. A warmer cluster could allow larger internuclear separation of the dissociating I_2, thereby requiring more time for diffusion of the separated iodine atoms to recombine. On the other hand, a relatively smaller cluster would increase the rate at which the diffusing iodine atoms would encounter one another.

3.3.4 Molecular Dynamics

In order to better quantify the results, we have done simulations of the dynamics of I_2 within macroclusters. The simulations begin with a given number of argon atoms (17, 44, 71) at positions similar to those corresponding to the pure argon clusters determined by electron diffraction.[4] The iodine atoms occupy two "would be" argon sites. Lennard-Jones potentials are used to describe the Ar-Ar interactions and the Ar-I interactions. Morse potentials are used for the states of I_2 (*B*, *A*, *A'*, and *X* states). The $C \cdot R^{-9}$ function is used for the $^1\Pi_{1u}$ state as suggested by Tellinghuisen.[12] All of the parameters for these potentials are given in Table I.

The trajectories consist of time integrations of Hamilton's equations. A fourth-order Runge-Kutta algorithm with a step controller to monitor accuracy is used for these integrations. The atoms are initially assigned a random velocity from a Gaussian-distribution-weighted random-number generator consistent with the cluster temperature (~30 K).[4] The system is allowed to relax for a couple of picoseconds with I_2 kept in the *X* state. The temperature (average kinetic energy) of the cluster is monitored every

picosecond and was used to adjust the velocity of the molecules so that the final temperature is within 20% of the initially assigned temperature. Then the pump energy places the iodine molecule onto the *B* state. The clock is reset to zero. The integration continues until the excess vibrational energy is transferred to the cluster such that the I_2 molecule is found at the point where the *B* state crosses the $^1\Pi_{1u}$ state (this point is approximately 2.9 Å with a potential energy of ~3500 cm^{-1}). The trajectory then switches to the $^1\Pi_{1u}$ state. When the two iodine atoms reach a separation >5 Å, we assume the system is now free to recombine along the *A* or *A'* state. Once the system reaches small separations and loses sufficient energy, it is assumed to be stable and the integration is stopped (more sophisticated simulations are currently underway, and can be found in future publications).

In considering the coupling between the *B* state and the repulsive $^1\Pi_{1u}$ potential, we have assumed the probability is unity at the crossing point and zero everywhere else. The probability for crossing to the $^1\Pi_{1u}$ state is of course a function of distance or energy with the maximum at the crossing point and we have not considered this distribution yet. This assumption is apt to give a shorter time scale for the dissociation. A break down of the Born-Oppenheimer approximation would also allow a coupling between the *B* state and the $^1\Pi_{1u}$ state at any energy and would not necessarily require vibrational relaxation on the *B* state prior to coupling. Despite these simplifications, however, the time scales calculated in this manner agree reasonably well with the experimental results.

Fig. 5 shows one typical trajectory with 44 argon atoms. The first panel shows the I-I internuclear separation. This trajectory takes ~10 ps to switch onto the $^1\Pi_{1u}$ state, after which the separation increases rapidly to ~5.4 Å. In this large cluster, the iodine atoms recombine as rapidly as they dissociate. After a mere 15 ps, the entire event is complete. The inset shows the vibration of the *B* state molecule prior to coupling onto the $^1\Pi_{1u}$ state. If a segment after recombination was similarly examined, the system would be seen to vibrate within the *A* or *A'* state potential. The second panel shows, that despite the

fact that the iodine recombination occurred very rapidly, the cluster is still evaporating argon atoms for some 100 ps later. An argon atom is assumed to be separated from the cluster it if reaches a radius of 15 Å from the center of mass. An important point to note is that the large cluster has lost more than 50% of the argon atoms in 100 ps. This point will be used below to explain the transients taken with a detection wavelength of 340 nm for smaller clusters.

The third panel shows the energy in the I_2 molecule. The zero is arbitrarily set to the energy of two free iodine atoms in their ground state. The recombination of the two iodine atoms is accompanied by a decrease in the I_2 energy below zero to a stable configuration. The time associated with the relaxation of vibrationally-hot *A* state I_2 to the bottom of the well is quite short. This is significant, since the relaxation mechanism discussed above (used to explain the slow rise in signal) cannot be due merely to "dark" vibrationally-hot *A* state molecules decaying into "bright" vibrationally-cold *A* state molecules. The temperature of the cluster (panel 4) is still high, and therefore justifies the continued loss of argon atoms from the cluster as seen in panel 2; the Ar-Ar van der Waals bond is only ~30 cm^{-1}. We have taken the recombination as a simple adiabatic process with a probability of unity at the critical internuclear distance. If the probability is less than one and non-adiabatic effects are important, the recombination time may become longer. This point will be examined in future simulations.

3.3.5 Smaller Clusters

Table II summarizes all of the measured time constants at various pressures with detection wavelengths of 340 nm and 400 nm. Fig. 6 shows a transient taken at 340 nm detection along with corresponding molecular simulations for $I_2 \cdot (Ar)_{17}$. Considering τ_1 first, the rate at which the I_2 is lost increases as the pressure is increased (detection at 340 nm). The kinetic model for this rate constant is similar to the scheme presented above except that the probe window includes only small clusters ($n<17$). Using the cluster size

vs. pressure relationships given by Farges *et al.*,[4] one could assume that at the lowest pressure used here, the average cluster size consists of ~10 argon atoms. The first solvent shell consists of ~17 argon atoms. With this in mind, one expects that as the pressure is increased, the average cluster size increases from ~10 argon atoms to ~70 argon atoms. This causes the effective coupling of the *B* state to the $^1\Pi_{1u}$ state to become stronger with the increased solvation. The coupling has been discussed at length in several papers with regard to the one-atom cage effect seen in $I_2 \cdot Ar$.[14] After a certain point (probably around ~17 argon atoms), this effect will level off because the addition of more solvent atoms will not perturb the I_2 to any greater extent. In fact, the time constant measured at the highest pressure while detecting at 340 nm is similar to the rate constant measured while detecting at 400 nm (which is not sensitive to pressure), consistent with the above discussion regarding the large clusters. These trends are in contrast to the cage exit effect mentioned above for dynamics in matrices.[18] In matrices, the dissociating iodine atoms would encounter an ever increasing "barrier" as the number of solvent molecules is increased. Thus, the rate for dissociation should decrease as the pressure is increased.

The other important point to make about these results is the relative importance of the electronic predissociation rate and the evaporation rate. For example, these processes, for 3 argon atoms, can be viewed as follows:

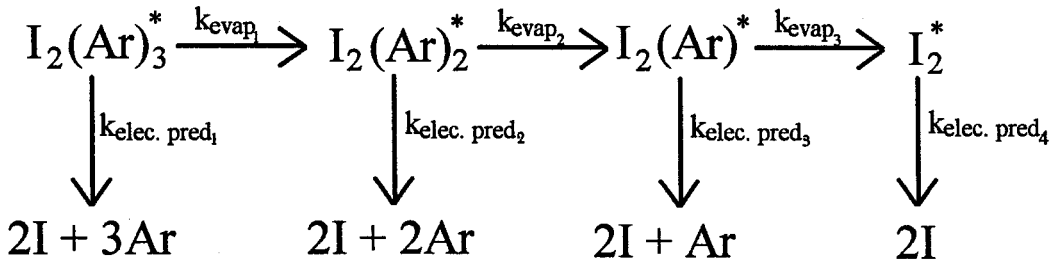

The experimentally measured rate constant τ_1, using this simplified model, would be multiexponential if we detected all of the bound species. One rate constant would equal

the sum of $k_{evap_1} + k_{elec.\ pred._1}$ and the second would equal $k_{evap_2} + k_{elec.\ pred._2}$ and so on. As the model is expanded to include still larger clusters (still capable of emitting at 340 nm) the decay of the signal will be ever more complicated. If on the other hand, one assumes all evaporation rates are essentially equal and likewise all electronic predissociation rates are equal then the measured decay would be "single" exponential. One would expect the evaporation rate to slow down as the cluster size is increased (based on statistical arguments), therefore, it appears that the first rate constant is dominated by the electronic predissociation process. Further experiments may shed some light on this step by lowering the pump energy such that system begins its trajectory closer to the crossing point of the *B* state and the $^1\Pi_{1u}$ state.

Considering τ_2, the pressure dependence of this rate constant is observed to be different depending upon whether the detection wavelength is 340 nm (small clusters) or 400 nm (large clusters). As the cluster size is increased from around 10 atoms to around 40 atoms, the separated iodine atoms are likely to find an increased volume in which to diffuse, thereby increasing the time scale for recombination. Beyond a certain point, however, the temperature of the cluster plays a more important role. A colder cluster would be more "crystalline" and would not allow the iodine internuclear separation to become very large; therefore, the time for recombination would likewise be shorter. Without further experiments it is difficult to be more than conjectory on this point.

An additional process must be considered for the transients taken when monitoring at 340 nm. The rise in signal is probably predominately reflecting the rate at which larger clusters, initially outside of the probe window, are evaporating sufficient argon atoms to enter the probe window. Our simulations of $I_2 \cdot (Ar)_{44}$ (Fig. 4 panel 2) indicate that indeed large clusters evaporate solvent atoms on a relatively slow time scale such that the transients taken with 340 nm detection should reflect this slow rate of evaporation.

Fig. 7 shows a simulation of evaporating clusters vs. time. The top panel starts with a cluster of 44 argon atoms. At 30 ps the I_2 molecule has dissociated and the cluster

still consists of ~42 argon atoms. By 60 ps the I_2 has reformed and the cluster size is difficult to assign since many of the solvent molecules are at large separations from the center of mass and are moving away. The time scales for evaporation of enough argon atoms to enter the probe window at 340 nm detection is consistent with our results. The lower panel illustrates the same effect for a starting cluster of only 17 argon atoms. In this case, after 60 ps, the cluster consists of perhaps only 3 solvent molecules surrounding the I_2 molecule. Based on these types of simulations, a conventional kinetic model is not entirely appropriate, however, it does provide a framework from which to discuss the trends observed. The molecular dynamics are very illustrative of the different steps and the pathways of the initially prepared wave packet.

Further studies at different energies and with other solvents, which cluster more strongly, might lead to further insights into this general problem of solute-solvent interactions, and to the primary changes in energetics and structure on their femtosecond-picosecond time scales.

Table I. Potential parameters used in the molecular dynamics simulations.

Lennard-Jones Parameters: $V(r) = 4D[(\sigma/r)^{12}-(\sigma/r)^{6}]$

	D (cm^{-1})	σ (Å)
Ar-Ar	84	3.40
Ar-I	209.7	3.59

Morse Parameters: $V(r) = D[\exp(-2\beta(r-r_e)) - 2\exp(-\beta(r-r_e))] + C$

States	D (cm^{-1})	r_e (Å)	β ($Å^{-1}$)	C (cm^{-1})
X	12547.2	2.656	1.875	0
A'	2506.0	3.073	1.608	0
A	1640.0	3.1	1.608	0
B	4381.8	3.03	1.75	7605.0

These values were taken from references 5 and 12.

Table II. Pressure dependance of the time constants fit to the experimental data in argon clusters[a] using a simple kinetic model A→B→C; where the probe window includes both A and C.

	340 nm detection		400 nm detection	
Pressure (atm)[b]	τ_1 (ps)	τ_2 (ps)	τ_1 (ps)	τ_2 (ps)
0.6	>40[c]			
0.9	23.4 ± 4.1[d]	36.9 ± 3.4	10.8 ± 4.2	64.8 ± 11.9
1.3	13.0 ± 4.2	58.2 ± 8.0	9.3 ± 4.4	33.9 ± 5.2
1.6	10.4 ± 3.4	50.8 ± 7.4	12.9 ± 8.5	22.0 ± 6.9

a) Values for τ_1 in helium were independent of pressure and equal to ~ 143 ps.
b) This pressure was measured with a baratron guage without further calibration.
c) This transient decayed to an asymptote of non-zero signal, and hence τ_2 could not be determined accurately.
d) The error bars given are 95% confidence limits from the nonlinear least squares fit.

3.4 References

1. a) J. Jortner, D. Scharf, N. Ben-Horin, U. Even, and U. Landman, in *Proceedings of the International School of Physics: The Chemical Physics of Atomic and Molecular Clusters*, edited by G. Scoles, North-Holland, New York (1990) p.43; b) R. S. Berry, *ibid* p.3; c) M. Kappes, and S. Leutwyler, in *Atomic and Molecular Beam Methods*, edited by G. Scoles, Oxford University Press, New York (1988) p.380.
2. A. H. Zewail, *Faraday Discuss. Chem. Soc.*, **91**, 207 (1991).
3. a) M. L. Alexander, N. E. Levinger, M. A. Johnson, D. Ray, W. C. Lineberger, *J. Chem. Phys.*, **88**, 6200 (1988); b) D. Ray, N. E. Levinger, J. M. Papanikolas, and W. C. Lineberger, *J. Chem. Phys.*, **91**, 6533 (1989); c) J. M. Papanikolas, J. R. Gord, N. E. Levinger, D. Ray, V. Vorsa, and W. C. Lineberger, *J. Phys. Chem.*, **95**, 8028 (1991); d) J. M Papanikolas, V. Vorsa, M. E. Nadal, P. J. Campagnola, J. R. Gord, W. C. Lineberger, Submitted for publication.
4. a) J. Farges, M. F. de Feraudy, B. Raoult, and G. Torchet, *J. Chem. Phys.*, **78**, 5067 (1983); b) J. Farges, M. F. de Feraudy, B. Raoult, and G. Torchet, *J. Chem Phys.*, **84**, 3491 (1986); c) O. F. Hagena, and W. Obert, *J. Chem. Phys.*, **56**, 1793 (1972).
5. a) F. G. Amar, and B. J. Berne, *J. Phys. Chem.*, **88**, 6720 (1984); b) J. N. Murrell, A. J. Stace, and R. Dammel, *J. Chem. Soc., Faraday Trans. 1*, **74**, 1532 (1978); c) A. J. Stace, *J. Chem. Soc. Farad. Trans. 2*, **75**, 2105 (1981); d) F. G. Amar, S. Weerasinghe, in *Proceedings of Quantum Chemistry Symposium*, edited by B. Pullman and J. Jortner, Kluwer Academic Publisher (1991).
6. a) R. M. Bowman, M. Dantus, and A. H. Zewail, *Chem. Phys. Lett.*, **161**, 297 (1989); b) M. Dantus, M. H. M. Janssen, and A. H. Zewail, *Chem. Phys. Lett.*, **181**, 281 (1991); c) M. Gruebele, and A. H. Zewail, *J. Chem. Phys.*--Submitted for publication.

7. a) Y. Yan, R. M. Whitnell, K. R. Wilson, and A. H. Zewail, *Chem. Phys. Lett.*, **193**, 402 (1992); b) A. H. Zewail, M. Dantus, R. M. Bowman, and A. Mokhtari, *J. Photochem. Photobiol. A: Chem.*, **62/3**, 301 (1992).

8. a) J. J. Breen, D. M. Willberg, and A. H. Zewail, *J. Chem. Phys.*, **93**, 9180 (1990); b) D. M. Willberg, M. Gutmann, J. J. Breen, and A. H. Zewail, *J. Chem. Phys.*, **96**, 198 (1992); c) M. Gutmann, D. M. Willberg, and A. H. Zewail, *J. Chem. Phys.*, in press.

9. J. Schroeder, and J. Troe, *Ann. Rev. Phys. Chem.*, **38**, 163 (1987).

10. a) T. J. Chuang, G. W. Hoffman, and K. B. Eisenthal, *Chem. Phys. Lett.*, **25**, 201 (1974); b) D. J. Nesbitt, J. T. Hynes, *J. Chem. Phys.*, 77, 2130 (1982); c) P. Bado, C. Pupuy, D. Magde, and K. Wilson, *J. Chem. Phys.*, **80**, 5531 (1984); d) A. L. Harris, J. K. Brown, and C. B. Harris, *Ann. Rev. Phys. Chem.*, **39**, 341 (1988), and references therein; e) N. F. Scherer, L. D. Zielgler, and G. R. Fleming, *J. Chem. Phys.*, **96**, 5544 (1992).

11. a) P. B. Beeken, E. A. Hanson, and G. W. Flynn, *J. Chem. Phys.*, **78**, 5892 (1983); b) M. Macler, and M. C. Heaven, *Chem. Phys.*, **151**, 219 (1991).

12. a) R. S. Mulliken, *J. Chem. Phys.*, **55**, 288, (1971); b) J. C. D. Brand, and A. R. Hoy, *Appl. Spect. Rev.*, **23**, 285 (1987); c) J. Tellinghuisen, *J. Chem. Phys.*, **76**, 4736 (1982); d) X. Zheng, S. Fei, M. C. Heaven, J. Tellinghuisen, *J. Chem. Phys.*, **96**, 4877 (1992); e) X. Zheng, S. Fei, M. C. Heaven, and J. Tellinghuisen, *J. Mol. Spectrosc.*, **149**, 399 (1991).

13. S. Fei, X. Zheng, M. C. Heaven, and J. Tellinghuisen, Submitted for publication.

14. a) J. J. Valentini and J. B. Cross, *J. Chem. Phys.*, 77, 572 (1982); b) J. A. Beswick, R. Monot, J.-M. Philippoz, and H. van den Bergh, *J. Chem. Phys.*, **86**, 3965 (1987); c) M. L. Burke and W. Klemperer, Submitted for publication.

15. I. R. Sims, M. Gruebele, E. D. Potter, and A. H. Zewail, *J. Chem. Phys.*, **97**, 4127 (1992).

16. a) R. E. Smalley, D. H. Levy, L. Wharton, *J. Chem. Phys.*, **64**, 3266 (1976); b) G. Kubiak, P. S. H. Fitch, L. Wharton, and D. H. Levy, *J. Chem. Phys.*, **68**, 4477 (1978); c) D. H. Levy, *Adv. Chem. Phys.*, **47**, part 1, 323 (1981).

17. N. Goldstein, T. L. Brack, and G. H. Atkinson, *J. Chem. Phys.*, **85**, 2684 (1986).

18. R. Alimi, R. B. Gerber, J. G. McCaffrey, H. Kunz, and N. Schwentner, *Phys. Rev. Lett.*, **69**, 856 (1992).

19. M. Chergui and N. Schwentner, in *Research Trends: Chemical Physics,* edited by J. Menon (Trirandum, India) 1992.

3.5 Figure Captions

1. Relevant potential energy curves of isolated I_2. A wavepacket is shown to represent the point at which our pump pulse prepares the system. The second panel shows a simulated cluster of 44 argon atoms surrounding I_2 (distances in Å). The radius of the iodine atoms is equal to the van der Waals radius. The radius of the the argon atoms are 1/4 the van der Waals radius, used in order to show the solvated I_2 molecule. The positions are those calculated in the manner described in the text (i.e., the system was allowed to relax from the electron diffraction positions, see text).
2. Dispersed fluorsecence spectra of I_2 in argon or helium: a) 1.6 atm argon, b) 0.6 atm argon, c) 1 atm helium. For traces a) and b) the monochromator resolution was 16 nm while trace c) was taken with 8 nm resolution.
3. Femtosecond transients of I_2 in the molecular beam. (a) Transient is obtained in ~1 atm. of helium. (b) Transient is obtained in ~1 atm. argon. The average signal level, for the helium scan decays with a time constant of ~143 ps, whereas the signal level for the argon scan decays appreciably in ~12 ps.
4. Femtosecond transients of I_2 taken with varying pressures of argon. The pump wavelength is 510 nm; the probe wavelength is 308 nm; and the detection wavelength is 400 nm. The pressures are: (A) 0.9 atm., (B) 1.3 atm., (C) 1.6 atm. All scans are normalized to one for ease of comparison.
5. Molecular dynamics results of a single trajectory for I_2 surrounded by 44 argon atoms. The details of this simulation are described in the text. The first panel shows the I-I internuclear separation vs. time. The second panel shows the cluster size vs. time. An argon atom is assumed to be separated from the cluster if its radius from the center of mass is >15 Å. The third panel shows the energy of the I_2 molecule vs. time. The zero is chosen as the energy of two isolated iodine atoms in their ground

der Waals bond energy for an Ar-Ar bond is ~30 cm^{-1}, evaporation continues to occur for at least 100 ps.

6. Femtosecond transients and molecular dynamics simulation for the smaller clusters (detection at 340 nm). The simulations shown are for I_2 surrounded by 17 argon atoms, which represents one solvent shell.

7. Snapshots of a simulated cluster at three different times. The top panel shows the dynamics for a cluster of 44 argon atoms and the bottom panel for 17 argon atoms surrounding I_2. These results illustrate the importance of evaporation, particularly in smaller clusters (see text).

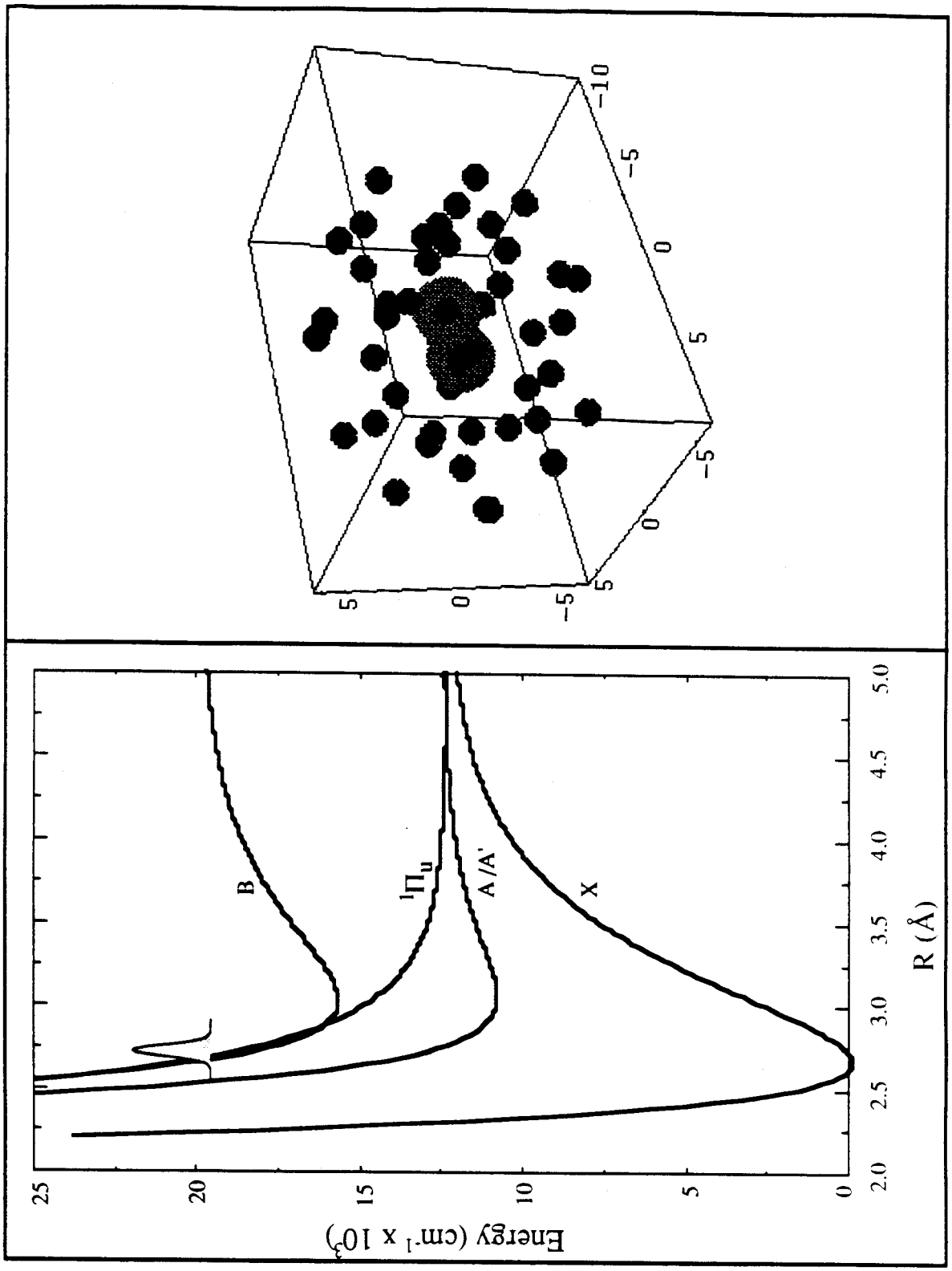
Energy (cm^{-1} x 10^3)
25
20
15
10
5
0
2.0
2.5
3.0
3.5
4.0
4.5
5.0
R (Å)
B
$^1\Pi_u$
A/A'
X
5
0
−5
5
0
−5
5
0
−5
−10

Figure 1.

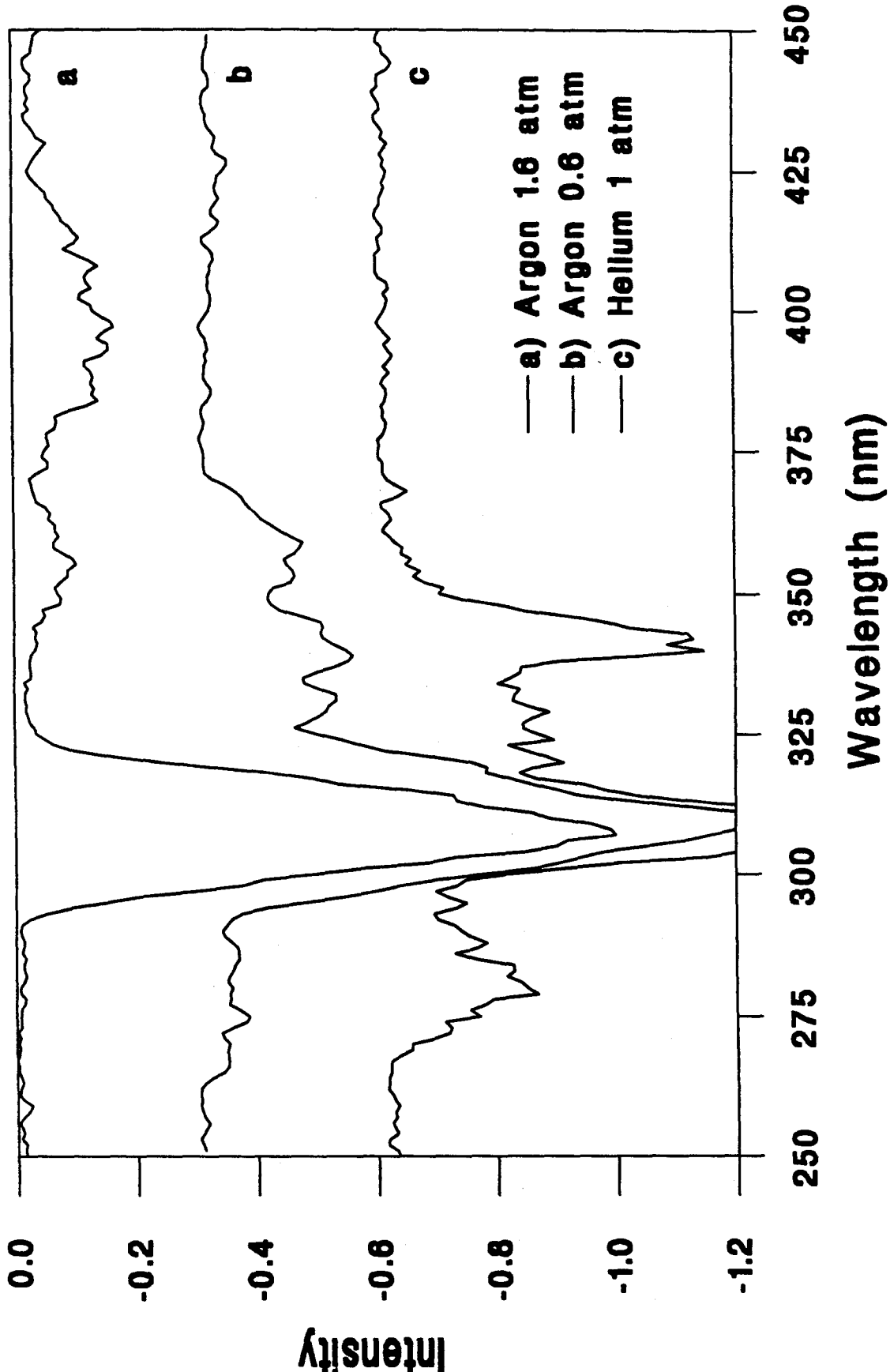
a
b
c
—a) Argon 1.6 atm
—b) Argon 0.8 atm
—c) Hellum 1 atm
Wavelength (nm)
250
275
300
325
350
375
400
425
450
Intensity
0.0
-0.2
-0.4
-0.6
-0.8
-1.0
-1.2

Figure 2.

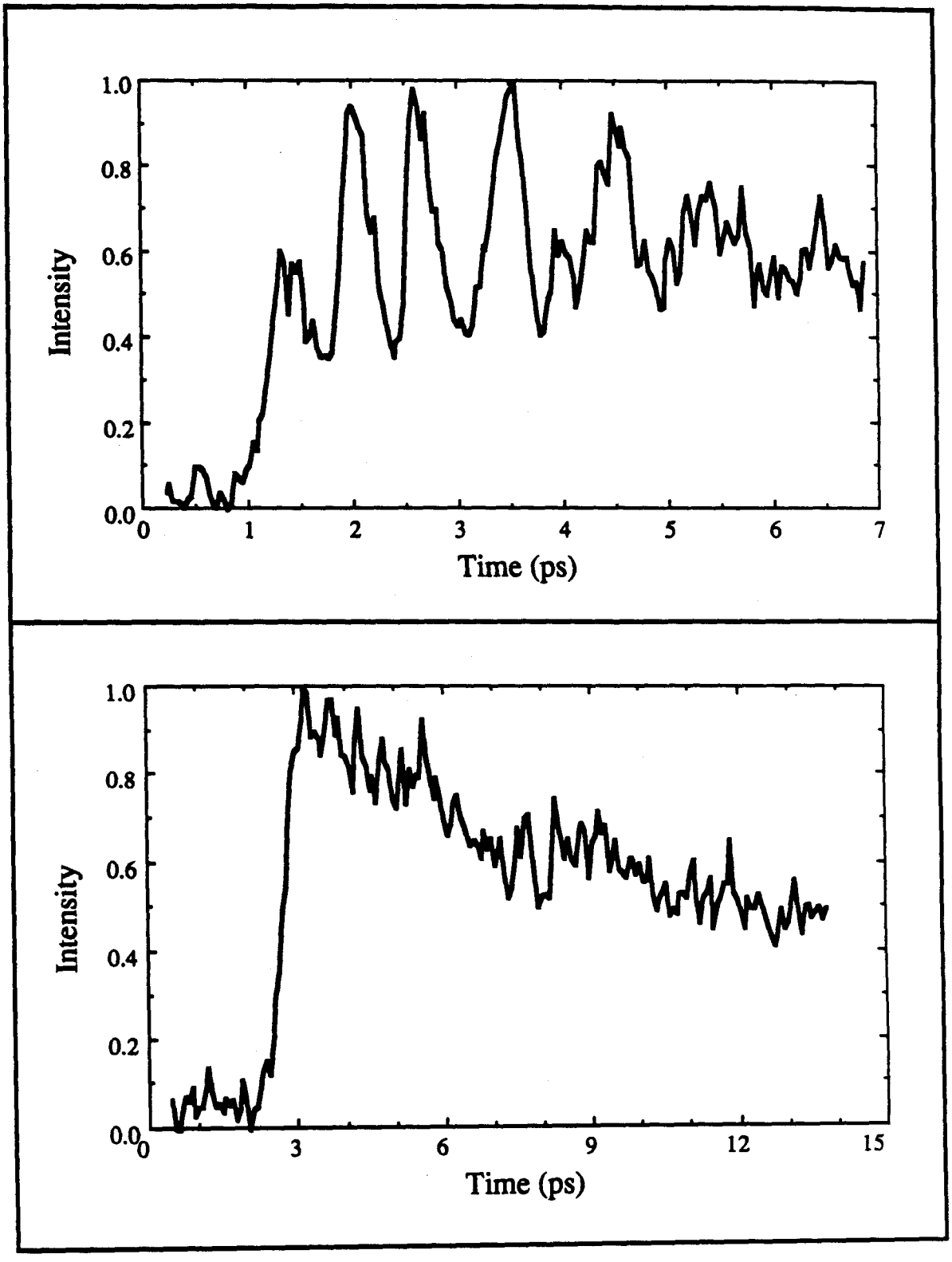
1.0
0.8
0.6
0.4
0.2
0.0
Intensity
0
1
2
3
4
5
6
7
Time (ps)
1.0
0.8
0.6
0.4
0.2
0.0
Intensity
0
3
6
9
12
15
Time (ps)

Figure 3.

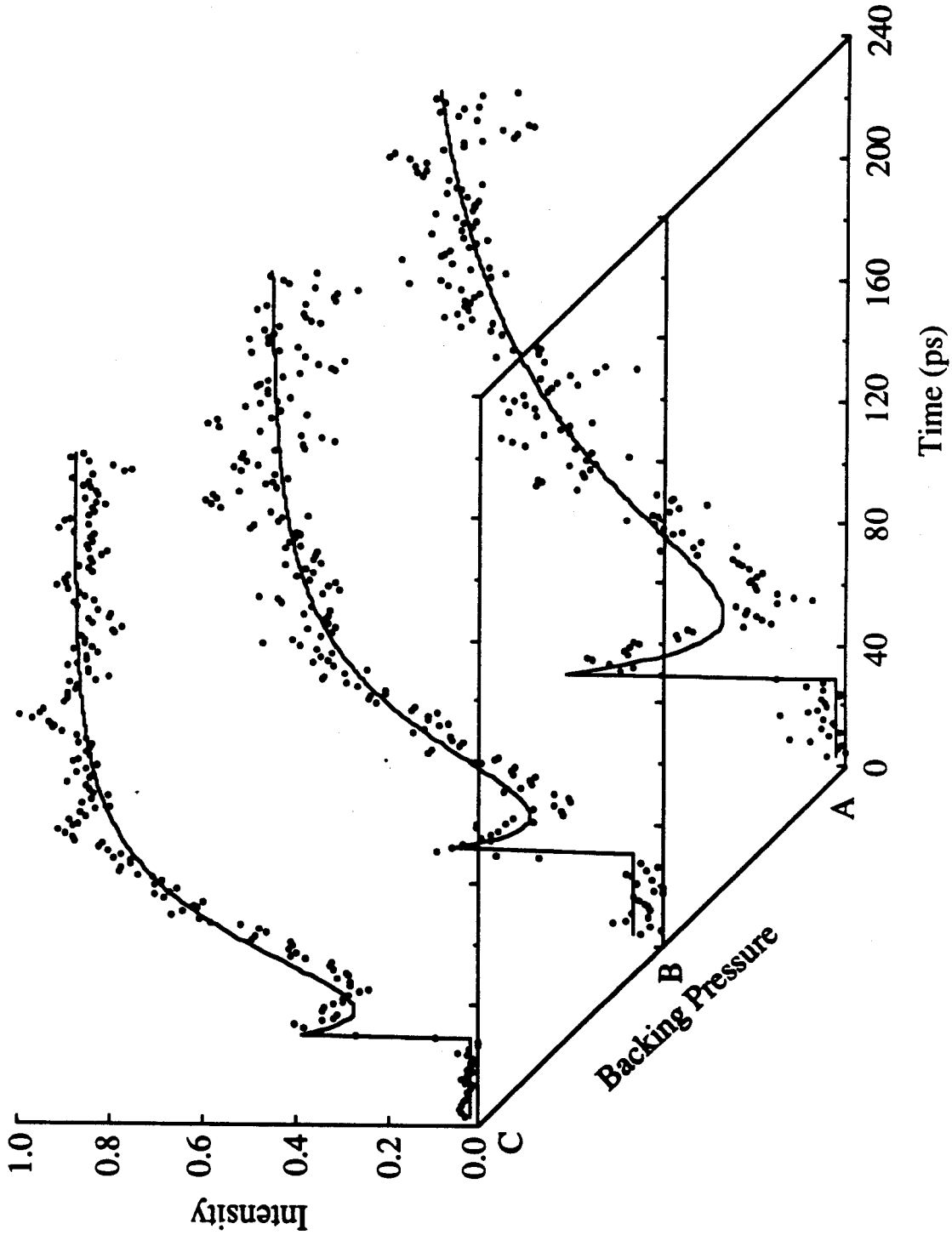
Intensity
1.0
0.8
0.6
0.4
0.2
0.0
C
B
A
Backing Pressure
0
40
80
120
160
200
240
Time (ps)

Figure 4.

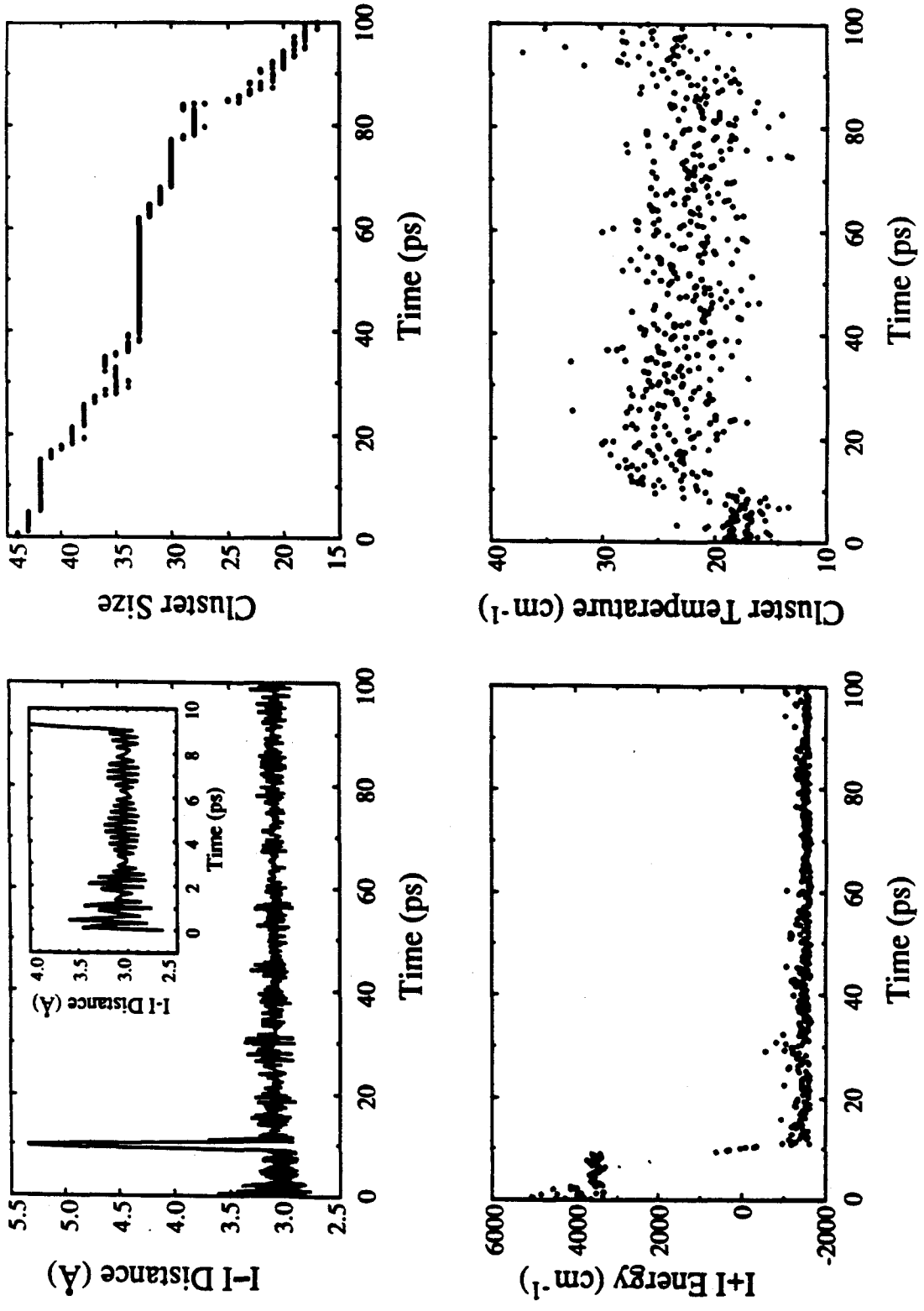
I-I Distance (Å)
Time (ps)
I-I Distance (Å)
Time (ps)
I+I Energy (cm-1)
Time (ps)
Cluster Size
Time (ps)
Cluster Temperature (cm-1)
Time (ps)

Figure 5.

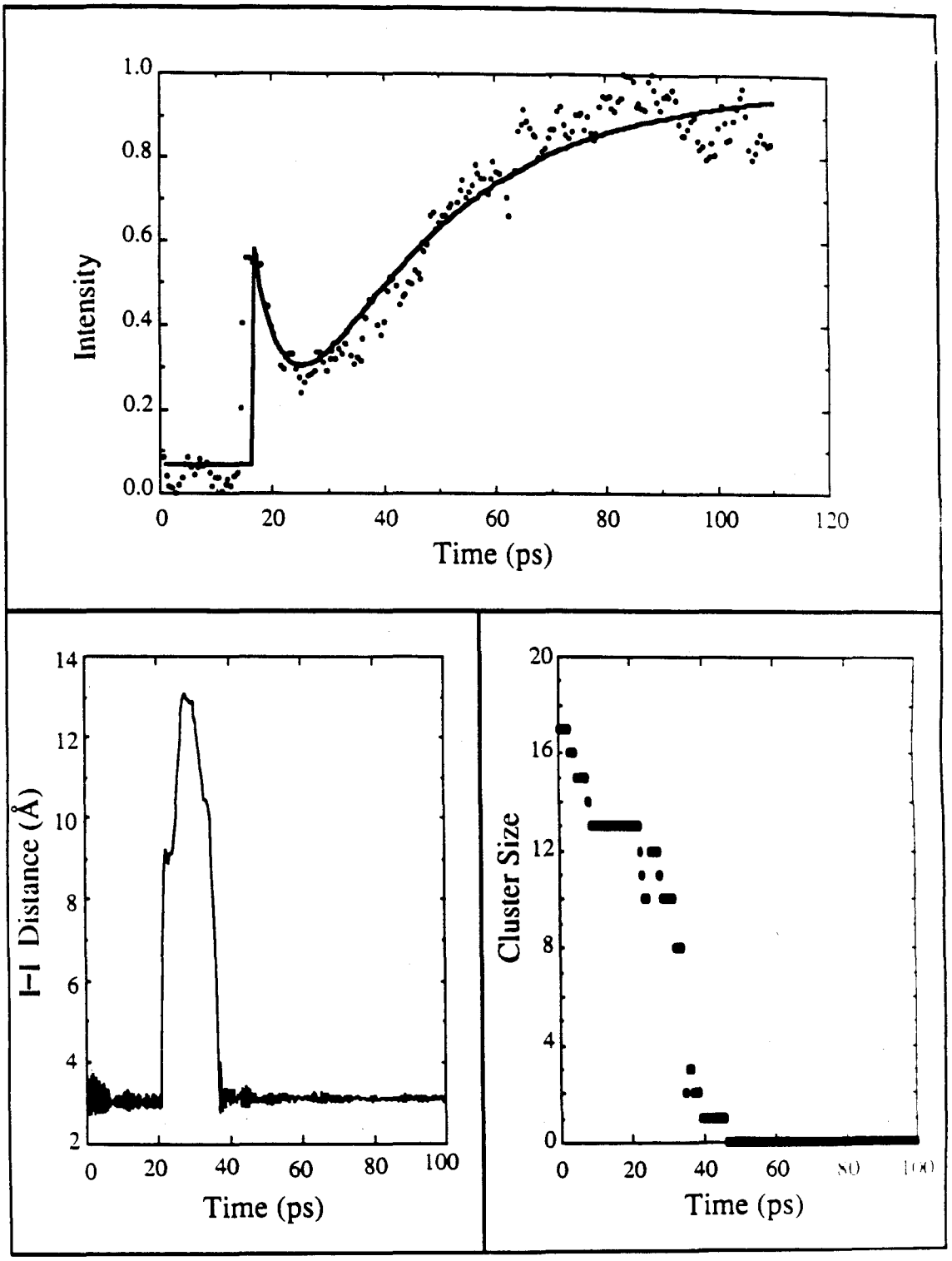

Figure 6.

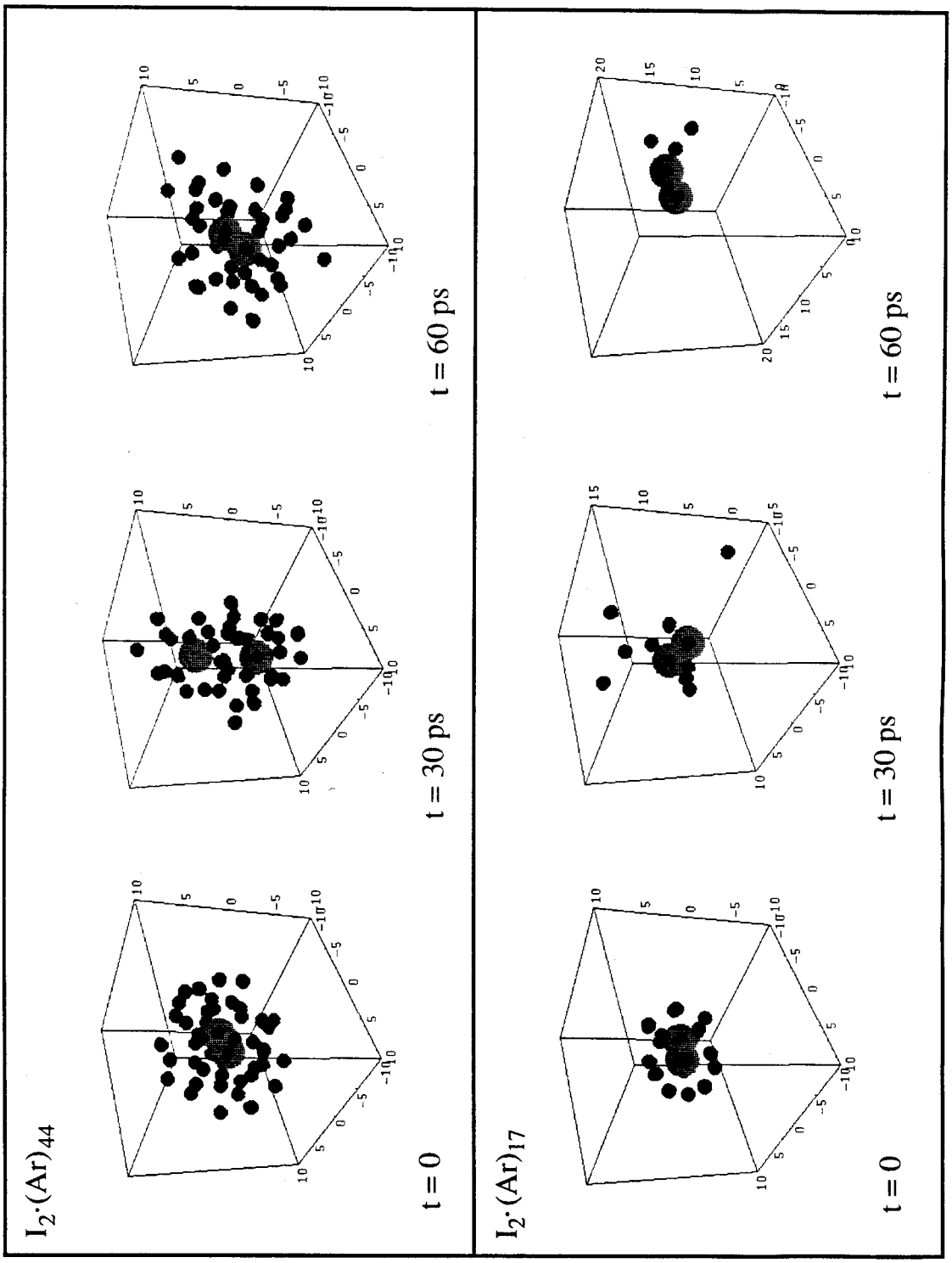

Figure 7.

Chapter 4

Ultrafast Dynamics of the Reaction:

$Xe + I_2 \rightarrow XeI^* + I$

4.1 Introduction

The reaction $Xe + I_2 \rightarrow XeI^* + I$ provides an excellent vehicle with which to study two distinctive issues in physical chemistry. The first involves controlling a chemical reaction such that a given product is produced at the expense of another, energetically allowed, product. The second issue involves the ultrafast dynamics of laser-assisted reactions (LAR) and the now classic, electron-hopping mechanism. LAR is a mechanism whereby a reaction proceeds only when two reactants and a photon collide simultaeously. In the nanosecond work described below, xenon, molecular iodine and a sufficiently energetic photon collide to form the excimer, XeI, through an electron-hopping step. However, this mechanism appears not to be operating in the femtosecond experiments described here.

4.1.1 Chemical Control

There is an extensive body of literature devoted to issues of control.[1-8] Much of the theoretical work involves light pulses or phase-locked beams which are experimentally difficult to prepare. Simultaneously, the Rice group[6] and the Zewail group[9] initiated work aimed at making a step towards showing limited control of a chemical reaction using experimentally feasible wavelengths and pulse characteristics. Our approach is explained below, but in the desire to be complete, the scheme designed by Amstrup *et al.*[6] will be included here (this experiment has not yet been performed but is similar in nature to the experiment described in this chapter). Simply, an initially prepared eigenstate of I_2 in the *B* state is dumped to high vibrational levels in the ground state via a 50 fs infrared pulse. The wave-packet thereby produced evolves on the ground state with a characteristic period of oscillation. A second near IR femtosecond pulse, resonant with the high lying vibrational levels of the ground state and the dissociate continuum states of the *B* state (which correlates with $I^* + I$), prepares the system to dissociate along the *B* state. As the delay between the dump pulse and the pump pulse is scanned, the production of spin-orbit

excited iodine will be modulated at the vibrational frequency of the high lying vibrational levels in the ground state. For reasons which will be evident later, the following quote from Amstrup *et al.*[6] justifies the approach to those who wish to discredit the work presented here.

> Our approach to the problem [of control] is to examine the modulation of the product yield in the photodissociation of a diatomic molecule as a function of the delay between pump and dump pulses. Although controlling the amount of product formed in the photodissociation of a diatomic molecule does not demonstrate the enhancement of the formation of a particular reaction product selected from a set of possible reaction products, it does depend on the same features of the wavepacket dynamics and wavepacket interference.

There have been several significant advances in laser technology which may give experimentalists the opportunity to undertake the schemes proposed thus far. Scherer *et al.*[10] have developed a way of phase-locking two femtosecond pulses. This technique allows one to prepare unique wavepackets as a result of the anharmonicity in the accessed upper state. After a single oscillation, the initially prepared wavepacket will interfere with a second wavepacket. This coherent superposition of the broadened first packet and the second ground-state reflected packet will lead to shapes not previously attainable. With a little bit of ingenuity, these unique wavepackets could be utilized in experiments similar to those discussed here to show greater control over product formation. On another front, at least two groups are actively developing techniques to generate ultrashort pulses with almost arbitrarily chosen phase and wavelength characteristics.[11] Again, these pulses could be used to generate wavepackets with shapes and phases quite distinct from the "natural" wavepackets created via conventional means. These techniques should allow full implementation of the theoretical schemes of Tannor and Rice.[1]

4.1.2 Mechanism

Setser *et al.*[12,13] have studied the xenon plus halogen reactions extensively over the last decade. Initially this work was directed to a better understanding of the states and relaxation mechanisms at work in the excimers, XeX^*--the obvious application of which was directed toward excimer laser technology. The early work demonstrated the feasibility and utility in the photoassociation reaction:[12]

$$Xe + X + h\nu_{laser} \rightarrow XeX^*$$

$$XeX^* \rightarrow Xe + X + h\nu_{emission}.$$

This technique was used to map out the spectroscopy of the excimer states in a way similar to that done on any ordinary bound-to-bound system. Recognition that such "termolecular" reactions could be studied led to the work on the LAR mechanism:[13]

$$Xe + X_2 + h\nu_{laser} \rightarrow XeX^* + X$$

$$XeX^* \rightarrow Xe + X + h\nu_{chemiluminescence}.$$

It is important to understand the distinction between LAR and reactive quenching:

$$X_2 + h\nu \rightarrow X_2^*$$

$$X_2^* + Xe \rightarrow XeX^* + X$$

$$XeX^* \rightarrow Xe + X + h\nu,$$

where in the former case the "collision complex" $Xe{\cdot}X_2$ is the absorber and in the latter, X_2 absorbs the photon prior to collision with a xenon atom .The second mechanism may also be carried out by exciting the atomic xenon, which subsequently collides with a ground state halogen molecule.

We combined the two areas of study--LAR and chemical control-- so as to utilize the work of Setser in demonstrating a simplified version of control over a chemical reaction. The method employed is shown in fig. 1 for the two alternate pathways (see discussion below). Without reference to the mechanism, molecular iodine is excited to the *B* electronic state via a short pulse laser. The wavepacket thus formed propagates along the potential energy curve with a period given by the inverse vibrational frequency of the vibrational levels excited. Some time later, a second short pulse is used to excite this

population to an upper ion-pair potential. At this energy the I_2^{**} reacts efficiently with xenon to form *B* state XeI^*, which subsequently fluoresces at 253 nm. The modulation of the signal at 253 nm is a direct consequence of the preferential absorption of the second femtosecond pulse on one or the other turning points within the I_2, *B* state.[14] When the photon energy matches the separation of the *B* state and the upper ion-pair state at one of the turning points, the system is excited to a reactive state.

4.2 Experimental

Half of this work was performed on a colliding pulse mode-locked (CPM) laser system which has been described in detail elsewhere.[15] The other half was carried out with the apparatus characterized in chapter 2. The CPM system operates at 620 nm with a pulse width of 60 fs in an ~80 MHz pulse train. This beam is amplified at 20 Hz with a Q-switched, DCR-3, Nd:YAG laser, the output of the amplifier is a 300 μJ pulse with negligible broadening (after dispersion compensation).

The amplified beam is split into two arms, both of which are used to generate white light continua. One arm, the pump, travels through a 510 nm, 10 nm FWHM interference filter. The low intensity beam is sent into the reaction cell directly. A second interference filter is used in the other arm to select the control pulse (~530 nm). The control pulse is amplified in a single stage amplifier pumped by the 355 nm light from the Q-switched laser. This amplification generated sufficient intensity to allow frequency doubling in a KDP crystal. The two beams were recombined with an appropriate dichroic beam splitter and propagated colinearly through the reaction cell. A 10 cm focal length lens focused both beams to a waist in the center of the cell. Lenses upstream were used to compensate for the differing focal points of the UV and visible beams.

The fluorescence was collected at right angles to the incoming beams via an F/1 lens. This beam is imaged onto the slits of an F/3.5, 34 cm monochromator prior to detection by a 1P28 pmt. The pmt output is integrated by an SRS boxcar integrator,

which is interfaced to a Macintosh personal computer. The computer controlled the linear stage used to delay one pulse relative to the other.

The pump pulse, centered at 510 nm, was ~50 μJ in intensity while the intensity of the probe pulse was at best 1 μJ. The overall response of the system was probably about 150 fs (estimated by the rise time and modulation depth in the isolated I_2 signal). The broadening was due in large part to double continua generation; this response was adequate to demonstrate the desired effect, however.

The reaction cell consisted of a quartz tube, 10 cm long, 4 cm in diameter, with a single O-ring valve stem used for cell preparation. Solid I_2 was placed in the cell, followed by evacuation to <1 torr total pressure (the room-temperature vapor pressure of I_2 is 0.33 torr). Xenon was back filled into the cell to a total pressure of ~50 torr. Other pressures were tried, *vide infra*, but generally the 50 torr sample worked best. For some of the experiments, the cell was heated to 40°C to raise the I_2 partial pressure to 1 torr.

4.3 Results

Figure 2 shows three dispersed fluorescence scans of cells containing varying pressures of xenon and 0.33 torr of I_2. These scans were obtained at a positive time delay (pump pulse preceding the probe pulse) with the monochromator set for 4 nm resolution. There are four distinct peaks in these spectra. The peaks at 253 nm and 320 nm may be assigned to the excimer XeI^*, $B \rightarrow X$ and $B \rightarrow A$ state emission respectively.[13] The dominate feature at 264 nm is the scattered light due to the probe pulse. The peak at 340 nm is isolated I_2, $D' \rightarrow A'$ emission.[14] The chemiluminescence signal reaches a maximum around 70 torr of xenon and then declines at higher pressures. This observation is in complete agreement with the VUV work of Donovon *et al.*[16]

Figure 3 shows transients with detection at either 253 nm or at 340 nm. The monochromator is kept at a given detection wavelength while the relative delay between the pump and probe pulses is scanned. These transients exhibit the characteristic I_2, *B*

state oscillations as a result of the wavepacket dynamics previously described in chapter 3 and in ref. 14. Most noteworthy is the similarity in the transients taken with 340 nm detection, due to isolated I_2, and 253 nm detection, due to excimer formation. The peaks and valleys match exactly between these two transients, indicating that the *B* state of I_2 is a common intermediate state for both processes.

Figure 4 displays a transient taken with 253 nm detection superimposed on the response function of the system. This response function was measured by ionization of diethyl analine (DEA). The 264 nm photon excites the molecule to S_1; the subsequent visible photon is sufficiently energetic to ionize the molecule out of S_1 giving a step function convoluted with the response function of the apparatus. The resulting signal was fit appropriately and the smooth fitted curve was differentiated in order to generate this figure. Since the window on the xenon/iodine cell may have a different amount of dispersion than the DEA cell, correction was made by measuring the effect of placing the quartz window of the DEA cell into the path of the beams prior to measuring a transient. This, compared to a transient without the window in place, leads to the dispersion due to the DEA cell window. This dispersion is then compared to the dispersion due to a window identical to that on the xenon/iodine cell. The difference was used to shift the DEA signal accordingly so as to correct for this small but measurable effect. The outcome of this experiment has been to show that absorption of the second photon, prior to excimer formation, occurs on the inner turning point of the I_2, *B* state.

The ionization experiment was performed in a small glass cell (4 cm long and 1.5 cm in diameter) with quartz windows. The cell is equipped with electrodes running the length of the cell separated by approximately 1 cm. The electrodes are placed in series with a 9 volt battery and the signal is detected by a current sensitive amplifier, the output of which is fed into the boxcar integrator.

Finally, an important indicator of whether LAR is the mechanism operating in these experiments, as opposed to excimer formation through a simple collision process, is

the time profile of the chemiluminescence signal.[13] If LAR is the mechanism at work, then the signal should be prompt and rise instantaneously. On the other hand, if collisions between excited I_2 and xenon are responsible for formation of xenon iodide, then the signal should build up with a time constant commensurate with the collision time between these two species at the given pressure. Figure 5 shows two such time profiles. Curve A represents the response of the electronics since the monochromator is set to detect only the probe beam scatter, which is obviously prompt and instantaneous. Curve B is a time profile of the 253 nm emission. These traces were obtained by sending a voltage ramp through a digital-to-analog converter from the computer to the boxcar integrator gate control, allowing the computer to control the gate delay. The scan was accomplished by scanning the gate across the signal in time. The gate was held at 3 ns and the step time was <1 ns. Obviously a narrower gate would be beneficial, but the signal level was altered dramatically by reducing the gate width to the minimum setting (1 ns); apparently the boxcar does not function well under these conditions. These two scans were taken without any change between them except to move the monochromator setting from 253 nm to 264 nm.

4.4 Discussion

The details of the reaction mechanism will be discussed first because these results directly influence the interpretation of the issues of control. The first concern addressed below, is what is the source of the 253 nm signal. Within the LAR mechanism, there are two schemes which could be responsible for the observed signal. Namely, the absorbing species could be molecular iodine which subsequently collides with a xenon atom simultaneous with absorption of the second photon; or the absorbing species may be a iodine/xenon complex. Furthermore, the nature of this "collision-complex" is important to ferreting out which of these two LAR schemes may be appropriate in describing these experiments (the complex could be a van der Waals molecule or merely a collision pair).

However, if the LAR mechanism is not operating, then a collisional process must be the source of the chemiluminescence, the consequences of which are described below.

4.4.1 Mechanism

On the basis of these experiments it may be concluded that, in contrast to the work of Setser *et al.*,[12,13] the chemiluminescence signal is not due to the LAR mechanism. The discussion below outlines the argument supporting this view.

A misconception held by this author when considering the LAR mechanism early on was to assume that the "collision-pair" responsible for generating the excimer was a van der Waals molecule. While a van der Waals molecule would indeed satisfy the conditions for LAR, and a finite number of such molecules do exist in the reaction cell, the relative concentration is so exceedingly small as to be irrelevant. Setser has shown, for example, this to be true for the case Xe + Cl $\leftrightarrow$ Xe·Cl using the appropriate partition functions to calculate the equilibrium constant.[12] The value thereby obtained was $\sim 10^{-24}$. Admittedly Xe + I_2 $\leftrightarrow$ Xe·I_2 is a different system (most importantly, the van der Waals well is deeper in the case of iodine), but certainly the equilibrium constant will not be twenty orders of magnitude larger. The equilibrium constant is unfavorable because the van der Waals well is relatively shallow and the molecule is formed at the expense of three translational degrees of freedom. This having been said, another source of the LAR chemiluminescence must be present.

Setser points out that most of the signal originates from true "collision-pairs."[12,13] A collision-pair is simply an I_2 molecule which is undergoing a random collision with a xenon atom during the laser excitation pulse. For example, during the 20 ns laser pulse employed in the work on the Kr + F system, the fluorine atom collides with a krypton atom ~10 times. This is easily calculated by the equation for collision frequency in a mixed gas:

$$Z_{12} = \pi\left(\frac{(d_{Kr} + d_F)}{2}\right)^2 \sqrt{\frac{8kt}{\pi\mu}} \tilde{N}_{Kr} \tilde{N}_F \qquad (4.1)$$

where d is the collision diameter, μ is the reduced mass and $\tilde{N}$ is the number density. This number represents the total number of collisions between krypton and fluorine per second per cubic meter. Changing this to collisions per 20 ns and dividing by the number density of fluorine gives the total number of collisions each fluorine atom will experience during the 20 ns laser pulse. Using the same expression for the Xe + I_2 case with a laser pulse width of 100 fs, one comes to the conclusion that only ~3 in 10^5 iodine molecules collide with a xenon atom during the 100 fs pulse.

Assuming that the experiment were somehow sensitive to this small number of collision-pairs, the following distinction in regard to the mechanism can be made immediately. The collision-pair exists for ~5 ps. This value is readily calculated by defining a collision-pair to be a situation where a xenon atom is within ~12 Å of an iodine molecule (12 Å is chosen since the experimentally determined cross sections for this type of electron-hopping reactions is on the order of 400 $Å^2$ [Ref. 17]). Using the relative velocities of these two species, one finds that it takes approximately 5 ps for the xenon atom to leave the 12 Å radius of the iodine molecule. This observation precludes the possibility that the collision-pair, which ultimately leads to excimer formation, originates on the *X* state of I_2. Experimentally, the I_2 may be allowed to propagate on the *B* state for tens of picoseconds prior to excitation with the second laser pulse. Therefore, any collision-pairs absorbing the first photon would no longer be collision-pairs by the time the second photon arrived. (There is not an enhanced signal at pump-probe delay times <10 ps, on the contrary the signal is quite constant for tens of picoseconds.) This does not, however, eliminate the possibility that the iodine molecules initially excited to the *B* state collide with a xenon atom simultaneous (or within several hundred femtoseconds) with the second photon. This alternative is addressed below.

If one is to assume that the small number of collision-pairs is somehow responsible for the observed signal, an argument must be made to show why these molecules react orders of magnitude more efficiently than isolated I_2^{**} colliding with xenon. The distinction between these two mechanisms is illustrated here taking into account the fact that the collision-pair must originate on the *B* state of I_2 because of the argument just discussed:

LAR:

$$I_2 (B \text{ state}) + Xe + h\nu \rightarrow XeI^* + I$$

Collision Mechanism:

$$I_2 (B \text{ state}) + h\nu \rightarrow I_2 (\text{ion-pair})$$

$$I_2 (\text{ion-pair}) + Xe \rightarrow XeI^* + I.$$

One might be inclined to argue that the LAR mechanism has an increased absorption cross section as compared with isolated *B* state iodine. However, the point has been made that the isolated halogen states mix with the xenon/halogen states so as to give oscillator strength to the LAR mechanism.[18] In other words, the absorption cross section of isolated I_2 should be nearly identical to the absorption cross section for $Xe{\cdot}I_2$.

It is possible, however, that if the ion-pair state of I_2 had a sufficiently short lifetime so as to preclude the reactive collision, one might be successful in claiming LAR as the dominate mechanism. As argued above, both the isolated I_2 and the $Xe{\cdot}I_2$ collision-pair should have comparable absorption cross sections; therefore, one need only compare the efficiencies of excimer production after absorption of the second photon. First, assume that the collision-pair reacts with unit efficiency after absorption of sufficient energy. Second, assume that ion-pair state I_2 will also react with unit efficiency as a result of collision with a xenon atom. These two assumptions are not unreasonable given the large reactive cross section for the electron-hopping mechanism. To estimate the amount of excimer formation from the collisional mechanism it is convenient to use the following

kinetic scheme which accounts for the competition between reactive quenching and spontaneous emission:

$$I_2^{**}\ (\text{ion-pair}) \xrightarrow{k_1} I_2^{*} + h\nu_{emission}$$

$$+$$

$$Xe$$

$$\downarrow k_2$$

$$XeI^{*} + I$$

where k_1 is the rate of spontaneous emission of isolated ion-pair state I_2, and k_2 is the collision rate for xenon colliding with I_2. Since the reaction is assumed to occur with unit efficiency, every collision should produce XeI^*; therefore, the reaction rate should be controlled by the collision frequency. Assuming the xenon concentration is constant (pseudo-first order kinetics), the concentration of excimer at $t = \infty$ is given by:

$$[XeI^{*}] = \frac{k_2[Xe]}{k_1 + k_2}. \qquad (4.2)$$

This assumption is valid since the concentration of xenon is >20 times the concentration of I_2 (to say nothing of I_2^{**}) under the conditions employed here. At the lowest pressure studied, 6.5 torr of xenon, the rate of collision is ~17 ns and the lifetimes of the ion-pair states of I_2 are all in the range of ~15 ns.[19] Therefore, based on these assumptions the decay of the ion-pair state cannot account for the 10^5 difference in concentration of isolated I_2^{**} and $Xe{\cdot}I_2$ collision pairs.

In addition to the arguments above, several other comparisons of our data with that found in ref. 13 further confirms that the collisional mechanism is responsible for excimer formation under the experimental conditions employed here. Setser makes the point that in the collisional mechanism the total emission due to the excimer cannot substantially exceed the signal due to isolated I_2 emission in the absence of xenon. While there are several assumptions necessary to arrive at this conclusion, the dispersed

fluorescence scans acquired with nanosecond excitation are quite different from those shown in fig. 2. The ratio of 253 nm emission (due to the excimer) to 340 nm emission (due to the D' $\rightarrow$ A' line in isolated I_2) is >10 for the nanosecond work,[13] whereas in this femtosecond experiment this ratio is <2 for all pressures studied.

It has also been suggested that in order for the electron-hopping mechanism to be efficient, the halogen molecule should be found at a large internuclear separation.[20] However, fig. 4 clearly shows that absorption of the second photon occurs on the inner turning point of the *B* state. Therefore, the halogen internuclear separation is close to the equilibrium bond length upon excitation to the energetically reactive state. If bond lengthening is indeed a prerequisite for reaction with xenon, it must occur on the upper ion-pair potential. The LAR mechanism implies that absorption of the second photon places the system directly on the coulomb potential responsible for excimer formation.

A pressure dependence of the 253 nm emission was carried out and found to be in agreement with the work of Donovan *et al.*[16] In their work, a simulation including all plausible relaxation pathways was performed and used to explain the measured pressure dependence. The conclusion was, as it is here, that the xenon collides with the ion-pair state I_2. In the LAR mechanism the pressure dependence should merely be first order in xenon over a broad pressure range[13] (other relaxation pathways are unimportant owing to the efficiency with which xenon iodide is formed from the collision-pair), but the results shown here are not consistent with this mechanism.

Finally, one of the most convincing pieces of evidence used to prove that LAR is the mechanism at work in the nanosecond experiments was the time profile of the fluorescence signal.[13] In LAR this signal should rise instantaneously, in contrast to a collisional process where the signal should rise at the collision rate. Fig. 5 shows our results. Since the boxcar gate was reasonably large these results are not definitive. Comparison of the scattered light profile with the excimer emission shows, to a limited extent, that the excimer signal does not rise instantaneously as the scattered light signal

does. A more precise analysis by convolution might strengthen this statement, but given the quality of the data this was deemed unnecessary.

With all of this evidence, it is safe to assume that the LAR mechanism will be difficult to study using femtosecond techniques. The number of collision pairs integrated over the pulse duration is exceedingly small compared to the number of isolated molecules. This is unfortunate in that, were LAR able to be studied with ultrashort pulses, a great many bimolecular experiments could be performed in a gas cell rather than necessitating the technique employed in the studies of $H + CO_2$ (Ref. 21) and $Br + I_2$ described in chapter 5.

4.4.2 Control

Now that the mechanism for reaction is clear, it is time to address the issue of whether or not we have demonstrated control over the reaction $I_2 + Xe \rightarrow XeI^* + I$. Afterall, an anonymous chemist quoted in C&E News claimed that these experiments did not demonstrate control unless the LAR mechanism was at work.[22] However, in comparing the scheme described here with that proposed by Rice,[6] the similarity is clear. In both cases the prepared wavepacket acts as a natural switch which controls whether or not reaction will occur. Admittedly, this outcome could be accomplished in a trivial manner, simply by placing a chopper wheel in the path of a continuous wave laser, but we contend that, while this work does not demonstrate a *useful* level of control, it does demonstrate the methodology proposed and justified in the quote from Rice given above.

4.5 Conclusion

This work provides a starting point from which further, more sophisticated control experiments may be undertaken--it may not be necessary to utilize complicated pulse sequences and experimentally difficult pulse characteristics to demonstrate a modicum of control over the outcome of a chemical reaction. Furthermore, once the techniques for

generating arbitrary pulse sequences becomes straightforward, this experiment may again represent the point from which further experiments will be launched.

In the scheme employed here, nothing was learned about the reactive event. It would be useful to somehow study this reaction in a way that allows one to measure the rate at which the electron-hop occurs. Such an experiment has been considered but may not prove to be viable based on work done by Soep *et al.*[23] If one were to start from a van der Waals molecule, formed in a molecular beam, it might be possible in principle to study the reaction in greater detail. However, in the work of Soep[23] it was found that the van der Waals complex $Xe \cdot I_2$ shows no emission whatsoever, indicating that the proximity of the xenon atom effectively relaxes the system prior to reaction or spontaneous emission. Nevertheless, it is worth the effort to at least attempt the experiment with ultrashort light pulses because successful results would be quite interesting.

4.6 References

1. D. J. Tannor, and S. A. Rice, *Adv. Chem. Phys.*, **LXX** (Part I), 441 (1988).
2. S. Mukamel, and K. Shan, *Chem. Phys. Lett.*, **117**, 489 (1985).
3. P. Brumer, and M. Shapiro, *Chem. Phys. Lett.*, **126**, 541 (1986).
4. S. Shi, A. Woody, and H. Rabitz, *J. Chem. Phys.*, **88**, 6870 (1988).
5. J. Manz, and C. S. Parmenter, *Chem. Phys.*, **139**, 1 (1989).
6. B. Amstrup, R. J. Carlson, A. Matro, and S. A. Rice, *J. Phys. Chem.*, **95**, 8019 (1991).
7. R. L. Vander Wal, J. L. Scott, and F. F. Crim, *J. Chem. Phys.*, **92**, 803 (1990).
8. D. J. Tannor, *Abs. Pap. ACS.*, **204**, 64 (1992).
9. E. D. Potter, J. L. Herek, S. Pedersen, Q. Liu, and A. H. Zewail, *Nature*, **355**, 66 (1992).
10. N. F. Scherer, A. J. Ruggiero, M. Du, and G. R. Fleming, *J. Chem. Phys.*, **93**, 856 (1990).
11. a) A. M. Weiner, J. P. Heritage, *Rev. Phys. Appl.*, **22**, 1619 (1987); b) F. Spano, M. Haner, W. S. Warren, *Chem. Phys. Lett.*, **135**, 97 (1987).
12. a) G. Inoue, J. K. Ku, and D. W. Setser, *J. Chem. Phys.*, **76**, 733 (1982); b) G. Inoue, J. K. Ku, and D. W. Setser, *J. Chem. Phys.*, **80**, 6006 (1984); c) A. W. McCown, and J. G. Eden, *J. Chem. Phys.*, **81**, 2933 (1984).
13. a) J. K. Ku, G. Inoue, and D. W. Setser, *J. Phys. Chem.*, **87**, 2989 (1983); b) E. Quiñones, Y. C. Yu, D. W. Setser, and G. Lo, *J. Chem. Phys.*, **93**, 333 (1990); c) T. O. Nelson, and D. W. Setser, *Chem. Phys. Lett.*, **170**, 430 (1990); d) J. Qin, T. O. Nelson, and D. W. Setser, *J. Phys. Chem.*, **95**, 5374 (1991).
14. R. M. Bowman, M. Dantus, and A. H. Zewail, *Chem. Phys. Lett.*, **161**, 297 (1989).
15. M. J. Rosker, M. Dantus, and A. H. Zewail, *J. Chem. Phys.*, **89**, 6113 (1988).
16. B. B. O'Grady, and R. J. Donovan, *Chem. Phys. Lett.*, **122**, 503 (1985).

17. M. R. Bruce, W. B. Layne, and J. W. Keto, *J. Chem. Phys.*, **92**, 428 (1990).

18. a) D. W. Setser, and J. Ku, *Photophysics and Photochemistry above 6 eV*, edited by F. Lahmani (Elsevier, Amsterdam, 1985), p. 621; b) J. Qin, and D. W. Setser, *Chem. Phys. Lett.*, **184**, 121 (1991).

19. J. C. D. Brand, and A. R. Hoy, *Appl. Spect. Rev.*, **23**, 285 (1987).

20. J. C. Tully, and R. K. Preston, *J. Chem. Phys.*, **55**, 562 (1971).

21. a) N.F. Scherer, L.R. Khundkar, R.B. Bernstein and A.H. Zewail, *J. Chem. Phys.*, **87**, 1451 (1987); b) N.F. Scherer, C. Sipes, R.B. Bernstein and A.H. Zewail, *J. Chem. Phys.*, **92**, 5239 (1990).

22. S. Borman, *C & E News*, **70** (1),7 (1992).

23. C. Jouvet, M. Boivineau, M.C. Duval, and B. Soep, *J. Phys. Chem.*, **91**, 5416 (1987).

24. K. Tamagake, D. W. Setser, and J. H. Kolts, *J. Chem. Phys.*, **74**, 4286 (1981).

4.7 Figure Captions

1. Three sections through the potential energy surface for the reaction Xe + $I_2 \rightarrow$ XeI + I. Left panel--potentials along the I-I vibrational coordinate. The *X*, *B*, and *f* states are shown (in increasing energy). The mechanism shown on this panel represents the collisional mechanism. Middle panel--potentials along the I_2-Xe coordinate. The same three states are shown except now they are nearly flat, representing the weak van der Waals interaction between molecular iodine and atomic xenon (merely schematic). The mechanism depicted is the laser assisted reaction. Right panel--XeI potentials. These are taken from ref. 24.
2. Dispersed fluorescence spectra taken with 510 nm pump and 264 nm probe pulses. The resolution of the monochromator is set to 4 nm. Xenon pressures: 6.5 torr, 200 torr, and 70 torr from top to bottom.
3. Transients taken with 510 nm pump, 264 nm probe and detection at 253 nm or 340 nm.
4. Transient, as in figure 3, superimposed on response function of the system. The transient was taken with 510 nm pump, 264 nm probe and detection at 253 nm. The response function was measured by ionizing diethyl analine. The curve shown is the derivative of the smooth curve fit to the experimental data.
5. Time profile of the dispersed fluorescence. The response of the system is embodied in the trace taken at 264 nm detection (probe beam scatter). The profile taken at 253 nm detection indicates the likelihood that the formation of the excimer proceeds by the collisional mechanism.

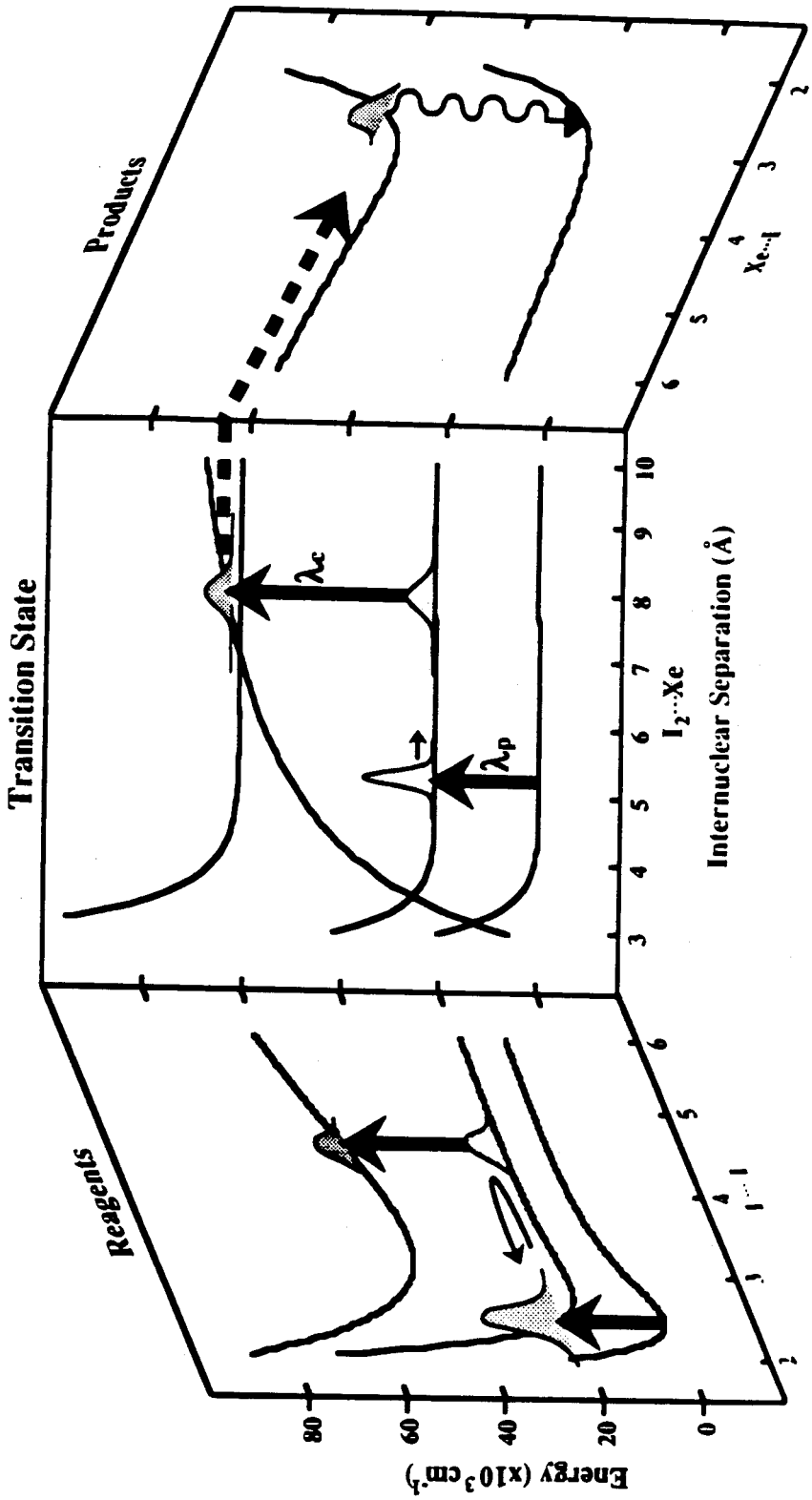
Products
Transition State
Reagents
λ_c
λ_p
I_2···Xe
Internuclear Separation (Å)
Energy (x10^3 cm^{-1})
80
60
40
20
0

Figure 1.

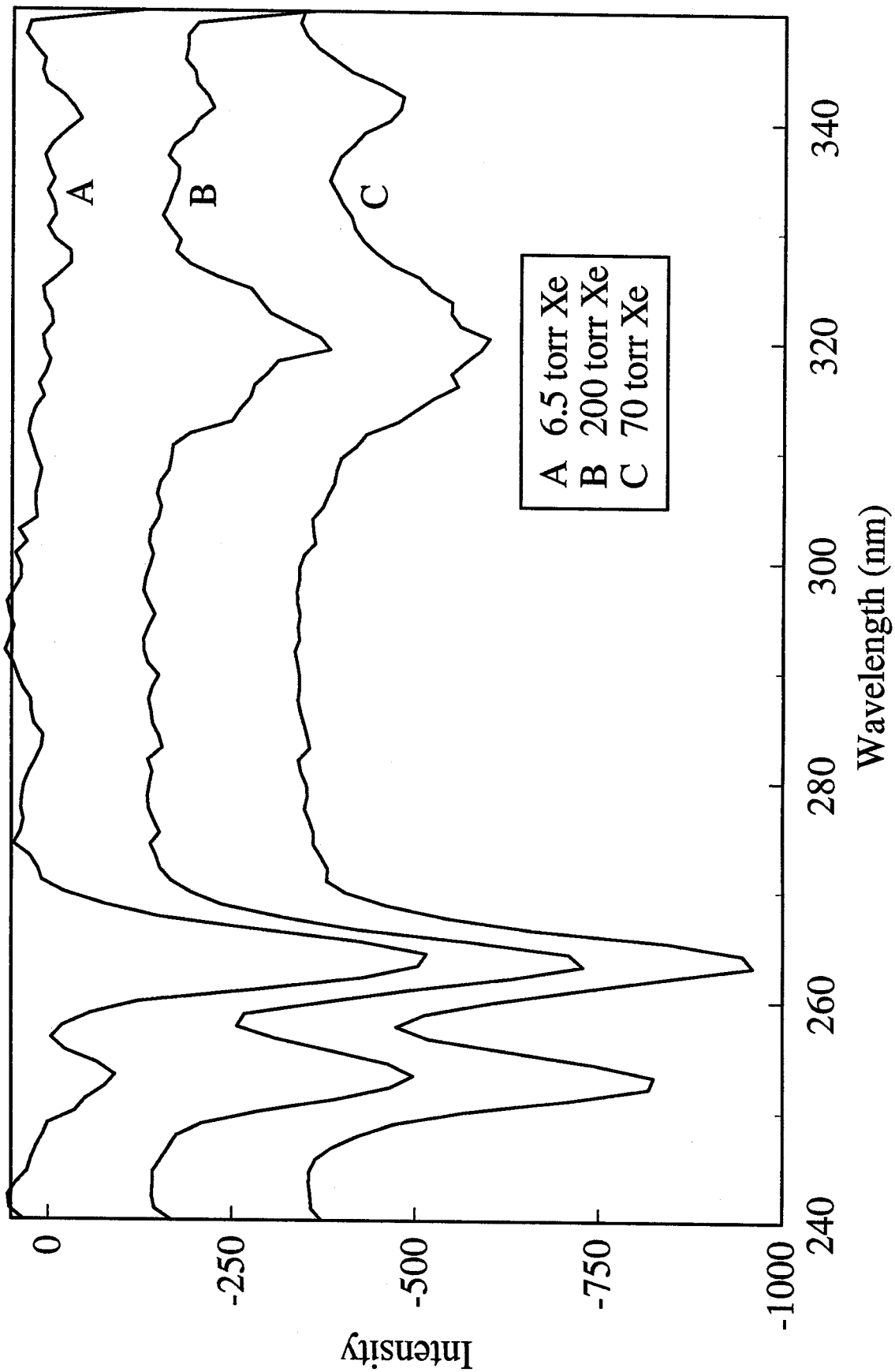
A
B
C
A 6.5 torr Xe
B 200 torr Xe
C 70 torr Xe
Intensity
0
-250
-500
-750
-1000
240
260
280
300
320
340
Wavelength (nm)

Figure 2.

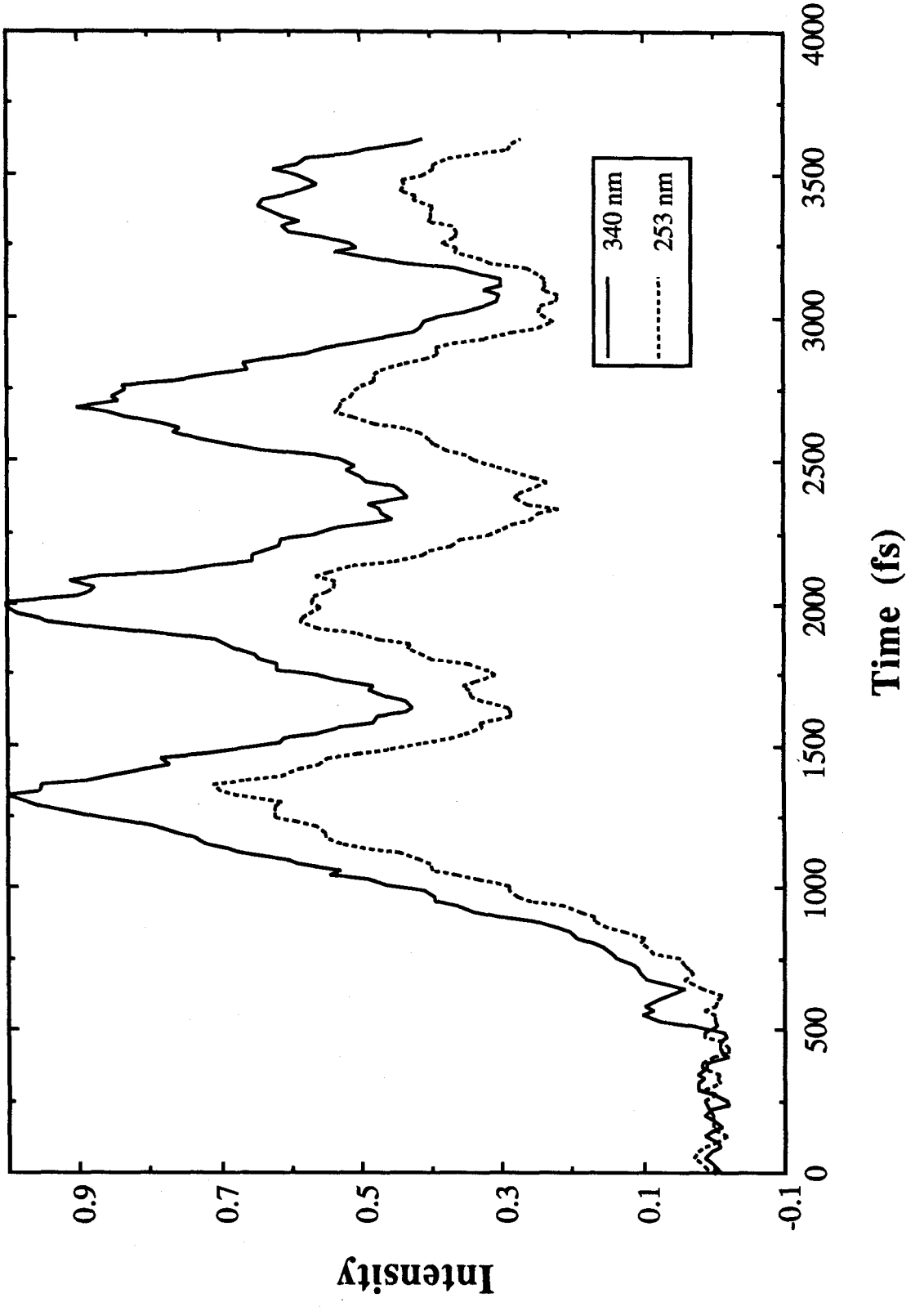
Intensity
0.9
0.7
0.5
0.3
0.1
-0.1
0
500
1000
1500
2000
2500
3000
3500
4000
Time (fs)
340 nm
253 nm

Figure 3.

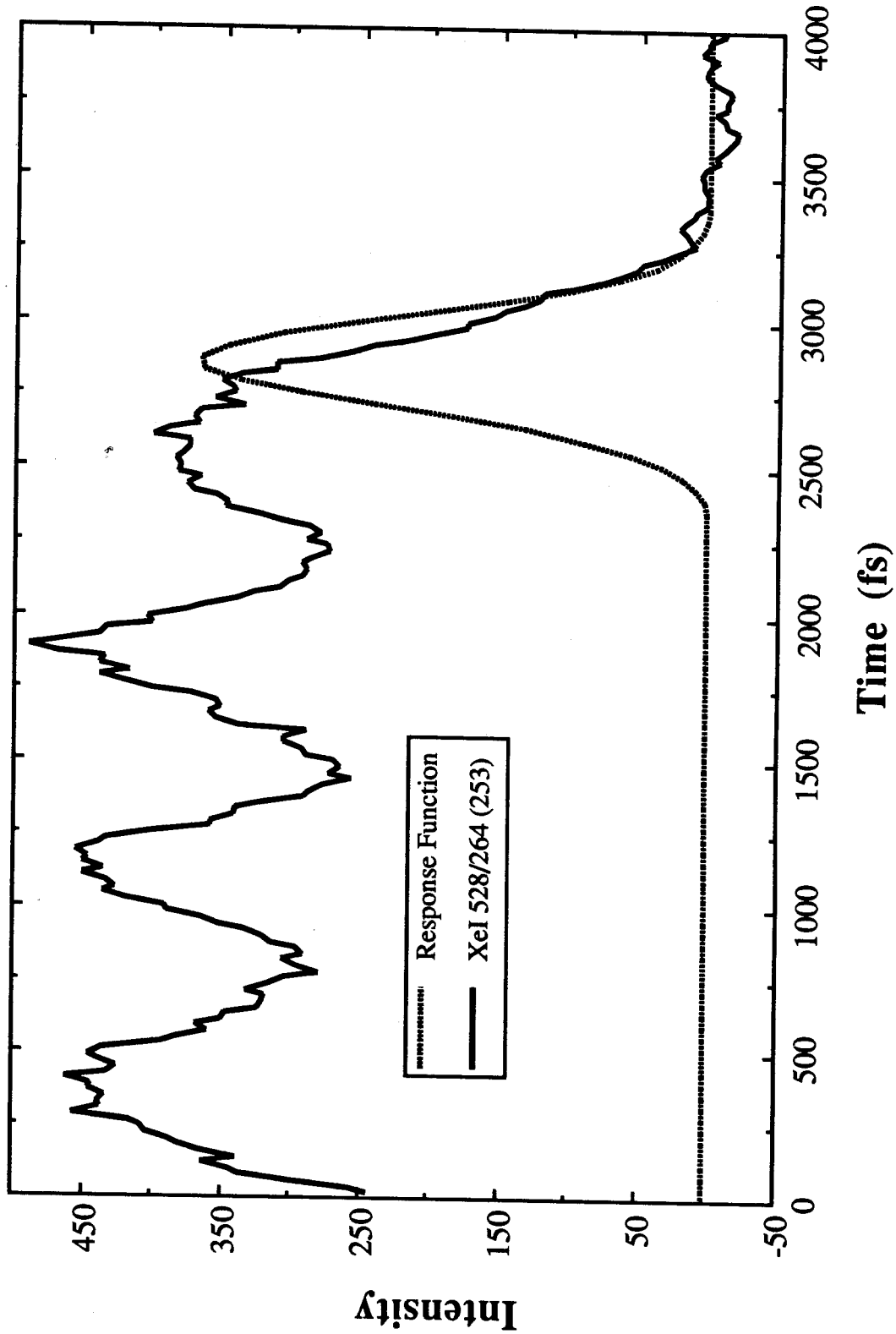
Intensity
450
350
250
150
50
-50
0
500
1000
1500
2000
2500
3000
3500
4000
Time (fs)
Response Function
XeI 528/264 (253)

Figure 4.

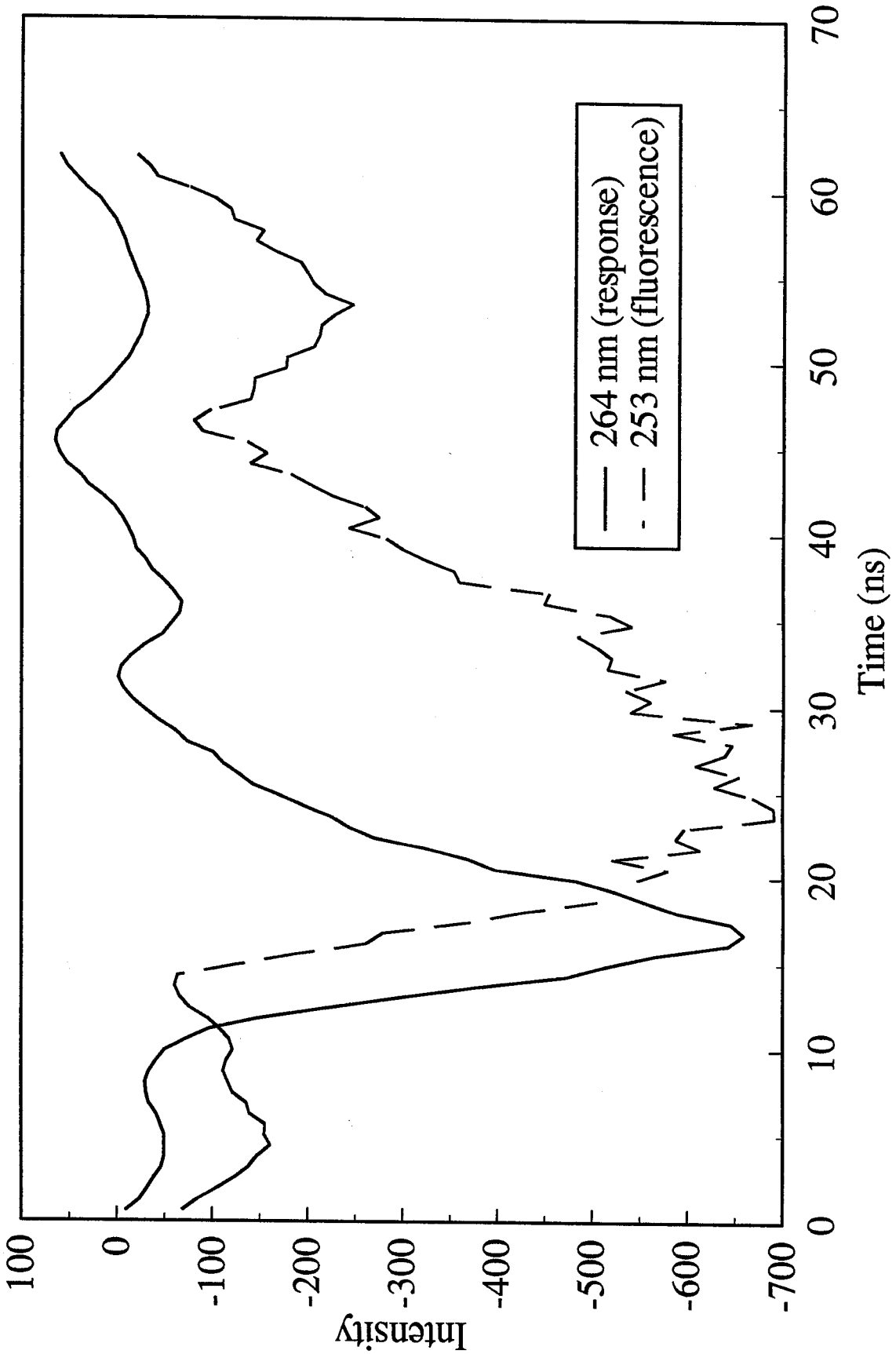
264 nm (response)
253 nm (fluorescence)
Intensity
Time (ns)
100
0
-100
-200
-300
-400
-500
-600
-700
0
10
20
30
40
50
60
70

Figure 5.

Chapter 5

Femtosecond Real-Time Probing of Reactions. VIII. The Bimolecular Reaction Br + I_2

In real-time studies of reaction dynamics, attention has been focused upon different types of unimolecular reactions, either on the femtosecond (fs) timescale, or on the picosecond (ps) time scale for reactions governed by energy redistribution.[1] The first example of a bimolecular reaction studied in real time is $H + CO_2 \rightarrow OH + CO$ within an $HI \cdot CO_2$ van der Waals complex.[2] In a recent communication,[3] we have reported on studies of a different class of bimolecular reactions, atom- (or radical-) molecule, with two objectives: (1) to extend the ps studies[2] to the femtosecond regime; and (2) to clock the bimolecular encounter under unperturbed and isolated conditions on the ground state potential energy surface (PES).

The femtosecond extension was achieved by building a new fs/molecular beam system, which is described in detail in Chapter 2. The study of isolated bimolecular reactions was initiated in halogen exchange reactions. By making the heavier atom or radical in the dissociated precursor the reactive partner, the lighter fragment rapidly departs from the scene and leaves the bimolecular reaction to occur unperturbed by the presence of a third body. The elementary reaction of interest for this study is:

$$Br + I_2 \rightarrow [BrI_2]^{\ddagger} \rightarrow BrI + I.$$

The zero-of-time is well defined since the reaction is initiated from the $HBr \cdot I_2$ van der Waals complex, and the light hydrogen atom is some 20 Å away from the field of the reaction in ~100 fs. A fuller account of the earlier communication[3] is given here.

This chapter is outlined as follows. First is a discussion of the problem establishing the zero-of-time in studies of bimolecular reactions, followed by a discussion of the $Br + I_2$ reaction and related systems, and a brief discussion of the experimental technique. Then a description of the experimental procedure unique to this system is included. The results are analyzed and discussed with focus on bonding in the collision complex and on the dynamics on the reactive surface. Classical trajectory simulations on an optimized PES are used as a guide, and comparison with experiments is made.

5.1 The zero-of-time, the reaction, and the technique

5.1.1 Establishing the zero-of-time

The problem of establishing the zero-of-time for a bimolecular reaction is different from that in unimolecular reactions. In the unimolecular case, a femtosecond pump laser pulse initiates the simultaneous dissociation of a large number of molecules which all pass essentially together through the transition state region and out to products. A second fs probe pulse can thus interact with a considerable concentration of transient species at any time during the reaction, as illustrated in the studies of many reactions.[1]

Bimolecular radical-molecule reactions are usually investigated by flowing a mixture of a molecular partner and a radical precursor in a cell, followed by photolysis of the precursor to generate radicals. These radicals then proceed to react after colliding with the molecular species. The progress of the reaction is then typically monitored by LIF (laser-induced fluorescence) of either the radical species or a reaction product. This method will not work, however, if we wish to probe short-lived intermediates or transition states of the bimolecular reaction. In the bimolecular case, the radicals produced by the pump laser pulse do not react with their molecular partners on a fs-ps time scale. Rather, a random delay is introduced prior to the reactive collision. This differs for each individual reactive event, lasting typically on the order of 100 ns (depending upon the pressure). Thus, the time resolution inherent to the ultrafast pump pulse is smeared out over this much longer time period in a random fashion. Furthermore, as a result, the concentration of intermediate or transition state species at any one time is significantly less for the probe laser to detect. Even in crossed molecular beams, the interaction region (8 mm^3 for skimmed beams) and beam velocities (typically 100-1000 m/s) result in an "interaction time" in the microsecond range--making temporal resolution of two reactant beams interacting with a laser beam impossible at the femtosecond level.

However, there are so far two ways of circumventing the problem.[2,4] In the approach by Scherer *et al.*[2] the two initial species, the radical precursor and the reagent molecule, are locked in a van der Waals complex using the elegant methodology (for studies of product state distributions) developed by the groups of Wittig[5] and Soep[6] in what can be called a "precursor geometry limited" (PGL) reaction. To define the zero-of-time, Scherer *et al.* used an initial ps pulse to photolyze the radical precursor. The newly produced radical partner collides with the molecule after a uniform and short (sub-picosecond to picosecond) delay. Subsequent production of reaction intermediates and decay products can then be observed by a second probe pulse which is able to interact with a considerable concentration of the transient species. The zero-of-time is thus defined by the pump pulse with a constant, short delay introduced by the van der Waals bond distance. For this reason, this class of reactions has been called van der Waals impacted bimolecular reactions (VIB).[2]

This technique has principally been applied to the reaction $H + CO_2 \rightarrow OH + CO$ within $IH \cdot CO_2$ to study the dynamics of the collision complex $[HOCO]^{\ddagger}$. For the $HCl \cdot CO_2$, $HBr \cdot CO_2$ and $HI \cdot CO_2$ van der Waals complexes, Wittig and co-workers have collected product state distributions,[5] and the cluster geometry has now been examined by infrared studies.[7] Thus, for the $H + CO_2$ reaction there is a considerable body of experimental[2,5,8] and theoretical[9,10,11] studies aimed at understanding the dynamics. Recent theoretical work by Shin, Wittig and Goddard[9] has highlighted the influence of the large, highly polarizable, halogen atom upon the subsequent course of the reaction. In their *ab initio* generalized valence bond-configuration interaction calculations on the $HBr \cdot CO_2$ system they find that the most favorable pathway for reaction is via a Br-C(O)-OH intermediate where the C-Br bond energy is calculated to be 63.4 kcal mol^{-1}. They advance arguments to explain the relatively cold OH distributions which they observe resulting from this reaction, in terms of the formation of this intermediate, and also suggest that formation of an analogous transient I-C(O)-OH intermediate could account

for the long lifetimes, and possibly the double exponential rise of the OH concentration.[2] These studies, while providing information relating to bulk bimolecular reactions, are possibly influenced by the presence of a third body.

A solution to this problem which still enables the establishment of a zero-of-time and subsequent time-resolved "clocking" of the reaction was recently proposed[12] and studied,[3] and is our focus here. The idea is to make the heavier atom or radical in the dissociated precursor the reactive partner, leaving the lighter fragment to rapidly depart from the scene while the bimolecular reaction between the heavier fragment and the other molecular participant in the complex proceeds unperturbed. The advantage of this method is that it enables a bimolecular reaction to be studied without the perturbation introduced in the earlier studies by the proximity of the halogen atom.

Further advantages include a much lower translational energy imparted to the reactive system, making it more sensitive to features of the underlying potential surface. In addition, the range of effective impact parameters is even more limited than in the case of a light precursor, due to smaller vibrational motions of the heavy precursor in the van der Waals cluster, and the low energy imparted from the initial photodissociation (*vide infra*). To deduce the impact parameter range, the geometry and large amplitude motions of the van der Waals precursor complex must still be known.

5.1.2 The Br + I_2 reaction and related systems.

The reaction Br + I_2 → BrI + I is calculated to be exoergic by 6.7 kcal mol^{-1} (ΔH°_{298} from bond strengths[13]). While a direct measurement of the rate of this reaction awaits determination, a pioneering crossed molecular beam study of this reaction was carried out by Lee, McDonald, LeBreton and Herschbach.[14] For an average collision energy in the center of mass frame of ~3 kcal mol^{-1} they found product IBr scattered to wide angles, and they concluded that there is little or no activation barrier to reaction, with the dominant short-range interaction being attractive. Furthermore, they proposed an "osculating complex" model[15] with a mean complex lifetime of ~5 ps, and estimated the

well depth for the $[BrI_2]^{\ddagger}$ to be ≥10 kcal mol^{-1}. This estimate for the lifetime is based on a number of assumptions which will be discussed below. However, the main points of relevance to this study are that the reaction proceeds on an essentially attractive potential energy surface via the formation of a long-lived intermediate complex. Further work by McDonald[16] reports the product translational energy distribution, which was analyzed using the osculating complex model.

A subsequent crossed beam study by Loesch and Beck[17] in which they measured angular product distributions for Br + I_2 under similar conditions is in good agreement with the work of Lee *et al.*[14] They investigated the reactions Cl + Br_2, Cl + I_2, Cl + BrI/IBr and Br + I_2, following the earlier study of Beck *et al.*[18] on the Cl + Br_2 reaction. They observed predominantly forward scattering in Cl + Br_2, I_2, and BrI (ClBr + I), increased backward intensity for Br + I_2 and nearly forward-backward symmetric scattering for Cl + IBr (ClI + Br), attributing this to a variation (in increasing order) of reaction time for these systems. They also observed energy partitioning favoring internal degrees of freedom and concluded that these reactions proceed with little or no activation barrier.

The halogen atom-molecule exchange reactions have been widely studied by crossed molecular beam techniques,[14,16-32] and were among the first to have been successfully investigated using "universal" crossed molecular beam machines with mass spectrometric detectors.[29] These reactions have relatively large cross sections (4-40 $Å^2$)[33] and appear to be dominated by attractive forces with little or no barrier to reaction.[33] Many of these, in particular F + XY reactions, have been studied by Grice and coworkers, both by crossed beam methods and theoretically.[23-28] As observed by Grice and coworkers,[23-28] Loesch and coworkers,[17,18] and other groups,[19-22] the reaction dynamics vary from "long-lived" collision complexes (e.g., Cl + IBr,[17,19,22]) via "osculating complexes" (e.g., Br + I_2[14,17]) to direct for most of the other systems studied (e.g., Cl + Br_2[14,16-21,29] or Cl + I_2[28]). In their comprehensive study of the Cl + Br_2

reaction, Valentini, Lee and Auerbach,[29] did conclude from their product recoil energy distributions at three collision energies that neither an osculating complex model nor a spectator stripping model fully describes the observed dynamics, which seem to change from complex to stripping as the collision energy is increased.

If a complex is long-lived, a "stable" trihalogen intermediate will be formed. In the gas phase, trihalogen radicals have long been understood to be important in halogen atom recombination reactions. The unusual efficiency of I_2 as a third body in I atom recombination was attributed by Bunker and Davidson[34] to the formation of a stable (by 5.3 kcal mol^{-1}) I_3 species. Porter[35] also presented evidence in support of the species. More recent gas phase kinetic studies[36-38] have also invoked a stable I_3 complex to explain experimental observations. Br_3 was observed in the gas phase by Sigrist *et al.*[39] as a result of $(Br_2)_2$ photodissociation, and Cl_3 was detected by laser-induced luminescence during Cl atom recombination in a study by Kawasaki, Sato and Inoue.[40]

In their early crossed molecular beam study, Lee *et al.*[19] comment on the stability of various trihalogen radicals, noting that radicals with the least electronegative atom in the central position are the most stable. In later crossed-beam studies of diatomic halogen reactions,[41-43] Lee and co-workers actually observed I_2F and ClIF resulting from an endoergic bimolecular reaction of F_2 with I_2 and ICl. Crossed beam studies of the F + I_2 reaction by Grice and co-workers,[23-27] along with LIF product distribution studies by Trickl and Wanner[30] and Girard *et al.*[31] have indicated the formation of a relatively long-lived FI_2 intermediate in which F atom migration takes place. In a very recent crossed-beam study, Girard *et al.*[32] were able to measure vibronic state-resolved differential cross sections for this reaction, and their overall results are compatible with FI_2 complex formation.

A number of trihalogen intermediates have been observed in matrix isolation studies, principally ClF_2,[44-48] and general agreement exists over a bent geometry with a F-Cl-F bond angle of ≥136°.[45,47] Cl_2F, BrF_2, Br_2F and possibly FI_2 have also been seen

in a matrix, but earlier reported observations of Cl_3 by Nelson and Pimentel[49] and Br_3 by Boal and Ozin[50] were later reassigned to their respective negative ions by Wight, Ault and Andrews,[51] as indicated by Jacox.[52] Several theoretical studies on the structure of the ClF_2 radical have been performed (e.g., Refs. 53-56), and there is now agreement over a bent geometry with an FClF bond angle of ~150°.

Direct kinetic measurements on halogen atom-molecule exchange reactions have been pursued in parallel with crossed molecular beam studies by a number of groups, driven in part by the need to provide independent determinations of integral reaction cross sections, which are difficult to measure accurately in crossed-beam systems.[57] Extensive studies by Clyne and co-workers of the kinetics of F atom[58,59] and Cl atom[57,59,60] reactions with halogen and interhalogen molecules show near collisional rates for almost all of these systems, consistent with reaction on an attractive potential energy surface with little or no barrier to complex formation. As expected, the rates increase gradually as the molecular partner is varied down the periodic group. Br atom kinetics have been less widely studied. Strattan and Kaufman[61] measured the rate of reaction with F_2 finding a value of 1.06×10^{-16} cm^3 $molecule^{-1}$ s^{-1} at room temperature, in accord with the other anomalously slow reaction rates of molecular fluorine with many atoms. An isotopic study of the Br + Br_2 reaction by Zaraga, Leone and Moore[62] gave a rate constant of 4×10^{-11} cm^3 $molecule^{-1}$ s^{-1} at room temperature, and Haugen, Weitz and Leone[63] found a rate constant of 4.6×10^{-11} cm^3 $molecule^{-1}$ s^{-1} for the reaction Br + IBr $\rightarrow$ Br_2 + I. In view of the observed trends, we expect that the room temperature rate constant for the reaction Br + I_2 $\rightarrow$ IBr + I studied here will be rapid, within a small factor of the collisional rate, consistent with its occurrence on an attractive potential energy surface with little or no barrier to complex formation.[64]

The influence of spin-orbit excitation on Br atom reactions has been investigated by Leone and co-workers for the reaction Br + IBr $\rightarrow$ Br_2 + I.[63,65] They found that the ground state reaction proceeded at a rate ≥40 times faster than the total rate of Br ($^2P_{1/2}$)

(Br^*) quenching and reaction with IBr. Comparison of the rate of the ground state reaction Br + Br_2 of 4 x 10^{-11} cm^3 $molecule^{-1}$ s^{-1} [Ref. 62] with that of the quenching + reaction rate for Br + Br_2 of 1.2 x 10^{-12} cm^3 $molecule^{-1}$ s^{-1} at room temperature determined by Wittig and co-workers[66] gives a similar factor of ~40. Wiesenfeld and Wolk studied the kinetics of the deactivation of I^* by Br_2 [Ref. 67,68] and found that the predominant product of this reaction is spin-orbit excited Br^*. Gordon *et al.*[69] have also studied spin-orbit effects in halogen atom-molecule reactions including the reaction Br + IBr $\rightarrow$ Br_2 + I, and proposed a conservation rule for the spin-orbit excited state, whereby the atomic spin-orbit state is not changed during the stay in the chemically bonded intermediate state. Thus the reaction of Br* with I_2 would be expected to be highly disfavored in comparison with the ground state reaction, as the pathway with spin-orbit conservation is endoergic due to the large spin-orbit splitting of I, as is found in these studies for the parallel reaction Br + IBr $\rightarrow$ Br_2 + I. Therefore any reaction with spin-orbit excited Br atoms may be discounted in the present study.

5.1.3 The technique.

The reaction is initiated by a UV pump laser pulse at 218 nm which causes photodissociation of the HBr precursor molecule, and IBr product is probed by LIF at 716.5 nm. HBr absorption in the near UV peaks near 180 nm and drops to a value of 80 liter mol^{-1} cm^{-1} by 218 nm.[70,71] The photolysis wavelength chosen for this study was a compromise between the efficiency of production of UV light, which falls rapidly in this region with decrease in wavelength, and the fall-off in absorption coefficient of HBr as the wavelength is increased.

Photodissociation of HBr at 193 nm produces 15% of Br atoms in the($^2P_{1/2}$) spin-orbit excited state.[72-74] While this proportion has not been measured for photolysis at 218 nm, it may be reasonable to assume by comparison with HI photolysis[74] that it will still be below 15% at this wavelength. Furthermore, as discussed above, reaction of I_2

with spin-orbit excited Br to yield ground state products is highly disfavored, and so can be discounted.

The HBr bond strength is listed as 87.56 kcal mol^{-1} [Ref. 13], leaving an excess energy after absorption of a 218 nm photon and dissociation, of 15,250 cm^{-1}. Considering only the (m = 79) isotope of Br for simplicity, momentum conservation dictates that the Br atom will receive only 1/80 of the total energy for HBr photodissociation, and 2/81 of the total for DBr, that is, 191 and 376 cm^{-1} respectively. This corresponds to Br atom velocities of 2.4 and 3.4 Å ps^{-1} respectively, and complementary H and D atom velocities of 190 and 130 Å ps^{-1}, indicating that the H or D atom is well clear of the reaction zone while complex formation and decay proceed.

The structure of the HBr·I_2 van der Waals complex remains as yet undetermined. Klemperer and co-workers have determined the structure of the HF·Cl_2 [Ref. 75] and HF·ClF[76] complexes by the molecular beam electric resonance technique. They find in both cases an anti-hydrogen bonded structure with a linear arrangement of the three heavy atoms. The trend for the van der Waals interaction of the heavier homologues (due to the higher polarizability of the homonuclear diatomic), suggests that HBr·I_2 is also expected to have the same basic linear, anti-hydrogen bonded structure. In any case, the energetics (low translational excitation of Br and van der Waals bonding) are such that there must be a Br + I_2 reactive channel for any precursor geometry, and only this channel is probed by the combination of laser wavelengths and filtered fluorescence used here, even if the H position is not exactly known.

The position of the light hydrogen atom is less easily predicted. Klemperer and co-workers determine an average H-F-Cl angle of 125° in the deuterated and undeuterated case. However, there is a large amplitude motion due to the bending vibration. For the case of HF·ClF,[76] Klemperer and co-workers concluded a bent equilibrium geometry (angle 125°) from the similarity of HF·ClF and DF·ClF dipole moments. While extrapolation of these results to HBr·I_2 should be viewed with caution, it is important to

note that the exact H-Br-I bond angle is not as critical in this case due to the proximity of the reagents and the low energy nature of the collision. Such is not the case in $XH{\cdot}CO_2$ (X = Cl, Br, I) hot-atom studies. The structural effects on the impact parameter are highlighted in Fig. 1 for several types of geometries, including crossed-beam, linear van der Waals cluster, the hydrogen off-axis, and a hypothetical hydrogen-bonded cluster.

For a linear, anti-hydrogen bonded complex structure of $HBr{\cdot}I_2$, the translational energy available for reaction can be calculated in the I_2-Br center-of-mass frame from the initial Br atom translational energies derived above. This amounts to 145 and 286 cm^{-1} for $HBr{\cdot}I_2$ and $DBr{\cdot}I_2$ respectively (neglecting effects of the van der Waals well discussed later). In contrast, the crossed-molecular beam studies employ available energies of the order of 1000 cm^{-1}, making them less sensitive to the lower energy features of the potential energy surface.

IBr product is probed by LIF via the $A^3\Pi_1(v'=21) \leftarrow X^1\Sigma^+(v''=1)$ transition at 716.5 nm, as observed by Selin.[77] Off-resonance fluorescence from this absorption is expected to lie principally to the red at 730 and 745 nm ($v'=21$, $v''=2,3$). The (A-X) system has also been studied by Brown,[78] but attention has primarily been focused on the visible (B-X) system, and a number of LIF studies have been carried out.[79-82] The $B^3\Pi$ (0^+) state of IBr is extensively predissociative,[80-83] and is not expected to play a role in the current study.

Our simulations of jet-cooled LIF spectra for I_2 in the 716.5 nm region indicate that there is no appreciable interference, and similarly the pump laser wavelength of 218 nm lies in a "window" in the I_2 absorption spectrum [see, for example, Refs. 84-87] at wavelengths longer than the $D(0_u^+) \leftarrow X(0_g^+)$ absorption band in the 176-200 nm region.

5.2 Experimental

The experimental arrangement can be found in the experimental chapter of this thesis. Only those details specific to these experiments will be included here.

5.2.1 Generation of the ultrafast pump and probe laser pulses

The gain medium used in the Satori was LDS722 (Exciton) in ethylene glycol, and the saturable absorber used was DDI (Exciton) in ethylene glycol. The laser was set to a wavelength of 716.5 nm, yielding 150-200 mW of light with a pulse autocorrelation of 350 fs. It was operated with this somewhat longer pulse to ensure stable operation, once the long (by the standards of this equipment) time scale of the Br + I_2 reaction had been established.

LDS750 (Exciton) laser dye in methanol was used in the first stage of the pulsed dye amplifier, followed by LDS722 (Exciton) in methanol in the last three stages to minimize ASE. The beam was focused through a 125 μm pinhole between the first and second stages: further precautions against ASE were found to be unnecessary. The 20 Hz amplified pulse energy was estimated to be ~60 μJ with ~20 μJ of ASE. For this experiment, pulse recompression was not used due to the time scales involved in the experiment.

The amplified beam was split using a pellicle beam splitter (Melles Griot uncoated 10% R/90% T or coated 30% R/70% T). The less intense reflected probe beam passed across to the optical delay section where it underwent one or two retro-reflections off appropriate reflectors mounted on the computer controlled linear stage. This in turn was mounted on the much longer low resolution manually controlled stage which facilitated location of the zero-of-time. After this variable optical delay, which required careful alignment to avoid problems of beam walk-off, the beam passed across to the molecular beam where it was focused into the reaction zone using a 50 cm fl (focal length) plcx (planoconvex) lens.

The stronger, transmitted component of the 716.5 nm beam was focused into a 1 cm path length, quartz cell containing D_2O (Aldrich). This provided a white light continuum, which was recollimated and directed through a 460 nm, 10 nm FWHM, interference filter (Corion) tilted to shift its center wavelength to 436 nm. The resulting

low intensity beam (estimated pulse energy ~50 nJ) was reamplified in three stages--side pumped by 355 nm laser light from the Q-switched Nd:YAG laser. The dye used was Coumarin 440 (Exciton) in methanol, and the radical scavenger diazabicyclo[2.2.2]octane (DABCO; Kodak) was added to prolong the dye lifetime. Even so, initial experiments were hindered due to a dye lifetime of one hour or less: increasing the dye volume, purging the solutions with nitrogen, and minimizing the 355 nm pump laser intensity, together enabled continuous runs of twelve hours or more, however.

The pulse energy of the second amplifier was measured as ~40 μJ amplified light and ~20 μJ ASE (the latter was essentially eliminated in the frequency doubling process). Again, pulse recompression, while provided for, was not used at this stage. The 436 nm beam passed over to the molecular beam apparatus, where the second harmonic was generated using a 300 μm thick BBO crystal (β-barium borate; Cleveland Crystals) placed about 1 cm before the focus of a 15 cm lens. The doubling efficiency at this wavelength appeared to be quite low, and the estimated pulse energy at 218 nm was ~1 μJ. An interference filter transmitting 35% at 218 nm (Acton Research) was used to check the intensity of the UV beam by blocking the fundamental. It was not used during the experiments in order to maximize the signal: tests were carried out with the residual 436 nm beam present to ensure that this had no influence on the results. The 218 nm beam was recollimated and focused into the chamber via a 50 cm fl plcx UV lens after reflection off a dichroic, beam combining, optic. Both beams entered the apparatus with vertical polarization.

5.2.2 Characterization of the pulses and the zero-of-time

The pulse width of the unamplified 716.5 nm beam was monitored by the real time scanning autocorrelator. Pulse widths of 350 fs were observed. The frequency tuning of the laser was controlled with reference to a monochromator/PMT set to 716.5 nm. The amplified beam pulse autocorrelation was determined using the linear stage and a 100 μm KD*P crystal; a FWHM of 380 fs was observed.

The main method used for characterizing the laser pulses was cross-correlation between the 218 nm pump and the 716.5 nm probe. This was achieved[88] using (1+1) photoionization of N,N dimethylaniline (Kodak) in a small ionization cell with an entrance window identical to the one on the reaction chamber--anti-reflection coated in the same batch. After alignment of the beams through the external pinhole, this cell was placed just in front of the focus, and a 9 V bias applied across the electrodes. The output current was amplified by a sensitive current-to-voltage converter (Keithley), and monitored by a boxcar integrator (PAR) interfaced to a computer.

Cross correlations were obtained by recording this signal as a function of translation stage position, and converting position to time delay via a previous calibration. The signal obtained was a combination of a very small steady state"step function" signal combined with a much larger peak. Presumably, the transient nature of the signal was due to extremely rapid IVR (intramolecular vibrational relaxation) within the molecule. Initial experiments with a recompressed 716.5 nm beam gave shorter cross correlation widths than were later determined for pulses used in the experiments described here, and so we are confident that the ionization peak well represents the cross correlation function of the two pulses, as well as providing an accurate indication of the zero-of-time. Spectra of the 716.5 and 436 nm beams yielded a time-bandwidth product 2-3 times the transform limit, due mainly to lack of recompression. It was not possible to take the spectrum of the 218 nm pump beam; its frequency bandwidth would be reduced with respect to the 10 nm FWHM 436 nm beam as a result of the limited acceptance angle of the BBO doubling crystal.

5.2.3 Formation and characterization of the $HBrI_2$ complex

The heatable pulsed valve was used for these experiments. This valve utilizes a solid sample reservoir attached to the front plate; a channel in the plate led from this external chamber containing I_2 to the gas stream just before the orifice. Two heating elements and a thermocouple mounted on this plate enabled the whole assembly to be

maintained at 160° C via an external temperature controller (Omega). It is estimated that the temperature of the I_2 reservoir, which was in good thermal contact with the face plate, would have been 10-20° C below that of the main assembly, thus ensuring that the valve did not clog with condensing I_2.

Both the duration, and pre-delay of the gas pulses with respect to the lasers were adjustable externally, and it was found that the clustering efficiency was very sensitive to these adjustments. The valve was operated with a ~400 μs pulse, and the time delay between the opening of the valve and the arrival of the laser pulses adjusted to optimize the concentration of the cluster at that time. He (Liquid Air) and HBr (Matheson) or DBr (99% isotopic purity; Cambridge Isotope Laboratories) were supplied from the external gas mixing manifold where their flows were limited by mass flow controllers (MKS), to a ratio of typically 3 sccm (standard cubic centimeters per minute) H(D)Br to 20 sccm He, though this was adjusted to maximize the $HBr{\cdot}I_2$ cluster signal. The backing pressure was monitored and was maintained in the range 1800-2600 torr. A typical example of an EI-TOFMS, after optimizing for $HBr{\cdot}I_2$ concentration, is shown in Figure 2.

5.2.4 LIF collection and signal processing

The laser beams, focused to an approximately 300 μm beam waist, intersected the molecular beam 20 mm downstream of the nozzle--corresponding to an X/D of 40. The emission, due to IBr, passed through a Schott RG9 filter to block light to the blue of 720 nm (the monochromator was not installed at this point). It was estimated that on-resonance LIF at 716.5 nm, along with laser probe scatter, would be cut by 50%, but background scatter and fluorescence resulting from the 218 nm pump beam would be cut dramatically. Another plcx lens (5 cm diameter, F/1.5) focused the fluorescence onto an adjustable slit to further discriminate against scattered light. Another F/1.5 lens recollimated the light and a final F/1.5 lens focused it onto the photocathode of a GaAs single photon counting PMT (Hamamatsu R943-02, chosen because of its high efficiency

in the near infra-red), mounted within a thermoelectrically cooled housing (Products For Research).

The signal was collected via the photon counter with the gate set to count typically from 0.5 to 3.5 μs after the arrival of the laser pulses. The counts were accumulated for 20 to 40 laser shots and fed to the computer via the RS-232 interface.

5.2.5 Signal Optimization

After optimization of pump and probe laser beam intensities and overlap, $HBr \cdot I_2$ mass spectral intensity, and pulsed valve delay time and width, a total photon count rate of 1-2 per pump/probe laser shot was obtained. Final optimization was carried out while monitoring the count rate with the optical delay set to its maximum value for the combined pump/probe beams.

The background was found to arise almost entirely from the UV pump beam, rather than the red probe beam or residual 436 nm fundamental of the doubled pump beam. While it does appear that the UV pump wavelength of 218 nm is in a "window" in the I_2 absorption spectrum, at these low count rates and high overall I_2 concentrations, even a very small absorption cross-section could result in such a background. This background signal was also observed with no HBr present. Girard *et al.*[31] observed intense fluorescence at wavelengths below 495 nm using a supersonic I_2 beam, but found this to be much reduced in a quasi-effusive beam, attributing this effect to $(I_2)_2$ formation. In our early experiments[3] we were able to detect some $(I_2)_2$ in our mass-spectral scans, and an experimental transient with a rapid rise time of ~5 ps was obtained with I_2 alone. However, under the optimized conditions employed here, no $(I_2)_2$ mass spectral peak could be seen, and no enhancement of signal over background was observed with I_2 alone.

To trace the origin of the signal to the $HBr \cdot I_2$ van der Waals cluster, enhancement was monitored as a function of the monomer, dimer and multimer concentrations. Enhancement was not observed with I_2 or HBr alone, and was found to be very sensitive to the concentration of $HBr \cdot I_2$ cluster as observed by TOFMS with both I_2 and HBr

present, but at low (<15% of $HBr{\cdot}I_2$) concentration of larger clusters, confirming its origin from the mixed dimer.

5.3 Results and Discussion

5.3.1 The lifetime of the collision complex

Our results for $HBr{\cdot}I_2$ and $DBr{\cdot}I_2$ are presented in Figures 3 and 4, and comprise weighted composites of several scans. Risetimes τ_{cc} (assumed to be exponential, see below) of (53 ± 4) ps and (44 ± 4) ps, respectively, were determined using non-linear least-squares analysis of the data, standard deviations being quoted at the $\pm 2\sigma$ level. All individual scans also showed this risetime difference. The DBr precursor reaction, leading to more energetic Br atoms, is seen to be significantly faster than the HBr precursor reaction.

These observations provide direct information about the collision complex: (1) The triatomic species $[BrII]^{\ddagger}$ is very stable on our (femtosecond) time scale, reflecting a "sticky" collision in the $Br + I_2$ encounter; (2) the observation indicates the presence of a well in the transition state region, capable of supporting a stable BrII molecule, and an exit channel barrier (see below) which significantly affects the threshold dynamics; (3) there is no entrance channel barrier, as evident from the threshold measurements and discussed below.

The threshold collision complex lifetimes allow a number of conclusions to be drawn about the well depth, possible barriers in the entrance and exit channels, and a number of other important features of the PES. In the following sections we shall focus our attention on the nature of bonding, the PES, the dynamics (via classical trajectories), and comparison with other methods for studying the dynamics.

5.3.2 Bonding in the collision complex

Parallel to experimental investigations, halogen atom--molecule exchange reactions [A + BC] have received a considerable amount of theoretical attention. For some of the

lighter trihalides, ground and excited electronic states have been calculated at the SCF or CI level.[55,56,89] For the heavier trihalides (X=Br,I), various semiempirical methods have seen continued application, due to the difficulties in dealing with many-electron systems by more rigorous methods.[54,90-94] For Br and I, spin-orbit coupling is an important contribution to the electronic energy, resulting in large splittings between electronic states that would otherwise be degenerate. Nonetheless, only the I_3 system has been studied by a relativistically corrected calculation.[95] In what follows, we shall first consider a nonrelativistic schematic of the contributing orbitals, which will then be followed by some more detailed considerations.

Consider the approach of a bromine atom ($4s^2\ 4p^5$) to an iodine molecule (n=5 valence shell) to form an open-shell 21 electron triatomic system. For the diatomic I_2, the MOs are the usual linear combinations of valence s and p orbitals (Fig. 5), which form the configuration $\sigma_g^2(s)\ \sigma_u^{*2}(s)\ \sigma_g^2(p_z)\ \pi_u^4(p_{x,y})\ \pi_g^{*4}(p_{x,y})$. The HOMO of the halogen molecule is therefore the π_g* while the LUMO is the σ_u* (p_z). The MOs of the complex BrI_2 (or more generally XY_2) form depending on the relative energies of the *ns* and *np* orbitals for X and Y. For light systems (e.g., ClF_2 in Fig. 5) the 2*s* orbitals of the F atoms are separated in energy, but the 3*s* orbital of the Cl atom is fairly close in energy to the fluorine 2*p* orbitals (Fig.5). Accordingly, there is extensive mixing between the chlorine 3*s* and the fluorine $2p_z$ orbitals. The MOs take on the form familiar in the literature,[23] and the odd electron resides in the σ_g* orbital. The bond order can be deduced by considering the nature of the orbitals (bonding (b), antibonding (*), or nonbonding (nb)) and in this case it is 1.5 (larger than the initial bond order of unity in F_2 + Cl). The LUMO will be of interest later in discussions of the frontier orbitals.

In "heavier" systems (e.g., IBrI), the *ns* orbitals are closer together and the *s-p* mixing is not as large. Consequently, the *s* orbital sub-system will mostly mix separately from the *p* sub-system. The MOs of the complex are shown in Fig 5. The nature of the

(b), (*), or (nb) character of the orbitals changes, and in fact for the same 21 valence electron system, the bond order could range from unity (if the σ_g(nb) lies at higher energy than the π_u* orbital) to 1.5 (in the reverse case). For asymmetric systems like BrI_2, the *u* and *g* symmetry labels are no longer valid, and a general numbering of the orbitals (which may now have asymmetric shapes discussed below) emerges, as shown in Fig. 5.

For the case of interest to us here (Br + I_2), the collinear approach will lead to a complex of the form BrII. The bond order depends on the composition of the 5σ orbital. Since the complex is not symmetric around the central atom, the 5σ orbital can be viewed as a linear combination of two orbitals formed by combining p_z orbitals of all three atoms (Fig. 6a), where one of the orbitals is bonding on the I-I and anti-bonding on I-Br, and vice-versa for the second one. When the coefficients $c_1 = c_2$ for symmetric systems (e.g., IBrI), the combination yields the nonbonding orbital shown in Fig. 5.

From the above discussion, it appears that the complex bonding in the nonrelativistic limit involves the σ system, and this simple picture is consistent with Fukui's frontier orbital approach.[96] The LUMO of I_2 is the σ_u*. If we consider the reaction as resulting from a transfer of charge density from the attacking atom Br HOMO (p_z in this case) to the LUMO of I_2, then we have, as shown in Fig. 6b, the completely anti-bonding orbital (6σ) and an orbital which is bonding on I-Br and has a node on the I-I (the $c_2 = 0$ limiting case). (Interestingly, side-on attack is predicted to have a higher energy barrier, neglecting spin-orbit excitation, since the net overlap is zero.) This latter orbital is a good zero-order description for the reaction: bond formation (I-Br) and bond breakage (I-I). Herschbach's description[97] of these halogen reactions in crossed-beam experiments is simply to make the σ and σ* orbitals shown in Fig. 6c, and one can now see the importance of the frontier orbitals. Furthermore, the analogy between X + Y_2 and hν + Y_2 reactions can now be physically understood: both create a node on the Y-Y bond. The effect of electronegativity of the atoms involved can also be appreciated. Since the

LUMO of the halogen molecule is anti-bonding, the orbital will be localized on the atom least in electronegativity, and the reacting atom will attack at such a point.

These observations are also supported by ab-initio calculations and more detailed considerations involving spin-orbit coupling; while some of the simpler calculational methods predict saddle points or very shallow wells for X_3 or XY_2,[98-101] more recent (semi-empirical/SCF/CI) calculations show that many trihalides have a bound ground state PES with a well-defined equilibrium geometry.[53,55,56,89] Consider Cl_3 as an example: one DIM (diatoms in molecules) study concludes that the molecule has only a saddle point on the ground state surface,[100] while the PES used by Thompson (based on the London equation)[102] shows a small symmetrically located well. LEPS and Sato surfaces from Ref. 101 show behavior ranging from saddle points to deep wells (8 kcal mol^{-1}). CNDO/2 and INDO calculations indicate a stable symmetric well (or a late well for some XY_2 species),[54,93] as do the available SCF/CI calculations (but the latter did not systematically sample the antisymmetric stretching mode).[89]

The consensus seems to be that the stability increases with heavier atoms, and decreases with the more electronegative atom located centrally in the case of asymmetric clusters, with only the most extreme cases of the latter showing a saddle point. The well is located near symmetrically or possibly 'late' in the exit channel of the heavier halogen atom. For several XY_2 clusters, stability has been verified experimentally by the analysis of infrared spectra in matrices,[48] and for others, beam scattering studies strongly suggest a bound ground state.[14,17,41-43]

5.3.3 Potential energy surface

Figure 7 represents a schematic view of a cut through the PES along the reaction coordinate and Fig. 8 shows the orbitals (including spin-orbit coupling) of the complex for different bond angles. To relate the dynamics on the PES to the experimental results reported here (real time studies of the collision complex) and to results reported earlier (scattering studies of the products), more quantitative features of the potential must be

considered. Several empirical approaches have been tested in the literature to generate model potentials for A + BC collision studies. One of the earliest models is the LEPS surface for collinear studies, which relies on the London formula. These surfaces have been used to unravel the nature of repulsive and attractive energy release, and the dependence on the location of the transition state along the reaction coordinate.[103] In a different approach, the total potential energy is represented by a sum of 'diatomic' Morse potentials, turned on and off at various internuclear distances via the use of a switching function.[104] A representation was also given in terms of a single Morse potential, with the dissociation energies and vibrational frequencies interpolated from reactants to products by a hyperbolic function along the collinear reaction coordinate.[105] For some collinear PESs a Morse potential was rotated about a point along the symmetric stretching coordinate in the r_{AB}-r_{BC} plane, varying the well depth and other parameters as a function of the rotation angle to yield a collinear PES.[106] Some of these PESs have been extended to include the bending mode, although not necessarily in a qualitatively correct global manner.[105]

We have chosen a somewhat different parameterization, which is more easily and symmetrically extended from two to three coordinates, and based on our previous studies of HgI_2[107] and our initial report on BrI_2.[3] Our goals were a fully symmetric treatment of all three diatom + atom limits, globally correct qualitative (or, if potential parameters can be determined with sufficient accuracy, quantitative) behavior for any location of the atoms. Likewise, we wanted easy constraint of parameters derivable from other sources (e.g., vibrational frequencies and dissociation energies of the diatomics), and easy adjustability of parameters that can be approximately determined by comparison to the experimental data (e.g., barrier heights, complex well depth or vibrational frequencies). Table I summarizes the various coefficients in the PES formula (seeAppendix), with a brief description of the physical meaning of each. In the present calculations, it was also necessary to introduce an exit channel barrier to reproduce the observed long lifetimes

(see Appendix for further details), and its parameters are also listed at the end of the table.

Fig. 9 shows a 3-D plot of the optimal PES for θ =150°; fig. 10 shows the PES at four different values of θ_3 (corresponding to a BrII rather than an IBrI complex), with the parameters given in Table I; this corresponds to one of the 'best fit' potentials discussed in the next section, with a significant well, an exit channel barrier, allowing only a small amount of interconversion near the reaction threshold to a less strongly bound IBrI conformer, and an equilibrium bond angle fixed near 150°.

5.3.4 Dynamics

A number of workers have reported classical trajectory calculations on trihalogen complexes. Thompson has performed Monte-Carlo trajectory calculations for $X + X_2$ (X = Cl, Br, and I) on surfaces based on the London or LEPS formalism.[102] In all three cases, the PESs contain shallow wells, and produce at least some long-lived trajectories indicative of a collision complex. Collisions of F with heavier halogens have been extensively discussed in the literature. The surface used by Fletcher and Whitehead contains a very shallow well, but they nonetheless find a symmetrical scattering distribution indicative of the formation of collision complexes.[106] Urrecha *et al.*[108] have studied the dynamics of the F + ICl reaction on surfaces with a 'late', deep well (31 kcal mol^{-1} with respect to reactants for attack on the I atom) and find lifetimes of up to 6 ps.[26] This results in a number of vibrational periods of the complex comparable to what is found in the present study, due to the smaller reduced mass and stronger bond in the FICl complex model than in the BrI_2 case. Finally, Borne and Bunker have reported three dimensional calculations on Br + I_2 on a variety of 'early' and 'late' surfaces.[109] They concluded that a potential well of 5-10 kcal mol^{-1} does not strongly affect the scattering angles, indicating the absence of long-lived complexes. This is in contrast to a later study by Fitz and Brumer, which shows that, as in the case of other trihalogen complexes, inclusion of a well in the PES results in the formation of collision complexes.[109]

In the present case, integration of Hamilton's equations of motion was carried out in space-fixed or triatomic center-of-mass coordinates, using a Bulirsch-Stoer routine with adaptive stepsize supported by an adaptive 4^{th} order Runge-Kutta method near singular points.[110] The stepsize was typically on the order of 0.5 to 5 fs, with an accuracy of at least one part in 10^7 per step. Trajectories were tested in a number of ways: energy conservation was enforced for all trajectories to 5 parts in 10^6 between beginning and end points. It was found that even at the maximum precision ($1{:}10^9$) of the integration procedure, trajectories could not be back-integrated reliably after more than 10 ps, where the accumulated deviation amounted to ~0.02 Å. This is due to the chaotic nature of the trajectories, and because of ergodicity does not effect averaged quantities (e.g., lifetimes) even at t larger than 10 ps.[111]

We now consider the results for reactions starting from the van der Waals impacted geometry, followed by calculations simulating crossed-beam scattering experiments .

5.3.4.1 Reactions from van der Waals impacted geometries

For the van der Waals precursor calculations, the following Monte Carlo selected initial conditions were used: the I_2 molecule was held in $v = 0$, with a random vibrational phase and zero space fixed angular momentum. The Br atom was placed near-collinearly at 5.47 ± 0.1 Å/ps from the I_2 center of mass with a small Gaussian spread in the plane normal to the I-I bond, corresponding to the non-axial intramolecular vibrations in the van der Waals precursor. The Br was given an initial velocity of 2.4 ± 0.1 Å/ps (HBr precursor) or 3.4 ± 0.1 Å/ps (DBr precursor) in the space-fixed frame. It was mentioned earlier that the equilibrium geometry of the complex is particularly uncertain as regards to the distribution of hydrogen orientations. Two types of calculations were carried out--with the most probable initial Br velocity vector oriented either along the Br-I-I axis, or at 55° from it. The large amplitude motion of the H was accounted for by a Gaussian spread of 12.5° HWHM (for the HBr case, correspondingly smaller for the DBr case). Where

appropriate, 2σ Monte Carlo uncertainties, derived by randomly binning trajectories into subsets and calculating standard deviations, are quoted.

Depending on whether the van der Waals kinetic energy was assigned randomly to the Br atom or not, trajectories ran either with an energy spread of ~20 cm^{-1} or ~150 cm^{-1}. The latter has the effect of smoothing somewhat the lifetime as a function of energy, but since the lifetime is still a sufficiently slowly varying function of energy in the region of interest, and considering the uncertainties inherent in the PES itself, small differences in the sampling of initial conditions were not found to lead to quantitatively significant differences. In either case, the reaction energy is somewhat below the threshold value possible in a scattering experiment, resulting in a "trapped" reaction with 100% reaction probability.

Table II summarizes typical results for the complex lifetimes (HBr precursor) as a function of the dimensionality of the PES, the well depth, and the exit channel barrier height. It can be seen from the barrier-free calculations, that the addition of the bending mode increases the lifetime of the complex by about a factor of three. However, it alone cannot account for the experimentally observed long lifetimes for any physically reasonable value of the well depth (25 kcal mol^{-1} with respect to reactants).

An exit channel barrier is required to reproduce lifetimes longer than about 10 ps, even close to the reaction threshold. Barrier heights between 2 and 4 kcal mol^{-1} (with respect to I + IBr), dependent on the depth of the well, yield the observed 50 ps lifetime for the HBr precursor reaction. There is clearly an indeterminacy, with lower barriers and deeper wells yielding similar results to higher barriers and shallower wells. In the extreme case, the complex can of course be trapped for an arbitrarily long time even in a very shallow well (measured with respect to the reactants).

This indeterminacy can be removed by considering the reaction at two different energies, as provided by the HBr and DBr precursors: the calculations now have to predict not just $\tau_{av} = (\tau_{HBr} + \tau_{DBr})/2$, but also the difference, τ_{HBr}-τ_{DBr}. For a very

shallow well to result in a 40 ps lifetime for the DBr case, the barrier height must be only slightly below the reaction energy. The HBr precursor trajectories would then be trapped, or at least much longer-lived than observed. On the other hand, for a very deep well and small barrier, the two precursors would result in nearly identical behavior, since an energy difference of only 145 cm^{-1} in the center of mass system, given a well of several 1000 cm^{-1} and an exothermic reaction, will have no pronounced effect on the lifetime.

This is illustrated in Table II, which shows trajectory lifetimes for HBr and DBr precursors for various well depths and barrier heights. We find that for a collinear approach geometry, a well depth of about 16 kcal mol^{-1} and a barrier height of about 3.3 kcal mol^{-1} yield the best agreement. For a 55° average approach angle, the lifetime increases by about 20% for a given set of potential parameters, and the best agreement with experiment is obtained for a well depth of about 15 kcal mol^{-1} and a barrier height of about 3.0 kcal mol^{-1}. These results are very similar to those we reported in a previous communication, using a different (r_1, r_2, θ rather than bond distance) parameterization of the PES.

Indeed, we find that the above results are relatively insensitive to the exact form of the PES used. Several trial PESs with a tighter or 'later' complex geometry (smaller r_{e1} value), different vibrational frequencies (β_{1i}) and different attainment of the asymptotic limits (γ), different barriers to rearrangement (IIBr to IBrI, D_1 and D_2) resulted in less than a 30% change in the lifetime, or well depths in the range 13-17 kcal mol^{-1} and barriers in the range of 3-4 kcal mol^{-1}.

The given ranges for the barrier and well are probably indicative of the accuracy of the QCT results. It should be noted that in order to reproduce τ_{HBr}-τ_{DBr} properly, the barrier height must be adjusted to a precision of 0.1 kcal mol^{-1}. The accuracy of this value will nonetheless be considerably lower (1 kcal mol^{-1}), as the nature of the I_2···Br attractive potential in the 4-5 Å range determines the initial reaction energy with respect to the products. As it changes by a few hundred wavenumbers, so must the exit channel

barrier to accommodate the experimental observations (e.g., while the present observations do not allow for a fully developed barrier in the entrance channel, an incipient barrier would raise the starting energy of the trajectories).

The above calculations were done with relatively large barriers to interconversion, typically allowing only 1-10% of trajectories to lead to the formation of the IBrI configuration. With very low barriers, the lifetime for a given exit channel barrier was lowered due to the shallower well of the symmetrical species. Should the interconversion probability be very high, the above results must be taken as averages over the available configurations, instead of reflecting the nature of a single potential well. Detailed *ab-initio* calculations will be required to resolve this problem.

Fig. 11 shows simulated transients for both the HBr and DBr precursor cases (conditions marked by an asterisk in Table II). They can be fitted by single exponentials, resulting in lifetimes close to those observed experimentally. The present Monte Carlo sampling is not yet accurate enough to reveal structure in the transients. The transients shown are for all vibrational levels, but since the $v = 1$ population amounts to half the $v = 0$ population (see below), multi-exponential behavior would be evident in the transients if the lifetime were strongly vibrationally dependent.

We have also investigated the possibility of off-resonant transients probing the BrII complex before complete separation into products occurs. To simulate a probe window, trajectories were weighted at each point in time by a Gaussian function located in the non-asymptotic range of the exit channel (near $r_{Br\text{-}I} = 2.47$ Å, $r_{I\text{-}I} = 3.9$ Å). The detuned transient is shown in Fig. 12. With only a fraction of the IBr molecules probed unperturbed, an "exponentially" decaying transient is observed, which levels off to a small non-zero value at long times. This falling transient resembles the statistical decay of the parent in a unimolecular process, but with a risetime limited by the complex formation time (0.5-1 ps). This 'quasi-unimolecular' behavior of the BrI_2 complex is to be expected, since the lifetime of the trihalogen is much longer than its 'preparation' time via the

reactive collision event. Otherwise, at least a biexponential would be required to fit the sequential formation and decay processes. The structure on the decay transient falls within the 2σ Monte Carlo limits of the simulation, although the possibility of structure on the decay transients, as on the rising transients, cannot be discounted, and might be observed in experiments.

Fig. 13 shows the change with time of the three bond coordinates for a typical trajectory, and Fig. 14 its power spectrum (obtained by Fourier transforming and summing the time series for the three bond coordinates), revealing a broad peak near 90 cm^{-1}. This regularity is due to the fact that the complex is still strongly bound in the symmetric stretching coordinate (by approximately the bond energy of I_2), although it is unbound in the antisymmetric normal coordinate. Due to the latter, the level density of quasibound 'symmetric resonances' (estimated to be ~10 cm^{-1} wide from Fig. 14) is high, which may mask the observation of an energy dependent resonance.

5.3.4.2 Reaction from fully impacted geometries

In addition to calculations near threshold, we have also performed QCT simulations of scattering experiments. Initial conditions were chosen in the standard way. The exact beam conditions are generally not stated in the literature, but the following should represent a reasonable approximation. The I_2 molecule was placed with its center of mass at the origin in $v = 0$, with a rotational temperature of 100 K and random vibrational phases and spatial orientation. The Br atom was set to approach with a Laval-type compressed thermal distribution (average space-fixed velocity 6.4 Å/ps) of translational energies,[16] similar to the conditions reported in Ref. 14. Impact parameters were sampled with the standard radial weighting factor up to 10 Å; at larger impact parameters, the reaction probability became negligibly small. At nearly 1000 cm^{-1} above the reaction threshold, the role of the exit channel barrier in the complex lifetime drastically decreases: we found an average lifetime of 8 ps. Comparing with Table II, this is similar to the value obtained at threshold with a 15 kcal mol^{-1} well, but no exit channel

barrier: at higher reaction energies, the effect of the well is thus still felt undiminished, resulting in a shorter lived complex, while the influence of the barrier has dwindled. The fact that the shorter lifetime is not due to the larger impact parameters in the scattering experiments is further supported by simulations under scattering conditions, but near threshold, which also show long lifetimes (30 ps). The smaller importance of the barrier at higher energies satisfactorily explains the (potentially) shorter lifetimes observed in the crossed-beam experiments (see below for a discussion of the crossed-beam lifetime estimates).[14]

5.3.4.3 The reaction at the asymptote

We have also calculated several asymptotic quantities, such as the translational energy distribution and the vibrational and rotational energy distributions. These are shown in Fig. 15 for the DBr precursor (The HBr curves are very similar), with and without a 3 kcal mol^{-1} exit channel barrier and a well depth of 15 kcal mol^{-1}. The product relative translational energy distribution shows marked threshold behavior, due to the presence of the exit-channel barrier. Correspondingly, the vibrational product distribution is much colder in the barrier case ($T_{eff} \sim 380$ K for $v = 0,1$, even lower for higher v states), since more energy is channeled into the translational degrees of freedom. The rotational temperature of the IBr released by the reaction is very similar, about 420 K. It would be interesting to perform experiments probing different IBr vibrational levels, to confirm the relatively cold product state distribution and the non-statistical behavior evident in some of the distributions.

Fig. 16 shows similar results for the scattering simulations. The relative I-IBr translational energy again shows threshold behavior in the case of an exit channel barrier, confirming tentative previous results (Fig. 17).[16] The distribution is much broader towards higher energies than in the threshold case, due to the ~3 kcal mol^{-1} higher average reaction energy. As expected, the distributions are somewhat 'hotter' than those calculated for the threshold case.

5.3.5 *The Lifetime from crossed-beam experiments*

The difference between the measured near-threshold complex lifetimes presented here and higher energy (1000 cm^{-1}) estimated values based on beam experiments, merits more detailed consideration. The lifetimes from scattering studies are obtained from the scattering asymmetry, with an estimated rotational period of the complex as a benchmark, as shown by Herschbach's group. To relate the lifetime to the scattering asymmetry, a simplified long-range potential and a number of other assumptions must be invoked in the analysis .

In somewhat more detail, the procedure adopted by Lee *et al.*[14] and McDonald[16] can be summarized as follows. At the larger impact parameters prevalent in scattering studies, the formation of a collision complex is postulated to depend on crossing the centrifugal barrier in the long range part of the effective interaction potential,

$$V_{\text{long}}(R,L) = \frac{L^2}{2\mu R^2} - \frac{C}{R^6}. \tag{5.1}$$

This approximate potential has a centrifugal barrier whose height W_L depends on the angular momentum $L = mvb$ (b is the impact parameter, L is the diatom-atom reduced mass, v the relative velocity):

$$W_L = \frac{L^3}{3\mu^{3/2}(6C)^{1/2}}. \tag{5.2}$$

At a given collision energy $E = \frac{1}{2}\mu v^2$, only trajectories with $E > W_L$ can clear the barrier and lead to a collision complex. There is thus a maximum value of the angular momentum (L_m) beyond which $W_L > E$ and no reaction occurs. For impact parameters b larger than $b_m = L_m/\mu v$, no collision complex is formed.

The idea is that for "long-lived" complexes, the scattering distribution $I(\theta)$ will be "forward-backward," while "short-lived" complexes should display an asymmetric scattering distribution $I'(\theta)$. The cross-over occurs when the lifetime τ_{cc} is comparable to

the rotational period τ_r of the complex--Herschbach's osculating complex model. In the simplest limit,[113] this can be approximated by

$$\tau_r \approx \frac{2\pi I^*}{L_m} \tag{5.3}$$

assuming a quasilinear complex with a moment of inertia I*. This is only a lower limit, since $L < L_m$ for many impact parameters.

More rigorously,[16,114] the total angular momentum of the complex will be $\mathbf{J} = \mathbf{L} + \mathbf{J}$, where J is the internal angular momentum of the reactants, and usually $\mathbf{J} = \mathbf{L}$. If one then postulates a *nearly collinear* collision complex, which can be approximated by a prolate, nearly symmetric top, uses a Boltzmann distribution for J, and assumes a *cutoff* for $\mathbf{J}$ given by L_m, one can derive an angular distribution. As the lifetime of the collision complex becomes longer than the rotational period, it becomes very difficult to deduce it from angular distributions. In scattering experiments, if the complex is "long-lived," the standard method is to increase the collision energy and observe the change in angular distribution. In some reactions, however, distributions do not follow the expected long to short lifetime change.[115] Comparisons between real-time data and crossed-beam results will be useful as one examines the collision complex dynamics and asymptotic regions of the reaction.

In the case of Br + I_2, some asymmetry was observed, indicating that the complex lifetime may be comparable to, or slightly larger than, its averaged rotational period (see Fig. 12). This leads to a lifetime on the order of 5 ps at a calculated excess energy of ~1000 cm^{-1}, since this corresponds approximately to the calculated effective rotational period of the "quasi-linear" complex after thermal and impact parameter averaging.[14] Our QCT calculations indicate a lifetime of 8 ps under these conditions, and show that the drastic shortening of the lifetime between (sub)threshold conditions and 1000 cm^{-1} is likely due to less sensitivity to the exit channel barrier at higher energies. Nonetheless, the well at the activated complex geometry still plays an important role even at 1000 cm^{-1}, since

otherwise a lifetime ~3ps would be expected. Since the crossed-beam study probed the reaction in a regime where the lifetime was almost too long for a reliable estimate based on the "osculating complex" model outlined above, further time-resolved studies with R-Br molecules resulting in higher translational energies of the bromine atom will be required to fully reveal the dependence of complex stability on reaction energy.

5.4 Conclusions

We have described the real-time technique we used for the determination of collision complex lifetimes of isolated bimolecular reactions, down to the 300 fs timescale, or better if necessary. This improved temporal resolution may well be required for the study of reactions which proceed via a shorter lived collision complex or even directly. The choice of binding partners to the precursor atom or radical opens up a wide energy range from threshold on up for direct time-resolved studies of such reactions.

The near-threshold information is sensitive to features on the PES, and allows one to study the effect of bonding (e.g., entrance or exit channel barriers, stable complex wells), on the reaction dynamics. The presence, absence, or quantitative nature of these effects can be studied, particularly if the time-domain data is combined with the wealth of available spectrally and spatially resolved experiments. As shown for the example given here, Br + I_2, the collision complex lifetime is directly related to the nature of the PES in the transition state region, and trajectory calculations[116] help elucidate the nature of the dynamics.

There are several improvements that we can add to a study of this type in the future. When off-resonance (complex) detection is made and the signal-to-noise ratio is improved, we may be able to resolve "structure" on the transients (steps, beats, biexponentiality or long-tail effects). Secondly, extension to other families of halogens, as was made in the pioneering crossed-beam studies, would be very valuable. Of particular interest is the study of light atom reactions with halogens in analogy with Polanyi's[116]

chemiluminescence, and photon + halogen, in analogy with Wilson's and Herschbach's studies. On the theoretical side, the calculation presented so far was classical, and future quantum calculations may indicate long-lived resonances[117,118] that have an overall effect on the lifetimes.

5.5 Appendix

When developing the model PES for this system, the following factors were taken into account.

1. There are 3 electronic states generated from the combination of a ground state atom and a ground state diatomic molecule. One state correlates to spin-orbit excited Br, which is unimportant due to symmetry considerations (see below). Another state is expected to have an entrance channel barrier and a shallow well (see Fig. 7). This leaves only one state to consider.

2. Based on Fig. 8 one can derive a strong propensity rule, as found experimentally in Ref. 62-69 and discussed in Ref. 95: due to the non-crossing rule for states of the same symmetry, and since Br* and I* both have $\Gamma_{1/2}$ symmetry and lie at higher energy than the $\Gamma_{3/2}$ ground state, *the reaction* $Br^* + I_2 \rightarrow BrI + I$ *is not allowed* via a bent complex, and allowed in the linear case only when a crossing of $\Gamma_{1/2}$ and $\Gamma_{3/2}$ states occurs.

3. Theoretical studies indicate that the complex should be linear or slightly bent (typically 150°) for XY_2 or X_3.[53,55,56,93] These results have been confirmed by more recent experimental reassignments of matrix-isolated IR spectra of trihalides.[48] As expected, the calculated barriers to linearity are fairly small in most cases, typically ranging from 1.5 kcal mol^{-1} (in I_3)[95] to 4 kcal mol^{-1} (in F_3)[94] and 2-6 kcal mol^{-1} (Cl_3).[89]

4. The presence of entrance or exit channel barriers has been debated theoretically.[101,108,119] However, the results from scattering experiments and this work suggest that there is not a signficant entrance channel barrier but a signficant exit channel barrier is present.

5. The complex with the less electronegative atom in the middle is expected to be more stable than alternate conformations.[97,120] Therefore, we have generally kept the interconversion barrier high enough so that the "insertion"configuration plays only a minor role.

The potential is expressed in terms of the three bond coordinates, rather than two coordinates and a bond angle, to emphasize the symmetry between the three different possible reactant combinations, complexes, and product combinations. The coordinates and numbering scheme are shown in Fig. 18. The general basis of our approach is a combination of a single global Morse potential with exponentially interpolated parameters,

$$V(r_1,r_2,r_3) = D(1-e^{-\beta x})^2 - D, \tag{5.A1}$$

where D is the dissociation energy measured from the bottom of the well, β the vibrational parameter ($= D_e/4\omega_e\chi_e$ in the diatomic limit), and x a distance parameter defined by

$$x(r_1,r_2,r_3) = \frac{x_1 e^{\gamma(r_2+r_3)} + x_2 e^{\gamma(r_1+r_3)} + x_3 e^{\gamma(r_1+r_2)}}{\Sigma} \tag{5.A2}$$

where Σ is the sum of the three exponential weighting factors in the numerator, and the x_i are the usual unitless Morse distance parameter $x_i = (r_i-r_e)/r_e$. γ defines the range over which the system is not separable into an atom and a diatomic molecule.

The changes in dissociation energy, vibrational frequencies and the local equilibrium bond distance at different bond distances can also be represented by exponential interpolation. However, in the case of D, β, and r_e, the additional ability to deviate from a smooth interpolation near the transition state is required. In general, a parameter like D, β, or r_e can be represented by $f = f_0 + f_1$, where f_0 is the smoothly interpolated part

$$f_0(r_1,r_2,r_3) = \frac{f_{01} e^{\gamma(r_2+r_3)} + f_{02} e^{\gamma(r_1+r_3)} + f_{03} e^{\gamma(r_1+r_2)}}{\Sigma}, \tag{5.A3}$$

and f_1 becomes important only near the transition state complex. (f_{oi} are the values in the corresponding isolated diatomic molecule, e.g., D_{02} the dissociation energy between atoms 2 and 3, see Fig. 18).

To allow for a well or saddle point near the transition state geometries, or adjust the vibrational parameters, the term f_1 must be included. There are in general three different equilibrium configurations (or saddle points), depending on which atom is centrally located. For a complex with equal bondlengths and a 60° equilibrium angle, a single minimum in D would be required. To break the symmetry between r_1, r_2 and r_3 at the three complex geometries with equilibrium angles of either θ_1, θ_2, or θ_3, and create three different minima, we introduce an effective equilibrium value for each bond distance,

$$\rho_i(r_j,r_k)=\sqrt{r_j^2+r_k^2-2r_j r_k cos(\theta_{ei})}. \tag{5.A4}$$

f_1 is then defined as

$$f_1(r_1,r_2,r_3)=\sum_{i=1}^{3} f_{1i}\, e^{-\left[(r_j-r_e)^2+(r_k-r_e)^2\right]/\sigma_{f1}^2-(r_i-\rho_i)^2/\sigma_{f2}^2}, \tag{5.A5}$$

with cyclic permutation. The result is that, as a complex is formed, f_1 becomes nonzero. In the case of the dissociation energy, the smooth change from diatom + atom reactants from products is now interrupted by either a well ($D_{1i} > 0$) or a saddle point ($D_{1i} < 0$). Note that the above definition can strictly be applied only to D and β; in the case of r_e, its occurrence in the Eq. [A5] must be replaced by r_{e0} or $r_{e0} + r_{e1}$, as r_e has not yet been evaluated. This, and the fact that a single value of r_e is used for all three bonds presents no problem in the present case where the equilibrium bond distances in the complex are similar ($\Delta r < 0.3$Å), and could easily be remedied in the more general case.

To allow the interconversion barriers and the bent-linear energy difference to be set independently, a term D_2 is required, which reduces the local dissociation energy for the linear configuration of the complex, effectively raising the energy difference between the linear and bent geometries,

$$D_2(r_1,r_2,r_3) = \sum_{i=1}^{3} D_{2i}\, e^{-\left[(r_j-r_e)^2+(r_k-r_e)^2\right]/\sigma_{D3}^2}, \qquad (5.A6)$$

with cyclic permutation. Physically, if the D_{2i} are chosen to be negative, but smaller than the D_{1i}, the bent-linear energy difference will be larger for a given interconversion barrier. In the surfaces we have used, both cases forbidding and allowing structural rearrangement have been considered. In all cases (see Table I), the IBrI well was made shallower than the BrII well, in accordance with the discussion presented in 5.4.2, and the linear-bent energy difference was kept near 500 cm^{-1}.

It should be pointed out that the Morse potential formulation presented above is not satisfactory at larger atom-diatom distances, since the exponential functions decay considerably faster than the van der Waals interaction between the Br and I_2. For example, for reasonable values of the potential parameters, at an atom-diatom separation of 6 Å, the above formalism predicts a lowering of the total energy of only 2.9 cm^{-1}, whereas the $-C_{Br\text{-}I_2}/r^6$ van der Waals energy amounts to -53 cm^{-1}. This has little effect on the van der Waals precursor calculation, where it only shifts the effective well depth and exit channel barrier height by a fraction of a kcal mol^{-1}, but can profoundly affect scattering calculations, which can be sensitive at large impact parameters to the location of the critical impact parameter. The latter is severely underestimated by an exponential function. This deficiency can be remedied by adding an interpolated van der Waals energy to the potential, which becomes isotropic at large distances and levels off to a constant at short distances:

$$\Delta V_{vdW}(r_1,r_2,r_3) = -\frac{C}{m^6+R^6}, \qquad (5.A7)$$

where m is a screening parameter that prevents the van der Waals correction from becoming very large at small internuclear distances. The van der Waals parameter C and the average distance R are again given by exponential interpolation,

$$C(r_1,r_2,r_3) = \frac{C_1 e^{\gamma(r_2+r_3)} + C_2 e^{\gamma(r_1+r_3)} + C_3 e^{\gamma(r_1+r_2)}}{\Sigma},$$

$$R(r_1,r_2,r_3) = \frac{R_{1-23} e^{\gamma(r_2+r_3)} + R_{2-13} e^{\gamma(r_1+r_3)} + R_{3-12} e^{\gamma(r_1+r_2)}}{\Sigma}, \qquad (5.A8)$$

where the $R_{i\text{-}jk}$ are the center-of-mass atom-diatom separations, and the C_i are the individual atom-atom van der Waals coefficients. At short interatomic distances, for a value of $m \sim 4.5$ Å, this adds a nearly constant value to the energy, which can be corrected for by slightly changing the D_i. The surfaces with or without the above correction are then in agreement to a fraction of a percent, except at distances > 4 Å, where the corrected surface is a much better approximation to the real interaction potential.

The exit channel barriers can be conveniently introduced by locally lowering the dissociation energy through another term, such as a Gaussian function centered at the required barrier location. For example, an exit channel barrier (in the present case, r_1 *or* r_3 small and approximately equal to the BrI bond distance, and r_2 larger) is obtained by adding a Gaussian barrier

$$B(r_1,r_2,r_3) = B_{01} G_1(r_1,r_2,r_3) + B_{03} G_3(r_1,r_2,r_3) \qquad (5.A9a)$$

to the local dissociation energy $D(r_1,r_2,r_3)$. The Gaussian function is defined as

$$G_i(r_1,r_2,r_3) = e^{-\left[(r_i-r_{Bi})^2/\sigma_{Bi}^2 + (r_2-r_{B2})^2/\sigma_{B2}^2 + (r_j-0.5r_{Bi}-r_{B2})^2/r_{Bi}^2\right]}, \qquad (5.A9b)$$

where $i = 1$ or 3 and $j = 3$ or 1. Entrance channel barriers can be obtained by appropriately permuting the indices.

Table I. Parameters for the optimal potential used in the Br + I_2 trajectory calculations described in the text. 28 different-valued parameters were used to describe the three-dimensional surface $V(r_1, r_2, r_3)$; 11 were fixed at values based on or derived from the literature, 13 were fixed at physically reasonable values determined by investigating derivatives and fixed points of the surface, and 4 were adjusted to bring the surface into concordance with the available temporal and scattering results.

Type	Name	Value	Unit	Description
Dissociation energy (DE)	$D_{01} = D_{03}$	14654	cm^{-1}	IBr DE*
	D_{02}	12439	cm^{-1}	I_2 DE
	$D_{11} = D_{13}$	4550	cm^{-1}	DE increase in complex (BrII)
	D_{12}	3270	cm^{-1}	DE increase in complex (IBrI)
	$D_{21} = D_{22} = D_{23}$	-500	cm^{-1}	DE correction linear vs. bent complex
	σ_{D1}	1.2	$Å^{-1}$	DE range parameter
	σ_{D2}	0.5	$Å^{-1}$	DE range parameter
	σ_{D3}	1.4	$Å^{-1}$	DE range parameter
Force Constant	$\beta_{01} = \beta_{03}$	4.65	-	IBr Morse force constant
	β_{02}	4.97	-	I_2 Morse force constant
	$\beta_{11} = \beta_{12} = \beta_{13}$	-3.5	-	Force constant change in complex
	$\sigma_{\beta 1}$	1.0	$Å^{-1}$	Force constant range parameter
	$\sigma_{\beta 2}$	0.9	$Å^{-1}$	Force constant range parameter
Bond length	$r_{e01} = r_{e03}$	2.47	Å	IBr equilibrium bond length
	r_{e02}	2.66	Å	I_2 equilibrium bond length
	$r_{e11} = r_{e12} = r_{e13}$	0.28	Å	Bond length change in complex
	σ_{r1}	1.0	$Å^{-1}$	Bond length range parameter
	σ_{r2}	0.4	$Å^{-1}$	Bond length range parameter
General constants	γ	1.5	$Å^{-1}$	Overall range parameter
	$\theta_1 = \theta_2 = \theta_3$	150	°	Complex near-equilibrium angles
Barriers	$B_{01} = B_{03}$	-2300	cm^{-1}	Exit channel decrease in DE
	$r_{B1} = r_{B3}$	3.9	Å	Exit channel barrier position
	r_{B2}	2.47	Å	Exit channel barrier position
	$\sigma_{B1} = \sigma_{B3}$	0.3	Å	Exit channel barrier width
	σ_{B2}	0.7	Å	Exit channel barrier width
van der Waals interaction	$C_1 = C_3$	2.71×10^6	$Å^6cm^{-1}$	Br-I vdW constant
	C_2	3.39×10^6	$Å^6cm^{-1}$	I-I vdW constant
	m	4.5	Å	Range parameter

* DE is the dissociation energy

Table II. Representative calculated complex lifetimes in ps under various conditions, including number of bonds (# bonds, 2 is collinear, 3 is a full calculation with three vibrational and three rotational degrees of freedom), well depth (well, in kcal mol^{-1}), exit channel barrier height (barrier, in kcal mol^{-1}), average hydrogen/deuterium binding angle for van der Waals precursor reactions (angle, degrees), van der Waals precursor or crossed beam calculation (vdW/CB), and translational energy of the Br atom (E_T in cm^{-1}, not including van der Waals interaction energy). The asterisks mark the optimal surface parameters used in the text.

	Lifetime	# bonds	Barrier	Well	Angle	vdW/CB	E_T
	6(1)	2	0	10	0	vdW	145
	6.2(5)	2	0	20	0	vdW	145
	11(1)	2	4	10	0	vdW	145
	3.0(5)	3	0	12.5	-	CB	980
	5.3(5)	3	0	15	0	vdW	290
	6.5(5)	3	0	15	0	vdW	145
	3.7(5)	3	0	15	-	CB	980
	7(1)	3	0	15	55	vdW	290
	8(1)	3	0	15	55	vdW	145
	20(4)	3	3.5	12.5	-	CB	290
	27(2)	3	3.0	15	0	vdW	290
	25(4)	3	2.9	15	0	vdW	290
	38(4)	3	3.0	15	0	vdW	145
*	41(5)	3	2.7	15	55	vdW	290
*	52(5)	3	2.7	15	55	vdW	145
*	8(1)	3	2.7	15	-	CB	980
	9(1)	3	3.5	15	-	CB	980
	51(5)	3	3.0	15	55	vdW	290
	64(6)	3	3.0	15	55	vdW	145
	40(4)	3	3.4	16.2	0	vdW	145
	35(4)	3	3.4	16.2	0	vdW	290
	38(4)	3	3.5	17.5	0	vdW	290
	58(4)	3	3.5	17.5	0	vdW	145

5.6 References

1. For reviews, see: a) A.H. Zewail, *Science,* **242**, 1645 (1988); b) M. Gruebele and A.H. Zewail, *Physics Today,* **43**, 24 (1990); c) L.R. Khundkar and A.H. Zewail, *Ann. Rev. Phys. Chem.*, **41**, 15 (1990).
2. a) N.F. Scherer, L.R. Khundkar, R.B. Bernstein and A.H. Zewail, *J. Chem. Phys.*, **87**, 1451 (1987); b) N.F. Scherer, C. Sipes, R.B. Bernstein and A.H. Zewail, *J. Chem. Phys.*, **92**, 5239 (1990).
3. M. Gruebele, I.R. Sims, E.D. Potter and A.H. Zewail, *J. Chem. Phys.*, **95**, 7763 (1991).
4. E.D. Potter, J.L. Herek, S. Pederson, Q. Liu and A.H. Zewail, *Nature,* **355**, 66 (1992).
5. a) S. Buelow, G. Radhakrishnan, J. Catanzarite and C. Wittig, *J. Chem. Phys.*, **83**, 444 (1985); b) G. Radhakrishnan, S. Buelow and C. Wittig, *J. Chem. Phys.*, **84**, 727 (1986); c) S. Buelow, M. Noble, G. Radhakrishnan, H. Reisler, C. Wittig and G. Hancock, *J. Phys. Chem.*, **90**, lO15 (1986); d) C. Wittig, S. Sharpe and R.A. Beaudet, *Acc. Chem. Res.*, **21**, 341 (1988); e) Y. Chen, G. Hoffmann, D. Oh and C. Wittig, *Chem. Phys. Lett.*, **159**, 426 (1989); f) C. Wittig, Y.M. Engel and R.D. Levine, *Chem. Phys. Lett.*, **153**, 411 (1988); g) SX. Shin, Y. Chen, D. Oh and C. Wittig, *Phil. Trans. R. Soc. Lond. A,* **332**, 361 (1990); h) G. Hoffmann, D. Oh, Y. Chen, Y.M. Engel and C. Wittig, *Isr. J. Chem.*, **30**, 115 (1990); i) S.K. Shin, Y. Chen, S. Nickolaisen, S.W. Sharpe, R.A. Beaudet and C. Wittig, *Advances in Photochemistry*, ed. D.H. Volman, to be published.
6. a) C. Jouvet and B. Soep, *Chem. Phys. Lett.*, **96**, 426 (1983); b) C. Jouvet and B. Soep, *J. Chem. Phys.*, **80**, 2229 (1984); c) W.H. Breckenridge, C. Jouvet Duval and B. Soep, *J. Phys. Chem.*, **91**, 5416 (1987); d) J.P. Visticot, B. Soep and C.J. Whitham, *J. Phys. Chem.*, **92**, 4574 (1988); e) C. Jouvet, M.C. Duval, B. Soep,

W.H. Breckenridge, C. Whitham and J.P. Visticot, *J. Chem. Soc. Faraday Trans II,* **85**, 1133 (1989); f) M.-C. Duval, B. Soep and W.H. Breckinridge, *J. Chem. Phys.,* **95**, 7145 (1991).

7. S.W. Sharpe, Y.P. Zeng, C. Wittig and R.A. Beaudet, *J. Chem. Phys.*, **92**, 943 (1990).

8. see: a) A. Jacobs, M. Wahl, R. Weller and J. Wolfrum, *Chem. Phys. Lett.*, **158**, 161 (1989); b) M.J. Frost, J.S. Salh and I.W.M. Smith, *J. Chem. Soc. Faraday Trans.*, **87**, 1037 (1991); c) for recent reviews see: J.A. Miller, R.J. Kee and C.K. Westbrook, *Ann. Rev. Phys. Chem.*, **41**, 345 (1990); d) R.E. Weston Jr., *J. Chem. Ed.*, **65**, 1062 (1988); e) G.W. Flynn, *Science,* **246**, 1009 (1989); f) J. K. Rice and A.P. Baronavski, *J. Chem. Phys.*, **94**, 1006 (1991).

9. S.K. Shin, C. Wittig and W.A. Goddard III, *J. Phys. Chem.*, **95**, 8048 (1991).

10. a) G.C. Schatz, M.S. Fitzcharles and L.B. Harding, *Faraday Disc. Chem. Soc.*, **84**, 359 (1987); b) G.C. Schatz and, M.S. Fitzcharles, in *Selectivity in Chemical Reactions*, ed. J.C. Whitehead (Kluwer, Dordrecht, 1988); c) K. Kudla and G.C. Schatz, *J. Phys Chem.*, **95**, 8267 (1991); d) K. Kudla, G.C. Schatz and A.F. Wagner, *J. Chem. Phys.*, **95**, 1635 (1991).

11. a) D. Feller, E.S. Huyser, W.T. Borden and E.R. Davidson, *J. Am. Chem. Soc.*, **105**, 1459 (1983); b) M. Aoyagi and S. Kato, *J. Chem. Phys.*, **88**, 6409 (1988); c) J. Brunning, D.W. Derbyshire, I.W.M. Smith and M.D. Williams, *J. Chem. Soc. Faraday Trans. 2,* **84**, 105, (1988); d) J.K. Rice, Y.C. Chung and A.P. Baronawski, *Chem. Phys. Lett.*, **167**, 151 (1990).

12. A.H. Zewail, *Faraday Discuss. Chem. Soc.*, **91**, 207 (1991).

13. *Handbook of Chemistry and Physics,* 71st edition, ed. D.R. Lide, CRC Press, Inc., Boca Raton (1990).

14. Y.T. Lee, J.D. McDonald, P.R. LeBreton and D.R. Herschbach, *J. Chem. Phys.*, **49**, 2447 (1968).

15. G.A. Fisk, J.D. McDonald and D.R. Herschbach, *Faraday Discuss. Chem. Soc.*, **44**, 228 (1967).

16. J.D. McDonald, Ph.D. Thesis, Harvard University (1971).

17. H.J. Loesch and D. Beck, *Ber. Bunsenges. Phys. Chem.*, **75**, 736 (1971).

18. D. Beck, F. Engelke and H.J. Loesch, *Ber. Bunsenges. Phys. Chem.*, **72**, 1105 (1968).

19. Y.T. Lee, P.R. LeBreton, J.D. McDonald and D.R. Herschbach, *J. Chem. Phys.*, **51**, 455 (1969).

20. J.B. Cross and N.C. Blais, *J. Chem. Phys.*, **50**, 4108 (1969).

21. N.C. Blais and J.B. Cross, *J. Chem. Phys.*, **52**, 3580 (1970).

22. J.B. Cross and N.C. Blais, *J. Chem. Phys.*, **55**, 3970 (1971).

23. C.F. Carter, M.R. Levy, K.B. Wooodall and R. Grice, *Faraday Discuss. Chem. Soc.*, **55**, 381 (1973).

24. N.C. Firth and R. Grice, *Mol. Phys.*, **60**, 1261 (1987).

25. N.C. Firth and R. Grice, *Mol. Phys.*, **60**, 1273 (1987).

26. N.C. Firth, D.J. Smith and R. Grice, *Mol. Phys.*, **61**, 859 (1987).

27. N.C. Firth, N.W. Keane, D.J. Smith and R. Grice, *Faraday Discuss. Chem. Soc.*, **84**, 53 (1987).

28. S.M.A. Hoffman, D.J. Smith and R. Grice, *Mol. Phys.*, **49**, 621 (1983).

29. J.J. Valentini, Y.T. Lee and D.J. Auerbach, *J. Chem. Phys.*, **67**, 4866 (1977).

30. T. Trickl and J. Wanner, *J. Chem. Phys.*, **78**, 6091 (1983).

31. B. Girard, N. Billy, G. Gouedard and J. Vigue, *Faraday Discuss. Chem. Soc.*, **84**, 65 (1987).

32. B. Girard, N. Billy, G. Gouedard and J. Vigue, *Europhys. Lett.*, **14**, 13 (1991).

33. J.C. Whitehead, *Comprehensive Chemical Kinetics*, **24**, 357 (1983).

34. D.L. Bunker and N. Davidson, *J. Am. Chem. Soc.*, **80**, 5090 (1958).

35. G. Porter, *Discuss. Faraday Soc.*, **33**, 198 (1962).

36. V.I. Balykin, V.S. Letokhov, V.I. Mishin and V.A. Semchishen, *Chem. Phys.*, **17**, 111 (1976).

37. J.L. Tellinghuisen, A.R. Whyte and L.F. Phillips, *J. Phys. Chem.*, **88**, 6084 (1984).

38. J.I. Cline and S.R. Leone, *J. Phys. Chem.*, **95**, 2917 (1991).

39. M.W. Sigrist, D.J. Krajnovich, F. Huisken, Z.J. Zhang, Y.T. Lee and Y.R. Shen, *Helv. Phys. Acta*, **53**, 289 (1980).

40. M. Kawasaki, H. Sato and G. Inoue, *J. Phys. Chem.*, **93**, 7571 (1989).

41. J.J. Valentini, M.J. Coggiola and Y.T.Lee, *J. Am. Chem. Soc.*, **98**, 853 (1976).

42. M.J. Coggiola, J.J. Valentini and Y.T.Lee, *Int. J. Chem. Kinet.*, **8**, 605 (1976).

43. J.J. Valentini, M.J. Coggiola and Y.T.Lee, *Faraday Discuss. Chem. Soc.*, **62**, 232 (1977).

44. G. Mamantov, D.G. Vickroy, E.J. Vasini, T. Maekwa and M.C. Moulton, *Inorg. Nucl. Chem. Letters*, **6**, 701 (1970).

45. G. Mamantov, E.J. Vasini, M.C. Moulton, D.G. Vickroy and T. Maekwa, *J. Chem. Phys.*, **54**, 3419 (1971).

46. M.R. Clarke, W.H. Fletcher, G. Mamantov, E.J. Vasini and D.G. Vickroy, *Inorg. Nucl. Chem. Letters*, **8**, 611 (1972).

47. E.S. Prochaska and L. Andrews, *Inorg. Chem.*, **16**, 339 (1977).

48. E.S. Prochaska, L. Andrews, N.R. Smyrl and G. Mamantov, *Inorg. Chem.*, **17**, 970 (1978).

49. L.Y. Nelson and G.C. Pimentel, *J. Chem. Phys.*, **47**, 3671 (1967).

50. D.H. Boal and G.A Ozin, *J. Chem. Phys.*, **55**, 3598 (1971).

51. C.A. Wight, B.S. Ault and L. Andrews, *J. Chem. Phys.*, **65**, 1244 (1976).

52. M.E. Jacox, *J. Phys. Chem. Ref. Data*, **13**, 945 (1984).

53. S.R. Ungemach and H.F. Schaefer III, *J. Am. Chem. Soc.*, **98**, 1658 (1976).

54. B.R. De and A.B. Sannigrahi, *Intern. J. Quntum Chem.*, **19**, 485 (1981).

55. A.B. Sannigrahi and S.D. Peyerimhoff, *Chem. Phys. Lett.*, **114**, 6 (1985).

56. V.L. Pershin and A.I. Boldyrev, *J. Mol. Struct. (Theochem)*, **150**, 171 (1987).

57. M.A.A. Clyne and H.W. Cruse, *J. Chem. Soc. Faraday Trans. II*, **68**, 1377 (1972).

58. E.H. Appelman and M.A.A. Clyne, *J. Chem. Soc. Faraday Trans. I*, **71**, 2072 (1975).

59. P.P. Bemand and M.A.A. Clyne, *J. Chem. Soc. Faraday Trans. II*, **72**, 191 (1975).

60. P.P. Bemand and M.A.A. Clyne, *J. Chem. Soc. Faraday Trans. II*, **71**, 1132 (1975).

61. L.W. Strattan and M.W. Kaufman, *J. Chem. Phys.*, **66**, 4963 (1977).

62. F. Zaraga, S.R. Leone and C.B. Moore, *Chem. Phys. Lett.*, **42**, 275 (1976).

63. H.K. Haugen, E. Weitz and S.R. Leone, *Chem. Phys. Lett.*, **119**, 75 (1985).

64. For a review, see a) I.W.M. Smith, *J. Chem. Soc. Faraday Trans.*, **87**, 2271 (1991); b) I.W.M. Smith, *Kinetics and Dynamics of Elementary Gas Reactions* (Butterworths, London, 1980).

65. H. Hofman and S.R. Leone, *Chem. Phys. Lett.*, **54**, 314 (1978).

66. A. Hariri, A.B. Peterson and C. Wittig, *J. Chem. Phys.*, **65**, 1872 (1976).

67. J.R. Wiesenfeld and G.L. Wolk, *J. Chem. Phys.*, **69**, 1797 (1978).

68. J.R. Wiesenfeld and G.L. Wolk, *J. Chem. Phys.*, **69**, 1805 (1978).

69. E.B. Gordon, A.I. Nadkhin, S.A. Sotnichenko and I.A. Boriev, *Chem. Phys. Lett.*, **86**, 209 (1982).

70. H. Okabe, *Photochemistry of Small Molecules* (Wiley-Interscience, New York, 1978).

71. B.J. Huebert and R.M. Martin, *J. Phys. Chem.*, **72**, 3046 (1968).

72. F. Magnotta, D.J. Nesbitt and S.R. Leone, *Chem. Phys. Lett.*, **83**, 21 (1981).

73. Z. Xu, B. Koplitz and C. Wittig, *J. Chem. Phys.*, **87**, 1062 (1987).

74. Z. Xu, B. Koplitz and C. Wittig, *J. Phys. Chem.*, **92**, 5518 (1988).

75. F.A. Baiocchi, T.A. Dixon and W. Klemperer, *J. Chem. Phys.*, **77**, 1632 (1982).

76. S.E. Novick, K.C. Janda and W. Klemperer, *J. Chem. Phys.*, **65**, 5115 (1977).

77. L.-E. Selin, *Arkiv för Fysik*, **21**, 479 (1962).

78. W.G. Brown, *Phys. Rev.*, **42**, 355 (1932).

79. E.M. Weinstock, *J. Mol. Spec.*, **61**, 395 (1976).

80. E.M. Weinstock and A. Preston, *J. Mol. Spec.*, **70**, 188 (1978).

81. M.A.A. Clyne and I.S. McDermid, *J. Chem. Soc. Faraday Trans II*, **72**, 2252 (1976).

82. T.A. Stephenson, W.R. Simpson, J.R. Wright, H.P.Schneider, J.W. Miller and K.E. Schultz, *J. Phys. Chem.*, **93**, 2310 (1989).

83. L.-E. Selin and B. Soderborg, *Arkiv för Fysik*, **21**, 515 (1962).

84. R.S. Mulliken, *J. Chem. Phys.*, **55**, 288 (1971) and references therein.

85. J. Tellinghuisen, *Chem. Phys. Lett.*, **99**, 373 (1983).

86. R.J. Donovan, B.V. O'Grady, K. Shobatake and A. Hiraya, *Chem. Phys. Lett.*, **122**, 612 (1985).

87. A. Hiraya, K. Shobatake, R.J. Donovan and A. Hopkirk, *J. Chem. Phys.*, **88**, 52 (1988).

88. N. F. Scherer, J.L. Knee, D.D. Smith and A.H. Zewail, *J. Phys. Chem.*, **89**, 5141 (1985); M. Rosker, M. Dantus and A.H. Zewail, *J. Chem. Phys.*, **89**, 6128 (1988).

89. A. B. Sannigrahi and S. D. Peyerimhoff, *Int. J. Quant. Chem.*, **30**, 413 (1986).

90. E. Vasini and E. Castro, *J. Mol. Struct.*, **22**, 415 (1974).

91. E. Castro and E Vasini, *Int. J. Quant. Chem.*, **22**, 433 (1982).

92. B. M. Deb, G. D. Mahajan and V. S. Vasan, *Pramana*, **9**, 93 (1977).

93. S. Bhattacharjee, A. B. Sannigrahi and D. C. Mukherjee, *Ind. J. Chem.*, **22A**, 1001 (1983).

94. B. R. De and A. B. Sannigrahi, *Int. J. Quant. Chem.*, **22**, 435 (1982).

95. A. Viste and P. Pyykko, *Int. J. Quant. Chem.*, **25**, 223 (1984).

96. K. Fukui, T. Yonezawa and H. Shingu, *J. Chem. Phys.*, **22**, 1423 (1954).

97. For a review and further references, see: D.R. Herschbach, in *The Chemical Bond*, p. 210, ed. A.H. Zewail (Academic Press, Boston, 1992).

98. M. Koshi, H. Ito and H. Matsui, *Chem. Phys. Lett.*, **103**, 180 (1983).

99. J. J. Duggan and Roger Grice, *J. Chem. Soc. Faraday Trans. II*, **80**, 795 (1984).

100. a) J. J. Duggan and Roger Grice, *J. Chem. Soc. Faraday Trans. II*, **80**, 809 (1984); b) J. J. Duggan and Roger Grice, *J. Chem. Soc. Faraday Trans. II*, **85**, 1081 (1984).

101. L. Dalla Riva, S. H. Lin and H. Eyring, *Anal. Asoc. Quim. Arg.*, **59**, 133 (1971).

102. a) D. L. Thompson, *J. Chem. Phys.*, **60**, 4557 (1974); b) D. L. Thompson, *Chem. Phys. Lett*, **55**, 424 (1978).

103. J. C. Polanyi, *Angew. Chem. Int. Ed. Engl.*, **26**, 952 (1987).

104. a) N. C. Blais and D. L. Bunker, *J. Chem. Phys.*, **37**, 2713 (1962); b) L. M. Raff and M. Karplus, *J. Chem. Phys.*, **44**, 1212 (1966).

105. a) D. L. Bunker and N. C. Blais, *J. Chem. Phys.*, **41**, 2377 (1964); b) D. L. Bunker and C. A. Parr, *J. Chem. Phys.*, **52**, 5700 (1970).

106. I. W. Fletcher and J. C. Whitehead, *J. Chem. Soc. Faraday Trans. II*, **78**, 1165 (1982).

107. M. Gruebele, G. Roberts and A. H. Zewail, *Phil. Trans. Roy. Soc. A*, **332**, 223 (1990).

108. I. Urrecha, I. SernaandJ. Iturbe, *Chem. Phys.*, **154**, 85 (1991).

109. a) T. B. Borne and D. L. Bunker, *J. Chem. Phys.*, **55**, 4861 (1971); b) D. E. Fitz and P. Brumer, *J. Chem. Phys.*, **69**, 1792 (1978).

110. W.H. Press, B.P. Flannery, S.A. Teukolsky and W.T. Vetterling, *Numerical Recipes* (CUP, Cambridge, 1986).

111. This deviation is not due to any deficiency in the routine, but rather to the presence of chaos. This was tested for by a method similar to that proposed in Ref. 113, by noting the exponential divergence of trajectories nearby in phase space and on the same energy shell (Lyapunov coefficient $3ps^{-1}$). The round-off error in the differential equation solver "seeds" this orbit divergence, but since the motion is

ergodic, average quantities are still correct as long as energy conservation is rigorously enforced.

112. G. Benettin and J.M. Strelcyn, *Phys. Rev. A*, **17**, 773 (1978).

113. M.M. Oprysko, F.J. Aoiz, M.A. McMahan and R.B. Bernstein, *J. Chem. Phys.*, **78**, 3816 (1983).

114. a) D.O. Ham and J.L. Kinsey, *J. Chem. Phys.*, **53**, 285 (1970); b) W.B. Miller, S.A. Safron and D.R. Herschbach, *J. Chem. Phys.*, **56**, 3580 (1972).

115. see e.g. a) L. Baffares and A.G. Urena, *J. Chem. Phys.*, **93**, 6473 (1990); b) L. Banares, A.G. Urena and A. A.-Navarro, *J. Chem. Soc. Faraday Trans.*, **86**, 2063 (1990).

116. see: J.C. Polanyi, in *The Chemical Bond: Structure and Dynamics*, ed. A.H. Zewail (Academic Press, Boston, 1992).

117. G. Schatz and J. Dyck, *Chem. Phys. Lett.*, **188**, 11 (1992).

118. See e.g., J.D. Kress, R.B. Walker and E.F. Hayes, *J. Chem. Phys.*, **93**, 8085 (1990).

119. I. Urrecha, F. Castano and J. Iturbe, *J. Chem. Soc. Faraday Trans. II*, **82**, 1077 (1986).

120. B. M. Gimalc, *Molecular Structure and Bonding* (Academic Press, Orlando, 1979).

5.7 Figure Captions

1. Schematic showing the effect of different impact geometries on the impact parameter distribution; (A) crossed-beam conditions, often leading to large impact parameters; (B) linear HBr - I_2 cluster; the displacement of the Br is negligible compared to the effect on its momentum vector due to the hydrogen large amplitude motion; (C) H off-axis linear HBr - I_2 cluster shows a somewhat increased impact parameter range; (D) hypothetical hydrogen-bonded configuration for reactive H + I_2. Note that the impact parameter of the hydrogen is influenced by its position as well as its momentum vector, as opposed to the Br, where only the momentum vector contributes significantly; this adds an additional b to the impact parameter. Also note that in this configuration, the H would lead to an undetecteable reaction or quickly depart, whereas the Br is still trapped. For configuration (D), a reactive Br + I_2 encounter requires the Br to turn around toward the I_2.
2. Time-of-flight mass spectrum obtained under typical operating conditions. The TOFMS deflection plates were set to bias for higher masses, and only the range from m/e ~80 and above is shown for clarity.
3. Experimental transient showing the time-resolved formation of IBr from the reaction Br + $I_2 \rightarrow$ BrI + I starting from an HBr·I_2 complex, as monitored by LIF. The data fit a rising exponential as indicated, with the zero-of-time being fixed by the photoionization cross-correlation (see text).
4. Experimental transient as in Fig. 5, but starting from a DBr·I_2 precursor, showing a faster risetime.
5. Schematic orbital diagram for various trihalogen systems. All relativistic corrections have been neglected, which would lift the degeneracy of the π orbitals. On the left is shown the standard correlation diagram for a homonuclear diatomic with more than half-filled *p*-shell, as applicable to I_2. The next diagram shows the formation of a

light symmetrical halogen complex, with notable *s* and *p* mixing; the third correlation diagram corresponds to the case of heavier halogens, where the amount of *s* and *p* mixing is decreased. For the asymmetrical complex case, such as BrI_2, the last digram shows the orbital numbering used in the text; the orbitals are now asymmetrical, and the 3π and 5σ orbitals may be shifted in order.

6. *Pz* orbital interaction possible as Br approaches I_2; refer to the text for a detailed discussion of the frontier orbital picture.
7. Reaction coordinate showing the effects of spin-orbit splitting. The three approaches of the Br *p* orbital to I_2 lead to three surfaces, of which only the lowest should play a major role in the present experimental investigation. Note that crossing from the Br/I to the Br*/I* surface is forbidden by a propensity rule. The exoergicity and well depth are also noted in kcal mol^{-1}.
8. Correlation diagram for the 21 valence electron system BrI_2. On the left are shown the atomic orbitals (4*s* and 4*p* for Br, 5*s* and 5*d* for I) which make the major contribution to the MO's of the linear complex. It can be seen that the HOMO has antibonding character, yielding an overall bond order of 1.5. (Orbitals are numbered starting in the valence shell). The degeneracies of the orbitals are lifted when spin-orbit coupling is considered: due to the unpaired electron, π states (ℓ = 1) lead to $\gamma_{1/2}$ and $\gamma_{3/2}$ states, while σ orbitals lead only to $\gamma_{1/2}$ orbitals. Upon bending the molecule to the C_s geometry, the HOMO energy increases; nonetheless, BrI_2 probably has a slightly bent geometry in its electronic ground state, due to the lowering of the 1π orbital energies.
9. Three-dimensional view of the reactive PES at a bond angle of 150°.
10. Cuts through the PES. (A) shows r_1 ($r_{Br\text{-}I}$) vs. r_2 ($r_{I\text{-}I}$) at 180°; (B) shows the lowering of the potential energy as the molecule is bent to 150°; (C) shows a very strongly bent, 60° configuration, where the arrow indicates a transition from an IBrI

to a BrII complex for a sufficiently energetic trihalogen molecule; (D) is a projection onto r_1-r_3 space, showing the symmetric dissociation limits of the IBrI complex.

11. Simulated transient from a 'best fit' PES for the reaction initiated with a DBr precursor (dotted line); the same for the case of the HBr precursor (solid line), shows the increase in lifetime at slightly lower reaction energy.

12. Theoretical simulation of the complex decay obtained by shifting the region where trajectories can lead to detection to smaller Br-I distances in the exit channel, the case of a perturbed BrI molecule. The noise is due to the Monte Carlo error in fully sampling 100 trajectories.

13. The beginning and end of a typical trajectory leading to IBr product formation. The oscillations in r_3 are seen to be slower than those in r_1 and r_2, since they are more strongly correlated to the bending mode in a Br-I-I configuration.

14. The power spectrum corresponding to Fig. 13, obtained by Fourier transformation, is representative of those found for all trajectories; the period near 55 cm^{-1} corresponds to bending motion, the broader peak near 90 cm^{-1} to stretching motions of the complex.

15. Product state distributions for the DBr precursor case; the solid lines correspond to a 3 kcal mol^{-1} exit channel barrier, the dotted lines to a PES without an exit channel barrier. Note that the energy stored in overall angular momentum L is not plotted, resulting in a slight energy defect if the other contributions are summed. Overall energy conservation was rigidly enforced.

16. Product state distribution for the crossed-beam simulation; the qualitative trend of the curves is similar to that of Fig. 15, but due to thermal averaging and the higher reaction energy, the distributions are considerably broader.

17. Crossed-beam results for Br + I_2 ($E_T \sim 980$ cm^{-1}) taken from Ref. 16. The upper panel shows the laboratory angle scattering and translational energy distributions, the lower panel the expected translational energy release; the solid line corresponds to a

nominal kinematic analysis, the dashed line to a collision-complex calculation; both show a maximum near 3 kcal mol^{-1}.

18. The numbering of the bond coordinates, angles and nuclei as used in the appendix.

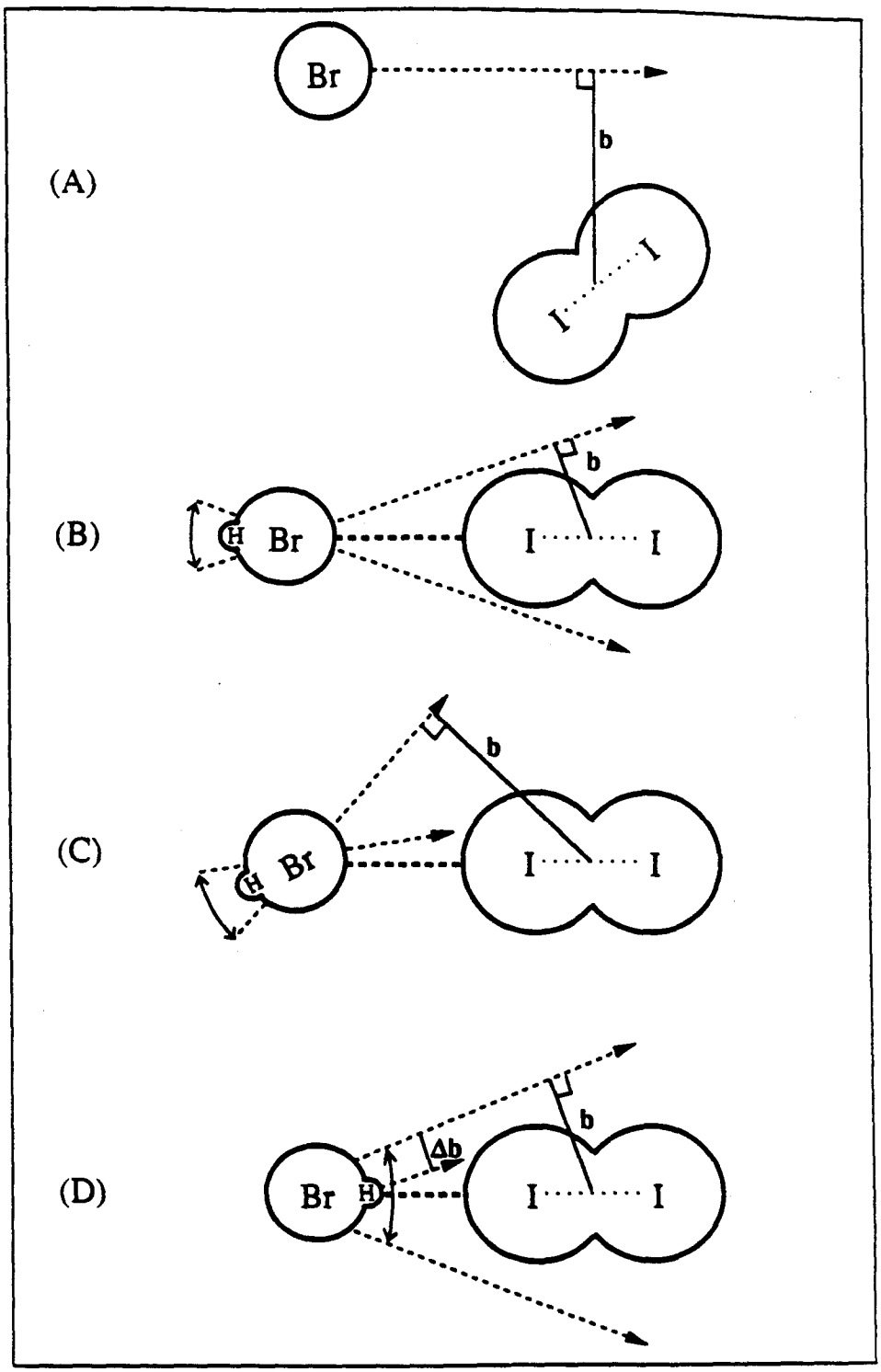

Figure 1.

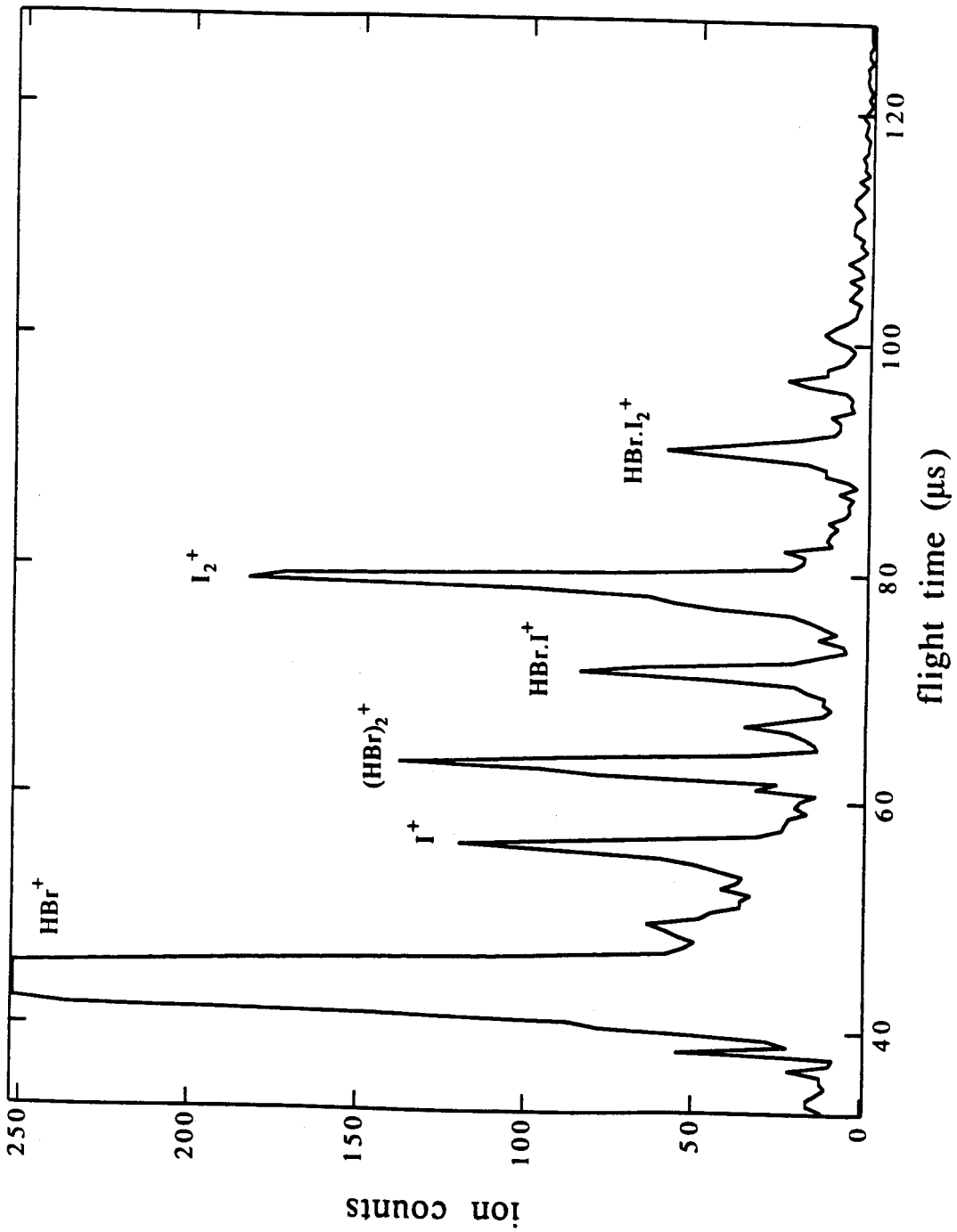
ion counts
flight time (μs)
HBr+
I+
(HBr)2+
I2+
HBr.I+
HBr.I2+
0
50
100
150
200
250
40
60
80
100
120

Figure 2.

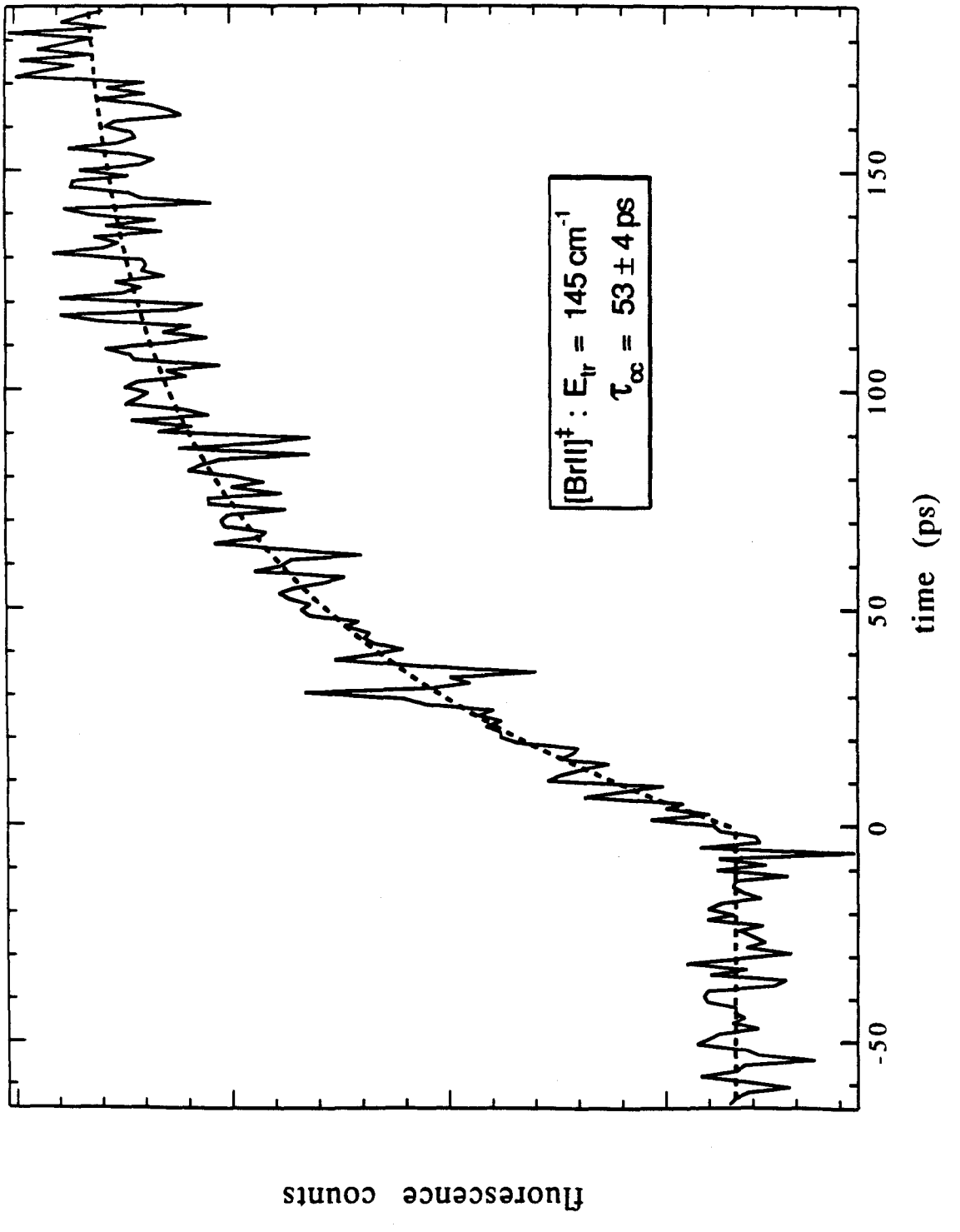
[BrII]‡ : Etr = 145 cm-1
τ∞ = 53 ± 4 ps
-50
0
50
100
150
time (ps)
fluorescence counts

Figure 3.

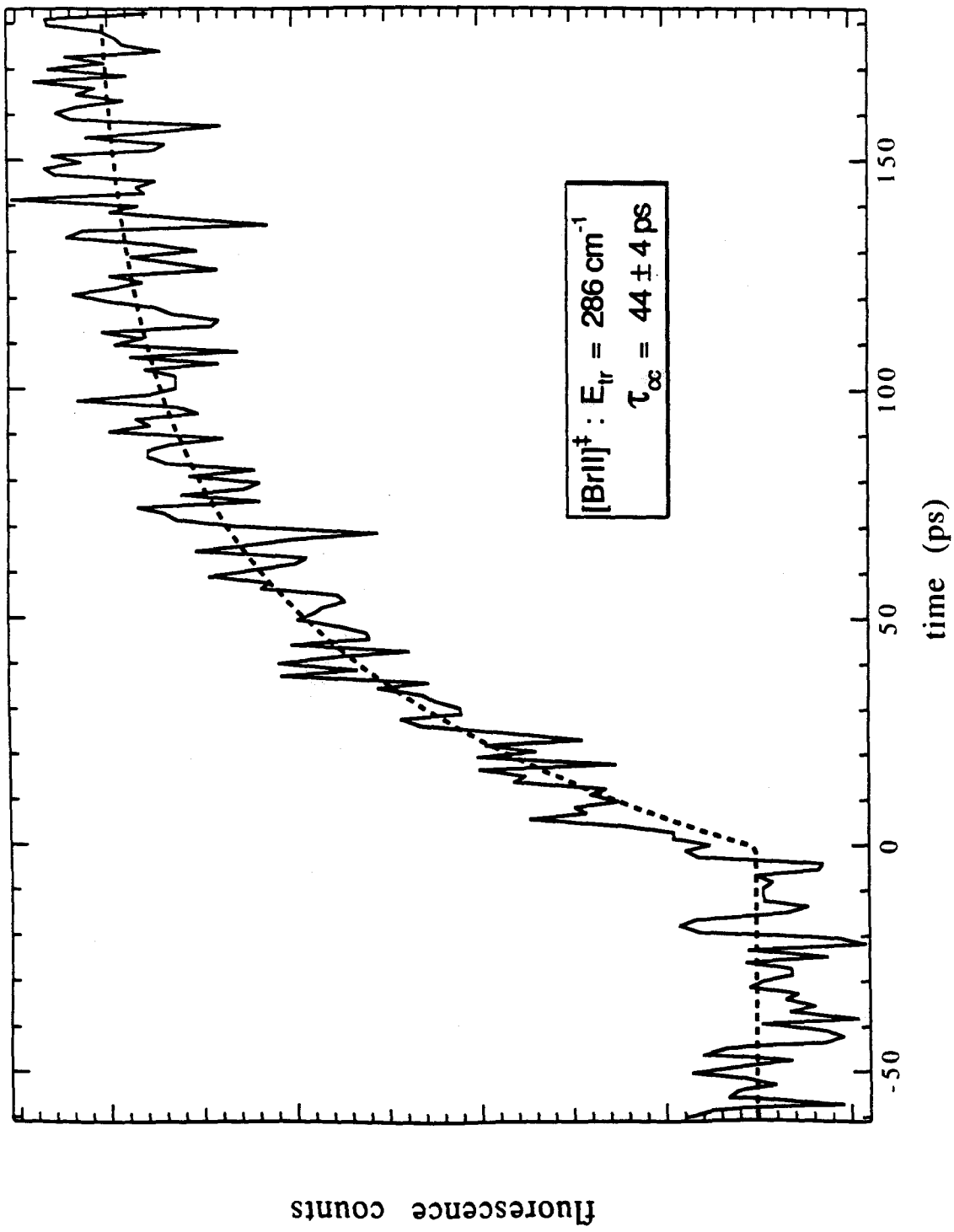
[BrII]‡ : Etr = 286 cm-1
τ∞ = 44 ± 4 ps
-50
0
50
100
150
time (ps)
fluorescence counts

Figure 4.

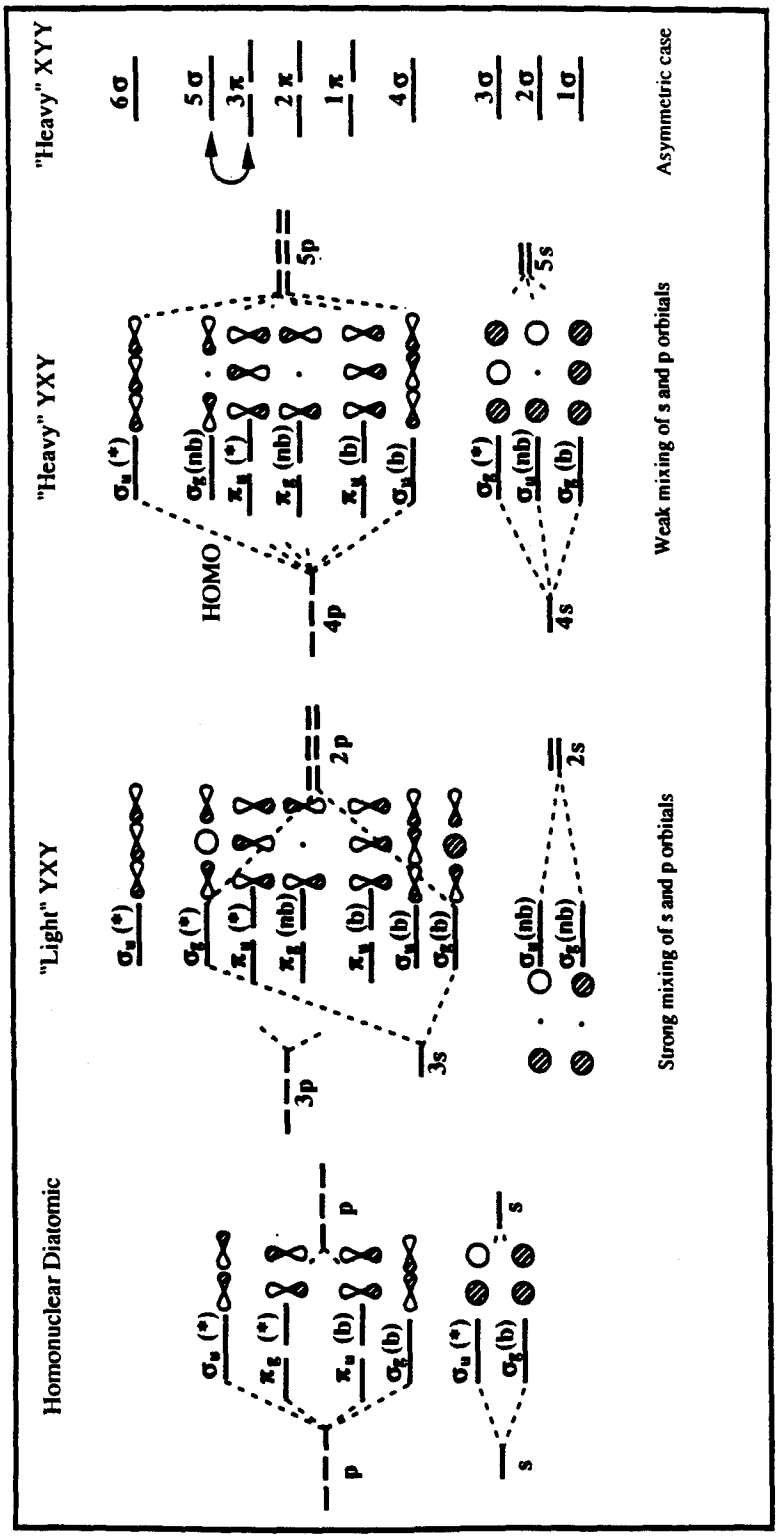
Homonuclear Diatomic
"Light" YXY
"Heavy" YXY
"Heavy" XYY
Strong mixing of s and p orbitals
Weak mixing of s and p orbitals
Asymmetric case
HOMO
6σ
5σ
3π
2π
1π
4σ
3σ
2σ
1σ
2p
3p
3s
4p
5p
4s
5s
2s
p
s

Figure 5.

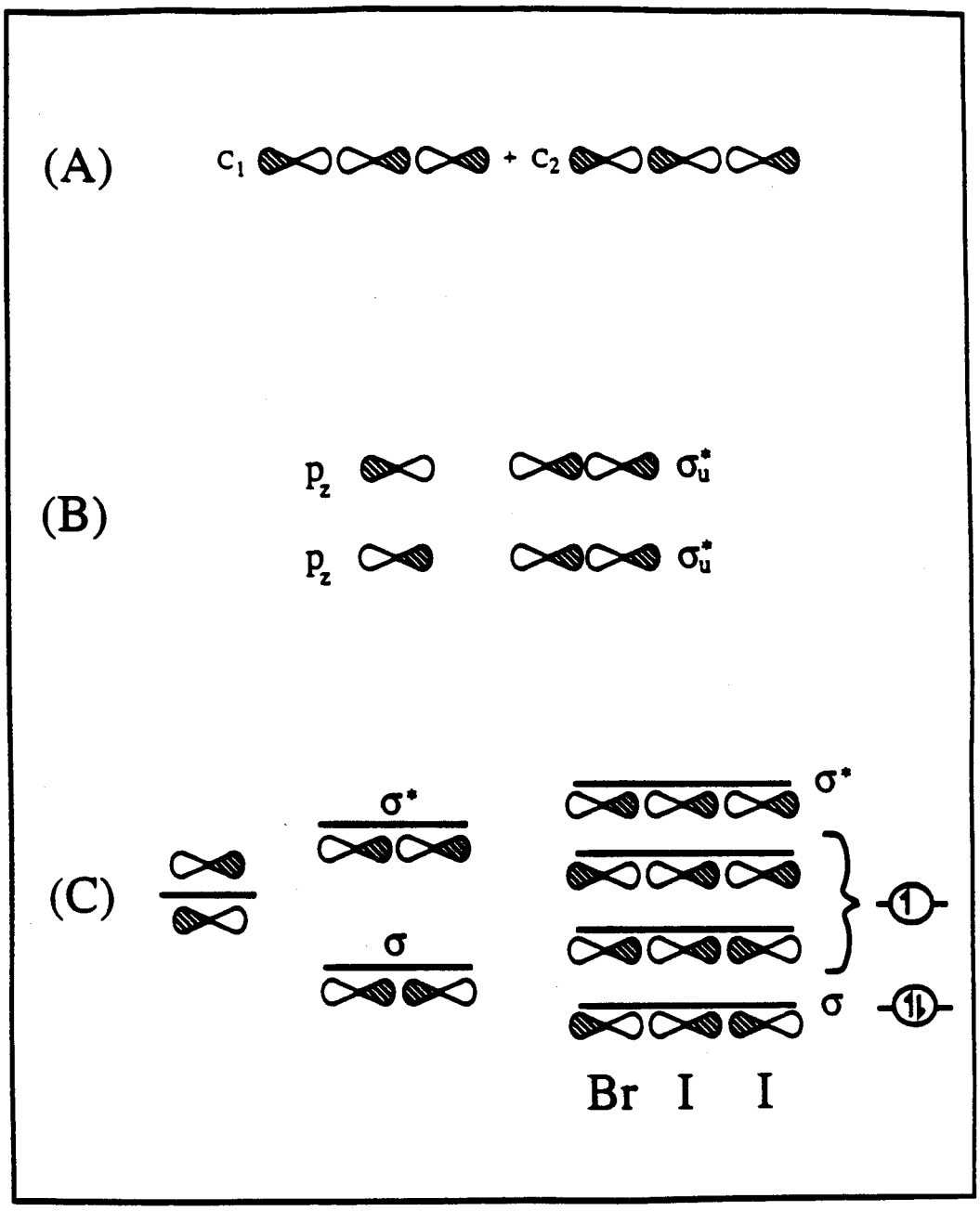

Figure 6.

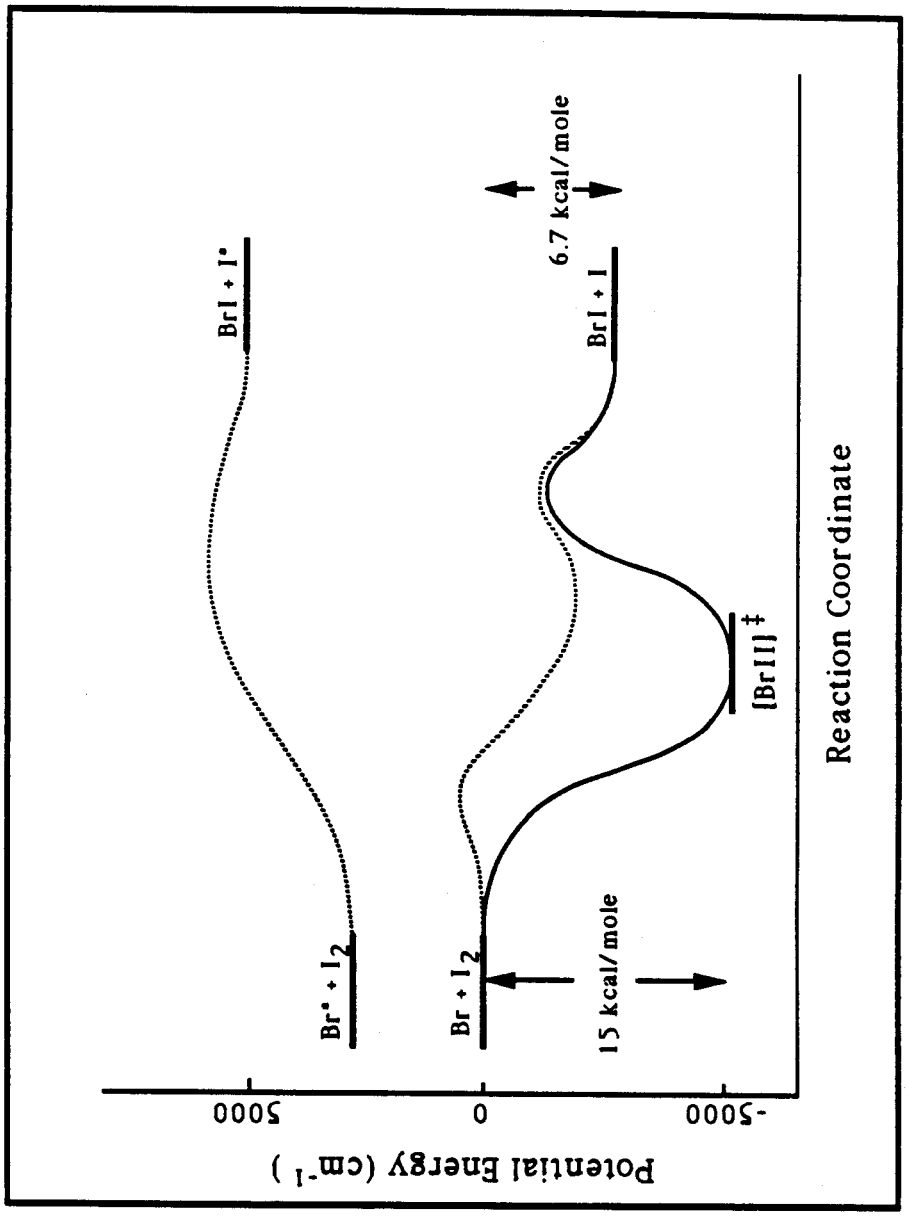
Potential Energy (cm-1)
5000
0
-5000
Reaction Coordinate
Br + I2
Br' + I2
BrI + I'
BrI + I
[BrII]‡
15 kcal/mole
6.7 kcal/mole

Figure 7.

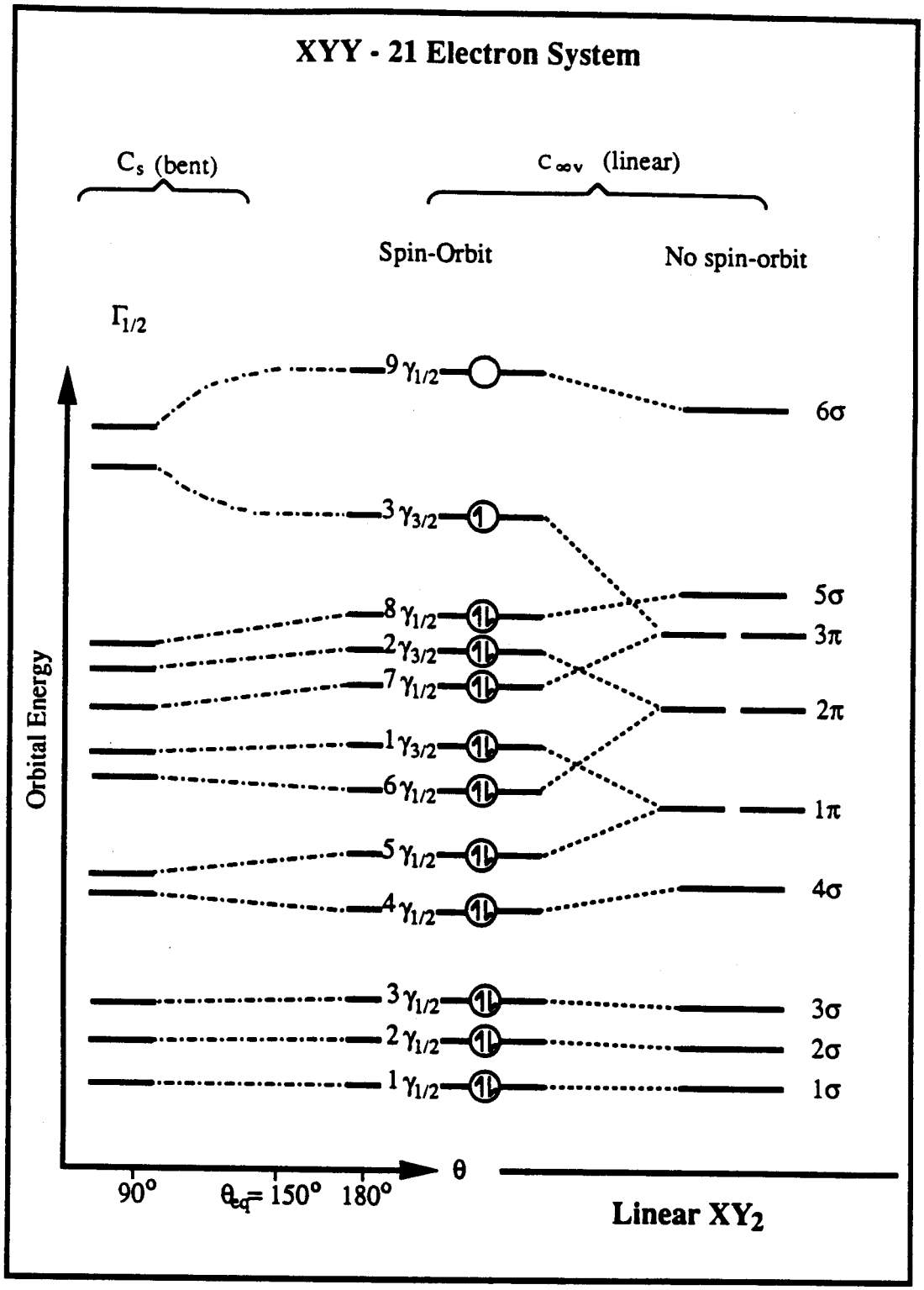
XYY - 21 Electron System
C_s (bent)
$C_{\infty v}$ (linear)
Spin-Orbit
No spin-orbit
$\Gamma_{1/2}$
$9\gamma_{1/2}$
6σ
$3\gamma_{3/2}$
$8\gamma_{1/2}$
5σ
$2\gamma_{3/2}$
3π
$7\gamma_{1/2}$
2π
$1\gamma_{3/2}$
$6\gamma_{1/2}$
1π
$5\gamma_{1/2}$
$4\gamma_{1/2}$
4σ
$3\gamma_{1/2}$
3σ
$2\gamma_{1/2}$
2σ
$1\gamma_{1/2}$
1σ
Orbital Energy
θ
90°
θ_{eq}= 150°
180°
Linear XY_2

Figure 8.

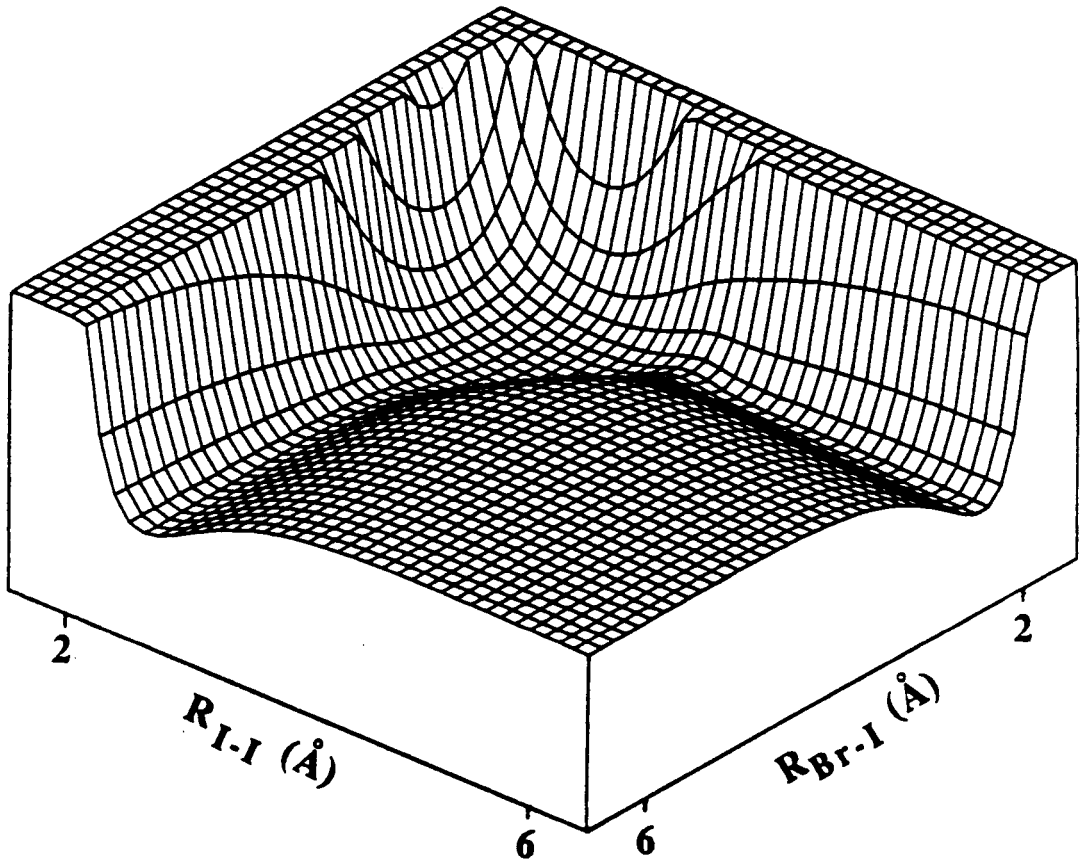

Figure 9.

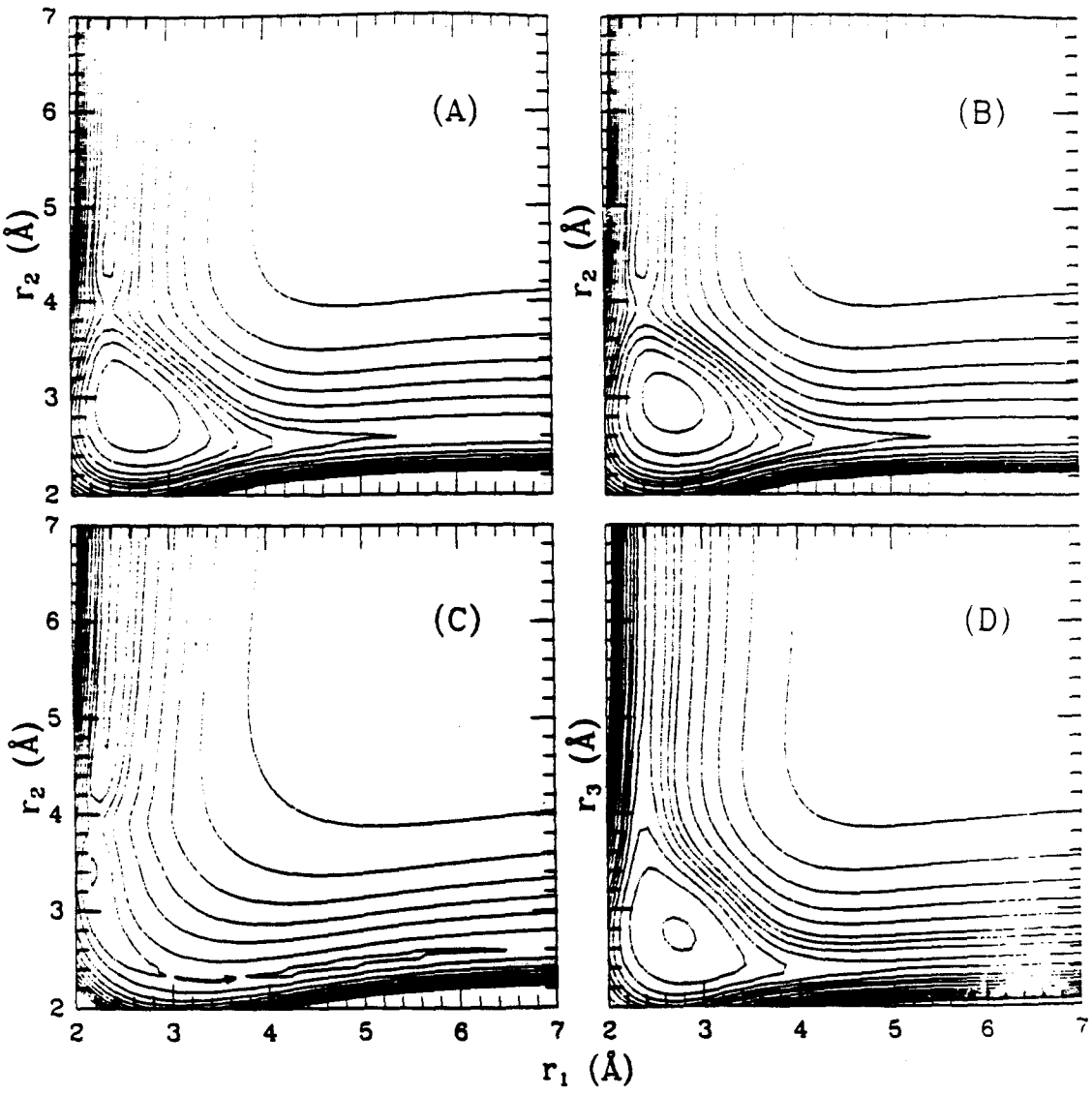

Figure 10.

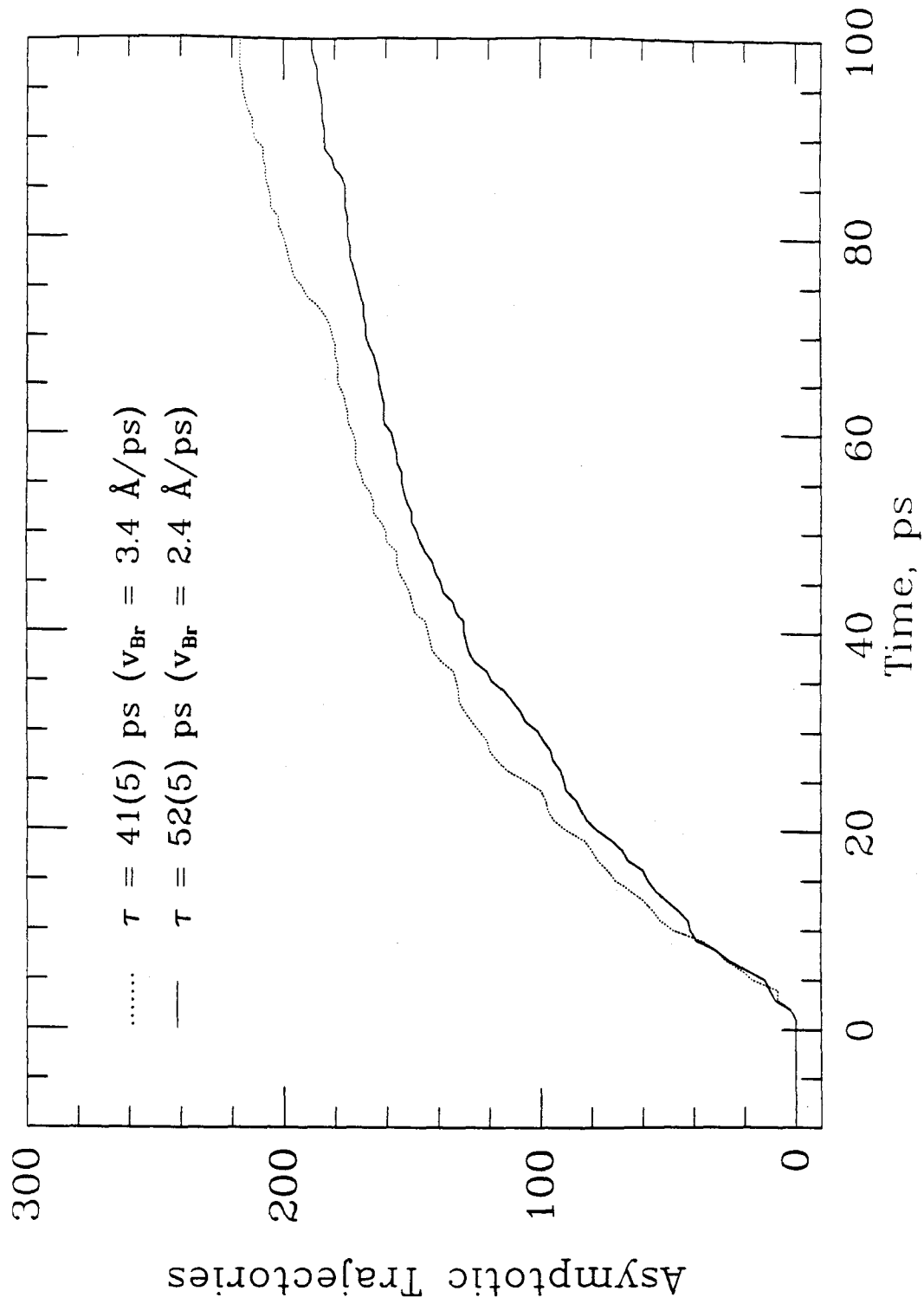
Asymptotic Trajectories
300
200
100
0
0
20
40
60
80
100
Time, ps
..... τ = 41(5) ps (v_{Br} = 3.4 Å/ps)
— τ = 52(5) ps (v_{Br} = 2.4 Å/ps)

Figure 11.

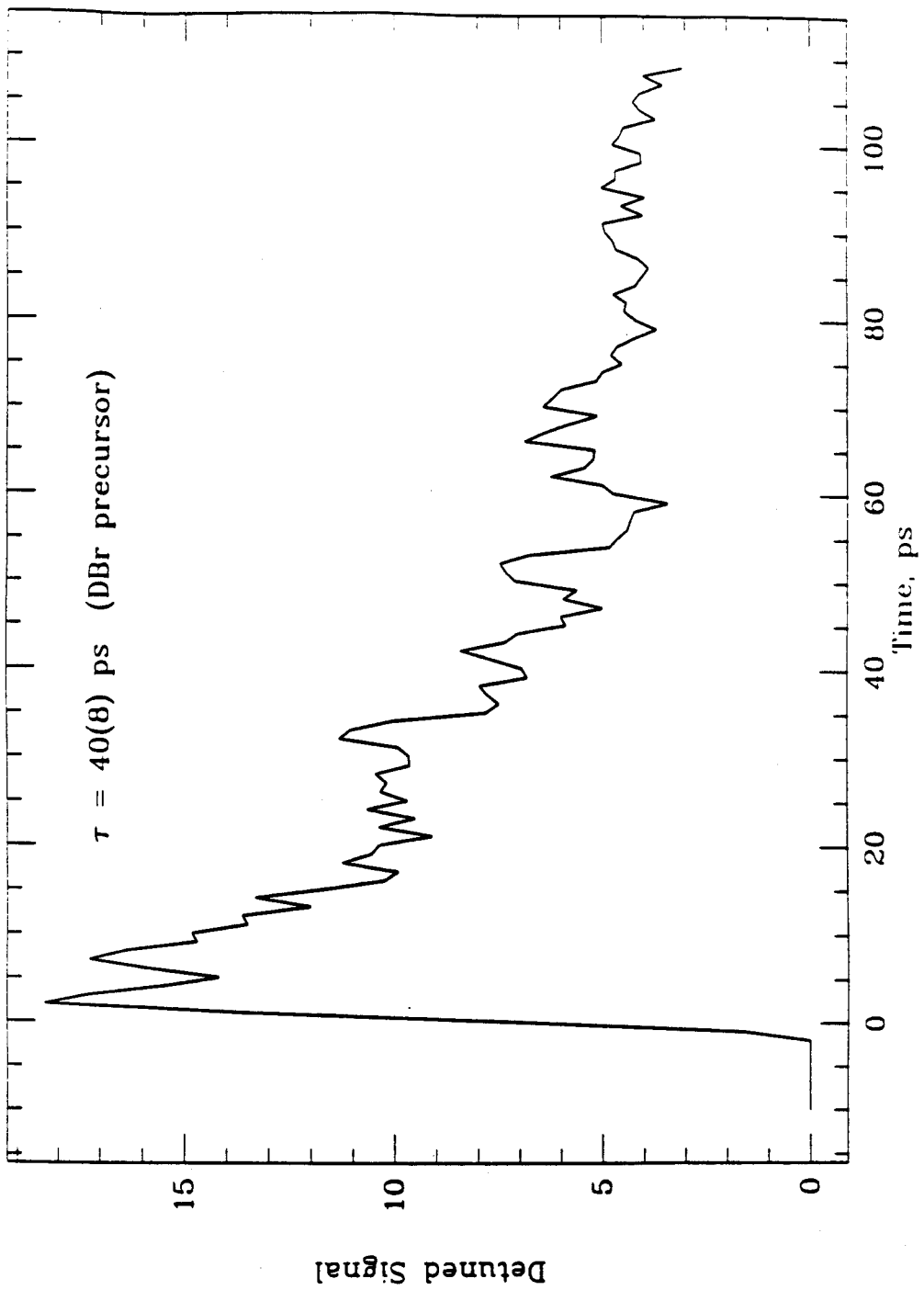
τ = 40(8) ps (DBr precursor)
Detuned Signal
Time, ps
0
5
10
15
0
20
40
60
80
100

Figure 12.

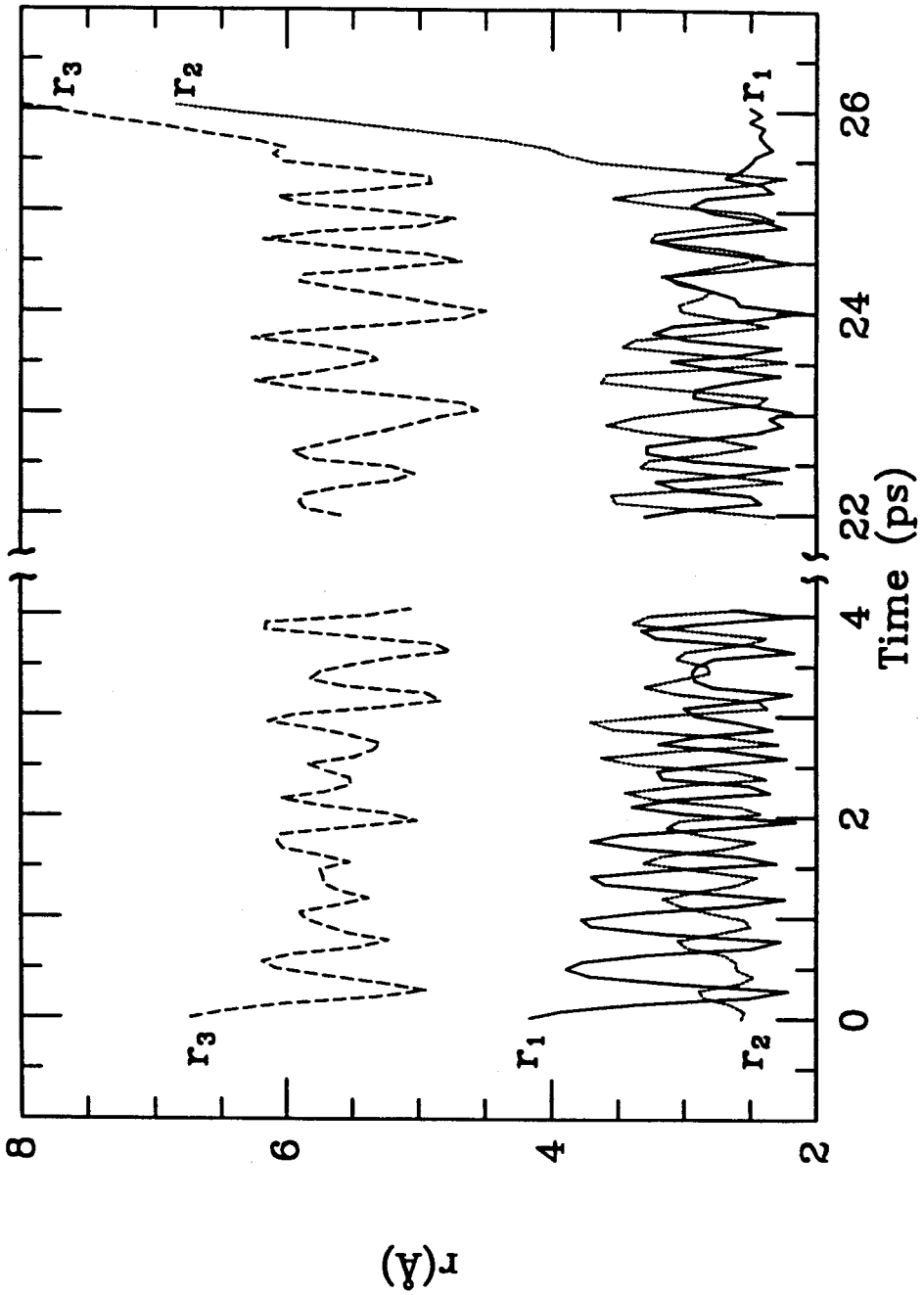

Figure 13.

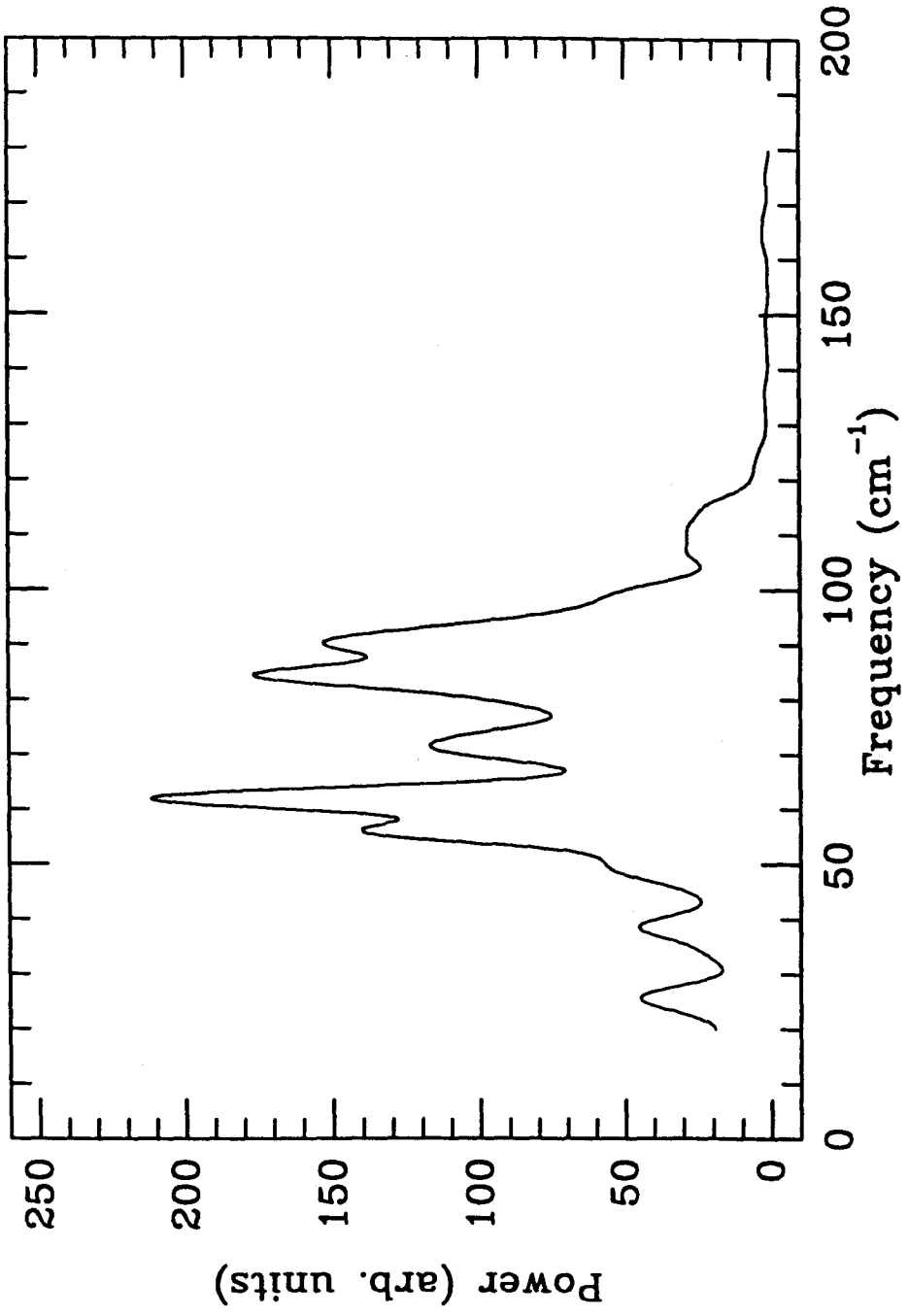
Power (arb. units)
250
200
150
100
50
0
0
50
100
150
200
Frequency (cm^{-1})

Figure 14.

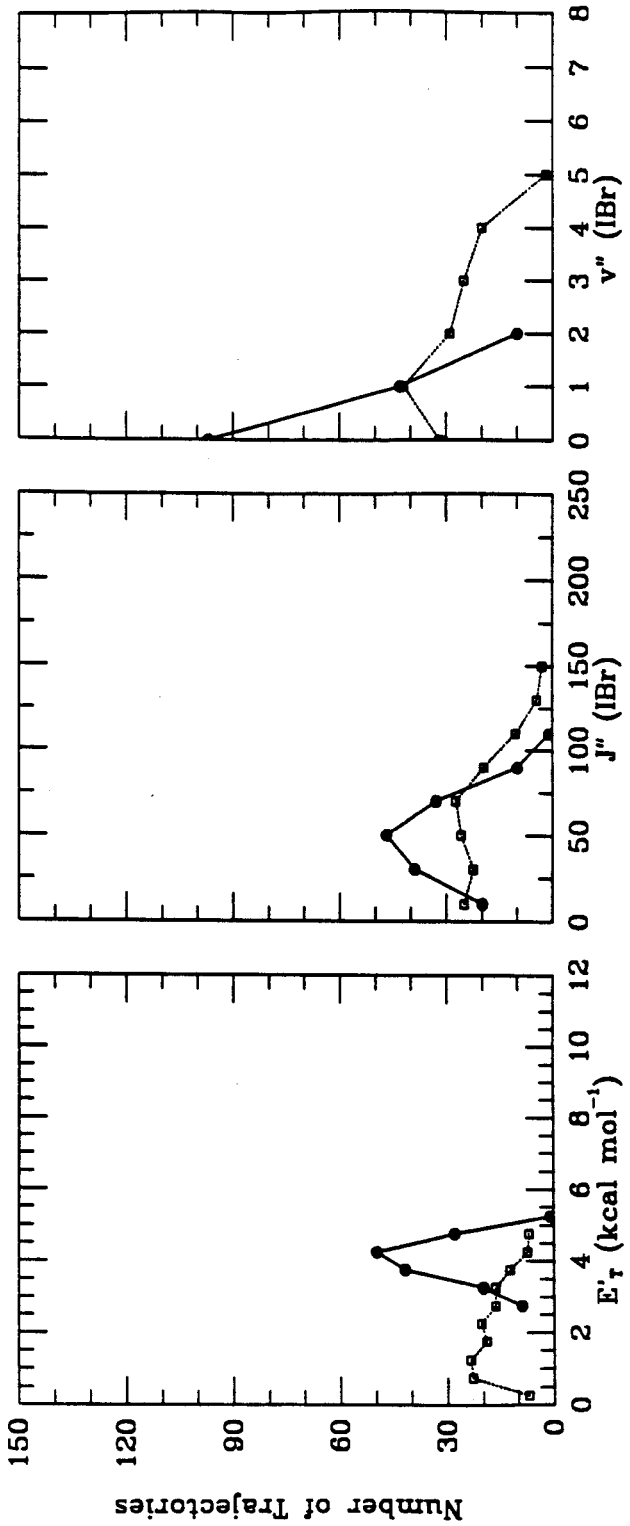
Number of Trajectories
150
120
90
60
30
0
0 2 4 6 8 10 12
E'T (kcal mol-1)
0 50 100 150 200 250
J" (IBr)
0 1 2 3 4 5 6 7 8
v" (IBr)

Figure 15.

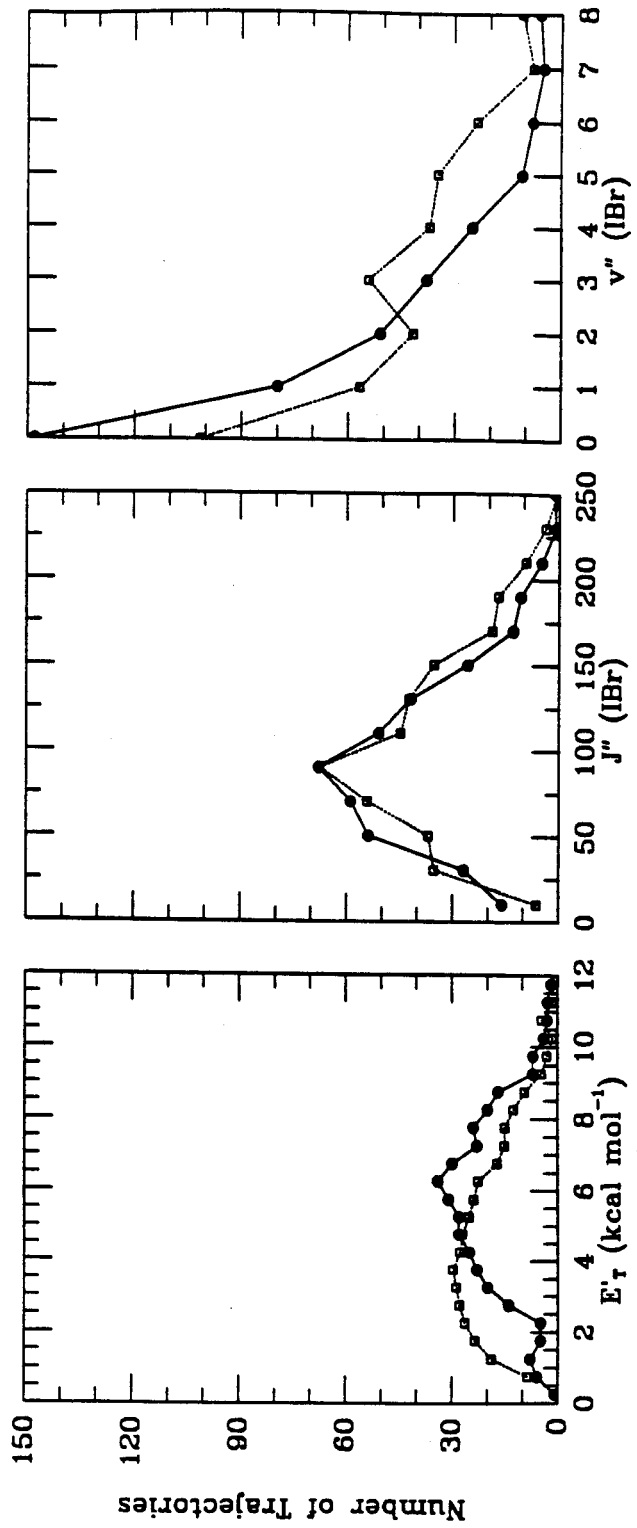
Number of Trajectories
150
120
90
60
30
0
0 2 4 6 8 10 12
E'T (kcal mol-1)
0 50 100 150 200 250
J" (IBr)
0 1 2 3 4 5 6 7 8
v" (IBr)

Figure 16.

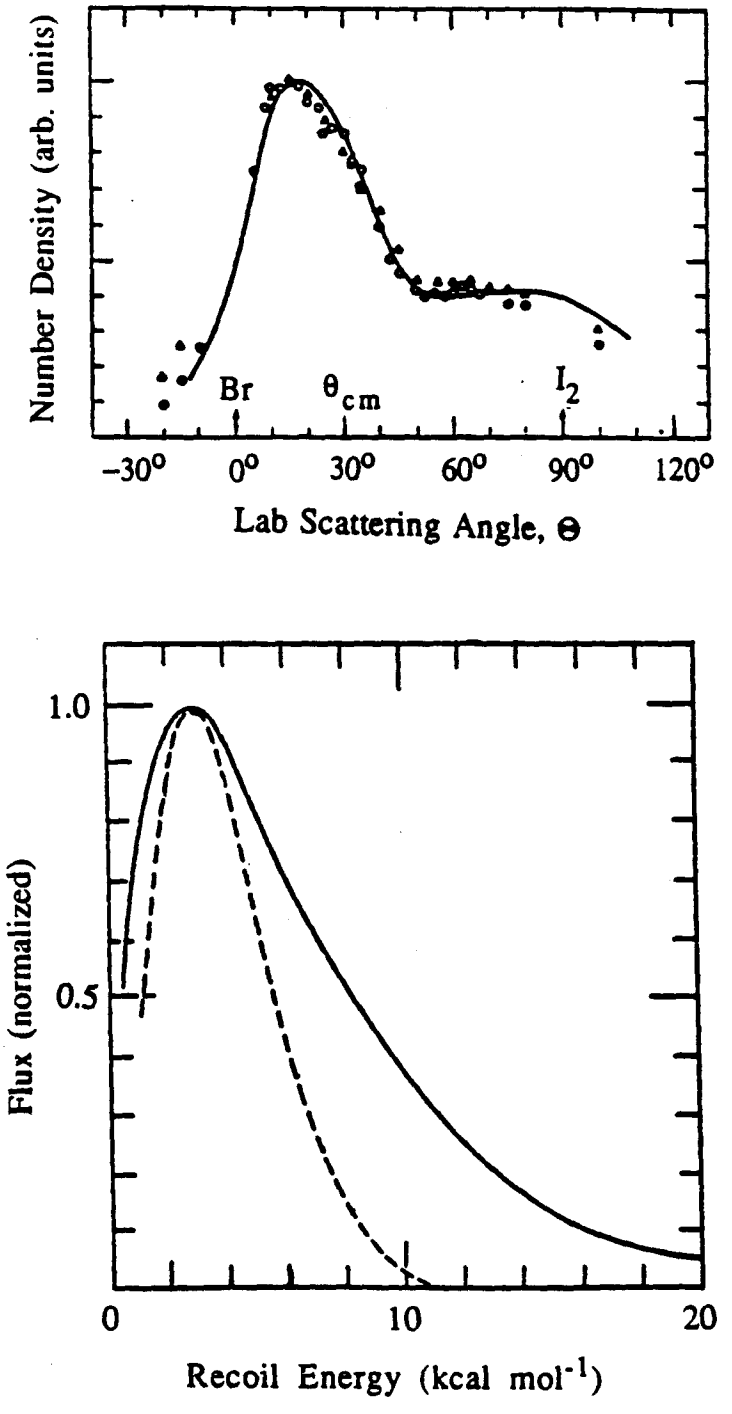
Number Density (arb. units)
Br
θcm
I2
-30°
0°
30°
60°
90°
120°
Lab Scattering Angle, Θ
Flux (normalized)
1.0
0.5
0
10
20
Recoil Energy (kcal mol-1)

Figure 17.

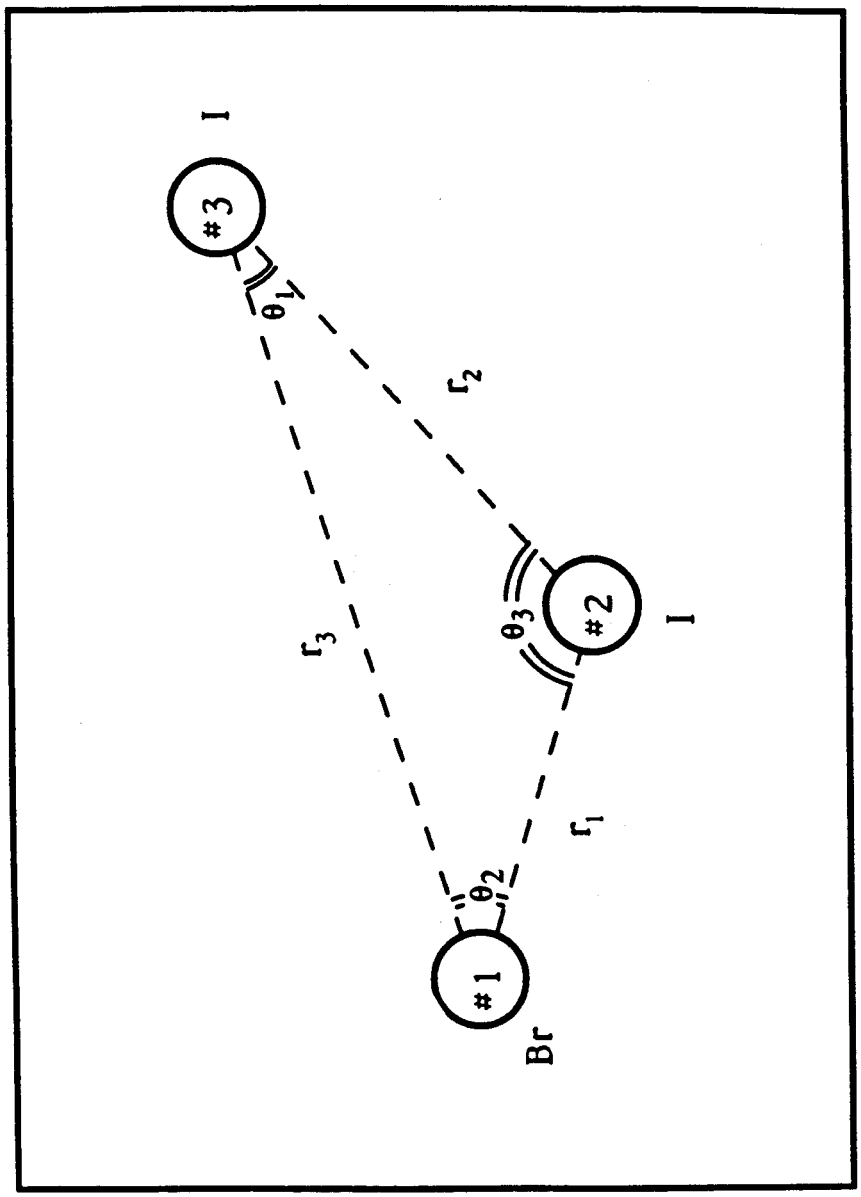

Figure 18.

Chapter 6

Picosecond Dissociation of Ketene: Experimental State-to-State Rates and Tests of Statistical Theories

6.1 Introduction

A number of theoretical approaches have been developed to describe unimolecular reactions, notably phase space theory (PST),[1] statistical adiabatic channel theory (SACM),[2] separate statistical ensembles (SSE)[3] and enhancements of classical RRKM theory.[4] Most of the comparisons between theory and experiment have been for product state distributions. Although slight deviations from PST product state distributions occur even for covalently bound reactants,[4] PST generally correctly predicts product state distributions. This is illustrated clearly for ketene dissociation in the work of the Moore group[5] in the dissociation of ketene to methylene (*subvibrational excitation*):

$$CH_2{=}C{=}O \rightarrow CH_2 + CO.$$

Recently, time resolved photofragment dynamics have been reported for a number of species.[6,7] In NCNO for example, PST or standard RRKM theory could not be brought into agreement with experimental observation:[6] PST predicts excessively high rates, while standard RRKM predicts lower rates, and even when arbitrarily adjusted for a looser transition state, accounts only for portions of the k(E) dependence. Clearly, a theory that can properly account for the energy dependence of the transition state is required, and has recently been proposed by Marcus and coworkers (variational RRKM).[4]

The photofragmentation of ketene is a prototype of unimolecular reactions and has been studied extensively at the bulk and state-to-state levels.[8-11] This makes it an excellent choice for further study of the discrepancy between product state measurements, which are well accounted for by PST (or SSE), and time resolved measurements, for which PST fails dramatically. The topology of the potential energy surface (PES) is known from several recent *ab initio* studies;[12,13] a simple one-dimensional picture, neglecting the complexities of conical intersections in the triplet manifold, is shown in Fig. 1.

In a series of studies, Moore and coworkers have examined the product state distributions and singlet-triplet branching ratios near threshold.[5,9-11] Here, we present measurements of methylene state-resolved reaction rates as a function of energy. As in the case of NCNO, PST and classical RRKM cannot explain the reaction rate over the full energy range studied here (500 to 5600 cm^{-1} above dissociation energy), with PST again failing on the high side even at the lowest energies. Better agreement with the rates is obtained by variational RRKM theory,[14] which also yields product state distributions surprisingly close to those predicted by PST, considering the adiabatic assumption made for the evolution of rovibrational states from the transition region to the products.

6.2 Experimental

The two color picosecond pump-probe experiment has been described in detail elsewhere.[7] Only a brief summary with emphasis on the ketene experiment is given here. A diagram of the pump-probe process is shown in Fig. 1. The pump beam (280-325 nm) excites the parent ketene molecule to the S_1 state, from which the molecule internally converts back to the ground state 450-5600 cm^{-1} above the singlet dissociation threshold at 30116 cm^{-1}. The time delayed probe beam (~600 nm) then excites the a^1A1 (bending mode $v_2 = 0, 1$) methylene fragments to the b^1B_1 electronic state, from which they are detected by laser induced fluorescence (LIF).

Two tunable laser sources were provided by an actively mode-locked, frequency doubled YAG synchronously pumping two picosecond dye lasers. The pulses were amplified in two separate multi-stage Q-switched YAG pumped dye amplifiers, resulting in visible power levels of 50-500 μJ/pulse at a 20 Hz repetition rate. A combination of spatial filters, low-pass filters and saturable absorbers was used to minimize ASE in the amplifiers. Pump radiation was generated by doubling one of the laser beams in a KDP, BBO or LiIO3 crystal. In some experiments, a single laser source was used, and the second frequency produced by continuum generation.

Birefringent filters in the dye lasers allowed frequency selection to 2.5 cm^{-1}, with the pulse duration generally within a factor of two of the uncertainty limit. The relatively long pulses (>5 ps Gaussian crosscorrelation HWHM) thus had sufficient spectral resolution to probe single lines or small portions of methylene rotational subbands with well defined rotational energies. Autocorrelations and crosscorrelations were taken before and after experiments to determine the pulse width.

The ketene was synthesized from acetic anhydride by distillation in a hot tungsten wire column and tested for purity by NMR and gas chromatography.[16] No significant changes in decay times were found with numerous batches over a period of several months. Ketene was held in a -63° C trap and seeded into a He (1.2-2 atm) pulsed (20 Hz) molecular beam, expanding through a 500 μm nozzle into an interaction region held to $<3 \times 10^{-4}$ torr by a rotary pump backed 6" oil diffusion pump. Several scans were done at varying He pressures, and even at the lowest excess energies, no significant variation in decay time was found. Above 2000 cm^{-1}, even an effusive ketene beam increased the rate by only 20%. The effective rotational temperature of the reactant in the beam (estimated to be less than 4 K) thus was sufficiently low not to interfere with the rate measurements.

Depending on the experiment, either the pump or the probe beam was delayed on a 20 μm resolution translation stage, before being colinearly recombined by a dichroic mirror and focused into the interaction region. The methylene LIF was detected by a right angle PMT and F/1 collimating lens. (000) fluorescence was detected with a UV cutoff filter, while (010) fluorescence was enhanced over the ground vibrational state product by two filters yielding a 517-581 nm bandpass. Excitation spectra were in agreement with reference[17] and sample spectra provided by Moore and coworkers.[18,19] The pump power was kept sufficiently low (<50 μJ) to avoid saturation effects: no changes in rates were evident over a factor of three change in visible and UV laser powers.

The photon count rate was sufficient to allow boxcar averaging of the signal over a 0.5-1 μs time window 0.5-1 μs from time zero as defined by the pump beam. The boxcar output (time constant typically 1 sec.) was read by an A/D converter into a control program running on an IBM PC AT. The translation stage controller also provided the timing for the computer.

Two types of experiments were performed. The pump laser dependence of the reaction time constant yields the dependence of the rate constant on excess energy over the range 500 to 5600 cm^{-1}. Tuning the probe laser to different methylene rovibronic transitions is sensitive to any product state variation of the rate constant. In the statistical limit, all product states satisfying angular momentum and energy constraints should have the same reaction rate at a given excess energy.

6.3 Results and Discussion

The optimal signal to noise ratio obtained for a given averaging time is illustrated in Fig. 2, showing a decay to the (000) methylene product. The half lives and rate constants for a variety of excess energies and $^1CH_2$ product states are given in Table I, and shown in Fig. 3 with two standard deviation error bars.

The errors exclude any possible systematic sources, such as saturation effects or high rotational excitation of the parent, which were, however, eliminated as discussed in the previous section. Several of the data points, marked by a * in Table I, are the result of two or more separate measurements, often separated by several months and using different conditions of laser power or He backing pressure. No statistically significant deviations were found in such cases, and the data and uncertainties averaged appropriately.

In the (000) data, no rotational dependence of the rate constant was evident for J = 1-4. A J = 8 state measurement at an excess energy of 2521 cm^{-1} turned out to be 122(14) ps, as opposed to 95(14) and 99(5) ps for lower rotational states, barely significant at the 2 standard deviation level. Unfortunately, many of the higher J CH_2 b

$\leftarrow a$ transitions are perturbed by a triplet state, with no combination differences available in the literature to decide whether the perturbation is in the lower state. That, and the lower signal to noise make it difficult to asses any rotational dependance above $J = 4$, but it certainly does not appear to be very large.

The (010) data points closely trail the ground state decay times, but lie slightly lower at higher excess energies. This might be a consequence of the lower signal to noise ((010) transitions are expected to be 2-16 times weaker than those of the fundamental over the energy range studied), but it is nonetheless interesting to speculate as to the source of the shift. If some of the reaction energy were locked in the vibrational mode(s) in the early stages of the transition state motion, one would expect this to lead to a lowering of the energy distributable among the remaining vibrations, including the reaction coordinate; if the further evolution to the product is vibrationally adiabatic, higher vibrationally excited product states might be expected to form with a slower decay rate. In the extreme case of a completely separate energy reservoir for a given vibration, the k(E) curve could be shifted by as much as the vibrational frequency for the first excited vibrational state.

We now turn to the more marked features of the reaction rate energy dependence. There has been some speculation in the literature as to the relative importance of internal conversion and dissociation from the S_1 surface in determining the observed rate constant. Between the triplet and singlet threshold, collisional deactivation experiments indicate that electronic relaxation to the ground state or intersystem crossing proceed on a shorter time scale than dissociation.[20] Similar behavior, 1832 cm^{-1} above the singlet threshold, indicates that internal conversion is still the fastest process.[20] PHOFEX experiments corroborate this near threshold, since the singlet methylene quantum yield appears to be proportional to the number of available product states, as expected from transition state theory.[5] Over the energy range of the present study, the Whitten-Rabinovich density of states of ketene increases only by a factor of three, and barring any dramatic changes in

the S_0-S_1 coupling matrix elements, internal conversion cannot explain the rapid rise of k(E) (Fig. 3), which would be expected to flatten out as intersystem crossing became predominant higher above threshold. One can therefore conclude that up to at least 5600 cm^{-1}, the observed rate is dominated by the actual S_0 unimolecular dissociation rate.

A number of estimates of the singlet dissociation rate have been made in the literature. Stern-Vollmer extrapolations from collisional quenching data 1832 cm^{-1} above the threshold indicate that the decay time should be approximately 100 ps.[8] From Fig. 3, the directly measured decay time at that energy is 160(20) ps (interpolated value). Chen *et al.*[5] have set a lower limit of 7×10^7 sec^{-1} on the threshold rate constant. Our 500 cm^{-1} data point indicates a rate of 9.8×10^8 sec^{-1}, and using the variational RRKM fit as an extrapolation (discussed below) we find a threshold rate near 2×10^8 sec^{-1}. With these values and Table I, an accurate experimental description of k(E) for the singlet channel is now available, which will hopefully be useful in reevaluating the detailed product state distribution and quantum yield measurements.

Several measurements are available in the literature of triplet to singlet channel fractional yields. At 125 cm^{-1}, Chen *et al.*[5] reported the triplet fractional yield to be 0.3. It decreases to 0.2 at 1832 cm^{-1} [Ref. 8] and less than 0.1 at 2350 cm^{-1} [Ref. 21]. At higher excess energy, the rate of methylene formation is thus essentially given by the measured singlet rate constant. At lower excess energies, measured quantum yields of singlet levels can be used to obtain a more accurate value for averaged triplet rate constants.

The question remains, how well various theoretical approaches can predict the experimental energy dependence of the reaction rate. Fig. 4 shows a plot of the (000) k(E) data and several theoretical rate dependences based on the following expression for the rate constant:

$$k(E) = N^{\ddagger}(E) / h\,\rho(E), \qquad (6.1)$$

where $\rho(E)$ is the ketene S_0 density of states. $N^{\ddagger}(E)$ is the number of accessible product channels at the transition state. In PST, the transition state is assumed to lie at "infinite" fragment separation, and $N^{\ddagger}(E)$ is simply the number of accessible ($\leq E$) product states satisfying angular momentum conservation. In classical RRKM, the transition state is assumed to be similar to the parent configuration, and $N^{\ddagger}(E)$ is simply the number of accessible states ($\leq E$) at the transition state with that configuration. In variational RRKM,[4] the transition state is chosen somewhat less arbitrarily to lie at the position of minimum flux (bottleneck) along the reaction coordinate, and the number of available channels is evaluated there.

The worst agreement is obtained by classical RRKM. The calculation in Fig. 4 uses the Whitten-Rabinovich vibrational state densities and a Haarhoff anharmonicity correction (which increases the level density by only a factor of 1.6-1.7 over the experimental energy range).[22] It is unlikely that the density of states is much higher than that calculated by the semiclassical anharmonic theory (3 - 11) x 10^4 per cm^{-1} over the energy range investigated), and the failure of classical RRKM in this case can be ascribed to the loose nature of the ketene transition state. The curve can be brought into qualitative agreement with the data by decreasing the unconserved vibrations (all bends other than the CH_2 bend) in the transition state configuration. However, no combination of densities of state calculation (direct count, semiclassical) and choice of frequencies brings the curve into quantitative agreement with experiment. In any case, such attempts, or a reduced number of 'effective' oscillators, shed no further light on the reaction mechanism.

The comparison with PST, which has very successfully predicted methylene product distributions and PHOFEX spectra of Ref. 5, is considerably more interesting. Fig. 4 shows two nearly identical PST calculations, both performed before the time resolved data became available. The one by Green *et al.*[11] calculates the density of states of ortho ketene by dividing the harmonic Whitten-Rabinovich result by two, and uses

explicit ortho methylene term values for the lower product states. They obtained the best PHOFEX fits using a strongly attractive interfragment potential, *i.e.*, nearly classical PST with the transition state essentially at infinity. The one by Klippenstein and Marcus[14] explicitly treats nuclear spin and parity conservation, but does not use experimental rovibrational energy levels for the lowest product states. They have considered a range of attractive potential parameters C_6 between 5×10^4 cm^{-1} (the value chosen by Green *et al.*) and infinity (corresponding to an infinitely loose transition state). Both groups also considered the effect of parent rotational excitation, and found a relatively small dependence of k(E) on J between $J = 0$-3 (<20%). Not too surprisingly, the two calculations are in good agreement except at the very lowest energies.

Both PST calculations predict rates faster by a factor of 4 to 8 over those observed experimentally in the energy range 500 to 5600 cm^{-1}. Anharmonic corrections (probably on the order of a 1.5 fold increase in the density of states) would make the agreement only worse, and it appears unlikely that the Whitten-Rabinovich expression seriously overestimates the density of states. A simple downward shift in the PST curve is therefore not possible because of the above argument, and because a match at high energies would drop the threshold rate significantly below the lower limit of 7×10^7 cm^{-1} set by Chen *et al.*,[5] and even further below our estimated threshold rate of 2×10^8 cm^{-1} .

However, PST fails not only at high excess energies, but also at 450-500 cm^{-1}, relatively close to threshold. Furthermore, the PST k(E) has a somewhat larger curvature than observed experimentally at low energies. All this leads to the conclusion that even at low energies, PST severely overestimates the number of accessible product states by positioning the transition state very loosely. While ketene, as illustrated by the failure of classical RRKM, certainly forms a loose transition state complex, it appears that a tightening to smaller values of the reaction coordinate takes place at relatively low energies. This then results in a more slowly rising rate, lower than PST by a factor of 3 at 500 cm^{-1}, and by a factor of 8 at 5600 cm^{-1}. On the other hand, the success of PST in

predicting PHOFEX experiments indicates that the nonadiabatic assumption in the product distribution may be sound.

Fig. 4 also shows a variational RRKM calculation by Klippenstein and Marcus.[14] The rate constant is increased considerably over its classical RRKM value by using a minimum flux criterion to select the position of the transition state, rather than arbitrarily fixing it near the parent configuration with its high vibrational frequencies. This allows the transition state to move inward on the reaction coordinate at higher energies, moving smoothly from more PST to more RRKM like behavior. The agreement of the variational RRKM calculation (using a potential surface interpolated between the parent and the fragments, and semiclassical harmonic level densities) with experiment is excellent over the entire energy range 450-5600 cm^{-1}, supporting the notion that the bottleneck of the reaction lies far out at low energies (PST like) and moves closer to the parent configuration as the reaction proceeds faster at high excess energies. It should be noted that at the very lowest excess energies, the experimentally observed rates seem to be slightly faster than predicted by variational RRKM, although still in much better agreement than with PST.

RRKM theory is generally not used to make predictions of product state distributions, since there is no clearcut 'correct' way of linking the transition state levels with the product state levels of interest. Recently, Marcus[15] has developed an extension of RRKM which calculates conserved vibrational product distributions assuming adiabaticity after the variational RRKM transition state is reached, but allowing rotational (and transition coordinate) nonadiabaticity to the PST angular momentum barrier (essentially at $r = \infty$ for large values of C_6). The PST-like evolution of the rotational distribution is very important, since adiabatic theories (SACM) have not predicted the ketene PHOFEX data,[5] presumably because of free rotational (and transitional coordinate) energy flow until the loose transition state is reached. This extension of RRKM thus yields rotational distributions in close agreement with PST, while leading to

higher excitation in the 'frozen' vibrational modes, similar to SSE or SACM theory. Fig. 5 shows the similarity between variational RRKM and PST rotational product distributions.

It thus appears that variational RRKM, with its adiabatic treatment of vibrations and a loose transition state for the rotational and transitional modes allow a simultaneous treatment of time resolved and product state data. One important question that remains open is the prediction of vibrational PSD's. In the time domain, the excited vibrational states appear to behave very similarly to the ground state, but it remains to be seen whether bending vibrations in CH_2 are indeed as highly excited as predicted by variational RRKM. Moore *et al.* are currently investigating the (010) and (020) product levels of singlet methylene by PHOFEX, and their experimental results will hopefully answer this question.[18] It would be interesting to compare our results, on ketene and NCNO dissociation state-to-state rates, with Quack and Troe's SACM theory to assess the role of full adiabaticity on reaction rates in these prototype systems.[23]

6.4 Conclusion

The singlet channel state-to-state dissociation rate of ketene to methylene varies between about 2×10^8 sec^{-1} at threshold and 5.6×10^{10} sec^{-1} at 5600 cm^{-1}. There is no significant J dependence of the rotational constant at low rotational product excitation, but there appears to be a slight difference in the rates for the (000) and (010) states. The energy dependence of $k(E)$ is in poor agreement with PST theory because of its loose transition state assumption. Much better agreement results with variational RRKM theory, which correctly predicts the rate, while yielding PST-like rotational product distributions. However, only a crude interpolated potential could be used in the calculations. An accurate and global theoretical potential energy surface and bending vibrational PSD's of the singlet methylene fragment are required to fully test variational RRKM in both the time and product state domains. The ketene reaction is the second example (after NCNO) from this group which shows that while PSD are describable by

PST, the state-to-state rates are not. Clearly, the PSD and rate measurements on the state-to-state level allow for a more stringent test of the various theories.

Table I. Ketene to methylene state-to-state rates.

	Excess Energy[a] (cm^{-1})	Probe λ (nm)	Transition[b]	τ (2σ) (ps)
(000)	*450[c]	590.60	$1_{01} \leftarrow 1_{11}$	907 (80)
	500	590.60	$1_{01} \leftarrow 1_{11}$	1020 (55)
	*1107	590.60	$1_{01} \leftarrow 1_{11}$	418 (70)
	1435	590.60	$1_{01} \leftarrow 1_{11}$	256 (24)
	1720	590.60	$1_{01} \leftarrow 1_{11}$	198 (50)
	2521	593.60	$2_{02} \leftarrow 3_{12}$	95 (14)
	*2521	594.28	$3_{03} \leftarrow 4_{13}$	98 (10)
	2521	594.28	$3_{03} \leftarrow 4_{13}$	122 (14)
	2565	594.28	$3_{03} \leftarrow 4_{13}$	118 (8)
	2665	594.28	$3_{03} \leftarrow 4_{13}$	99 (16)
	2942	594.28	$3_{03} \leftarrow 4_{13}$	72 (6)
	3217	594.28	$3_{03} \leftarrow 4_{13}$	63 (8)
	3217	590.60	$1_{01} \leftarrow 1_{11}$	70 (4)
	3538	594.28	$3_{03} \leftarrow 4_{13}$	52 (2)
	3744	590.74	$3_{03} \leftarrow 3_{13}$	50 (14)
	3782	594.28	$3_{03} \leftarrow 4_{13}$	63 (24)
	4367	590.60	$1_{01} \leftarrow 1_{11}$	29 (2)
	*4870	590.60	$1_{01} \leftarrow 1_{11}$	22 (8)
	4920	590.74	$3_{03} \leftarrow 3_{13}$	21 (6)
	5598	590.74	$3_{03} \leftarrow 3_{13}$	18 (4)
(010)	2501	610.20	$1_{10} \leftarrow 0_{00}$	96 (15)
	3351	610.80	$1_{11} \leftarrow 1_{01}$	80 (18)
	3351	609.56	$2_{11} \leftarrow 1_{01}$	84 (24)
	3555	610.20	$1_{10} \leftarrow 0_{00}$	53 (5)
	*3782	609.56	$2_{11} \leftarrow 1_{01}$	75 (8)
	3956	610.80	$1_{11} \leftarrow 1_{01}$	63 (8)

a) Energy above dissociation at 30,116cm^{-1}
b) From Ref. 16.
c) Represents multiple transients averaged together.

6.5 References

1. P. Pechukas and J. C. Light, *J. Chem. Phys.*, **42**, 3238 (1965)
2. M. Quack and J. Troe, *Ber. Bunsenges.*, **78**, 240 (1974).
3. C. Wittig, I. Nadler, H. Reisler, M. Noble, J. Catanzarite and G. Radhakrishnan, *J. Chem. Phys.*, **83**, 5581 (1985).
4. a) D. M. Wardlaw and R. A. Marcus, *Adv. Phys. Chem*, **70**, 231 (1988); b) S. R. Klippenstein and R. A. Marcus, *J. Phys. Chem.*, **92**, 5412 (1988).
5. I.-C. Chen, W. H. Green and C. B. Moore, *J. Chem. Phys.*, **89**, 314 (1988).
6. L. R. Khundkar, J. L. Knee and A. H. Zewail, *J. Chem. Phys.*, **87**, 77 (1987).
7. a) N. F. Scherer and A. H. Zewail, *J. Chem. Phys.*, **87**, 77 (1987); b) J. L. Knee and A.H. Zewail, *Spectroscopy*, **5**, 44, (1988).
8. V. Zabransky and R. W. Carr, Jr., *J. Chem. Phys.*, **79**, 1618 (1975).
9. H. Bitto, I.-C. Chen, and C. B. Moore, *J. Chem. Phys.*, **85**, 5101 (1986).
10. D. J. Nesbitt, H. Petek, M. F. Foltz, S. V. Filseth, D. J. Banford and C. B. Moore, *J. Chem. Phys.*, **83**, 223 (1985).
11. W. H. Green,Jr., I.-C. Chen and C. B. Moore, *Ber. Bunsenges. Phys. Chem.*, **84**, 389 (1988).
12. S. Yamabe and K. Morokuma, *J. Am. Chem. Soc.*, **100**, 7551 (1978).
13. W. D. Allen, H. F. Schaefer III, *J. Chem. Phys.*, **89**, 329 (1988).
14. S. R. Klippenstein and R. A. Marcus, *J. Chem. Phys.*, **91**, 2280 (1989).
15. R. A. Marcus, *Chem. Phys. Lett.*, **144**, 208 (1988).
16. J. Firl and W. Runge, *Angew. Chemie*, **85**, 668 (1973).
17. H. Petek, Ph.D. thesis, University of California at Berkeley, 1985.
18. C. B. Moore, private communication.
19. S. K. Klippenstein and R. A. Marcus, private communication.

20. a) G. A. Taylor and G. B. Porter, *J. Chem. Phys.*, **36**, 1353 (1962); b) A. N. Strachnan and D. E. Thornton, *Can. J. Chem.*, **46**, 2353 (1968).

21. G. C. Hayden, D. M. Neumark, K. Shobatake, R. K. Sparks and Y. T. Lee, *J. Chem. Phys.*, **76**, 3607 (1982).

22. P. C. Haarhoff, *Mol. Phys.*, **7**, 101 (1963).

23. J. Troe, private communication.

6.6 Figure Captions

1. Picosecond pump-probe scheme on a simplified potential energy diagram of the ketene unimolecular dissociation process. Also shown are the singlet vibrational levels of methylene accessed by the probe laser.
2. LIF transient probing of the 4_{13} (000) product state of singlet methylene. The solid line represents a non-linear least-squares fit of the data to a single exponenetial rise, taking into account the finite pulse width of the lasers. The pump wavelength is 594.3nnm.
3. Reaction rate vs. excess energy, with two standard deviation error bars.
4. (000) reaction rate and theoretical curves; classical RRKM underestimates, and PST overestimates the observed rates.
5. $^1CH_2$ rotational product state distribution (J) in the (000) state; the variational RRKM curve (o) is remarkably close to the PST distribution (+); reproduced from reference 14 by permission.

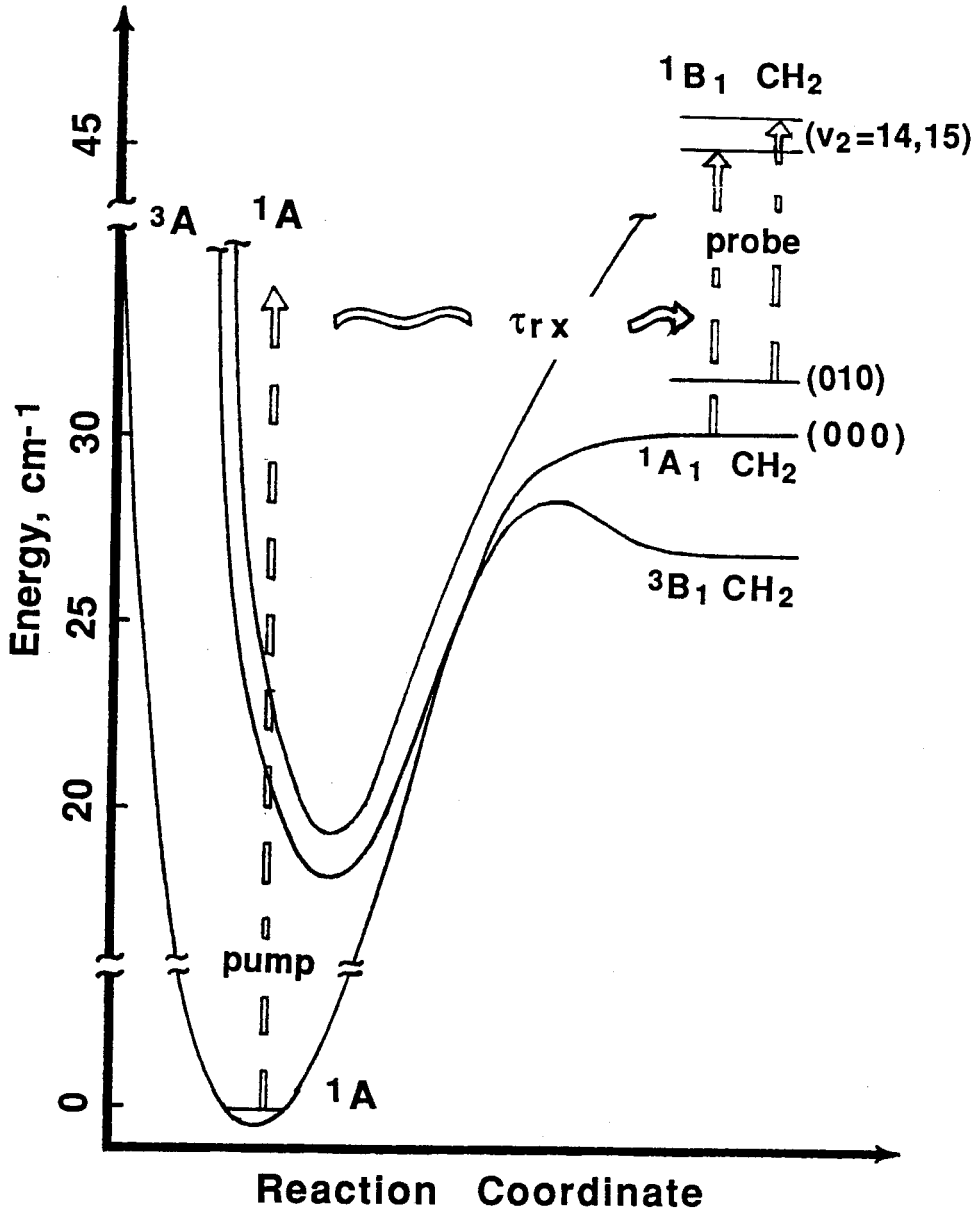
Energy, cm-1
45
30
25
20
0
3A
1A
pump
1A
τrx
1B1 CH2
(v2=14,15)
probe
(010)
(000)
1A1 CH2
3B1 CH2
Reaction Coordinate

Figure 1.

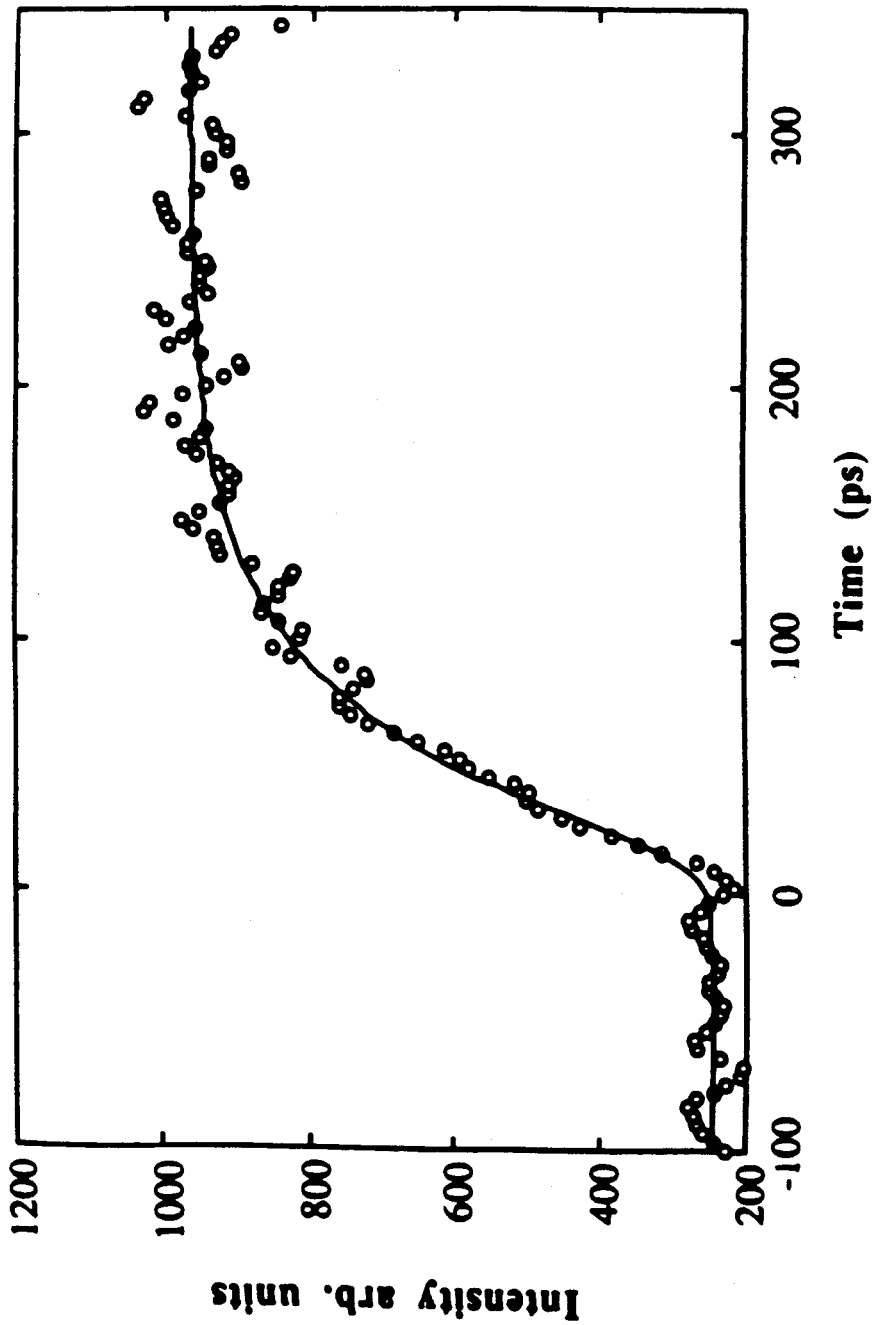
Intensity arb. units
1200
1000
800
600
400
200
-100
0
100
200
300
Time (ps)

Figure 2.

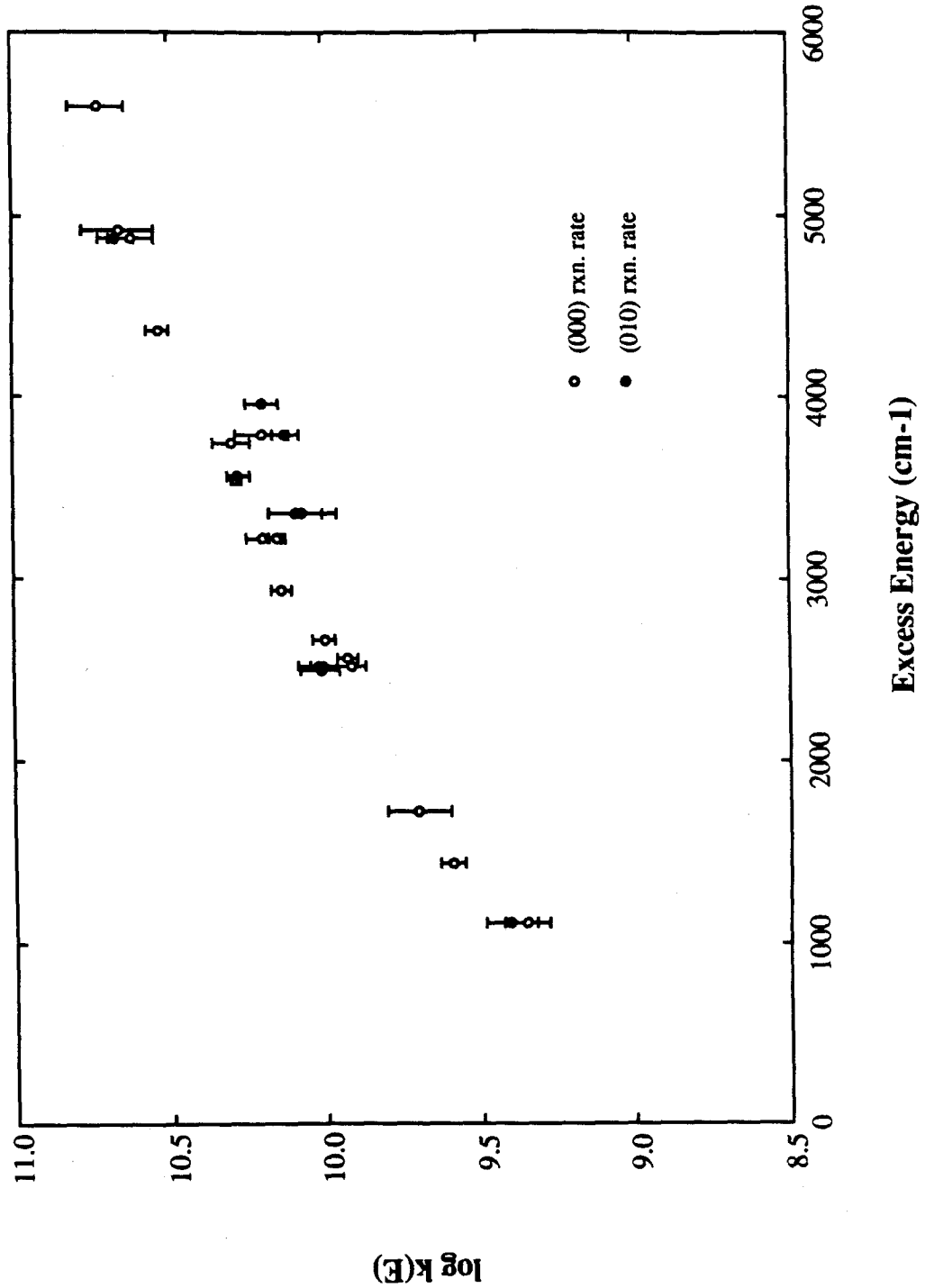
log k(E)
11.0
10.5
10.0
9.5
9.0
8.5
0
1000
2000
3000
4000
5000
6000
Excess Energy (cm-1)
(000) rxn. rate
(010) rxn. rate

Figure 3.

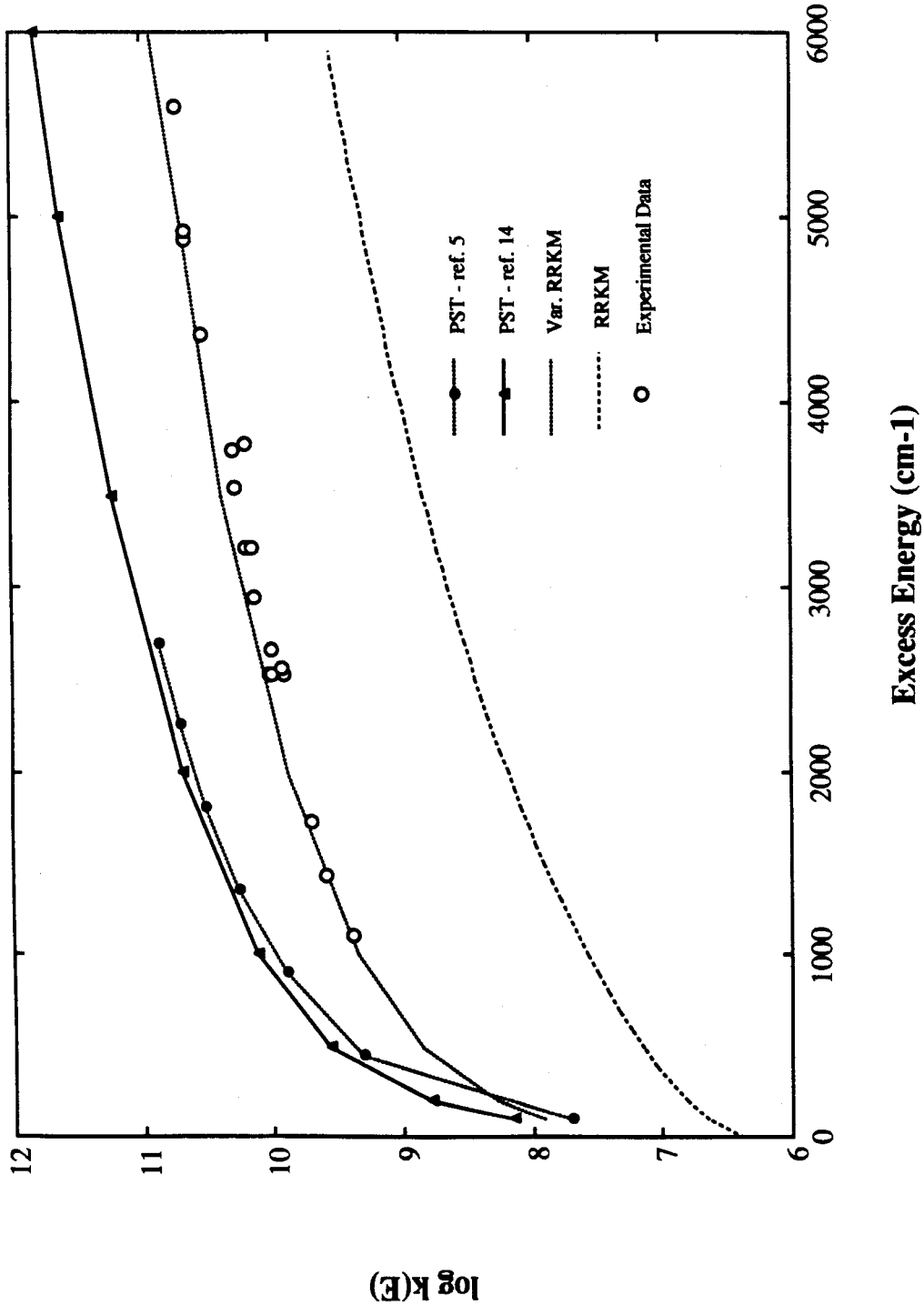
log k(E)
Excess Energy (cm-1)
PST - ref. 5
PST - ref. 14
Var. RRKM
RRKM
Experimental Data
12
11
10
9
8
7
6
0
1000
2000
3000
4000
5000
6000

Figure 4.

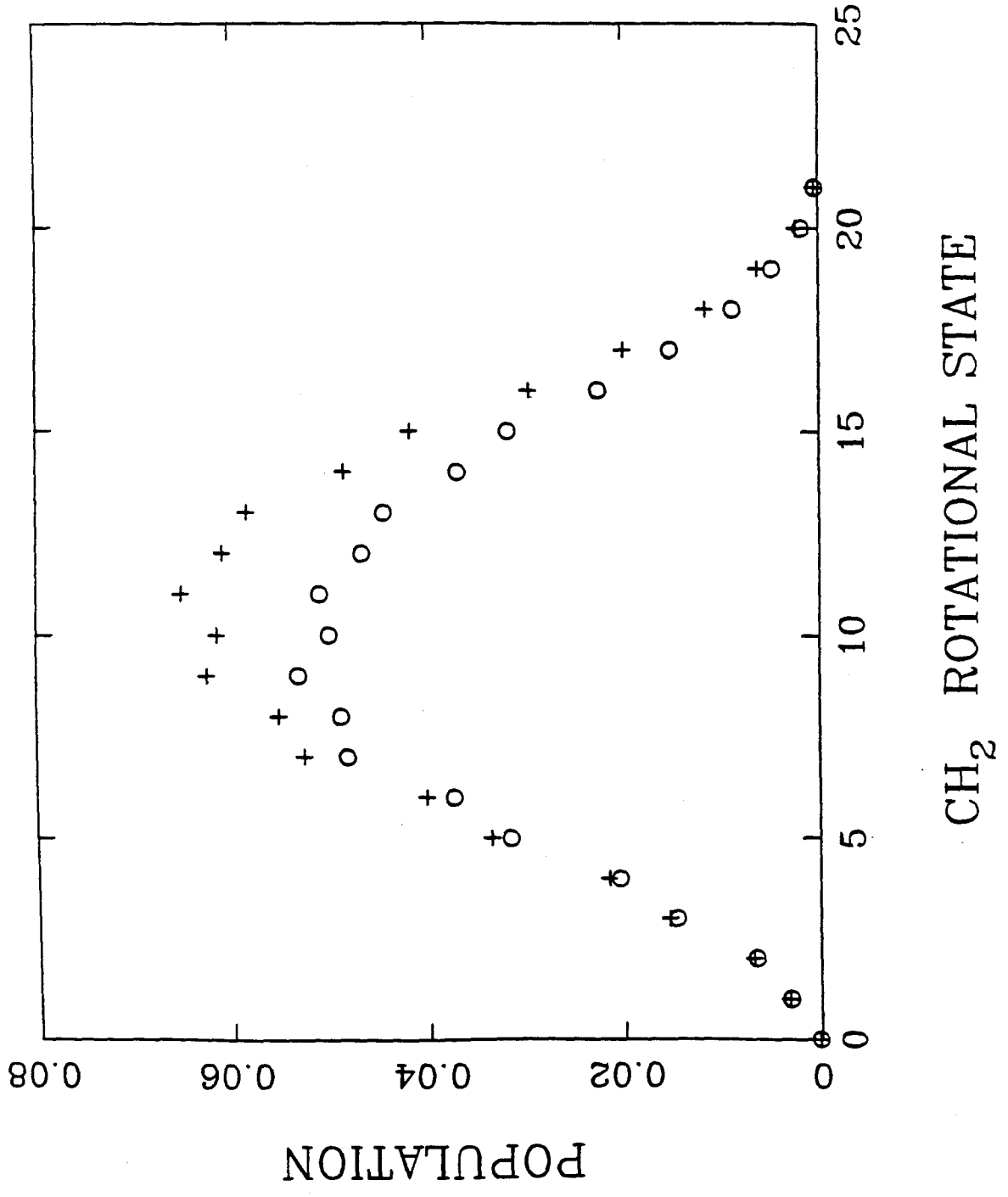
POPULATION
0
0.02
0.04
0.06
0.08
0
5
10
15
20
25
CH_2 ROTATIONAL STATE

Figure 5.

Appendix A

Data Acquisition Program

Main Module

```
'*****************************************************************
'*                                                               *
'*                      Subroutine Declarations                  *
'*                                                               *
'*****************************************************************

DECLARE SUB FILESAVE (MODE%, NPTS%, AV%, HEADER1$, HEADER2$)
DECLARE SUB FIVESCAN (AV%, MODE%, NPTS%)
DECLARE SUB DAC (CHANNEL%, DIGITAL%)
DECLARE SUB DACMENU ()
DECLARE SUB INITMONO (MONOAVAILABLE%)
DECLARE SUB MONOCHROMETER ()
DECLARE SUB SCANSUB (YMIN!, YMAX!, INDEXMIN%, INDEXMAX%)
DECLARE SUB SETUPSUB ()
DECLARE SUB MODE1PARAMETERS ()
DECLARE SUB MODE2PARAMETERS ()
DECLARE SUB MODE3PARAMETERS ()
DECLARE SUB MODE4PARAMETERS ()
DECLARE SUB DEFAULTSUB ()
DECLARE SUB MODE1GO (YMIN!, YMAX!, INDEXMIN%, INDEXMAX%)
DECLARE SUB MODE2GO (YMIN!, YMAX!, INDEXMIN%, INDEXMAX%)
DECLARE SUB RESETPARAMETERS (FIL$)
DECLARE SUB SAVEPARAMETERS (FIL$)
DECLARE SUB DISPLAYSUB (YMIN!, YMAX!, INDEXMIN%, INDEXMAX%)
DECLARE SUB JOG ()
DECLARE SUB DATASUB (YMIN!, YMAX!, INDEXMIN%, INDEXMAX%)
DECLARE SUB DISPLAY (YMIN!, YMAX!, INDEXMIN%, INDEXMAX%)
DECLARE SUB MODE4GO (YMIN!, YMAX!, INDEXMIN%, INDEXMAX%)
DECLARE SUB MOTION (COMM$, REPORT$)
DECLARE SUB SMOOTH3 (YMIN!, YMAX!, INDEXMIN%, INDEXMAX%)
DECLARE SUB GETSTRING (ROW%, COL%, LONGEST%, XP$)
DECLARE SUB KEYBOARDCLEAR ()
DECLARE SUB MODE3GO (YMIN!, YMAX!, INDEXMIN%, INDEXMAX%)
DECLARE SUB SQWAVE (FREQ!)
DECLARE SUB DAS (CHANNEL%, DIO%)
DECLARE SUB MMENU ()
DECLARE SUB FILENAME (ROW%, COL%, FIL$)
DECLARE SUB MCLEAR ()
DECLARE SUB SCLEAR ()

'*****************************************************************
'*          Input/Output Buffers (see Quckcomm manual for description)          *
'*****************************************************************
```

```
DIM TXBUF2(20), RXBUF2(20), TXBUF3(20), RXBUF3(20), TXBUF6(20),
RXBUF6(20)
COMMON SHARED /BUFFERS/ TXBUF2(), RXBUF2(), TXBUF3(), RXBUF3(),
TXBUF6(), RXBUF6()

**********************************************************************
*                    Dimension and Declare Global variables          *
**********************************************************************

DIM LT%(6)                          ' LT%() is used for A/D conversion
COMMON SHARED /GLOBAL/ NPTS%, MODE%, ERRORCODE%
            ' NPTS% is # of data pts. in scan
            ' MODE% is an index referring to boxcar or photon-counter
            ' ERRORCODE% used for error trapping. see end of main module
COMMON SHARED /DAS8/ LT%()
TYPE DATAPAIR                       ' data structure for x,y data pairs
      X AS SINGLE
      Y AS SINGLE
END TYPE
DIM DAT(1000) AS DATAPAIR
COMMON SHARED /D/ DAT() AS DATAPAIR
REM $DYNAMIC              'Allows array space to be cleared after use
REM $INCLUDE: 'QB.BI'     'Include file contains declarations needed for directory
                                function.  See below for printout.
REM $INCLUDE: 'user.inc'  'More subroutine declarations. See below for printout.
DIM SHARED BASADR%  'Base address for A/D converter.
DIM SHARED PARAMETERS(4, 6) AS SINGLE  'List of setup parameters for
                                                    instruments.
DIM SHARED PHOTON$(2, 33)     'Photon counter parameters.  See manual.
DIM SHARED TEMPLATE$(65)      'Used for generating the photon counter parameter
                                    file.
DIM SHARED CALIB, CALIB2      'Calibration factors for delay line.
OPEN "C:\QB45\PROGRAMS\DAS8.ADR" FOR INPUT AS #1  'File containing base
                                                    address of A/D.
INPUT #1, BASADR%
CLOSE #1
FOR i = 1 TO 33
      READ PHOTON$(1, i)        'See data list below for photon counter commands.
NEXT i
CALL RESETPARAMETERS("DATA\DEFAULT.DAT") 'Default parameters are saved
                                                    in file DEFAULT.DAT.
CLS
DO    'Determine which calibration factor to use for delay line.
      LOCATE 2, 2
      PRINT "WHICH GEAR BOX IS BEING USED? ( <1> 261:1   <2> 76:1  )";
```

```
        GB$ = INKEY$
LOOP UNTIL VAL(GB$) = 1 OR VAL(GB$) = 2
IF VAL(GB$) = 1 THEN
        CALIB = .1994          'fs/encoder count 261:1 gear box
        CALIB2 = 29.89         'nm/encoder count
ELSE
        CALIB = .68595         'fs/encoder count 76:1 gear box
        CALIB2 = 102.82        'nm/encoder count
END IF
CALL MOTION("1MN", REPORT$)          'Turn delay line motor on.
CALL MOTION("1SV50", REPORT$)        'Set velocity to 50 (reduced hysteresis).

'*****************************************************************
'*                          Prepare screen                       *
'*****************************************************************

SCREEN 9    'Best screen value for our current monitor. Could be upgraded.
LINE (0, 34)-(639, 349), 1, B: LINE (0, 6)-(639, 32), 1, B
CALL MCLEAR       'Clears menu line.
PRINT "LOCATING INTERFACE BOARDS"
FLAG% = 1
MD% = 0
CALL DAS8(MD%, BASADR%, FLAG%) 'A/D access routine.  See Metrabyte manual.
IF FLAG% <> 0 THEN
   DO
      TIMES% = TIMES% + 1
      CALL DAS8(MD%, VARPTR(BASADR%), FLAG%)
      IF TIMES% = 5 THEN
            PRINT "INSTALLATION ERROR"
            END
      END IF
   LOOP UNTIL FLAG% = 0
END IF
CALL INITMONO(MONOAVAILABLE%)  'Initialize monochromator.  See manual.
CALL MCLEAR: CALL MMENU   'Main menu prints onto menu line.
DO              'Get keyboard response to main menu.
      FK% = 0
      KBD$ = INKEY$
      IF LEN(KBD$) = 2 THEN FK% = ASC(RIGHT$(KBD$, 1))
      IF FK% = 59 THEN CALL SCANSUB(YMIN!, YMAX!, INDEXMIN%,
INDEXMAX%)                    'F1 key.
      IF FK% = 60 THEN CALL DISPLAYSUB(YMIN!, YMAX!, INDEXMIN%,
INDEXMAX%)                    'F2 key.
      IF FK% = 61 THEN JOG    'F3 key.
```

```
        IF FK% = 62 AND MONOAVAILABLE% = 1 THEN CALL
MONOCHROMETER                   'F4 key (as long as mono. is o.k.).
        IF FK% = 63 THEN CALL DATASUB(YMIN!, YMAX!, INDEXMIN%,
INDEXMAX%)                      'F5 key.
LOOP UNTIL FK% = 64

END

DATA        'Valid communication commands for the photon counter
CM,CI0,CI1,CI2,CP,NP,NE,DT,AS,AM,SD,TS,TL,DS0,DS1,DS2,DM0,DM1,DM2
DATA DY0,DY1,DY2,DL0,DL1,DL2,GM0,GM1,GY0,GY1,GD0,GD1,GW0,GW1

HANDLER:        'Error trapping routine.  Send error back and resume one line later.

        ERRORCODE% = ERR
        RESUME NEXT
```

Subroutines

```
*****************************************************************
*                Read A/D converter without using DAS8 command                *
*****************************************************************
SUB DAS (CHANNEL%, DIO%)    'CHANNEL% is the number of the conversion
                                channel.  DIO% is the data.

OUT BASADR% + 2, CHANNEL% 'Send out channel number on second byte.
OUT BASADR% + 1, 0          'Send out zero on first byte.
DO
      STATUS = INP(BASADR% + 2)    'Wait until
LOOP UNTIL STATUS < 128
XL% = INP(BASADR%)                 'Low data byte is at base address
XH% = INP(BASADR% + 1)             'High data byte is at base address plus one.
DIO% = 16 * XH% + XL% / 16 - 2048  'Form the data from the two bytes.

END SUB

*****************************************************************
*                Subroutine active when F5 is hit from main menu.             *
*****************************************************************
SUB DATASUB (YMIN!, YMAX!, INDEXMIN%, INDEXMAX%) 'YMIN! is the
      minimum value of the data set.  YMAX! the maximum.  INDEXMIN%, and
      INDEXMAX% are the indices of the first data point displayed and the last.

DIM MENU(5500) AS INTEGER   'For each menu, need to set aside an array for what
                                is behind the menu so it can be returned.
DIM X(1000), Y(1000)
GET (405, 34)-(530, 190), MENU   'Make menu
LINE (405, 34)-(530, 190), 1, BF
LINE (409, 34)-(526, 186), 0, BF
COLOR 15, 0
LOCATE 2, 56: PRINT "F5:MISC"
COLOR 1, 0
LOCATE 4, 53: PRINT "F1:CONVERT TO"
LOCATE 5, 57: PRINT "MAC FILE"
LOCATE 7, 53: PRINT "F2:3-POINT"
LOCATE 8, 56: PRINT "SMOOTH"
LOCATE 10, 53: PRINT "F3:RETRIEVE"
LOCATE 11, 56: PRINT "DATA# FILE"
LOCATE 13, 53: PRINT "F4:DAC"
DO                                  'Get keyboard response.
      KBD$ = INKEY$
      IF LEN(KBD$) = 2 THEN FK% = ASC(RIGHT$(KBD$, 1))
```

```
SELECT CASE FK%
  CASE 59                    'F1 key.
       COLOR 15, 0
       LOCATE 4, 53: PRINT "F1:CONVERT TO"
       LOCATE 5, 57: PRINT "MAC FILE"
       CALL MCLEAR
       PRINT "                PLACE DATA DISK IN DRIVE A:"
       CALL FILENAME(130, 250, F$)    'FILENAME is a routine designed to
                                            get a filename from the user.
       FIL$ = "A:" + LEFT$(F$, LEN(F$) - 4) + "MAC" 'Get rid of the DAT ext.
       F$ = "DATA\" + LEFT$(F$, LEN(F$) - 1)
       OPEN F$ FOR INPUT AS #1        'Input data from file.
       OPEN FIL$ FOR OUTPUT AS #2     'Output data onto floppy drive.
       INPUT #1, M%
       INPUT #1, YMIN!, YMAX!, NPTS%, AV%
       INPUT #1, COMMENT$
       INPUT #1, D$
       INPUT #1, DUMMY$, DUMMY$
       DO UNTIL EOF(1)   'Eliminate file info on new file.
            INPUT #1, X, Y       'x,y data pair from file
            PRINT #2, X, Y       'x,y data pair to new file.
       LOOP
       CLOSE #1: CLOSE #2
       CALL MCLEAR        'Clear menu line.
       CALL MMENU         'Print main menu.
       EXIT DO            'Leave this do loop.
  CASE 60                 'F2 key.
       COLOR 15, 0
       LOCATE 7, 53: PRINT "F2:3-POINT"
       LOCATE 8, 56: PRINT "SMOOTH"
       COLOR 1, 0
       CALL SMOOTH3(YMIN!, YMAX!, INDEXMIN%, INDEXMAX%)
                  '3-point smooth directly from Bevington.
       PUT (405, 34), MENU, PSET
       ERASE MENU
       CALL SCLEAR        'SCLEAR clears the data screen.
       CALL DISPLAY(YMIN!, YMAX!, INDEXMIN%, INDEXMAX%)
            'DISPLAY redisplays the now smoothed data.
       COLOR 1, 0
       LOCATE 2, 56: PRINT "F5:DATA"
       EXIT SUB     'Return to main menu.
  CASE 61           'F3 key.
       COLOR 15, 0
       LOCATE 10, 53: PRINT "F3:RETRIEVE"
       LOCATE 11, 56: PRINT "DATA# FILE"
```

```
            OPEN "I", #2, "STATUS"    'STATUS holds the current file number, e.g.
                                      xei321.dat, where the 321 is held in the file.
            INPUT #2, TOTALSCANS%
            CLOSE #2
            COLOR 1, 0
            CALL MCLEAR
            INPUT "WHICH FILE NUMBER WOULD YOU LIKE TO
RETRIEVE"; FINU%                  'Program saves data every five files.  File number is
                                      then number of scans/5.
            CALL MCLEAR
            PRINT "UNDER WHAT NAME WOULD YOU LIKE TO SAVE THIS
DATA"
            CALL FILENAME(100, 250, FIL$)  'Save this data as FIL$.
            FIL$ = LEFT$(FIL$, LEN(FIL$) - 1)
            FIL$ = "DATA\" + FIL$ + RIGHT$(STR$(TOTALSCANS%),
LEN(STR$(TOTALSCANS%)) - 1) + ".DAT"
            OPEN FIL$ FOR OUTPUT AS #2
            F$ = "DATA\DATA" + LTRIM$(STR$(FINU%)) + ".DAT"
            OPEN F$ FOR INPUT AS #1
            INPUT #1, MD%
            PRINT #2, MD%
            DO          'Save data to file.

                INPUT #1, X(i), Y(i)
                IF i = 0 THEN
                        YMIN! = Y(0): YMAX! = Y(0)
                ELSE
                        IF YMAX! < Y(i) THEN YMAX! = Y(i)
                        IF YMIN! > Y(i) THEN YMIN! = Y(i)
                END IF
                i = i + 1
            LOOP UNTIL EOF(1)
            PRINT #2, YMIN!, YMAX!, i, FINU% * 5
            CALL MCLEAR
            PRINT "COMMENTS:"
            CALL GETSTRING(2, 12, 76, COMMENT$)
            PRINT #2, LEFT$(COMMENT$, LEN(COMMENT$) - 1)
            PRINT #2, DATE$
            WRITE #2, "TIME (fs)", "INTENSITY"
            FOR P = 0 TO i - 1
                    PRINT #2, X(P), Y(P)
            NEXT P
            CLOSE #1
            CLOSE #2
            CALL MCLEAR
```

```
            PRINT "SAVED AS "; FIL$; "                    HIT <RETURN> TO
CONTINUE"
            KBD$ = ""
            DO UNTIL KBD$ <> ""       'Pause until user hits a key.
                KBD$ = INKEY$
            LOOP
            TOTALSCANS% = TOTALSCANS% + 1   'Increment the file counter.
            OPEN "O", #1, "STATUS"
            PRINT #1, TOTALSCANS%
            CLOSE #1
            PUT (405, 34), MENU, PSET
            ERASE MENU
            CALL MCLEAR
            CALL MMENU
            EXIT SUB     'Return to main menu.
        CASE 62          'F4 key.
            LOCATE 13, 53: COLOR 15, 0: PRINT "F4:DAC"
            CALL DACMENU   'DACMENU routine controls the D/A converter.
            LOCATE 13, 53: COLOR 1, 0: PRINT "F4:DAC"
            FK% = 0
    END SELECT
LOOP UNTIL KBD$ = CHR$(27)   'Finished with menu.
PUT (405, 34), MENU, PSET    'Put data back on screen behind menu.
ERASE MENU                   'Erase the array MENU in order to save memory.
COLOR 1, 0
LOCATE 2, 56: PRINT "F5:MISC"

END SUB


*****************************************************************
*                  Subroutine active under setup when F3 is hit.  .                  *
*****************************************************************

SUB DEFAULTSUB          'Gives menu for resetting or saving default parameters.

DIM MENU2(1 TO 13084) AS INTEGER  'Menu array
DIM DOTPOS(1 TO 4) AS INTEGER     'Bullets used in the menu
DOTPOS(1) = 146: DOTPOS(2) = 188: DOTPOS(3) = 230: DOTPOS(4) = 272
INDEX% = 1                        'Bullet is set to the first menu item.
GET (180, 100)-(420, 310), MENU2  'Get data behind menu.
LINE (180, 100)-(420, 310), 1, BF 'Make box for menu.
LINE (184, 104)-(416, 306), 0, BF
LOCATE 9, 32: PRINT "PARAMETER FILES"
COLOR 1, 0
```

```
LOCATE 11, 25: PRINT "1 ( ) SAVE PARAMETERS UNDER"
LOCATE 12, 32: PRINT "DEFAULT.DAT"
LOCATE 14, 25: PRINT "2 ( ) SAVE PARAMETERS UNDER"
LOCATE 15, 32: PRINT "OTHER NAME"
LOCATE 17, 25: PRINT "3 ( ) RESET PARAMETERS TO"
LOCATE 18, 32: PRINT "DEFAULT.DAT"
LOCATE 20, 25: PRINT "4 ( ) SET PARAMETERS TO"
LOCATE 21, 32: PRINT "THOSE IN OTHER FILE"
CIRCLE (220, DOTPOS(INDEX%)), 3, 15, , , 1.2: PAINT (220, DOTPOS(INDEX%)),
15

DO          'Get keyboard response.
    KBD$ = INKEY$
    FK% = 0
    IF LEN(KBD$) = 2 THEN FK% = ASC(RIGHT$(KBD$, 1))
    IF FK% = 72 THEN          'If the up arrow is hit, move bullet up one.
        PAINT (220, DOTPOS(INDEX%)), 0, 0
        IF INDEX% = 1 THEN INDEX% = 4 ELSE INDEX% = INDEX% - 1
        CIRCLE (220, DOTPOS(INDEX%)), 3, 15, , , 1.2
        PAINT (220, DOTPOS(INDEX%)), 15
    END IF
    IF FK% = 80 THEN          'If the down arrow is hit, move bullet down one.
        PAINT (220, DOTPOS(INDEX%)), 0, 0
        IF INDEX% = 4 THEN INDEX% = 1 ELSE INDEX% = INDEX% + 1
        CIRCLE (220, DOTPOS(INDEX%)), 3, 15, , , 1.2
        PAINT (220, DOTPOS(INDEX%)), 15
    END IF
    IF KBD$ = CHR$(13) THEN          'If one of the items is chosen.
        SELECT CASE INDEX%
            CASE 1                   'Save current parameters under default.dat.
                COLOR 15, 0
                LOCATE 11, 31
                PRINT "SAVE PARAMETERS UNDER"
                LOCATE 12, 32
                PRINT "DEFAULT.DAT"
                CALL SAVEPARAMETERS("DATA\DEFAULT.DAT")
                COLOR 1, 0
                LOCATE 11, 31
                PRINT "SAVE PARAMETERS UNDER"
                LOCATE 12, 32
                PRINT "DEFAULT.DAT"
            CASE 2                   'Save parameters under different filename.
                COLOR 15, 0
                LOCATE 14, 31
                PRINT "SAVE PARAMETERS UNDER"
```

```
                    LOCATE 15, 32
                    PRINT "OTHER NAME"
                    ROW% = 190: COL% = 450
                    CALL FILENAME(ROW%, COL%, FIL$)
                    CALL SAVEPARAMETERS("DATA\" + LTRIM$(FIL$))
                    COLOR 1, 0
                    LOCATE 14, 31
                    PRINT "SAVE PARAMETERS UNDER"
                    LOCATE 15, 32
                    PRINT "OTHER NAME"
                CASE 3              'Reset parameters to those in default.dat.
                    COLOR 15, 0
                    LOCATE 17, 31
                    PRINT "RESET PARAMETERS TO"
                    LOCATE 18, 32
                    PRINT "DEFAULT.DAT"
                    CALL RESETPARAMETERS("DATA\DEFAULT.DAT")
                    COLOR 1, 0
                    LOCATE 17, 31
                    PRINT "RESET PARAMETERS TO"
                    LOCATE 18, 32
                    PRINT "DEFAULT.DAT"
                CASE 4              'Set parameters to those in filename.
                    COLOR 15, 0
                    LOCATE 20, 31
                    PRINT "SET PARAMETERS TO"
                    LOCATE 21, 32
                    PRINT "THOSE IN OTHER FILE"
                    ROW% = 270: COL% = 450
                    CALL FILENAME(ROW%, COL%, FIL$)
                    CALL RESETPARAMETERS("DATA\" +
LTRIM$(FIL$))
                    COLOR 1, 0
                    LOCATE 20, 31
                    PRINT "SET PARAMETERS TO"
                    LOCATE 21, 32
                    PRINT "THOSE IN OTHER FILE"

            END SELECT
        END IF
LOOP UNTIL KBD$ = CHR$(27)
PUT (180, 100), MENU2, PSET     'Put data back behind menu.
ERASE MENU2                     'Erase array memory so not to use up memory.

END SUB
```

```
**********************************************************************
*                        Subroutine used to display data  .                        *
**********************************************************************

SUB DISPLAY (YMIN!, YMAX!, INDEXMIN%, INDEXMAX%)
                'YMIN! is the minimum y value in the data set.  YMAX! is
                maximum.  'INDEXMIN% is the indece of the first x value.
        VIEW (0, 34)-(639, 349)       'use only the data window.
        WINDOW (2 * DAT(INDEXMIN%).X - DAT(INDEXMIN% + 1).X,
YMAX! + .1 * ABS(YMAX! - YMIN!))-(2 * DAT(INDEXMAX%).X -
DAT(INDEXMAX% - 1).X, YMIN! - .1 * ABS(YMAX! - YMIN!))  'Set new
    coordinates for data window.
        FOR i = INDEXMIN% + 1 TO INDEXMAX%  'Plot data.
            LINE (DAT(i - 1).X, DAT(i - 1).Y)-(DAT(i).X, DAT(i).Y), 15
        NEXT i
        VIEW: WINDOW     'Set window to normal coordinates.

END SUB

**********************************************************************
*                    Subroutine active when F2 is hit from main menu.                *
**********************************************************************

SUB DISPLAYSUB (YMIN!, YMAX!, INDEXMIN%, INDEXMAX%)

DIM MENU(5700) AS INTEGER
GET (105, 34)-(260, 173), MENU
LINE (105, 34)-(260, 173), 1, BF
LINE (109, 34)-(256, 169), 0, BF
COLOR 15, 0
LOCATE 2, 18: PRINT "F2:DISPLAY"
COLOR 1, 0
LOCATE 4, 16: PRINT "F1:DISPLAY FILE"
LOCATE 6, 16: PRINT "F2:CLEAR SCREEN"
LOCATE 8, 16: PRINT "F3:SHIFT"
LOCATE 10, 16: PRINT "F4:EXPAND"
LOCATE 12, 16: PRINT "F5:DIR"
ERRORCODE% = 0
DO              'Get keyboard response.
    KBD$ = "": FK% = 0
    KBD$ = INKEY$
    IF LEN(KBD$) = 2 THEN FK% = ASC(RIGHT$(KBD$, 1))
    IF FK% = 59 THEN   'F1 key.
        PUT (105, 34), MENU, PSET
```

```
ERASE MENU
CALL FILENAME(50, 250, FIL$)
IF FIL$ = "ESC" THEN
        COLOR 1, 0
        LOCATE 2, 18: PRINT "F2:DISPLAY"
        VIEW: WINDOW
        EXIT SUB
END IF
IF INSTR(FIL$, "*") THEN  'If filename has a wildcard in it.
        path$ = "DATA\" + LEFT$(FIL$, LEN(FIL$) - 1)
        CALL DIRECTORY(path$, FIL$)    'Get disk directory routine.
        IF FIL$ = "ESC" THEN
                COLOR 1, 0
                LOCATE 2, 18: PRINT "F2:DISPLAY"
                VIEW: WINDOW
                EXIT SUB
        END IF
        FIL$ = LEFT$(FIL$, LEN(FIL$) - 2)
        FIL$ = RTRIM$(FIL$)
END IF
FIL$ = "DATA\" + RTRIM$(LEFT$(FIL$, LEN(FIL$) - 1))
ON ERROR GOTO HANDLER
OPEN FIL$ FOR INPUT AS #1
DO WHILE ERRORCODE% <> 0   'If error occurs this will handle.
        SELECT CASE ERRORCODE%     'If filename is invalid this
        routine will allow user to try again without crashing program.
                CASE 53
                        CALL MCLEAR
                        COLOR 15, 0
                        PRINT "FILE NOT FOUND.   TRY AGAIN"
                        COLOR 1, 0
                        CALL FILENAME(50, 250, FIL$)
                        IF FIL$ = "ESC" THEN
                                COLOR 1, 0
                                CALL MCLEAR
                                CALL MMENU
                                VIEW: WINDOW
                                EXIT SUB
                        END IF
                        FIL$ = "DATA\" + LEFT$(FIL$, LEN(FIL$) - 1)
                        ERRORCODE% = 0
                        OPEN FIL$ FOR INPUT AS #1
                        CALL MCLEAR
                        CALL MMENU
                CASE 64
```

```
                        ERRORCODE% = 0
                        CALL MCLEAR
                        COLOR 15, 0
                        PRINT "BAD FILE NAME.   TRY AGAIN"
                        COLOR 1, 0
                        CALL FILENAME(50, 250, FIL$)
                        IF FIL$ = "ESC" THEN
                                COLOR 1, 0
                                CALL MCLEAR
                                CALL MMENU
                                VIEW: WINDOW
                                EXIT SUB
                        END IF
                        FIL$ = "DATA\" + LEFT$(FIL$, LEN(FIL$) - 1)
                        ERRORCODE% = 0
                        OPEN FIL$ FOR INPUT AS #1
                        CALL MCLEAR
                        CALL MMENU
                CASE ELSE
                        ON ERROR GOTO 0
        END SELECT
    LOOP
    ON ERROR GOTO 0
    INPUT #1, M%                'Input the data.
    INPUT #1, YMIN!, YMAX!, NPTS%, AV%
    INPUT #1, COMMENT$
    INPUT #1, D$
    INPUT #1, DUMMY$, DUMMY$
    P% = 0
    DO UNTIL EOF(1)
        INPUT #1, DAT(P%).X, DAT(P%).Y
        P% = P% + 1
    LOOP
    INDEXMIN% = 0: INDEXMAX% = NPTS% - 1    'Display data.
    CALL DISPLAY(YMIN!, YMAX!, INDEXMIN%, INDEXMAX%)
    COLOR 1, 0
    LOCATE 2, 18: PRINT "F2:DISPLAY"
    CLOSE #1
    VIEW: WINDOW
    EXIT SUB
END IF
IF FK% = 60 THEN                'F2 key.  Clear the data screen.
    PUT (105, 34), MENU, PSET       'Put data back behind menu.
    ERASE MENU                      'Erase menu array.
    CALL SCLEAR                     'Clear data screen.
```

```
            COLOR 1, 0
            LOCATE 2, 18: PRINT "F2:DISPLAY"
            EXIT SUB                              'Return to main menu.
        END IF
        IF FK% = 61 THEN                          'F3 key.  Not used yet.
        END IF
        IF FK% = 62 THEN                    'F4 key.  Cursors and expand.
            PUT (105, 34), MENU, PSET       'Put data back behind menu.
            ERASE MENU                      'Erase menu array.
            CALL MCLEAR                     'Clear menu line.
            COLOR 1, 0
            LOCATE 2, 2
            PRINT "F10:TOGGLE  "; CHR$(27); ":LEFT   "; CHR$(26); ":RIGHT"
                        'Print new menu line.
            STEPSIZE% = 1       'Cursor stepsize.
            LIX% = 10           'Left cursor starts at the tenth point from left.
            RIX% = 10           'Right cursor starts at the tenth point from the right.
            TOGGLE% = 1         '1--Left cursor.  2--Right cursor.
            LOCATE 2, 34
            PRINT USING "######.##"; DAT(INDEXMIN% + LIX%).X; : PRINT
"fs  ";     'Time in fs of left cursor.
            PRINT USING "+####.##"; DAT(INDEXMIN% + LIX%).Y; : PRINT "
";          'Intensity of left cursor position.
            PRINT USING "######.##"; DAT(INDEXMAX% - RIX%).X; : PRINT
"fs  ";     'Time in fs of right cursor.
            PRINT USING "+####.##"; DAT(INDEXMAX% - RIX%).Y
            'Intensity of right cursor position.
            DELTAY! = 1.2 * ABS(YMAX! - YMIN!) / 315    'Y axis is the
difference between YMAX! and YMIN!  + 20% (315 is due to screen coordinates).
            YTOP! = YMAX! + .1 * ABS(YMAX! - YMIN!) - DELTAY!
            YBOTTOM! = YMIN! - .1 * ABS(YMAX! - YMIN!) + DELTAY!
            VIEW (0, 34)-(639, 349)     'Use only the data screen.
            WINDOW (2 * DAT(INDEXMIN%).X - DAT(INDEXMIN% + 1).X,
YTOP! + DELTAY!)-(2 * DAT(INDEXMAX%).X - DAT(INDEXMAX% - 1).X,
YBOTTOM! - DELTAY!)         'Set new coordinates for the data screen.
            K$ = ""
            DO UNTIL K$ = CHR$(27)  'If esc is hit then exit cursor mode.
                K$ = "": FK% = 0
                K$ = INKEY$
                IF LEN(K$) = 2 THEN FK% = ASC(RIGHT$(K$, 1))
                LINE (DAT(INDEXMIN% + LIX%).X, YTOP!)-
(DAT(INDEXMIN% + LIX%).X, YBOTTOM!), 1, , &HCCCC    'Make dashed line at
left side.
```

```
                LINE (DAT(INDEXMAX% - RIX%).X, YTOP!)-
(DAT(INDEXMAX% - RIX%).X, YBOTTOM!), 1, , &HCCCC   'Make dashed line at
right side.
                IF K$ = CHR$(13) THEN    'If Return, expand data screen.
                    CALL SCLEAR          'Clear data screen.
                    YMIN! = DAT(INDEXMIN% + LIX%).Y: YMAX! =
DAT(INDEXMIN% + LIX%).Y    'Reset the YMIN! and YMAX!.
                    INDEXMIN% = INDEXMIN% + LIX%: INDEXMAX%
= INDEXMAX% - RIX%         'Reset the x coordinate indices.
                    FOR P% = INDEXMIN% TO INDEXMAX%
      'Determine new YMIN! and YMAX!.
                        IF DAT(P%).Y > YMAX! THEN YMAX! =
DAT(P%).Y
                        IF DAT(P%).Y < YMIN! THEN YMIN! =
DAT(P%).Y
                    NEXT P%
                    CALL DISPLAY(YMIN!, YMAX!, INDEXMIN%,
INDEXMAX%)             'Display expanded data set.
                    CALL MCLEAR          'Clear menu line.
                    CALL MMENU           'Print main menu.
                    EXIT SUB             'Return to main menu.
                END IF
                SELECT CASE FK%
                    CASE 68
                        IF TOGGLE% = 1 THEN TOGGLE% = 2 ELSE
TOGGLE% = 1            'Toggle between left and right cursor.
                    CASE 75
                        IF TOGGLE% = 1 THEN    'Left arrow, left cursor
                            LINE (DAT(INDEXMIN% + LIX%).X,
YTOP!)-(DAT(INDEXMIN% + LIX%).X, YBOTTOM!), 0, , &HCCCC
                            PSET (DAT(INDEXMIN% + LIX%).X,
DAT(INDEXMIN% + LIX%).Y)
                            LIX% = LIX% - STEPSIZE%
                            IF LIX% < 0 THEN BEEP: LIX% = LIX%
+ STEPSIZE%             'If too far left then beep and reset new position.
                            LOCATE 2, 34
                            PRINT USING "######.##";
DAT(INDEXMIN% + LIX%).X;   'Print time of new position.
                            LOCATE 2, 46
                            PRINT USING "+####.##";
DAT(INDEXMN% + LIX%).Y;    'Print intensity of new position.
                        ELSE           'Left arrow, right cursor.
                            LINE (DAT(INDEXMAX% - RIX%).X,
YTOP!)-(DAT(INDEXMAX% - RIX%).X, YBOTTOM!), 0, , &HCCCC
```

```
                                        PSET (DAT(INDEXMAX% - RIX%).X,
DAT(INDEXMAX% - RIX%).Y)
                                        RIX% = RIX% + STEPSIZE%
                                        IF RIX% > INDEXMAX% - INDEXMIN%
THEN BEEP: RIX% = RIX% - STEPSIZE%      'If too far left then beep and reset
                                                new position.
                                        LOCATE 2, 59
                                        PRINT USING "######.##";
DAT(INDEXMAX% - RIX%).X;                'Print new time.
                                        LOCATE 2, 72
                                        PRINT USING "+####.##";
DAT(INDEXMAX% - RIX%).Y;                'Print new intensity.
                                END IF
                            CASE 77     'Right arrow.
                                IF TOGGLE% = 1 THEN     'Right arrow, left
                                                            cursor.
                                        LINE (DAT(INDEXMIN% + LIX%).X,
YTOP!)-(DAT(INDEXMIN% + LIX%).X, YBOTTOM!), 0, , &HCCCC
                                        PSET (DAT(INDEXMIN% + LIX%).X,
DAT(INDEXMIN% + LIX%).Y)
                                        LIX% = LIX% + STEPSIZE%
                                        IF LIX% > INDEXMAX% - INDEXMIN%
THEN BEEP: LIX% = LIX% - STEPSIZE%
                                        LOCATE 2, 34
                                        PRINT USING "######.##";
DAT(INDEXMIN% + LIX%).X;
                                        LOCATE 2, 46
                                        PRINT USING "+####.##";
DAT(INDEXMIN% + LIX%).Y;

                                ELSE            'Right arrow, right cursor.
                                        LINE (DAT(INDEXMAX% - RIX%).X,
YTOP!)-(DAT(INDEXMAX% - RIX%).X, YBOTTOM!), 0, , &HCCCC
                                        PSET (DAT(INDEXMAX% - RIX%).X,
DAT(INDEXMAX% - RIX%).Y)
                                        RIX% = RIX% - STEPSIZE%
                                        IF RIX% < 0 THEN BEEP: RIX% = RIX%
+ STEPSIZE%
                                        LOCATE 2, 59
                                        PRINT USING "######.##";
DAT(INDEXMAX% - RIX%).X;
                                        LOCATE 2, 72
                                        PRINT USING "+####.##";
DAT(INDEXMAX% - RIX%).Y;
```

```
                        END IF
                    CASE 72     'Up arrow, used to increase stepsize.
                        STEPSIZE% = STEPSIZE% + 10
                    CASE 80     'Down arrow, used to decrease stepsize.
                        STEPSIZE% = STEPSIZE% - 10
                        IF STEPSIZE% < 0 THEN STEPSIZE% =
STEPSIZE% + 10          'Stepsize cannot go negative.
                    END SELECT
                    FK% = 0
                LOOP        'If esc then eliminate cursors and return to main menu.
                LINE (DAT(INDEXMIN% + LIX%).X, YTOP!)-(DAT(INDEXMIN% +
LIX%).X, YBOTTOM!), 0, , &HCCCC
                LINE (DAT(INDEXMAX% - RIX%).X, YTOP!)-(DAT(INDEXMAX% -
RIX%).X, YBOTTOM!), 0, , &HCCCC
                PSET (DAT(INDEXMIN% + LIX%).X, DAT(INDEXMIN% +
LIX%).Y), 1
                PSET (DAT(INDEXMAX% - RIX%).X, DAT(INDEXMAX% -
RIX%).Y), 1
                CALL MCLEAR
                CALL MMENU
                EXIT SUB
        END IF
        IF FK% = 63 THEN        'F5 key, directory function.
                PUT (105, 34), MENU, PSET
                CALL MCLEAR
                INPUT "INPUT FILE SPECIFICATION (path): ", path$
                CALL DIRECTORY(path$, DUMMY$)
                CALL MCLEAR
                CALL MMENU
                ERASE MENU
                EXIT SUB
        END IF
        FK% = 0
LOOP UNTIL KBD$ = CHR$(27)
PUT (105, 34), MENU, PSET
ERASE MENU
COLOR 1, 0
LOCATE 2, 18: PRINT "F2:DISPLAY"

END SUB

*****************************************************************
*                   Subroutine used to move the delay line.     *
*****************************************************************
```

```
SUB JOG

DIM MENU(8050) AS INTEGER          'Make menu.
GET (210, 34)-(350, 236), MENU
LINE (210, 34)-(350, 236), 1, BF
LINE (214, 34)-(346, 232), 0, BF
LOCATE 4, 30: PRINT "CURRENT POS"
LOCATE 7, 31: PRINT "STEP SIZE:"
LOCATE 9, 32: PRINT "MOTIONS:"
LOCATE 10, 30: PRINT "GOTO 0 <HOME>"
LOCATE 11, 29: PRINT "POS <+> NEG <->"
LOCATE 12, 29: PRINT "NEG BELOW ZERO:"
LOCATE 13, 31: PRINT "<SHIFT ->"
LOCATE 15, 30: PRINT "DEFINE HOME:"
LOCATE 16, 30: PRINT "<CTRL-HOME>"
SS$ = "1"              'Initial stepsize is one step.
CALL MOTION("1MN", REPORT$)        'Motion is the general controller of the delay
                                        line.  Turns motor on.
CALL MOTION("1TP", POSITION$)      'Get current position in encoder counts.
DO UNTIL POSITION$ <> "        "   'Keep requesting position until non-null value
                                        is returned.
        CALL MOTION("1TP", POSITION$)
LOOP
COLOR 15, 0
LOCATE 5, 30
IF VAL(POSITION$) >= 0 THEN        'Places a '+' or '-' in front of position number.
        PRINT "+";
ELSE
        PRINT "-";
        POSITION$ = RIGHT$(POSITION$, LEN(POSITION$) - 1)
END IF
PRINT POSITION$
LINE (228, 55)-(322, 69), 15, B
COLOR 1, 0
LOCATE 6, 28: PRINT USING "##.##"; VAL(POSITION$) * CALIB2 / 1000000!; :
PRINT "mm"             'Print position in milimeters.
LOCATE 6, 36: PRINT USING "###.##"; VAL(POSITION$) * CALIB / 1000; : PRINT
"ps"                   'Print position in picoseconds.
COLOR 15, 0
LOCATE 8, 33: PRINT SS$  'Print stepsize.
CALL KEYBOARDCLEAR  'KEYBOARDCLEAR clears the keyboard buffer.
DO                         'Get response from keyboard.
        KBD$ = "": FK% = 0
        KBD$ = INKEY$
        IF LEN(KBD$) = 2 THEN FK% = ASC(RIGHT$(KBD$, 1))
```

```
        IF KBD$ = "+" THEN          'Move stage positive by SS$.
                COLOR 15, 0
                LOCATE 11, 29: PRINT "POS <+>"
                CMD$ = "1MR" + SS$
                IF VAL(POSITION$) + VAL(SS$) > 20 * 1000000! / CALIB2 THEN
CMD$ = "1MR0"       'If request to move is beyond range of stage then no motion.
                CALL MOTION(CMD$, REPORT$)          'Execute move.
                POSITION$ = "NOTHING"
                DO              'Get new position until returns same value twice, then the
stage has stopped.
                        OLDREPORT$ = POSITION$
                        CALL MOTION("1TP", POSITION$)
                LOOP UNTIL OLDREPORT$ = POSITION$ AND POSITION$ <> "

                LOCATE 5, 30
                IF VAL(POSITION$) >= 0 THEN    'Print new position.
                        PRINT "+";
                ELSE
                        PRINT "-";
                        POSITION$ = RIGHT$(POSITION$, LEN(POSITION$) - 1)
                END IF
                PRINT POSITION$
                LINE (228, 55)-(322, 69), 15, B
                COLOR 1, 0
                LOCATE 6, 28: PRINT USING "##.##"; VAL(POSITION$) * CALIB2 /
1000000!
                LOCATE 6, 36: PRINT USING "###.##"; VAL(POSITION$) * CALIB /
1000
                LOCATE 11, 29: PRINT "POS <+>"
                PARAMETERS(MODE%, 6) = VAL(POSITION$)'Starting position of
        scan setup is updated to this new location.  This is really an unnecessary feature.
        END IF
        IF KBD$ = "-" OR KBD$ = "_" THEN        'Negative motion requested.
                COLOR 15, 0
                LOCATE 11, 37: PRINT "NEG <->"
                CMD$ = "1MR-" + SS$
                IF KBD$ = "-" THEN
                        IF VAL(POSITION$) - VAL(SS$) < 0 THEN CMD$ = "1MR0"
                                'If request is below zero then do nothing.
                END IF
                CALL MOTION(CMD$, REPORT$)
                POSITION$ = "NOTHING"
                DO              'Wait until motor has stopped.
                        OLDREPORT$ = POSITION$
                        CALL MOTION("1TP", POSITION$)
```

```
            LOOP UNTIL OLDREPORT$ = POSITION$ AND POSITION$ <> "
"
            LOCATE 5, 30
            IF VAL(POSITION$) >= 0 THEN    'Print new position.
                  PRINT "+";
            ELSE
                  PRINT "-";
                  POSITION$ = RIGHT$(POSITION$, LEN(POSITION$) - 1)
            END IF
            PRINT POSITION$
            LINE (228, 55)-(322, 69), 15, B
            COLOR 1, 0
            LOCATE 6, 28: PRINT USING "##.##"; VAL(POSITION$) * CALIB2 /
1000000!
            LOCATE 6, 36: PRINT USING "###.##"; VAL(POSITION$) * CALIB /
1000
            LOCATE 11, 37: PRINT "NEG <->"
            PARAMETERS(MODE%, 6) = VAL(POSITION$)'Update new starting
                                                                  point.
      END IF
      IF KBD$ >= "0" AND KBD$ <= "9" THEN 'If digit is hit then assume a new
                                                  stepsize is being input.
            COLOR 15, 0
            LOCATE 7, 31: PRINT "STEP SIZE:"       'Get new stepsize.
            SS$ = KBD$
            LOCATE 8, 33: PRINT "      "       'Cover up old stepsize.
            LOCATE 8, 33: PRINT SS$;
            INPUT "", TEMP$    'Get rest of stepsize string.
            SS$ = SS$ + TEMP$
            COLOR 1, 0
            LOCATE 7, 31: PRINT "STEP SIZE:"
      END IF
      IF FK% = 71 THEN           'Home is hit.
            COLOR 15, 0
            LOCATE 10, 30: PRINT "GOTO 0 <HOME>"
            CMD$ = "1GH"
            CALL MOTION(CMD$, REPORT$)
            POSITION$ = "NOTHING"
            DO             'Wait for stage to stop moving.
                  OLDREPORT$ = POSITION$
                  CALL MOTION("1TP", POSITION$)
            LOOP UNTIL OLDREPORT$ = POSITION$ AND POSITION$ <> "
"
            LOCATE 5, 30
```

```
            IF VAL(POSITION$) >= 0 THEN   'Print new position (it sometimes
                                                  come back as 1 or -1.
                PRINT "+";
            ELSE
                PRINT "-";
                POSITION$ = RIGHT$(POSITION$, LEN(POSITION$) - 1)
            END IF
            PRINT POSITION$
            LINE (228, 55)-(322, 69), 15, B
            COLOR 1, 0
            LOCATE 6, 28: PRINT USING "##.##"; VAL(POSITION$) * CALIB2 /
1000000!
            LOCATE 6, 36: PRINT USING "###.##"; VAL(POSITION$) * CALIB /
1000
            LOCATE 10, 30: PRINT "GOTO 0 <HOME>"
            PARAMETERS(MODE%, 6) = VAL(POSITION$)
        END IF
        IF FK% = 119 THEN          'Ctrl-Home if hit to reset the zero position.
            COLOR 15, 0
            LOCATE 16, 30: PRINT "<CTRL-HOME>"
            CALL MOTION("1DH", DUMMY$)
            CALL MOTION("1MN", REPORT$)        'Need to turn motor on again,
                                                      I guess.
            CALL MOTION("1TP", POSITION$)      'Get new position.
            DO UNTIL POSITION$ <> "          "
                CALL MOTION("1TP", POSITION$)
            LOOP
            COLOR 15, 0
            LOCATE 5, 30
            IF VAL(POSITION$) >= 0 THEN
                PRINT "+";
            ELSE
                PRINT "-";
                POSITION$ = RIGHT$(POSITION$, LEN(POSITION$) - 1)
            END IF
            PRINT POSITION$
            LINE (228, 55)-(322, 69), 15, B
            COLOR 1, 0
            LOCATE 6, 28: PRINT USING "##.##"; VAL(POSITION$) * CALIB2 /
1000000!; : PRINT "mm"
            LOCATE 6, 36: PRINT USING "###.##"; VAL(POSITION$) * CALIB /
1000; : PRINT "ps"
            LOCATE 16, 30: PRINT "<CTRL-HOME>"
        END IF
LOOP UNTIL KBD$ = CHR$(27)
```

```
COLOR 1, 0
CLOSE #1
PUT (210, 34), MENU, PSET        'Return to main menu.
ERASE MENU

END SUB

*****************************************************************
*                Subroutine used check the status of the Antares shutter.          *
*****************************************************************

SUB LASER (OUT$, IN$)   'This routine is currently not being used.  If the Antares is
      unstable and long scans are necessary then this routine should be reincorporated.  I
      will explain this routine in more detail in the experimental section of my thesis.

PORT% = 3: BAUD% = 9600
CALL QCINIT(4, 3, 0, 1, PORTSTATUS%, QCERROR%)
CALL COPEN(PORT%, BAUD%, 1, 0, 8, 0, 20, 20, TXBUF3(), RXBUF3(),
QCERROR%)
CALL CBUFCLR(2, 3, QCERROR%)
OUT$ = OUT$ + CHR$(13)
CALL CPRINT(PORT%, OUT$, QCERROR%)
DO
      CALL CBUFFER(PORT%, RECV%, XMIT%, QCERROR%)
LOOP UNTIL XMIT% = 20
RELPOS% = 0: KB% = 0: FLAG% = 0
IN$ = SPACE$(20)
CALL CINPUT(PORT%, IN$, RELPOS%, 0, "", "", KB%, FLAG%)
CALL CCLOSE(PORT%, QCERROR%)
CALL QCEXIT

END SUB

*****************************************************************
*                Subroutine to take data by scanning the boxcar gate.          *
*****************************************************************

SUB MODE1GO (YMIN!, YMAX!, INDEXMIN%, INDEXMAX%)
      'This routine is not currently used as is.  It could be adapted easily to collect data
            on any instrument.

OPEN "I", #2, "STATUS"    'Get the scan number.
INPUT #2, TOTALSCANS%
CLOSE #2
```

```
CALL SCLEAR             'Clear data screen.
CALL MCLEAR             'Clear menu line.
PRINT "COLLECTING DATA"
MD% = 1
LT%(0) = 0
LT%(1) = 0
FLAG% = 1
CALL DAS8(MD%, LT%(0), FLAG%)     'Initialize the A/D converter.
IF FLAG% <> 0 THEN                'Error trap for the A/D.
        CALL MCLEAR
        PRINT "ERROR IN MODE1 ON THE DAS BOARD   ERROR #:"; FLAG%
        END
END IF
FOR P = 0 TO PARAMETERS(1, 3)     'Reset the x and y values.
        DAT(P).X = P * PARAMETERS(1, 5)
        DAT(P).Y = 0
NEXT P
VIEW (0, 34)-(639, 349)           'Set the data screen coordinates.
WINDOW (2 * DAT(0).X - DAT(1).X, 2048)-(2 * DAT(PARAMETERS(1, 3)).X -
DAT(PARAMETERS(1, 3) - 1).X, -2048)
CALL DAC(0, INT(PARAMETERS(1, 1))) 'Set D/A converter to initial point.
STEPSIZE! = (PARAMETERS(1, 2) - PARAMETERS(1, 1)) / PARAMETERS(1, 3)
AV% = 0                 'Number of scans.
DO UNTIL KBD$ <> ""
  FOR P = 0 TO PARAMETERS(1, 3)
        TIMEIN! = TIMER           'Delay for the step time.
        DO
                TIMEOUT! = TIMER
        LOOP UNTIL TIMEOUT! - TIMEIN > PARAMETERS(1, 4)
        CALL DAS(0, DIO%)         'Read A/D converter.
        DAT(P).Y = (DAT(P).Y * AV% + DIO%) / (AV% + 1)    'Update the y value.
        CALL DAC(0, INT(STEPSIZE! * P + PARAMETERS(1, 1)))     'Move the gate
        PSET (DAT(P).X, DAT(P).Y), 15           'Plot the point on the screen.
  NEXT P
        AV% = AV% + 1             'Increment the number of scans.
        CALL FIVESCAN(AV%, MODE%, INT(PARAMETERS(1, 3))) 'Save data
                                                          every five scans.
        LOCATE 2, 50: PRINT "# OF SCANS COMPLETED: "; AV%
        CALL SCLEAR       'Clear data screen
        YMIN! = DAT(0).Y: YMAX! = DAT(0).Y
        FOR i = 1 TO PARAMETERS(1, 3)          'Find new YMIN! and YMAX!.
                IF DAT(i).Y < YMIN! THEN YMIN! = DAT(i).Y
                IF DAT(i).Y > YMAX! THEN YMAX! = DAT(i).Y
        NEXT i
```

```
        CALL DISPLAY(YMIN!, YMAX!, 0, INT(PARAMETERS(1, 3))) 'Display new
                                                                data.
        VIEW (0, 34)-(639, 349)       'Reset the screen coordinates.
        WINDOW (2 * DAT(0).X - DAT(1).X, YMAX! + .1 * ABS(YMAX! - YMIN!))-
(2 * DAT(PARAMETERS(1, 3)).X - DAT(PARAMETERS(1, 3) - 1).X, YMIN! - .1 *
ABS(YMAX! - YMIN!))
        CALL DAC(0, INT(PARAMETERS(1, 1))) 'Return gate to initial point.
        KBD$ = INKEY$
LOOP                                    'Do another scan unless key has been hit.
VIEW: WINDOW            'Return the screen coordinates to the original coordinates.
CALL FILESAVE(1, INT(PARAMETERS(1, 3)), AV%, "TIME", "INTENSITY")
                        'Save the data.
          CALL MCLEAR   'Clear menu line.
          CALL MMENU    'Print main menu.

END SUB

*********************************************************************
*                  Subroutine used to get parameters for MODE1                  *
*********************************************************************

SUB MODE1PARAMETERS

DIM MENU3(11500)  AS INTEGER          'Make menu.
DIM MESSAGEPOS$(5, 2)
GET (460, 70)-(630, 320), MENU3
LINE (460, 70)-(630, 320), 1, BF
LINE (464, 74)-(626, 316), 0, BF
MESSAGEPOS$(1, 1) = "START DAC POINT:": MESSAGEPOS$(1, 2) = "9"
MESSAGEPOS$(2, 1) = "END DAC POINT:": MESSAGEPOS$(2, 2) = "12"
MESSAGEPOS$(3, 1) = "# OF STEPS:": MESSAGEPOS$(3, 2) = "15"
MESSAGEPOS$(4, 1) = "STEP TIME:": MESSAGEPOS$(4, 2) = "18"
MESSAGEPOS$(5, 1) = "TIME FACTOR:": MESSAGEPOS$(5, 2) = "21"
ITEMINDEX% = 1
COLOR 1, 0: LOCATE 7, 61: PRINT "MODE 1 PARAMETERS"
COLOR 15, 0: LOCATE 9, 60: PRINT MESSAGEPOS$(1, 1)
LOCATE 10, 67: PRINT USING "####"; PARAMETERS(1, 1)
COLOR 1, 0: LOCATE 12, 60: PRINT MESSAGEPOS$(2, 1)
COLOR 15, 0: LOCATE 13, 67: PRINT USING "####"; PARAMETERS(1, 2)
COLOR 1, 0: LOCATE 15, 60: PRINT MESSAGEPOS$(3, 1);
COLOR 15, 0: LOCATE 15, 72: PRINT USING "###"; PARAMETERS(1, 3)
COLOR 1, 0: LOCATE 18, 60: PRINT MESSAGEPOS$(4, 1)
COLOR 15, 0: LOCATE 19, 68: PRINT USING "##.##"; PARAMETERS(1, 4)
COLOR 1, 0: LOCATE 21, 60: PRINT MESSAGEPOS$(5, 1)
COLOR 15, 0: LOCATE 22, 68: PRINT USING "##.##"; PARAMETERS(1, 5)
```

```
DO              'Get keyboard response.
        KBD$ = INKEY$
        FK = 0
        IF LEN(KBD$) = 2 THEN FK = ASC(RIGHT$(KBD$, 1))
        IF FK = 72 THEN             'Up arrow.
                COLOR 1, 0
                LOCATE VAL(MESSAGEPOS$(ITEMINDEX%, 2)), 60
                PRINT MESSAGEPOS$(ITEMINDEX%, 1)
                COLOR 15, 0
                IF ITEMINDEX% = 1 THEN ITEMINDEX% = 5 ELSE ITEMINDEX%
= ITEMINDEX% - 1
                LOCATE VAL(MESSAGEPOS$(ITEMINDEX%, 2)), 60
                PRINT MESSAGEPOS$(ITEMINDEX%, 1)
        END IF
        IF FK = 80 THEN             'Down arrow.
                COLOR 1, 0
                LOCATE VAL(MESSAGEPOS$(ITEMINDEX%, 2)), 60
                PRINT MESSAGEPOS$(ITEMINDEX%, 1)
                COLOR 15, 0
                IF ITEMINDEX% = 5 THEN ITEMINDEX% = 1 ELSE ITEMINDEX%
= ITEMINDEX% + 1
                LOCATE VAL(MESSAGEPOS$(ITEMINDEX%, 2)), 60
                PRINT MESSAGEPOS$(ITEMINDEX%, 1)
        END IF
        IF KBD$ = CHR$(13) THEN         'Return.
                SELECT CASE ITEMINDEX%
                        CASE 1          'Parameters (1,1).
                                LINE (530, 127)-(558, 140), 0, BF
                                LINE (530, 127)-(558, 138), 1, BF
                                XP$ = ""
                                CALL GETSTRING(10, 67, 4, XP$)
                                PARAMETERS(1, 1) = VAL(XP$)
                                LOCATE 10, 67
                                PRINT USING "####"; PARAMETERS(1, 1)
                        CASE 2          'Parameters (1,2).
                                LINE (530, 168)-(558, 180), 0, BF
                                LINE (530, 168)-(558, 180), 1, BF
                                XP$ = ""
                                CALL GETSTRING(13, 67, 4, XP$)
                                PARAMETERS(1, 2) = VAL(XP$)
                                LOCATE 13, 67
                                PRINT USING "####"; PARAMETERS(1, 2)
                        CASE 3          'Parameters (1,3)
                                LINE (568, 197)-(590, 209), 0, BF
                                LINE (568, 197)-(590, 209), 1, BF
```

```
                XP$ = ""
                CALL GETSTRING(15, 72, 3, XP$)
                PARAMETERS(1, 3) = VAL(XP$)
                LOCATE 15, 72
                PRINT USING "###"; PARAMETERS(1, 3)
            CASE 4      'Parameters (1,4).
                LINE (544, 253)-(575, 265), 1, BF
                XP$ = ""
                CALL GETSTRING(19, 69, 5, XP$)
                PARAMETERS(1, 4) = VAL(XP$)
                LOCATE 19, 68
                PRINT USING "##.##"; PARAMETERS(1, 4)
            CASE 5      'Parameters (1,5).
                LINE (544, 294)-(583, 306), 0, BF
                LINE (544, 294)-(583, 306), 1, BF
                XP$ = ""
                CALL GETSTRING(22, 69, 5, XP$)
                PARAMETERS(1, 5) = VAL(XP$)
                LOCATE 22, 69
                PRINT USING "##.##"; PARAMETERS(1, 5)
        END SELECT
    END IF

LOOP UNTIL KBD$ = CHR$(27)   'Esc returns to calling routine.

PUT (460, 70), MENU3, PSET   'Put data back behind the menu.

END SUB


*****************************************************************
*           Subroutine to take data with boxcar and delay line.                 *
*****************************************************************

SUB MODE2GO (YMIN!, YMAX!, INDEXMIN%, INDEXMAX%)

STATIC AV%, XMIN!, XMAX!, NPTS%  'Retain these numbers in order to continue
                                  scan.
MD% = 1             'Initialize the A/D.
LT%(0) = 0
LT%(1) = 0
FLAG% = 0
CALL DAS8(MD%, LT%(0), FLAG%)
IF FLAG% <> 0 THEN
    CALL MCLEAR
```

```
        PRINT "ERROR IN MODE1 ON THE DAS BOARD   ERROR #:"; FLAG%
        END
END IF
CALL MOTION("1MN", REPORT$)          'Turn motor on.
CALL MOTION("1TP", POS$)             'Get position.
COLOR 15, 0
CALL MCLEAR                          'Clear menu line.
INPUT "CONTINUE CURRENT SCAN (Y OR y)"; CONTINUE$          'New scan?
IF CONTINUE$ <> "Y" OR CONTINUE$ <> "y" THEN
        AV% = 0: XMIN! = 0: YMIN! = 0: XMAX! = 0: YMAX! = 0: NPTS% =
PARAMETERS(2, 1)
        FOR P = 0 TO PARAMETERS(2, 1)
                DAT(P).X = P * PARAMETERS(2, 2) * CALIB: DAT(P).Y = 0
        NEXT P
        CALL SCLEAR
END IF
CALL MCLEAR
VIEW (0, 34)-(639, 349)              'Set data screen coordinates.
WINDOW (-PARAMETERS(2, 2) * CALIB, 2048)-((PARAMETERS(2, 1) + 1) *
PARAMETERS(2, 2) * CALIB, -2048)
PRINT "COLLECTING DATA"
KBD$ = ""
DO UNTIL KBD$ <> ""                  'Go.
        FOR P = 0 TO PARAMETERS(2, 1)
                NEXTPOSITION& = PARAMETERS(2, 6) + P * PARAMETERS(2, 2)
                        'Calculate the next delay line position.
                CMD$ = "1MA" + RIGHT$(STR$(NEXTPOSITION&),
LEN(STR$(NEXTPOSITION&)) - 1)
                CALL MOTION(CMD$, REPORT$)          'Move delay line.
                DO              'Wait until stage has stopped.
                        OLDPOS$ = POS$
                        CALL MOTION("1TP", POS$)
                LOOP UNTIL OLDPOS$ = POS$
                STARTTIME! = TIMER                  'Wait the step time.
                DO
                        TIMENOW! = TIMER
                LOOP UNTIL (TIMENOW! - STARTTIME!) >= PARAMETERS(2, 3)
                CALL DAS(0, DIO%)          'Read A/D.
                DAT(P).Y = (DAT(P).Y * AV% + DIO%) / (AV% + 1)   'Update y value.
                PSET (DAT(P).X, DIO%), 1           'Plot new point on the screen.
                STOP$ = INKEY$     'S stops the scan and anything stops after scan.
                IF KBD$ = "" THEN KBD$ = STOP$
                IF STOP$ = "P" OR STOP$ = "p" THEN     'P allows restarting of scan.
                        STOP$ = ""
                        DO UNTIL STOP$ <> ""
```

```
                    STOP$ = INKEY$
                LOOP
                STOP$ = "": KBD$ = ""
            END IF
            IF STOP$ = "S" OR STOP$ = "s" THEN EXIT DO 'Stop immediately.
        NEXT P
            AV% = AV% + 1               'Increment the number of scans.
            CALL FIVESCAN(AV%, MODE%, INT(PARAMETERS(2, 1))) 'Save
                                                data after every five scans.
            LOCATE 2, 50
            PRINT "# OF SCANS COMPLETED: "; AV%
            CMD$ = "1MR-" + STR$(PARAMETERS(2, 1) * PARAMETERS(2, 2)
+ 100)
            CALL MOTION(CMD$, REPORT$)      'Return delay line to starting pt.
                plus 100 points in order to eliminate backlash.
            CALL SCLEAR         'Clear data screen.
            YMIN! = DAT(0).Y: YMAX! = DAT(0).Y  'Find new YMIN! and
                                                        YMAX!.
            FOR i = 1 TO PARAMETERS(2, 1) - 1
                IF DAT(i).Y < YMIN! THEN YMIN! = DAT(i).Y
                IF DAT(i).Y > YMAX! THEN YMAX! = DAT(i).Y
            NEXT i
            CALL DISPLAY(YMIN!, YMAX!, 0, INT(PARAMETERS(2, 1)))
                    'Redisplay the new averaged data.
            VIEW (0, 34)-(639, 349)
            WINDOW (2 * DAT(0).X - DAT(1).X, YMAX! + .1 * ABS(YMAX! -
YMIN!))-(2 * DAT(PARAMETERS(2, 1) - 1).X - DAT(PARAMETERS(2, 1) - 1).X,
YMIN! - .1 * ABS(YMAX! - YMIN!))
            DO              'Has the delay line stopped?
                OLDPOS$ = POS$
                CALL MOTION("1TP", POS$)
            LOOP UNTIL OLDPOS$ = POS$
            CMD$ = "1MA" + STR$(PARAMETERS(2, 6))   'Move to starting
                                                        point.
            CALL MOTION(CMD$, REPORT$)
LOOP
VIEW: WINDOW
CALL FILESAVE(2, INT(PARAMETERS(2, 1)), AV%, "TIME (fs)", "INTENSITY")
                                                    'Save data.
CALL MCLEAR
CALL MMENU

END SUB

*****************************************************************
```

```
*              Subroutine to get parameters for boxcar/delay line scan.              *
*****************************************************************

SUB MODE2PARAMETERS

DIM MENU3(1 TO 12100) AS INTEGER          'Make menu.
DIM MESSAGEPOS$(6, 2)
MESSAGEPOS$(1, 1) = "# OF DATA POINTS:": MESSAGEPOS$(1, 2) = "7"
MESSAGEPOS$(2, 1) = "STEPSIZE:": MESSAGEPOS$(2, 2) = "10"
MESSAGEPOS$(3, 1) = "TIME BETWEEN STEPS:": MESSAGEPOS$(3, 2) = "12"
MESSAGEPOS$(4, 1) = "INVERT:  ": MESSAGEPOS$(4, 2) = "15"
MESSAGEPOS$(5, 1) = "FULL SCALE VOLTAGE:": MESSAGEPOS$(5, 2) = "17"
MESSAGEPOS$(6, 1) = "START SCANNING AT:": MESSAGEPOS$(6, 2) = "20"
GET (460, 42)-(630, 315), MENU3
ITEMINDEX% = 1                    'Start at first menu item.
IF PARAMETERS(2, 4) = 1 THEN INV$ = "YES" ELSE INV$ = "NO "
LINE (460, 42)-(630, 315), 1, BF
LINE (464, 46)-(626, 311), 0, BF
COLOR 1, 0: LOCATE 5, 61: PRINT "MODE 2 PARAMETERS"
COLOR 15, 0: LOCATE 7, 60: PRINT MESSAGEPOS$(1, 1)
LOCATE 8, 66: PRINT USING "####"; PARAMETERS(2, 1)
COLOR 1, 0: LOCATE 10, 60: PRINT MESSAGEPOS$(2, 1)
COLOR 15, 0: LOCATE 10, 70: PRINT USING "####"; PARAMETERS(2, 2)
COLOR 1, 0: LOCATE 12, 60: PRINT MESSAGEPOS$(3, 1)
COLOR 15, 0: LOCATE 13, 66: PRINT USING "##.##"; PARAMETERS(2, 3)
COLOR 1, 0: LOCATE 15, 60: PRINT MESSAGEPOS$(4, 1)
COLOR 15, 0: LOCATE 15, 69: PRINT INV$
COLOR 1, 0: LOCATE 17, 60: PRINT MESSAGEPOS$(5, 1)
COLOR 15, 0: LOCATE 18, 66: PRINT USING "##.##"; PARAMETERS(2, 5)
COLOR 1, 0: LOCATE 20, 60: PRINT MESSAGEPOS$(6, 1)
COLOR 15, 0: LOCATE 21, 66: PRINT USING "###,###"; PARAMETERS(2, 6)
DO                        'Get keyboard response.
        KBD$ = INKEY$
        FK = 0
        IF LEN(KBD$) = 2 THEN FK = ASC(RIGHT$(KBD$, 1))
        IF FK = 72 THEN           'Down arrow.
                COLOR 1, 0
                LOCATE VAL(MESSAGEPOS$(ITEMINDEX%, 2)), 60
                PRINT MESSAGEPOS$(ITEMINDEX%, 1)
                COLOR 15, 0
                IF ITEMINDEX% = 1 THEN ITEMINDEX% = 6 ELSE ITEMINDEX%
= ITEMINDEX% - 1
                LOCATE VAL(MESSAGEPOS$(ITEMINDEX%, 2)), 60
                PRINT MESSAGEPOS$(ITEMINDEX%, 1)
        END IF
```

```
        IF FK = 80 THEN             'Up arrow.
                COLOR 1, 0
                LOCATE VAL(MESSAGEPOS$(ITEMINDEX%, 2)), 60
                PRINT MESSAGEPOS$(ITEMINDEX%, 1)
                COLOR 15, 0
                IF ITEMINDEX% = 6 THEN ITEMINDEX% = 1 ELSE ITEMINDEX%
= ITEMINDEX% + 1
                LOCATE VAL(MESSAGEPOS$(ITEMINDEX%, 2)), 60
                PRINT MESSAGEPOS$(ITEMINDEX%, 1)
        END IF
        IF KBD$ = CHR$(13) THEN         'Return hit.
                SELECT CASE ITEMINDEX%
                        CASE 1                  'Parameters (2,1).
                                LINE (520, 98)-(551, 110), 1, BF
                                XP$ = ""
                                CALL GETSTRING(8, 66, 4, XP$)
                                PARAMETERS(2, 1) = VAL(XP$)
                                LOCATE 8, 66: COLOR 15, 0
                                PRINT USING "####"; PARAMETERS(2, 1)
                        CASE 2                  'Parameters (2,2).
                                LINE (552, 126)-(582, 138), 1, BF
                                XP$ = ""
                                CALL GETSTRING(10, 70, 4, XP$)
                                PARAMETERS(2, 2) = VAL(XP$)
                                LOCATE 10, 70: COLOR 15, 0
                                PRINT USING "####"; PARAMETERS(2, 2)
                        CASE 3                  'Parameters (2,3).
                                LINE (500, 168)-(600, 180), 0, BF
                                LINE (526, 168)-(557, 180), 1, BF
                                XP$ = ""
                                CALL GETSTRING(13, 66, 5, XP$)
                                PARAMETERS(2, 3) = VAL(XP$)
                                LOCATE 13, 66: COLOR 15, 0
                                PRINT USING "##.##"; PARAMETERS(2, 3)
                        CASE 4      'Parameters (2,4) (this parameter is not used).
                                IF PARAMETERS(2, 4) = 1 THEN
                                        PARAMETERS(2, 4) = 0
                                        INV$ = "NO "
                                        COLOR 15, 0
                                        LOCATE 15, 69
                                        PRINT INV$
                                ELSE
                                        PARAMETERS(2, 4) = 1
                                        INV$ = "YES"
                                        COLOR 15, 0
```

```
                        LOCATE 15, 69
                        PRINT INV$
                    END IF
                CASE 5              'Parameters (2,5).
                    LINE (500, 239)-(600, 251), 0, BF
                    LINE (521, 239)-(557, 251), 1, BF
                    XP$ = ""
                    CALL GETSTRING(18, 66, 5, XP$)
                    PARAMETERS(2, 5) = VAL(XP$)
                    LOCATE 18, 66: COLOR 15, 0
                    PRINT USING "##.##"; PARAMETERS(2, 5)
                CASE 6              'Parameters (2,6).
                    LINE (480, 280)-(600, 292), 0, BF
                    LINE (522, 280)-(567, 292), 1, BF
                    XP$ = ""
                    CALL GETSTRING(21, 66, 7, XP$)
                    PARAMETERS(2, 6) = VAL(XP$)
                    LOCATE 21, 66: COLOR 15, 0
                    PRINT USING "###,###"; PARAMETERS(2, 6)
            END SELECT
            COLOR 1, 0
        END IF
LOOP UNTIL KBD$ = CHR$(27)          'Esc returns to calling routine.
PUT (460, 42), MENU3, PSET
ERASE MENU3

END SUB

*****************************************************************
*                Subroutine to take data as if strip chart recorder.            *
*****************************************************************

SUB MODE3GO (YMIN!, YMAX!, INDEXMIN%, INDEXMAX%)
    'This routine acts like a strip chart recorder.  Only one scan is possible.  This
    routine is not really very useful.

OPEN "I", #2, "STATUS"              'Get scan number.
INPUT #2, TOTALSCANS%
CLOSE #2
MD% = 1             'Initialize the A/D board.
LT%(0) = 0
LT%(1) = 0
FLAG% = 1
CALL DAS8(MD%, VARPTR(LT%(0)), FLAG%)
IF FLAG% <> 0 THEN
```

```
        CALL MCLEAR
        PRINT "ERROR IN INITIALIZING DAS8 BOARD"
        FOR i = 1 TO 10000: NEXT i
        CALL MCLEAR
        CALL MMENU
        EXIT SUB
END IF
CALL MCLEAR
PRINT "COLLECTING DATA          COLLECTION WILL TAKE ";
PARAMETERS(3, 1) * PARAMETERS(3, 2); " SECONDS"
KBD$ = ""
MD% = 4              'This mode triggers the A/D by software.
FLAG% = 1
INTO! = TIMER
FOR P = 0 TO PARAMETERS(3, 1) - 1
        START! = TIMER
        DO
                NOW! = TIMER
        LOOP UNTIL NOW! - START! >= PARAMETERS(3, 2)
        CALL DAS8(MD%, VARPTR(LT%(0)), FLAG%) 'Trigger A/D after set time.
        DAT(P).Y = LT%(0)          'LT%(0) contains the conversion value.
NEXT P
OUTOF! = TIMER
LOCATE 12, 12: PRINT OUTOF! - INTO!
FOR P = 0 TO PARAMETERS(3, 1) - 1      'Find YMIN! and YMAX! and set x value.
        IF P = 0 THEN
                YMAX! = DAT(P).Y
                YMIN! = DAT(P).Y
        END IF
        IF DAT(P).Y > YMAX! THEN YMAX! = DAT(P).Y
        IF DAT(P).Y < YMIN! THEN YMIN! = DAT(P).Y
        DAT(P).X = P * PARAMETERS(3, 2) * PARAMETERS(3, 4)
NEXT P
CALL DISPLAY(YMIN!, YMAX!, 0, PARAMETERS(3, 1) - 1)   'Display data.
CALL FILESAVE(3, INT(PARAMETERS(3, 1)), AV%, "TIME (fs)", "INTENSITY")
VIEW:WINDOW
CALL MCLEAR
CALL MMENU

END SUB

*****************************************************************
*                    Subroutine to get parameters for mode3     .                  *
*****************************************************************
```

```
SUB MODE3PARAMETERS

DIM MENU3(1 TO 11000)  AS INTEGER 'Make menu.
DIM MESSAGEPOS$(4, 2)
GET (460, 70)-(630, 290), MENU3
MESSAGEPOS$(1, 1) = "TOTAL # OF STEPS:": MESSAGEPOS$(1, 2) = "9"
MESSAGEPOS$(2, 1) = "STEP TIME:": MESSAGEPOS$(2, 2) = "12"
MESSAGEPOS$(3, 1) = "INVERT:": MESSAGEPOS$(3, 2) = "15"
MESSAGEPOS$(4, 1) = "TIME FACTOR:": MESSAGEPOS$(4, 2) = "18"
ITEMINDEX% = 1
INV$ = "NO"
LINE (460, 70)-(630, 290), 1, BF
LINE (464, 74)-(626, 286), 0, BF
COLOR 1, 0: LOCATE 7, 61: PRINT "MODE 1 PARAMETERS"
COLOR 15, 0: LOCATE 9, 60: PRINT MESSAGEPOS$(1, 1)
LOCATE 10, 63: PRINT USING "###,###"; PARAMETERS(3, 1)
COLOR 1, 0: LOCATE 12, 60: PRINT MESSAGEPOS$(2, 1)
COLOR 15, 0: LOCATE 13, 67: PRINT USING "###"; PARAMETERS(3, 2)
COLOR 1, 0: LOCATE 15, 60: PRINT MESSAGEPOS$(3, 1);
COLOR 15, 0: LOCATE 15, 69: PRINT INV$
COLOR 1, 0: LOCATE 18, 60: PRINT MESSAGEPOS$(4, 1)
COLOR 15, 0: LOCATE 19, 68: PRINT USING "##.##"; PARAMETERS(3, 4)
DO              'Get keyboard response.
        KBD$ = INKEY$
        FK = 0
        IF LEN(KBD$) = 2 THEN FK = ASC(RIGHT$(KBD$, 1))
        IF FK = 72 THEN             'Up arrow.
                COLOR 1, 0
                LOCATE VAL(MESSAGEPOS$(ITEMINDEX%, 2)), 60
                PRINT MESSAGEPOS$(ITEMINDEX%, 1)
                COLOR 15, 0
                IF ITEMINDEX% = 1 THEN ITEMINDEX% = 4 ELSE ITEMINDEX%
= ITEMINDEX% - 1
                LOCATE VAL(MESSAGEPOS$(ITEMINDEX%, 2)), 60
                PRINT MESSAGEPOS$(ITEMINDEX%, 1)
        END IF
      ' IF FK = 80 THEN             'Down arrow.
                COLOR 1, 0
                LOCATE VAL(MESSAGEPOS$(ITEMINDEX%, 2)), 60
                PRINT MESSAGEPOS$(ITEMINDEX%, 1)
                COLOR 15, 0
                IF ITEMINDEX% = 4 THEN ITEMINDEX% = 1 ELSE ITEMINDEX%
= ITEMINDEX% + 1
                LOCATE VAL(MESSAGEPOS$(ITEMINDEX%, 2)), 60
                PRINT MESSAGEPOS$(ITEMINDEX%, 1)
```

```
    END IF
    IF KBD$ = CHR$(13) THEN          'Return is hit.
        SELECT CASE ITEMINDEX%
            CASE 1                   'Parameters (3,1).
                LINE (495, 127)-(560, 140), 0, BF
                LINE (505, 127)-(550, 138), 1, BF
                XP$ = ""
                CALL GETSTRING(10, 64, 6, XP$)
                PARAMETERS(3, 1) = VAL(XP$)
                LOCATE 10, 63
                PRINT USING "###,###"; PARAMETERS(3, 1)
            CASE 2                   'Parameters (3,2).
                LINE (530, 168)-(550, 180), 1, BF
                XP$ = ""
                CALL GETSTRING(13, 67, 3, XP$)
                PARAMETERS(3, 2) = VAL(XP$)
                LOCATE 13, 67
                PRINT USING "##.##"; PARAMETERS(3, 2)
            CASE 3                   'Parameters (3,3).
                IF PARAMETERS(3, 3) = -1 THEN
                    PARAMETERS(3, 3) = 1
                    INV$ = "NO "
                    COLOR 15, 0
                    LOCATE 15, 69
                    PRINT INV$
                ELSE
                    PARAMETERS(3, 3) = -1
                    INV$ = "YES"
                    COLOR 15, 0
                    LOCATE 15, 69
                    PRINT INV$
                END IF
            CASE 4                   'Parameters (3,4).
                LINE (544, 253)-(575, 265), 1, BF
                XP$ = ""
                CALL GETSTRING(19, 69, 4, XP$)
                PARAMETERS(3, 4) = VAL(XP$)
                LOCATE 19, 68
                PRINT USING "##.##"; PARAMETERS(3, 4)
        END SELECT
    END IF

LOOP UNTIL KBD$ = CHR$(27)   'Esc returns to calling routine.

PUT (460, 70), MENU3, PSET       'Put data back behind menu.
```

```
END SUB

**********************************************************************
*              Subroutine to take data with photon counter and delay line.          *
**********************************************************************

SUB MODE4GO (YMIN!, YMAX!, INDEXMIN%, INDEXMAX%)

STATIC AV%, XMIN!, XMAX!     'Allows you to continue scan after stopping.
OPEN "I", #2, "STATUS"       'Get scan number.
INPUT #2, TOTALSCANS%
CLOSE #2
CALL MOTION("1MN", REPORT$)      'Turn motor on.
CALL MOTION("1TP", POS$)         'Get current position.
OPEN "COM1:9600,N,8,2,CS,DS,CD" FOR RANDOM AS #2     'Communication with
                                                       photon counter.
PRINT #2, "   "
PRINT #2, "CR;CH"  'See photon counter manual for communication commands.
COLOR 15, 0
CALL MCLEAR
INPUT "CONTINUE CURRENT SCAN (Y OR y)"; CONTINUE$        'New scan?
IF CONTINUE$ <> "Y" OR CONTINUE$ <> "y" THEN
        AV% = 0: XMIN! = 0: YMIN! = 0: XMAX! = 0: YMAX! = 0
        FOR P = 0 TO PARAMETERS(4, 1)
                DAT(P).X = P * PARAMETERS(4, 2) * CALIB: DAT(P).Y = 0
        NEXT P
        CALL SCLEAR
END IF
CALL MCLEAR              'Clear menu line.
VIEW (0, 34)-(639, 349)      'Set screen coordinates.
WINDOW (-PARAMETERS(4, 2) * CALIB, PARAMETERS(4, 5))-
((PARAMETERS(4, 1) + 1) * PARAMETERS(4, 2) * CALIB, -PARAMETERS(4, 5) *
.05)
PRINT "COLLECTING DATA"
KBD$ = ""
DO UNTIL POS$ <> "?"      'Find current position.
        CALL MOTION("1TP", POS$)
LOOP
DO
        CMD$ = "1MR" + LTRIM$(STR$(PARAMETERS(4, 6) - VAL(POS$)))
        CALL MOTION(CMD$, REPORT$)        'Go to beginning point on stage.
        DO              'Wait until stage stops moving.
                OLDPOS$ = POS$
                CALL MOTION("1TP", POS$)
```

```
        LOOP UNTIL OLDPOS$ = POS$
LOOP UNTIL ABS(VAL(POS$) - PARAMETERS(4, 6)) <= 4     'Get within 4 encoder
        counts of desired starting point.  Something is wrong with this routine.
DO UNTIL KBD$ <> ""       'Begin scan.
        FOR P% = 0 TO PARAMETERS(4, 1)       'From zero to # of pts.
                NEXTPOSITION& = PARAMETERS(4, 6) + P% * PARAMETERS(4,
2)
                CMD$ = "1MA" + LTRIM$(STR$(NEXTPOSITION&))
                CALL MOTION(CMD$, REPORT$)          'Move to next point.
                DO              'Wait for stage to stop.
                        NEWPOS$ = POS$
                        CALL MOTION("1TP", POS$)
                LOOP UNTIL NEWPOS$ = POS$
                PSET (DAT(P%).X, DAT(P%).Y), 0   'Put a black point on old data point.
                PRINT #2, "CS"        'Start collecting data for preset triggers.
                DO                    'Wait until data is ready.
                        PRINT #2, "SS1"
                        INPUT #2, DATAREADYBIT%
                LOOP UNTIL DATAREADYBIT%
                PRINT #2, "QA"        'Get data from photon counter.
                INPUT #2, NEWDATA%
                DAT(P%).Y = (DAT(P%).Y * AV% + NEWDATA%) / (AV% + 1)
                                'Update new y value.
                IF P% = 0 THEN        'Find YMAX! and YMIN!.
                        YMAX! = DAT(P%).Y
                        YMIN! = DAT(P%).Y
                END IF
                IF DAT(P%).Y > YMAX! THEN YMAX! = DAT(P%).Y
                IF DAT(P%).Y < YMIN! THEN YMIN! = DAT(P%).Y
                PSET (DAT(P%).X, DAT(P%).Y), 1          'Plot point.  Could use the
                                                display routine here as in other modes.
                STOP$ = INKEY$     'stop immediately with "S", stop at end of scan any
                                                other key.  P will pause the scan.
                IF KBD$ = "" THEN KBD$ = STOP$
                IF STOP$ = "P" OR STOP$ = "p" THEN
                        STOP$ = ""
                        DO UNTIL STOP$ <> ""
                        STOP$ = INKEY$
                        LOOP
                        STOP$ = "": KBD$ = ""
                END IF
                IF STOP$ = "S" OR STOP$ = "s" THEN EXIT DO
        NEXT P%               'Next scan.
                AV% = AV% + 1       '# of averages.
```

```
            CALL FIVESCAN(AV%, MODE%, INT(PARAMETERS(4, 1))) 'Save
                                                    every five scans.
            LOCATE 2, 50
            PRINT "# OF SCANS COMPLETED: "; AV%
            CMD$ = "1MR-" + LTRIM$(STR$(PARAMETERS(4, 1) *
PARAMETERS(4, 2) + 100))
            CALL MOTION(CMD$, REPORT$)        'Go back to starting point,
                                        plus 100 points to avoid backlash.
            PRINT #2, "CR;CH"                 'Reset photon counter.
            DO                                'Wait until stage stops.
                OLDPOS$ = POS$
                CALL MOTION("1TP", POS$)
            LOOP UNTIL OLDPOS$ = POS$
            CMD$ = "1MA" + LTRIM$(STR$(PARAMETERS(4, 6)))
            CALL MOTION(CMD$, REPORT$)        'Go to starting point.
            'CALL CHECKLASER(shutter1%)  'Used to check whether the laser
                                    shutter is open.  Not used currently.
            'CALL CHECKLASER(shutter2%)
            'IF shutter1% <> shutter2% THEN
             '    CALL CHECKLASER(shutter3%)
              '   shutter% = (shutter1% + shutter2% + shutter3%) / 3
            'ELSE
             '    shutter% = shutter1%
          ' END IF
            'IF shutter% = 0 THEN
             '    KBD$ = "ANTARES"
              '   CALL MCLEAR
               '  PRINT "      STOPPED DUE TO ANTARES SHUTTER
CLOSED"
            'END IF
LOOP
CLOSE #2            'close communication with photon counter.
VIEW: WINDOW        'Reset screen coordinates.
CALL FILESAVE(4, INT(PARAMETERS(4, 1)), AV%, "TIME (fs)", "INTENSITY")
                                                        'Save data.
CALL MCLEAR         'Clear menu line.
CALL MMENU          'Print main menu.

END SUB

*****************************************************************
*                  Subroutine to get parameters for mode 4.                  *
*****************************************************************

SUB MODE4PARAMETERS
```

```
DIM MENU3(1 TO 12100) AS INTEGER  'Make menu.
DIM MESSAGEPOS$(6, 2)
MESSAGEPOS$(1, 1) = "# OF DATA POINTS:": MESSAGEPOS$(1, 2) = "7"
MESSAGEPOS$(2, 1) = "STEPSIZE:": MESSAGEPOS$(2, 2) = "10"
MESSAGEPOS$(3, 1) = "LASER SHOTS/STEP:": MESSAGEPOS$(3, 2) = "12"
MESSAGEPOS$(4, 1) = "INVERT:  ": MESSAGEPOS$(4, 2) = "15"
MESSAGEPOS$(5, 1) = "COUNTS FULL SCALE:": MESSAGEPOS$(5, 2) = "17"
MESSAGEPOS$(6, 1) = "START SCANNING AT:": MESSAGEPOS$(6, 2) = "20"
GET (460, 42)-(630, 315), MENU3
ITEMINDEX% = 1
IF PARAMETERS(4, 4) = 1 THEN INV$ = "YES" ELSE INV$ = "NO "
LINE (460, 42)-(630, 315), 1, BF
LINE (464, 46)-(626, 311), 0, BF
COLOR 1, 0: LOCATE 5, 61: PRINT "MODE 4 PARAMETERS"
COLOR 15, 0: LOCATE 7, 60: PRINT MESSAGEPOS$(1, 1)
LOCATE 8, 66: PRINT USING "####"; PARAMETERS(4, 1)
COLOR 1, 0: LOCATE 10, 60: PRINT MESSAGEPOS$(2, 1)
COLOR 15, 0: LOCATE 10, 70: PRINT USING "####"; PARAMETERS(4, 2)
COLOR 1, 0: LOCATE 12, 60: PRINT MESSAGEPOS$(3, 1)
COLOR 15, 0: LOCATE 13, 66: PRINT USING "###"; PARAMETERS(4, 3)
COLOR 1, 0: LOCATE 15, 60: PRINT MESSAGEPOS$(4, 1)
COLOR 15, 0: LOCATE 15, 69: PRINT INV$
COLOR 1, 0: LOCATE 17, 60: PRINT MESSAGEPOS$(5, 1)
COLOR 15, 0: LOCATE 18, 66: PRINT USING "####"; PARAMETERS(4, 5)
COLOR 1, 0: LOCATE 20, 60: PRINT MESSAGEPOS$(6, 1)
COLOR 15, 0: LOCATE 21, 66: PRINT USING "###,###"; PARAMETERS(4, 6)
DO                    'Get keyboard response.
        KBD$ = INKEY$
        FK = 0
        IF LEN(KBD$) = 2 THEN FK = ASC(RIGHT$(KBD$, 1))
        IF FK = 72 THEN     'Up arrow.
                COLOR 1, 0
                LOCATE VAL(MESSAGEPOS$(ITEMINDEX%, 2)), 60
                PRINT MESSAGEPOS$(ITEMINDEX%, 1)
                COLOR 15, 0
                IF ITEMINDEX% = 1 THEN ITEMINDEX% = 6 ELSE ITEMINDEX%
= ITEMINDEX% - 1
                LOCATE VAL(MESSAGEPOS$(ITEMINDEX%, 2)), 60
                PRINT MESSAGEPOS$(ITEMINDEX%, 1)
        END IF
        IF FK = 80 THEN     'Down arrow.
                COLOR 1, 0
                LOCATE VAL(MESSAGEPOS$(ITEMINDEX%, 2)), 60
                PRINT MESSAGEPOS$(ITEMINDEX%, 1)
```

```
            COLOR 15, 0
            IF ITEMINDEX% = 6 THEN ITEMINDEX% = 1 ELSE ITEMINDEX%
= ITEMINDEX% + 1
            LOCATE VAL(MESSAGEPOS$(ITEMINDEX%, 2)), 60
            PRINT MESSAGEPOS$(ITEMINDEX%, 1)
        END IF
        IF KBD$ = CHR$(13) THEN         'Return hit.
            SELECT CASE ITEMINDEX%
                CASE 1          'Parameters (4,1).
                    LINE (520, 98)-(551, 110), 1, BF
                    XP$ = ""
                    CALL GETSTRING(8, 66, 4, XP$)
                    PARAMETERS(4, 1) = VAL(XP$)
                    LOCATE 8, 66
                    PRINT USING "####"; PARAMETERS(4, 1)
                    OPEN "COM1:9600,N,8,2,CS,DS,CD" FOR RANDOM
AS #2
                        CMD$ = "NP" +
LTRIM$(STR$(INT(PARAMETERS(4, 1))))
                        PRINT #2, CMD$
                    CLOSE #2
                CASE 2          'Parameters (4,2).
                    LINE (552, 126)-(582, 138), 1, BF
                    XP$ = ""
                    CALL GETSTRING(10, 70, 4, XP$)
                    PARAMETERS(4, 2) = VAL(XP$)
                    LOCATE 10, 70
                    PRINT USING "####"; PARAMETERS(4, 2)
                CASE 3          'Parameters (4,3).
                    LINE (500, 168)-(600, 180), 0, BF
                    LINE (530, 168)-(550, 180), 1, BF
                    XP$ = ""
                    CALL GETSTRING(13, 67, 5, XP$)
                    PARAMETERS(4, 3) = VAL(XP$)
                    LOCATE 13, 67
                    PRINT USING "###"; PARAMETERS(4, 3)
                    OPEN "COM1:9600,N,8,2,CS,DS,CD" FOR RANDOM
AS #2
                        PRINT #2, "CM"
                        INPUT #2, COUNTINGMODE%
                        IF COUNTINGMODE% = 3 THEN
                            CMD$ = "CP1," +
LTRIM$(STR$(PARAMETERS(4, 3)))
                            PRINT #2, CMD$
                        ELSE
```

```
                                        CMD$ = "CP2," +
LTRIM$(STR$(PARAMETERS(4, 3)))
                                        PRINT #2, CMD$
                                    END IF
                                CLOSE #2
                            CASE 4      'Parameters (4,4).  Not used now.
                                IF PARAMETERS(4, 4) = 1 THEN
                                    PARAMETERS(4, 4) = 0
                                    INV$ = "NO "
                                    COLOR 15, 0
                                    LOCATE 15, 69
                                    PRINT INV$
                                ELSE
                                    PARAMETERS(4, 4) = 1
                                    INV$ = "YES"
                                    COLOR 15, 0
                                    LOCATE 15, 69
                                    PRINT INV$
                                END IF
                            CASE 5      'Parameters (4,5).
                                LINE (500, 239)-(590, 251), 0, BF
                                LINE (521, 239)-(550, 251), 1, BF
                                XP$ = ""
                                CALL GETSTRING(18, 66, 5, XP$)
                                PARAMETERS(4, 5) = VAL(XP$)
                                LOCATE 18, 66
                                PRINT USING "####"; PARAMETERS(4, 5)
                            CASE 6      'Parameters (4,6).
                                LINE (480, 280)-(600, 292), 0, BF
                                LINE (522, 280)-(567, 292), 1, BF
                                XP$ = ""
                                CALL GETSTRING(21, 66, 7, XP$)
                                PARAMETERS(4, 6) = VAL(XP$)
                                LOCATE 21, 66
                                PRINT USING "###,###"; PARAMETERS(4, 6)
                        END SELECT
                    END IF
LOOP UNTIL KBD$ = CHR$(27)   'Esc returns to calling routine.
PUT (460, 42), MENU3, PSET   'Put data back behind menu.
ERASE MENU3                  'Return memory.

END SUB

**********************************************************************
```

```
*                    Subroutine to control the delay line.                    *
*************************************************************************

SUB MOTION (COMM$, REPORT$)        'This routine is a general communication
        routine for the delay line by microkinetics.  See the experimental section of my
        thesis for explanation.

CALL QCINIT(4, 3, 0, 1, PORTSTATUS%, QCERROR%)
CALL COPEN(2, 9600, 1, 0, 8, 0, 20, 20, TXBUF2(), RXBUF2(), QCERROR%)
CALL CBUFCLR(2, 3, QCERROR%)
CODE$ = MID$(COMM$, 2, 2)
SELECT CASE CODE$
        CASE "MR", "MA", "GH", "MN", "DH", "AB", "SV"
                SEN$ = COMM$ + CHR$(13)
                CALL CPRINT(2, SEN$, QCERROR%)
                FOR i = 1 TO 1000: NEXT i
                DO
                        CALL CBUFFER(2, RECV%, XMIT%, QCERROR%)
                LOOP UNTIL XMIT% = 20
                REPORT$ = "NO RETURN VALUE"
        CASE "TP", "TE", "TV"
                SEN$ = COMM$ + CHR$(13)
                CALL CPRINT(2, SEN$, QCERROR%)
                FOR i = 1 TO 1000: NEXT i
                DO
                        CALL CBUFFER(2, RECV%, XMIT%, QCERROR%)
                LOOP UNTIL XMIT% = 20
                REPORT$ = SPACE$(20)
                RELPOS% = 0: FLAG% = 1
                CALL CINPUT(2, REPORT$, RELPOS%, 0, "", "", KB%, FLAG%)
                REPORT$ = RIGHT$(REPORT$, LEN(REPORT$) - INSTR(REPORT$,
" "))
                REPORT$ = LEFT$(REPORT$, 10)
END SELECT
CALL CCLOSE(2, QCERROR%)
CALL QCEXIT

END SUB

*************************************************************************
*                Subroutine to reset the scan parameters to those in FIL$.        *
*************************************************************************

SUB RESETPARAMETERS (FIL$) 'The file structure can be seen elsewhere in the
        appendix.  These files have titles for each entry, therefore the input routine must
```

accept these unnecessary fields (DUMMY$). These titles are kept in the array TEMPLATE$() in order to save the parameters the same way.

```
OPEN FIL$ FOR INPUT AS #1
INPUT #1, DUMMY$
MODE% = VAL(RIGHT$(DUMMY$, LEN(DUMMY$) - 8))
TEMPLATE$(1) = LEFT$(DUMMY$, 8)
INPUT #1, DUMMY$: INPUT #1, DUMMY$: TEMPLATE$(2) = SPACE$(19):
TEMPLATE$(3) = DUMMY$
FOR i = 1 TO 4
        INPUT #1, DUMMY$
        PARAMETERS(1, i) = VAL(RIGHT$(DUMMY$, LEN(DUMMY$) - 19))
        TEMPLATE$(i + 3) = LEFT$(DUMMY$, 19)
NEXT i
INPUT #1, DUMMY$: INPUT #1, DUMMY$: TEMPLATE$(8) = SPACE$(19):
TEMPLATE$(9) = DUMMY$
FOR i = 1 TO 6
        INPUT #1, DUMMY$
        PARAMETERS(2, i) = VAL(RIGHT$(DUMMY$, LEN(DUMMY$) - 19))
        TEMPLATE$(i + 9) = LEFT$(DUMMY$, 19)
NEXT i
INPUT #1, DUMMY$: INPUT #1, DUMMY$: TEMPLATE$(16) = SPACE$(19):
TEMPLATE$(17) = DUMMY$
FOR i = 1 TO 5
        INPUT #1, DUMMY$
        PARAMETERS(3, i) = VAL(RIGHT$(DUMMY$, LEN(DUMMY$) - 19))
        TEMPLATE$(i + 17) = LEFT$(DUMMY$, 19)
NEXT i
INPUT #1, DUMMY$: INPUT #1, DUMMY$: TEMPLATE$(23) = SPACE$(19):
TEMPLATE$(24) = DUMMY$
FOR i = 1 TO 6
        INPUT #1, DUMMY$
        PARAMETERS(4, i) = VAL(RIGHT$(DUMMY$, LEN(DUMMY$) - 19))
        TEMPLATE$(i + 24) = LEFT$(DUMMY$, 19)
NEXT i
INPUT #1, DUMMY$: INPUT #1, DUMMY$: TEMPLATE$(31) = SPACE$(19):
TEMPLATE$(32) = DUMMY$
FOR i = 1 TO 33
        INPUT #1, DUMMY$
        PHOTON$(2, i) = RIGHT$(DUMMY$, LEN(DUMMY$) - 19)
        TEMPLATE$(i + 32) = LEFT$(DUMMY$, 19)
NEXT i
CLOSE #1
```

```
OPEN "COM1:9600,N,8,2,CS,DS,CD" FOR RANDOM AS #1      'Send these
                                                      parameters to the photon counter.
PRINT #1, "   "
IF VAL(PHOTON$(2, 1)) = 3 THEN PHOTON$(1, 5) = PHOTON$(1, 5) + "1" ELSE
PHOTON$(1, 5) = PHOTON$(1, 5) + "2"
FOR i = 1 TO 33 'Some commands require a comma in between command and parameter.
        SELECT CASE i
                CASE 2, 3, 4, 5, 14 TO 33
                        PRINT #1, PHOTON$(1, i) + "," + PHOTON$(2, i)
                CASE ELSE
                        PRINT #1, PHOTON$(1, i) + PHOTON$(2, i)
        END SELECT
NEXT i

CLOSE #1

END SUB


**********************************************************************
*                    Subroutine to save current parameters in FIL$.                    *
**********************************************************************

SUB SAVEPARAMETERS (FIL$)  'This routine is the inverse of the
                           RESETPARAMETERS(FIL$) routine.  This is
                           where TEMPLATE$() comes in handy.

OPEN FIL$ FOR OUTPUT AS #1
PRINT #1, TEMPLATE$(1) + STR$(MODE%)
PRINT #1, TEMPLATE$(2): PRINT #1, TEMPLATE$(3)
FOR i = 1 TO 4
        PRINT #1, TEMPLATE$(i + 3) + STR$(PARAMETERS(1, i))
NEXT i
PRINT #1, TEMPLATE$(8): PRINT #1, TEMPLATE$(9)
FOR i = 1 TO 6
        PRINT #1, TEMPLATE$(i + 9) + STR$(PARAMETERS(2, i))
NEXT i
PRINT #1, TEMPLATE$(16): PRINT #1, TEMPLATE$(17)
FOR i = 1 TO 5
        PRINT #1, TEMPLATE$(i + 17) + STR$(PARAMETERS(3, i))
NEXT i
PRINT #1, TEMPLATE$(23): PRINT #1, TEMPLATE$(24)
FOR i = 1 TO 6
        PRINT #1, TEMPLATE$(i + 24) + STR$(PARAMETERS(4, i))
NEXT i
```

```
PRINT #1, TEMPLATE$(31): PRINT #1, TEMPLATE$(32)

OPEN "COM1:9600,N,8,2,CS,DS,CD" FOR RANDOM AS #2     'Get parameters from
                                                      the photon counter.
PRINT #2, "   "
PRINT #2, PHOTON$(1, 1)
INPUT #2, MD%
PHOTON$(1, 5) = LEFT$(PHOTON$(1, 5), 2)
IF MD% = 3 THEN PHOTON$(1, 5) = PHOTON$(1, 5) + "1" ELSE PHOTON$(1, 5) =
PHOTON$(1, 5) + "2"
FOR i = 1 TO 33
        PRINT #2, PHOTON$(1, i)
        INPUT #2, DUMMY!
        PRINT #1, TEMPLATE$(i + 32) + STR$(DUMMY!)
NEXT i

CLOSE #1
CLOSE #2

END SUB

*********************************************************************
*                  Subroutine to give scan menu (F1 from main menu).                  *
*********************************************************************

SUB SCANSUB (YMIN!, YMAX!, INDEXMIN%, INDEXMAX%)

DIM MENU1(1 TO 2700)  AS INTEGER   'Make menu.
GET (26, 34)-(136, 124), MENU1
LINE (26, 34)-(136, 124), 1, BF
LINE (30, 34)-(132, 120), 0, BF
COLOR 15, 0
LOCATE 2, 7: PRINT "F1:SCAN"
COLOR 1, 0
LOCATE 4, 6: PRINT "F1:GO"
LOCATE 6, 6: PRINT "F2:SETUP"
LOCATE 8, 6: PRINT "F3:DEFAULTS"
DO              'Get keyboard response.
        KBD$ = INKEY$
        IF LEN(KBD$) = 2 THEN FK = ASC(RIGHT$(KBD$, 1))
        IF FK = 59 THEN             'F1 key.
                PUT (26, 34), MENU1, PSET       'Put data back behind menu.
                SELECT CASE MODE%     'Scan using whatever mode is chosen.
                        CASE 1
```

```
                        CALL MODE1GO(YMIN!, YMAX!, INDEXMIN%,
INDEXMAX%)
                CASE 2
                        CALL MODE2GO(YMIN!, YMAX!, INDEXMIN%,
INDEXMAX%)
                CASE 3
                        CALL MODE3GO(YMIN!, YMAX!, INDEXMIN%,
INDEXMAX%)
                CASE 4
                        CALL MODE4GO(YMIN!, YMAX!, INDEXMIN%,
INDEXMAX%)
            END SELECT
            COLOR 1, 0
            EXIT SUB
        END IF
        IF FK = 60 THEN     'F2 key.  Used to get to next menu.
            COLOR 15, 0
            LOCATE 6, 6: PRINT "F2:SETUP"
            CALL SETUPSUB
            COLOR 1, 0
            LOCATE 6, 6: PRINT "F2:SETUP"
        END IF
        IF FK = 61 THEN     'F3 key. Used to get to next menu.
            COLOR 15, 0
            LOCATE 8, 6: PRINT "F3:DEFAULTS"
            CALL DEFAULTSUB
            COLOR 1, 0
            LOCATE 8, 6: PRINT "F3:DEFAULTS"
        END IF
        FK = 0
LOOP UNTIL KBD$ = CHR$(27)   'Esc returns to main menu.
PUT (26, 34), MENU1, PSET    'Put data back behind menu.
ERASE MENU1                  'Return memory.
COLOR 1, 0
LOCATE 2, 7: PRINT "F1:SCAN"

END SUB


*****************************************************************
*                    Subroutine to give setup menu.             *
*****************************************************************

SUB SETUPSUB
```

```
DIM MENU2(1 TO 11844)  AS INTEGER 'Make menu.
DIM DOTPOS(1 TO 4) AS INTEGER
DOTPOS(1) = 146: DOTPOS(2) = 174: DOTPOS(3) = 202: DOTPOS(4) = 244
GET (180, 100)-(420, 290), MENU2
LINE (180, 100)-(420, 290), 1, BF
LINE (184, 104)-(416, 286), 0, BF
COLOR 15, 0
LOCATE 9, 30: PRINT "MODES OF OPERATION"
COLOR 1, 0
LOCATE 11, 25: PRINT "1 ( ) SCAN BOXCAR GATE"
LOCATE 13, 25: PRINT "2 ( ) BOXCAR/INTERNAL DELAY"
LOCATE 15, 25: PRINT "3 ( ) SCAN PHOTON COUNTER"
LOCATE 16, 35: PRINT "GATE DELAY"
LOCATE 18, 25: PRINT "4 ( ) PHOTON COUNTER/"
LOCATE 19, 35: PRINT "INTERNAL DELAY"
CIRCLE (220, DOTPOS(MODE%)), 3, 15, , , 1.2: PAINT (220, DOTPOS(MODE%)),
15

DO              'Get keyboard response.
        KBD$ = INKEY$
        FK = 0
        IF LEN(KBD$) = 2 THEN FK = ASC(RIGHT$(KBD$, 1))
        IF FK = 72 THEN      'Up arrow.
                PAINT (220, DOTPOS(MODE%)), 0, 0
                IF MODE% = 1 THEN MODE% = 4 ELSE MODE% = MODE% - 1
                CIRCLE (220, DOTPOS(MODE%)), 3, 15, , , 1.2: PAINT (220,
DOTPOS(MODE%)), 15
        END IF
        IF FK = 80 THEN      'Down arrow.
                PAINT (220, DOTPOS(MODE%)), 0, 0
                IF MODE% = 4 THEN MODE% = 1 ELSE MODE% = MODE% + 1
                CIRCLE (220, DOTPOS(MODE%)), 3, 15, , , 1.2: PAINT (220,
DOTPOS(MODE%)), 15
        END IF
        IF KBD$ = CHR$(13) THEN          'Return hit.
                SELECT CASE MODE%
                        CASE 1                  'Mode 1.
                                COLOR 15, 0
                                LOCATE 11, 31: PRINT "SCAN BOXCAR GATE"
                                CALL MODE1PARAMETERS
                                COLOR 1, 0
                                LOCATE 11, 31: PRINT "SCAN BOXCAR GATE"

                        CASE 2                  'Mode 2.
                                COLOR 15, 0
```

```
                    LOCATE 13, 31: PRINT "BOXCAR/INTERNAL
DELAY"
                    CALL MODE2PARAMETERS
                    COLOR 1, 0
                    LOCATE 13, 31: PRINT "BOXCAR/INTERNAL
DELAY"
                CASE 3              'Mode 3.
                    COLOR 15, 0
                    LOCATE 15, 31: PRINT "SCAN PHOTON COUNTER"
                    LOCATE 16, 35: PRINT "GATE DELAY"
                    CALL MODE3PARAMETERS
                    COLOR 1, 0
                    LOCATE 15, 31: PRINT "SCAN PHOTON COUNTER"
                    LOCATE 16, 35: PRINT "GATE DELAY"
                CASE 4              'Mode 4.
                    COLOR 15, 0
                    LOCATE 18, 31: PRINT "PHOTON COUNTER/"
                    LOCATE 19, 35: PRINT "INTERNAL DELAY"
                    CALL MODE4PARAMETERS
                    COLOR 1, 0
                    LOCATE 18, 31: PRINT "PHOTON COUNTER/"
                    LOCATE 19, 35: PRINT "INTERNAL DELAY"
            END SELECT
        END IF
LOOP UNTIL KBD$ = CHR$(27)          'Esc returns to calling routine.

PUT (180, 100), MENU2, PSET         'Put data back behind menu.
ERASE MENU2                         'Return memory.

END SUB
```

Monochromator Module

```
*****************************************************************
*                Subroutine declarations for those used in these subroutines          *
*****************************************************************

DECLARE SUB FILESAVE (MODE%, NPTS%, AV%, HEADER1$, HEADER2$)
DECLARE SUB FIVESCAN (AV%, MODE%, NPTS%)
DECLARE SUB SCLEAR ()
DECLARE SUB FILENAME (ROW%, COL%, FIL$)
DECLARE SUB DISPLAY (YMIN!, YMAX!, INDEXMIN%, INDEXMAX%)
DECLARE SUB DAS (CHANNEL%, DIO%)
DECLARE SUB MONOSCAN (MNPARA!())
DECLARE SUB MONOPARA (MNPARA!(), PARAMETERSAVAILABLE%)
DECLARE SUB GETSTRING (ROW%, COL%, LONGEST%, XP$)
DECLARE SUB MMENU ()
DECLARE SUB MCLEAR ()
DECLARE SUB READPOSITION (POSITION!)
DECLARE SUB MN (INTO$, OUTOF$)
DECLARE SUB INITMONO (MONOAVAILABLE%)
'*  Set up the RS232 buffers  *
DIM TXBUF2(20), RXBUF2(20), TXBUF3(20), RXBUF3(20), TXBUF6(20),
RXBUF6(20)
COMMON SHARED /BUFFERS/ TXBUF2(), RXBUF2(), TXBUF3(), RXBUF3(),
TXBUF6(), RXBUF6()
TYPE DATAPAIR          'Define data structure
     X AS SINGLE
     Y AS SINGLE
END TYPE
DIM DAT(1000) AS DATAPAIR
COMMON SHARED /D/ DAT() AS DATAPAIR
REM $DYNAMIC           'Make memory dynamic
HANDLER:               'Error handler--just returns program to line after error.

     ERRORCODE% = ERR
     RESUME NEXT

REM $STATIC

*****************************************************************
*                          Initialize the monochromator                          *
*****************************************************************
SUB INITMONO (MONOAVAILABLE%)          'Returns 1 if mono is available

PORT% = 4
```

```
CALL QCINIT(4, 3, 0, 1, PORTSTATUS%, QCERROR%)
CALL COPEN(PORT%, 9600, 1, 0, 8, 0, 40, 40, TXBUF6(), RXBUF6(), QCERROR%)
NUMTRIES% = 0
DO                      'Call at least 10 times before returning 0.
    NUMTRIES% = NUMTRIES% + 1     '# of tries
    CALL CBUFCLR(PORT%, 3, QCERROR%) 'Clear buffers
    CALL CPUTCHAR(PORT%, 32, QCERROR%)     'Put a return on the output line.
    NOW! = TIMER
    DO              'loop until a chr$(70) is returned
        CALL CBUFREC(PORT%, STATUS%, QCERROR%)  'wait until buffer sees
                a character or until 5 seconds have elapsed.
        LATER! = TIMER
        IF LATER! - NOW! > 5 THEN EXIT DO
    LOOP UNTIL STATUS% = 1  'Something is in buffer.
    CHAR% = 0
    CALL CGETCHAR(PORT%, CHAR%, STATUS%) 'Get buffer contents.
    IF CHAR% = 70 THEN          'Mono is available.
        MONOAVAILABLE% = 1
        CALL CCLOSE(PORT%, QCERROR%)'Close buffers.
        CALL QCEXIT
        EXIT SUB
    END IF
    IF NUMTRIES% = 10 THEN  'Mono is not available.
        CALL MCLEAR             'Clear menu line.
        INPUT "MONOCHROMETER NOT RESPONSING
CONTINUE (Hit n to end, else any key to continue)"; DUMMY$
        IF DUMMY$ = "N" OR DUMMY$ = "n" THEN
            CLS
            END
        ELSE                'Continue without the use of the monochromator.
            MONOAVAILABLE% = 0
            CALL CCLOSE(PORT%, QCERROR%)
            CALL QCEXIT
            EXIT SUB
        END IF
    END IF
LOOP UNTIL CHAR% = 42           'After the 70 a 42 should be returned.
FOR I = 1 TO 500: NEXT I            'Pause.
CALL CBUFCLR(PORT%, 3, QCERROR%)        'clear the buffers.
    CALL CPUTCHAR(PORT%, 247, QCERROR%)     'Put a 247 out to mono.
    DO              'Wait until the receive buffer gets something in return.
        CALL CBUFREC(PORT%, STATUS%, QCERROR%)
    LOOP UNTIL STATUS% = 1
    CALL CGETCHAR(PORT%, CHAR%, STATUS%) 'Get the character
FOR I = 1 TO 500: NEXT I  'Pause.
```

```
CALL CBUFCLR(PORT%, 3, QCERROR%)        'clear buffers.
    STRNG$ = "O2000" + CHR$(&H0)        'Send O2000 + chr$(&h0).
    CALL CPRINT(PORT%, STRNG$, QCERROR%)
    DO              'Wait until something is returned.
        CALL CBUFREC(PORT%, STATUS%, QCERROR%)
    LOOP UNTIL STATUS% = 1
    CALL CGETCHAR(PORT%, CHAR%, STATUS%) 'Get character.
FOR I = 1 TO 500: NEXT I            'Pause.
CALL CBUFCLR(PORT%, 3, QCERROR%)        'Clear buffers.
    STRNG$ = "B14,300,450,2000" + CHR$(13)  'Initialize if mono has just been
                                                turned on.
    CALL CPRINT(PORT%, STRNG$, QCERROR%)    'Send to the port.
    DO              'Wait until mono sends something back.
        CALL CBUFREC(PORT%, STATUS%, QCERROR%)
    LOOP UNTIL STATUS% = 1
    CALL CGETCHAR(PORT%, CHAR%, STATUS%) 'Get character.
MONOAVAILABLE% = 1              'Mono is available.
CALL CCLOSE(PORT%, QCERROR%)    'close buffers.
CALL QCEXIT

END SUB

SUB MN (INTO$, OUTOF$)          'General communication protocol with the mono.

PORT% = 4                       'mono hooked up to com4.
CALL QCINIT(4, 3, 0, 1, PORTSTATUS%, QCERROR%)      'initialize port.
CALL COPEN(PORT%, 9600, 1, 0, 8, 0, 40, 40, TXBUF6(), RXBUF6(), QCERROR%)
CALL CBUFCLR(PORT%, 3, QCERROR%)        'Open and clear port buffers.
CALL CPRINT(PORT%, INTO$, QCERROR%)     'Send out the command.
DO          'Loop until the receive buffer has something.
    CALL CBUFFER(PORT%, RECV%, XMIT%, QCERROR%)
LOOP UNTIL RECV% <> 0
CMND$ = LEFT$(INTO$, 1)         'Just need the command character (see manual).
SELECT CASE CMND$       'Different commands send back different things.
    CASE "A", "B", "F", "G", "L", "p", "q", "v"     'These commands send back 1 char.
        CALL CGETCHAR(PORT%, CHAR%, STATUS%)    'Get char.
        OUTOF$ = CHR$(CHAR%)        'Set OUTOF$ to this char.
    CASE "C", "H", "r", "s", "t"                'These send a string of char.
        OUTOF$ = ""
        DO          'Keep getting char. until return or space is returned.
            FOR I = 1 TO 200: NEXT I  'Slight pause.
            CALL CGETCHAR(PORT%, CHAR%, STATUS%)        'Get char.
            IF CHAR% <> 32 OR CHAR% <> 13 THEN OUTOF$ = OUTOF$ +
CHR$(CHAR%)       'Generate the desired string.
        LOOP UNTIL CHAR% = 13
```

```
    CASE "E", "K"           'These commands send back two characters.
        CALL CGETCHAR(PORT%, CHAR%, STATUS%)
        OUTOF$ = CHR$(CHAR%)
        CALL CGETCHAR(PORT%, CHAR%, STATUS%)
        OUTOF$ = OUTOF$ + CHR$(CHAR%)
END SELECT

CALL CCLOSE(PORT%, QCERROR%)    'Close port.
CALL QCEXIT                     'Close communication protocols.

END SUB

SUB MONOCHROMETER STATIC        'Sub to make menu for mono. functions.

DIM MENU(10050) AS INTEGER  'Get what is behind menu.
DIM MNPARA!(5, 2)           'Array used for mono. parameters.
LOCATE 2, 42: COLOR 15, 0: PRINT "F4:MONOCHR"   'Print menu option in bold.
GET (290, 34)-(440, 284), MENU          'Make menu.
LINE (290, 34)-(440, 284), 1, BF
LINE (294, 34)-(436, 280), 0, BF
LOCATE 4, 41: PRINT "CURRENT POS"
LOCATE 7, 42: PRINT "MOVE TO:"
LOCATE 8, 38: PRINT "(or calibrate to)"
LOCATE 11, 43: COLOR 15, 0: PRINT "ACTIONS"
LOCATE 13, 39: COLOR 15, 0: PRINT "MOVE:": LOCATE 13, 52: COLOR 1, 0:
PRINT "<+>"
LOCATE 15, 39: COLOR 15, 0: PRINT "CALIBRATE:"
LOCATE 16, 46: COLOR 1, 0: PRINT "<CTRL-F5>"
LOCATE 17, 39: COLOR 15, 0: PRINT "SCAN SET-UP:"
LOCATE 18, 46: COLOR 1, 0: PRINT "<CTRL-F9>"
LOCATE 19, 39: COLOR 15, 0: PRINT "START SCAN:"
LOCATE 20, 46: COLOR 1, 0: PRINT "<CTRL-F4>"
CALL READPOSITION(POSITION!)        'Get current position of mono.
LOCATE 5, 42: PRINT USING "###.##"; POSITION!; : PRINT "nm"
LINE (318, 55)-(402, 69), 15, B
LOCATE 9, 48: PRINT "nm"
LINE (318, 111)-(402, 126), 15, B
LINE (328, 113)-(375, 123), 15, BF
GOTNUMBER% = 0: GOTPOINT% = 0: GOTPARAMETERS% = 0
DO              'Get keyboard response for menu.
    KBD$ = "": FK% = 0
    KBD$ = INKEY$
    IF LEN(KBD$) = 2 THEN FK% = ASC(RIGHT$(KBD$, 1))
    IF KBD$ = "+" THEN   'Move mono. if a value has been input.
        IF GOTNUMBER% = 1 THEN   'A target value has been input.
```

```
                LOCATE 13, 52: COLOR 15, 0: PRINT "<+>"
                MR! = NM! - POSITION!    'Find the difference of current pos. and target
                IF MR! < 0 THEN    'If negative then remove backlash of 300 steps.
                    CALL MN("F0," + LTRIM$(STR$(MR! * 20 - 300)) + CHR$(13),
OUTOF$)    'Move to target minus 300 steps.
                    DO      'Wait until stopped.
                        CALL MN("E", OUTOF$)
                    LOOP UNTIL RIGHT$(OUTOF$, 1) = "z"
                    CALL MN("F0,300" + CHR$(13), OUTOF$) 'Move forward 300
steps.
                    DO      'Wait until stopped.
                        CALL MN("E", OUTOF$)
                    LOOP UNTIL RIGHT$(OUTOF$, 1) = "z"
                ELSEIF MR! > 0 THEN      'If pos. then backup 300 and then go.
                    CALL MN("F0,-300" + CHR$(13), OUTOF$)   'Backup 300.
                    DO      'Wait until stopped.
                        CALL MN("E", OUTOF$)
                    LOOP UNTIL RIGHT$(OUTOF$, 1) = "z"
                    CALL MN("F0," + LTRIM$(STR$(MR! * 20 + 300)) + CHR$(13),
OUTOF$)      'Move forward to target.
                    DO      'Wait until stopped.
                        CALL MN("E", OUTOF$)
                    LOOP UNTIL RIGHT$(OUTOF$, 1) = "z"
                END IF
                CALL READPOSITION(POSITION!)      'Read current position.
                LOCATE 5, 42: PRINT USING "###.##"; POSITION!; : PRINT "nm"
                LINE (318, 55)-(402, 69), 15, B
                LOCATE 13, 52: COLOR 1, 0: PRINT "<+>"
            END IF
        ELSEIF KBD$ >= "0" AND KBD$ <= "9" THEN      'If a # is hit then assume
target value is being input.
            LINE (328, 112)-(375, 123), 15, BF
            GOTNUMBER% = 1      'Target available.
            NM$ = KBD$
            LOCATE 9, 42: COLOR 15, 0: PRINT NM$;
            DO          'Piece together string of target value.
                TEMP$ = INKEY$
                IF (TEMP$ >= "0" AND TEMP$ <= "9") OR TEMP$ = "." THEN
                    IF GOTPOINT% = 0 OR TEMP$ <> "." THEN
                        NM$ = NM$ + TEMP$
                        PRINT TEMP$;
                    END IF
                    IF TEMP$ = "." THEN GOTPOINT% = 1
                END IF
            LOOP UNTIL TEMP$ = CHR$(13)      'Until return is hit.
```

```
            NM! = VAL(NM$)          'NM! is the target position.
            LOCATE 9, 42: COLOR 1, 0: PRINT USING "###.##"; NM!
            LOCATE 9, 48: PRINT "nm"
            LINE (318, 111)-(402, 126), 1, B
            GOTPOINT% = 0
        END IF
        SELECT CASE FK%
            CASE 98             ' calibrate
                IF GOTNUMBER% = 1 THEN      'If input is for calibration.
                    LOCATE 16, 46: COLOR 15, 0: PRINT "<CTRL-F5>"
                    CALL MN("G0," + LTRIM$(STR$(NM! * 20)) + CHR$(13),
OUTOF$)     'Call calibrate command.
                    CALL READPOSITION(POSITION!)        'Read pos.
                    LOCATE 5, 42: PRINT USING "###.##"; POSITION!; : PRINT
"nm"
                    LINE (318, 55)-(402, 69), 15, B
                    LOCATE 16, 46: COLOR 1, 0: PRINT "<CTRL-F5>"
                END IF
            CASE 102            ' input scan parameters
                LOCATE 18, 46: COLOR 15, 0: PRINT "<CTRL-F9>"
                CALL MONOPARA(MNPARA!(), PARAMETERSAVAILABLE%)
                LOCATE 18, 46: COLOR 1, 0: PRINT "<CTRL-F9>"
            CASE 97             ' begin scan
                IF PARAMETERSAVAILABLE% = 1 THEN  'If no parameters, no scan.
                    COLOR 1, 0
                    PUT (290, 34), MENU, PSET  'Erase menu on screen.
                    ERASE MENU 'Return memory.
                    CALL MONOSCAN(MNPARA!())    'call scan routine.
                    CALL MCLEAR: CALL MMENU     'Clear menu line and return to
                                                main menu.
                    EXIT SUB
                END IF
        END SELECT
LOOP UNTIL KBD$ = CHR$(27)   'Loop until escape is hit.
COLOR 1, 0
PUT (290, 34), MENU, PSET          'Erase menu on screen.
ERASE MENU                  'Return memory.
LOCATE 2, 42: COLOR 1, 0: PRINT "F4:MONOCHR"

END SUB

SUB MONOPARA (MNPARA!(), PARAMETERSAVAILABLE%)        'Routine to get
                                    mono. parameters.

DIM MENU3(1 TO 12100) AS INTEGER  'New menu to be made.
```

```
DIM MESSAGEPOS$(6, 2)
MESSAGEPOS$(1, 1) = "START POSITION:": MESSAGEPOS$(1, 2) = "7"
MESSAGEPOS$(2, 1) = "STOP POSITION:": MESSAGEPOS$(2, 2) = "10"
MESSAGEPOS$(3, 1) = "# OF POINTS:": MESSAGEPOS$(3, 2) = "13"
MESSAGEPOS$(4, 1) = "INTEGRATION TIME:  ": MESSAGEPOS$(4, 2) = "16"
MESSAGEPOS$(5, 1) = "MAX. # OF SCANS:": MESSAGEPOS$(5, 2) = "19"
GET (60, 42)-(230, 315), MENU3
ITEMINDEX% = 1          'Index of which parameters is being changed.
LINE (60, 42)-(230, 315), 1, BF
LINE (64, 46)-(226, 311), 0, BF
COLOR 1, 0: LOCATE 5, 10: PRINT "SCAN PARAMETERS"
COLOR 15, 0: LOCATE 7, 10: PRINT MESSAGEPOS$(1, 1)
COLOR 1, 0: LOCATE 10, 10: PRINT MESSAGEPOS$(2, 1)
COLOR 1, 0: LOCATE 13, 10: PRINT MESSAGEPOS$(3, 1)
COLOR 1, 0: LOCATE 16, 10: PRINT MESSAGEPOS$(4, 1)
COLOR 1, 0: LOCATE 19, 10: PRINT MESSAGEPOS$(5, 1)
IF PARAMETERSAVAILABLE% = 1 THEN        'If already available, print values.
    LOCATE 8, 15: PRINT USING "###.##"; MNPARA!(1, 1); : PRINT "nm"
    LOCATE 11, 15: PRINT USING "###.##"; MNPARA!(2, 1); : PRINT "nm"
    LOCATE 14, 18: PRINT USING "###"; MNPARA!(3, 1)
    LOCATE 17, 17: PRINT USING "#.##"; MNPARA!(4, 1); : PRINT "sec"
    LOCATE 20, 18: PRINT USING "###"; MNPARA!(5, 1)
END IF
DO          'Get keyboard response to change parameters.
    KBD$ = INKEY$
    FK% = 0
    IF LEN(KBD$) = 2 THEN FK% = ASC(RIGHT$(KBD$, 1))
    IF FK% = 72 THEN    'Down arrow hit.
        COLOR 1, 0
        LOCATE VAL(MESSAGEPOS$(ITEMINDEX%, 2)), 10
        PRINT MESSAGEPOS$(ITEMINDEX%, 1)
        COLOR 15, 0
        IF ITEMINDEX% = 1 THEN ITEMINDEX% = 5 ELSE ITEMINDEX% =
ITEMINDEX% - 1
        LOCATE VAL(MESSAGEPOS$(ITEMINDEX%, 2)), 10
        PRINT MESSAGEPOS$(ITEMINDEX%, 1)
    END IF
    IF FK% = 80 THEN    'Up arrow is hit.
        COLOR 1, 0
        LOCATE VAL(MESSAGEPOS$(ITEMINDEX%, 2)), 10
        PRINT MESSAGEPOS$(ITEMINDEX%, 1)
        COLOR 15, 0
        IF ITEMINDEX% = 5 THEN ITEMINDEX% = 1 ELSE ITEMINDEX% =
ITEMINDEX% + 1
        LOCATE VAL(MESSAGEPOS$(ITEMINDEX%, 2)), 10
```

```
    PRINT MESSAGEPOS$(ITEMINDEX%, 1)
END IF
IF KBD$ = CHR$(13) THEN    'Return is hit.
    SELECT CASE ITEMINDEX%  'Which item is being changed.
        CASE 1        'Starting point.
            LINE (112, 98)-(158, 110), 1, BF
            XP$ = ""
            CALL GETSTRING(8, 15, 6, XP$)
            MNPARA!(1, 1) = VAL(XP$)
            LOCATE 8, 15
            PRINT USING "###.##"; MNPARA!(1, 1); : PRINT "nm"
            MNPARA!(1, 2) = 1
        CASE 2        'Ending point.
            LINE (112, 140)-(158, 152), 1, BF
            XP$ = ""
            CALL GETSTRING(11, 15, 6, XP$)
            MNPARA!(2, 1) = VAL(XP$)
            LOCATE 11, 15
            PRINT USING "###.##"; MNPARA!(2, 1); : PRINT "nm"
            MNPARA!(2, 2) = 1
        CASE 3        '# of points.
            LINE (136, 182)-(158, 194), 1, BF
            XP$ = ""
            CALL GETSTRING(14, 18, 3, XP$)
            MNPARA!(3, 1) = VAL(XP$)
            LOCATE 14, 18
            PRINT USING "###"; MNPARA!(3, 1)
            MNPARA!(3, 2) = 1
        CASE 4        'Time between steps.
            LINE (128, 224)-(158, 234), 1, BF
            XP$ = ""
            CALL GETSTRING(17, 17, 4, XP$)
            MNPARA!(4, 1) = VAL(XP$)
            LOCATE 17, 17
            PRINT USING "#.##"; MNPARA!(4, 1); : PRINT "sec"
            MNPARA!(4, 2) = 1
        CASE 5        'Max # of scans.
            LINE (136, 266)-(158, 278), 1, BF
            XP$ = ""
            CALL GETSTRING(20, 18, 3, XP$)
            MNPARA!(5, 1) = VAL(XP$)
            LOCATE 20, 18
            PRINT USING "###"; MNPARA!(5, 1)
            MNPARA!(5, 2) = 1
    END SELECT
```

```
    END IF

LOOP UNTIL KBD$ = CHR$(27)   'Loop until escape is hit.
PUT (60, 42), MENU3, PSET    'Erase menu on screen.
ERASE MENU3                  'Return memory.
FOR I = 1 TO 5       'All parameters must be available before scan function can be used.
    IF MNPARA!(I, 2) = 1 THEN
        PARAMETERSAVAILABLE% = 1      'Parameters available.
    ELSE
        PARAMETERSAVAILABLE% = 0      'Not available.
        EXIT FOR
    END IF
NEXT I

END SUB

SUB MONOSCAN (MNPARA!())  'Scan routine. Similar to delay line scans found in
                                main module.

AV% = 0      '# of averages.
CALL MCLEAR      'Clear main menu line.
PRINT "COLLECTING DATA"
LOCATE 2, 50: PRINT "# OF SCANS COMPLETED: "; AV%
CALL SCLEAR      'Clear data screen.
FOR I = 0 TO MNPARA!(3, 1)       'Clear the data arrays.
    DAT(I).X = I * (MNPARA!(2, 1) - MNPARA!(1, 1)) / MNPARA!(3, 1) +
MNPARA!(1, 1)
    DAT(I).Y = 0
NEXT I
VIEW (0, 34)-(639, 349)      'Set data screen to desired coordinates.
WINDOW (2 * DAT(0).X - DAT(1).X, 2048)-(2 * DAT(MNPARA!(3, 1)).X -
            DAT(MNPARA!(3, 1) - 1).X, -2048)
KBD$ = ""
CALL READPOSITION(POSITION!)      'Get current position.
STARTPOSITION! = MNPARA!(1, 1)    'Set starting point.
MR! = STARTPOSITION! - POSITION!  'Move relative.
IF MR! <= 0 THEN   'If negative then go back to target less 300 steps (eliminate
                                                                    backlash).
    CALL MN("F0," + STR$(MR! * 20 - 300) + CHR$(13), OUTOF$)  'Move
    DO       'Wait until stopped.
        CALL MN("E", OUTOF$)
    LOOP UNTIL LEFT$(OUTOF$, 2) = "oz"
    CALL MN("F0,300" + CHR$(13), OUTOF$)  'Move forward 300 steps.
    DO       'Wait until stopped.
        CALL MN("E", OUTOF$)
```

```
    LOOP UNTIL LEFT$(OUTOF$, 2) = "oz"
ELSE            'If positive then just move to target position.
    CALL MN("F0," + STR$(MR! * 20) + CHR$(13), OUTOF$)'Move.
    DO          'Wait until stopped.
        CALL MN("E", OUTOF$)
    LOOP UNTIL LEFT$(OUTOF$, 2) = "oz"
END IF
SS! = (MNPARA!(2, 1) - MNPARA!(1, 1)) / MNPARA!(3, 1) * 20          'Define step
                                                                    size for scan.
FOR J = 1 TO MNPARA!(5, 1)      'Begin scan--do not exceed max. # of scans.
    FOR I = 0 TO MNPARA!(3, 1) 'Begin scan from 0 to # of points.
        TIMEIN! = TIMER         'Start timer.
        DO          'Wait until necessary time has elapsed.
            TIMEOUT! = TIMER
        LOOP UNTIL TIMEOUT! - TIMEIN! > MNPARA!(4, 1)
        CALL DAS(0, DIO%)       'Get A/D conversion.
        PSET (DAT(I).X, DIO%), 15       'Plot point.
        DAT(I).Y = (DAT(I).Y * AV% + DIO%) / (AV% + 1)  'Update the running
                                                                    average.
        CALL READPOSITION(POSITION!)    'Read position.
        MR! = (I + 1) * SS! + STARTPOSITION! * 20 - POSITION! * 20  'Calculate
                                                        new position for next point.
        CALL MN("F0," + STR$(MR!) + CHR$(13), OUTOF$)'Move.
        DO          'Wait until stopped.
            CALL MN("E", OUTOF$)
        LOOP UNTIL LEFT$(OUTOF$, 2) = "oz"
    NEXT I          'Next point.
    AV% = AV% + 1       'Update average total.
    CALL FIVESCAN(AV%, 5, INT(MNPARA!(3, 1)))  'After every 5th scan data is
            saved in temporary files in case of computer crash or signal disappearing.
    LOCATE 2, 50: PRINT "# OF SCANS COMPLETED: "; AV%
    CALL SCLEAR 'Clear data screen.
    YMIN! = DAT(0).Y: YMAX! = DAT(0).Y     'Find new YMIN! and YMAX!.
    FOR I = 1 TO MNPARA!(3, 1)
        IF DAT(I).Y < YMIN! THEN YMIN! = DAT(I).Y
        IF DAT(I).Y > YMAX! THEN YMAX! = DAT(I).Y
    NEXT I
    CALL DISPLAY(YMIN!, YMAX!, 0, INT(MNPARA!(3, 1)))       'Display new
                                                                    average scan.
    VIEW (0, 34)-(639, 349)         'Reset screen coordinates.
    WINDOW (2 * DAT(0).X - DAT(1).X, YMAX! + .1 * ABS(YMAX! - YMIN!))-(2
* DAT(MNPARA!(3, 1)).X - DAT(MNPARA!(3, 1) - 1).X, YMIN! - .1 * ABS(YMAX!
- YMIN!))
    CALL READPOSITION(POSITION!) 'Read mono. position.
```

```
    MR! = (STARTPOSITION! - POSITION!) * 20 - 300'Scan back to starting position
                                                plus 300 more steps to eliminate backlash.
    CALL MN("F0," + STR$(MR!) + CHR$(13), OUTOF$)       'Move.
    DO      'Wait until stopped.
        CALL MN("E", OUTOF$)
    LOOP UNTIL LEFT$(OUTOF$, 2) = "oz"
    CALL MN("F0,300" + CHR$(13), OUTOF$)  'Move forward 300 steps.
    DO      'Wait until stopped.
        CALL MN("E", OUTOF$)
    LOOP UNTIL LEFT$(OUTOF$, 2) = "oz"
    KBD$ = INKEY$       'If a key has been hit during scan then stop scan.
    IF KBD$ <> "" THEN EXIT FOR
NEXT J      'Continue unless max. # of scans exceeded.
CALL MN("v", OUTOF$)    'Make sure mono. has stopped moving.
VIEW: WINDOW    'Return screen coordinates to defaults.
CALL FILESAVE(5, INT(MNPARA!(3, 1)), AV%, "LAMBDA (nm)", "INTENSITY")
      'Save last scan.

END SUB

SUB READPOSITION (POSITION!)        'Read current mono. position routine.

CALL MN("H0" + CHR$(13), OUTOF$)    'Send command to mono.
POSITION$ = LEFT$(OUTOF$, LEN(OUTOF$) - 1)      'Useful information is in the
                                                middle of the returned string.
POSITION$ = RIGHT$(POSITION$, LEN(POSITION$) - 1)
POSITION% = VAL(POSITION$)
POSITION! = POSITION% / 20!     'Change to nm.

END SUB
```

Utility Module

```
*****************************************************************
*                Subroutine declarations for those used in these subroutines          *
*****************************************************************


DECLARE SUB DAC (CHANNEL%, DIGITAL%)
DECLARE SUB FILENAME (ROW%, COL%, FIL$)
DECLARE SUB SCLEAR ()
DECLARE SUB MMENU ()
DECLARE SUB MCLEAR ()
DECLARE SUB GETSTRING (ROW%, COL%, LONGEST%, XP$)
DECLARE SUB KEYBOARDCLEAR ()
DECLARE SUB SMOOTH3 (YMIN!, YMAX!, INDEXMIN%, INDEXMAX%)
TYPE DATAPAIR
     X AS SINGLE
     Y AS SINGLE
END TYPE
DIM DAT(1000) AS DATAPAIR
COMMON SHARED /D/ DAT() AS DATAPAIR
HANDLER:

     ERRORCODE% = ERR
     RESUME NEXT


SUB DAC (CHANNEL%, DIGITAL%)   'taken out of DAC-02 manual p.3-4.

DH% = INT(DIGITAL% / 16)       'generate high byte
DL% = DIGITAL% - 16 * DH%      'get remainder to be put into low byte
DL% = 16 * DL%                 'shift over 4 places to the left (12 bit resolution instead of
16)
SELECT CASE CHANNEL%
     CASE 0                    'converter number 0
          OUT &H330, DL%
          OUT &H331, DH%
     CASE 1                    'converter number 1
          OUT &H332, DL%
          OUT &H333, DH%
END SELECT

END SUB

SUB DACMENU STATIC   'Routine to make DAC menu.
```

```
DIM MENU(3500) AS INTEGER   'Make menu.
DIM MNU$(2)                 'There is only two items on this menu.
GET (405, 210)-(530, 310), MENU
LINE (405, 210)-(530, 310), 1, BF
LINE (409, 214)-(526, 306), 0, BF
MNU$(0) = "DAC 0:"
MNU$(1) = "DAC 1:"
LOCATE 17, 53: COLOR 15, 0: PRINT MNU$(0)
LOCATE 20, 53: COLOR 1, 0: PRINT MNU$(1)
LOCATE 18, 57: PRINT USING "####"; DAC0%
LOCATE 21, 57: PRINT USING "####"; DAC1%
IF DAC0% < 0 OR DAC0% > 4095 THEN DAC0% = 0
IF DAC1% < 0 OR DAC1% > 4095 THEN DAC1% = 0
CALL DAC(0, DAC0%): CALL DAC(1, DAC1%)
INDEX% = 0          'Index for menu (0 for DAC 0 and 1 for DAC1).
DO                  'Get keyboard response.
    KBD$ = INKEY$
    IF LEN(KBD$) = 2 THEN FK% = ASC(RIGHT$(KBD$, 1))
    IF FK% = 72 OR FK% = 80 THEN    'Up or Down arrow--move highlighted item.
        LOCATE 3 * INDEX% + 17, 53: COLOR 1, 0: PRINT MNU$(INDEX%)
        IF INDEX% = 0 THEN INDEX% = 1 ELSE INDEX% = 0
        LOCATE 3 * INDEX% + 17, 53: COLOR 15, 0: PRINT MNU$(INDEX%)
        FK% = 0
    END IF
    IF KBD$ >= "0" AND KBD$ <= "9" THEN   'If a # is hit.
        SELECT CASE INDEX%          'Act on DAC chosen.
          CASE 0          'DAC 0.
            LINE (455, 238)-(478, 250), 15, BF 'Get desired output voltage.
            X$ = KBD$
            LOCATE 18, 57: COLOR 1, 0: PRINT X$;
            DO            'Assemble output voltage as a string.
                TEMP$ = INKEY$
                IF TEMP$ >= "0" AND TEMP$ <= "9" THEN
                    X$ = X$ + TEMP$
                    PRINT TEMP$;
                END IF
            LOOP UNTIL TEMP$ = CHR$(13) 'Get response until return is hit.
            DAC0% = VAL(X$)         'Convert to integer.
            LOCATE 18, 57: PRINT USING "####"; DAC0% 'Print value.
            CALL DAC(0, DAC0%)              'Send voltage out to DAC 0.
          CASE 1          'DAC 1--same routine as for DAC 0.
            LINE (455, 280)-(478, 293), 15, BF
            X$ = KBD$
            LOCATE 21, 57: COLOR 1, 0: PRINT X$;
```

```
                DO
                    TEMP$ = INKEY$
                    IF TEMP$ >= "0" AND TEMP$ <= "9" THEN
                        X$ = X$ + TEMP$
                        PRINT TEMP$;
                    END IF
                LOOP UNTIL TEMP$ = CHR$(13)
                DAC1% = VAL(X$)
                LOCATE 21, 57: PRINT USING "####"; DAC1%
                CALL DAC(1, DAC1%)      'Send voltage out to DAC 1.
            END SELECT
        END IF
    LOOP UNTIL KBD$ = CHR$(27)   'Return to main menu when esc is hit.
    PUT (405, 210), MENU, PSET   'Return screen behind menu.
    ERASE MENU                   'Return memory.

    END SUB

    SUB FILENAME (ROW%, COL%, FIL$)   'Get a filename for saving data.

    DIM MENU(1 TO 1000) AS INTEGER     'Make menu.
    ROW% = (ROW% \ 14) * 14: COL% = (COL% \ 8) * 8     'Find a good spot for the
                                                        menu based on the values sent into routine.
    GET (COL%, ROW% - 2)-(COL% + 112, ROW% + 30), MENU   'Save stuff behind
                                                                menu.
    LINE (COL%, ROW% - 2)-(COL% + 112, ROW% + 30), 15, B    'Make box.
    LOCATE ROW% \ 14 + 1, COL% \ 8 + 2
    PRINT "FILENAME:"
    LINE (COL% + 8, ROW% + 14)-(COL% + 103, ROW% + 27), 1, BF
    FIL$ = ""
    CALL GETSTRING(ROW% \ 14 + 2, COL% \ 8 + 2, 12, FIL$)    'Get keyboard string.
    FIL$ = UCASE$(FIL$)        'Convert to uppercase.
    PUT (COL%, ROW% - 2), MENU, PSET   'Return screen behind menu.
    ERASE MENU                 'Return memory.

    END SUB

    SUB FILESAVE (MODE%, NPTS%, AV%, HEADER1$, HEADER2$)  'Saves data
                                                          into a standard file type.

    OPEN "I", #2, "STATUS"     'STATUS contains the running total of files.
    INPUT #2, TOTALSCANS%          'Get total number of files.
    CLOSE #2                   'Close file.
    SAVE2:    FIL$ = ""            'Save the data.
            CALL FILENAME(50, 290, FIL$)   'Get filename.
```

```
        IF LEFT$(FIL$, 1) < "A" OR LEFT$(FIL$, 1) > "Z" THEN        'May not wish
                                                                    to save the data.
          CALL MCLEAR
          INPUT "ARE YOU CERTAIN YOU DO NOT WISH TO SAVE THE
DATA"; S$
          IF LEFT$(S$, 1) = "Y" OR LEFT$(S$, 1) = "y" THEN
               CALL MMENU       'If not save then return to main menu.
               EXIT SUB
          END IF
          GOTO SAVE2            'If yes then return to the save routine above.
        END IF
        CALL MCLEAR
        PRINT "COMMENTS:"       'Get the comment string.
        COMMENT$ = ""
        CALL GETSTRING(2, 12, 76, COMMENT$)
        FIL$ = LEFT$(FIL$, LEN(FIL$) - 1)       'Eliminate the return character.
        F$ = "DATA\" + FIL$ + RIGHT$(STR$(TOTALSCANS%),   'Save data in the
                                                          DATA subdirectory.
        LEN(STR$(TOTALSCANS%)) - 1) + ".DAT"      'Add the DAT extension.
        ON ERROR GOTO HANDLER     'If bad filename.
        OPEN "O", #1, F$    'Open file for output.
        DO WHILE ERRORCODE% <> 0          'Error handling routine.
              SELECT CASE ERRORCODE%
                   CASE 53        'File not found.  Only appropriate if opening a file.
                        CALL MCLEAR
                        COLOR 15, 0
                        PRINT "FILE NOT FOUND.   TRY AGAIN"
                        COLOR 1, 0
                        CALL FILENAME(50, 250, FIL$)
                        FIL$ = LEFT$(FIL$, LEN(FIL$) - 1)
                        F$ = FIL$ + RIGHT$(STR$(TOTALSCANS%),
LEN(STR$(TOTALSCANS%)) - 1) + ".DAT"
                        ERRORCODE% = 0
                        OPEN F$ FOR OUTPUT AS #1
                        CALL MCLEAR
                   CASE 64        'Bad file name.
                        CALL MCLEAR
                        COLOR 15, 0
                        PRINT "BAD FILE NAME.    TRY AGAIN"
                        COLOR 1, 0
                        CALL FILENAME(50, 250, FIL$)
                        FIL$ = LEFT$(FIL$, LEN(FIL$) - 1)
                        F$ = FIL$ + RIGHT$(STR$(TOTALSCANS%),
LEN(STR$(TOTALSCANS%)) - 1) + ".DAT"
                        ERRORCODE% = 0
```

```
                    OPEN F$ FOR OUTPUT AS #1
                    CALL MCLEAR
                CASE ELSE
                    ON ERROR GOTO 0
            END SELECT
        LOOP
        ON ERROR GOTO 0
        YMIN! = DAT(0).Y: YMAX! = DAT(0).Y 'Find new YMIN! and YMAX!
                                                values.
        FOR P = 1 TO NPTS%
          IF YMIN! > DAT(P).Y THEN YMIN! = DAT(P).Y
          IF YMAX! < DAT(P).Y THEN YMAX! = DAT(P).Y
        NEXT P
        PRINT #1, MODE% 'Print data to the file.
        PRINT #1, YMIN!, YMAX!, NPTS%, AV%
        PRINT #1, LEFT$(COMMENT$, LEN(COMMENT$) - 1)
        D$ = DATE$
        PRINT #1, D$
        PRINT #1, HEADER1$, HEADER2$
        FOR P = 0 TO NPTS%
          PRINT #1, DAT(P).X, DAT(P).Y
        NEXT P
        CLOSE #1            'Close the file.
        CALL MCLEAR         'Clear menu line.
        PRINT "SAVED AS "; F$; : PRINT "                    HIT <RETURN> TO
CONTINUE"
        DO UNTIL K$ = CHR$(13)
          K$ = INKEY$
        LOOP
        TOTALSCANS% = TOTALSCANS% + 1  'Update the running scan total.
        OPEN "O", #1, "STATUS"   'Save the new scan total.
        PRINT #1, TOTALSCANS%
        CLOSE #1

END SUB

SUB FIVESCAN (AV%, MODE%, NPTS%)        'Saves data in temporary files every
                                                5th scan.

        IF AV% \ 5 = AV% / 5 THEN     'Is it a 5th scan?
            F$ = "DATA\DATA" + LTRIM$(STR$(AV% \ 5)) + ".DAT"       'Save
                                            the data in files DATA#.DAT.
            OPEN "O", #3, F$     'Open file for output.
            WRITE #3, MODE%'Print data into file.
            FOR P = 0 TO NPTS%
```

```
                PRINT #3, DAT(P).X, DAT(P).Y
            NEXT P
            CLOSE #3
        END IF

END SUB

SUB GETSTRING (ROW%, COL%, LONGEST%, XP$)  'Get a string from the
            keyboard one character at a time and generate the output string XP$.

    COLOR 15, 0
    CALL KEYBOARDCLEAR    'Clear the keyboard buffer.
DO          'Loop until return or escape is hit.

    KBD$ = INKEY$         'Get first character.
    IF KBD$ = CHR$(27) THEN   'Exit loop if escape is hit.
        XP$ = "ESC"
        EXIT DO
    END IF
    IF KBD$ <> "" THEN   'Any other char.
        IF LEN(KBD$) = 1 THEN         'If a 2 bit char then forget it.
            IF LEN(XP$) <> 0 OR KBD$ <> CHR$(8) THEN 'No space.
                IF KBD$ = CHR$(8) THEN    'Space.
                    XP$ = LEFT$(XP$, LEN(XP$) - 1)       'Eliminate space.
                    LOCATE ROW%, COL%
                    PRINT XP$; " "
                ELSE
                    XP$ = XP$ + KBD$       'Generate string char. by char.
                    LOCATE ROW%, COL% + LEN(XP$) - 1
                    PRINT KBD$      'Print new char.
                    IF LEN(XP$) >= LONGEST% THEN    'Cannot exceed max.
                                                        length.
                        DO UNTIL KBD$ = CHR$(13)     'Wait for return.
                            KBD$ = INKEY$
                        LOOP
                        EXIT DO
                    END IF
                END IF
            END IF
        END IF
    END IF
LOOP UNTIL KBD$ = CHR$(13)   'Return is hit.
COLOR 1, 0

END SUB
```

```
SUB KEYBOARDCLEAR   'Clear keyboard buffer.

    DEF SEG = 0
    POKE 1050, PEEK(1052)
    DEF SEG

END SUB

SUB MCLEAR          'Clear main menu line.

    VIEW
    WINDOW
    LINE (1, 7)-(638, 31), 0, BF     'Draw a filled in black box over menu line.
    LOCATE 2, 2

END SUB

SUB MMENU           'Print main menu.

LOCATE 2, 2
COLOR 1, 0
PRINT "   F1:SCAN   F2:DISPLAY   F3:JOG   F4:MONOCHR   F5:MISC
F6:EXIT";

END SUB

SUB SCLEAR          'Clear data screen.

    VIEW
    WINDOW
    LINE (1, 35)-(638, 348), 0, BF 'Draw a filled in black box over data screen.

END SUB

SUB SMOOTH3 (YMIN!, YMAX!, INDEXMIN%, INDEXMAX%)      '3 point
                                                      smooth.

' this subroutine was taken directly from Bevington page 260
YI! = DAT(INDEXMIN%).Y
YMAX! = DAT(INDEXMIN%).Y: YMIN! = DAT(INDEXMIN%).Y
IF YMAX! = 0 THEN YMAX! = 10
FOR P% = INDEXMIN% TO INDEXMAX% - 1
    YNEW! = (YI! + 2 * DAT(P%).Y + DAT(P% + 1).Y) / 4
    YI! = DAT(P%).Y
```

```
        DAT(P%).Y = YNEW!
        IF DAT(P%).Y > YMAX! THEN YMAX! = DAT(P%).Y
        IF DAT(P%).Y < YMIN! THEN YMIN! = DAT(P%).Y
NEXT P%
DAT(INDEXMAX%).Y = (YI! + 3 * DAT(INDEXMAX%).Y) / 4

END SUB
```

Directory Module

```
*****************************************************************
*                Subroutine declarations for those used in these subroutines      *
*****************************************************************

'These routines came as an application note from Microsoft directly. This is designed to
        retrieve the directory of a given path. There are no comments since I have never
bothered to figure out how these routines work. Questions, call Microsoft

REM $INCLUDE: 'user.inc'
REM $INCLUDE: 'QB.BI'

SUB CalculateAssign (FileInfoBlock() AS FileInfo, BUFFER AS FileFindBuf, counter)
        FileInfoBlock(counter).FILENAME = BUFFER.FILENAME
        FileInfoBlock(counter).Size = STR$(BUFFER.FileSize)
        FileInfoBlock(counter).Seconds = STR$(BUFFER.CreateTime AND &H1F)
        FileInfoBlock(counter).Minutes = STR$((BUFFER.CreateTime AND &H7E0) \
32)
        ' If BUFFER.CreateTime is negative add 64 K to make unsigned integer:
        IF BUFFER.CreateTime < 0 THEN
                FileInfoBlock(counter).Hours = STR$(((BUFFER.CreateTime + 2 ^ 16)
AND &HF800) \ 2048)
        ELSE
                FileInfoBlock(counter).Hours = STR$((BUFFER.CreateTime AND
&HF800) \ 2048)
        END IF
        FileInfoBlock(counter).Day = STR$(BUFFER.AccessDate AND &H1F)
        FileInfoBlock(counter).Month = STR$((BUFFER.AccessDate \ 32) AND &HF)
        FileInfoBlock(counter).Year = STR$((BUFFER.AccessDate \ 512) + 1980)
END SUB

SUB DIRECTORY (path$, FILE$)

DIM BUFFER AS FileFindBuf
DIM FileInfoBlock(300) AS FileInfo
DIM MENU(15000) AS INTEGER
CALL setdta(BUFFER)
fa% = 16 ' A value of 16 includes directory names.
counter = 0
IF (firstfm(path$, fa%) = 0) THEN
        DO
                counter = counter + 1
                CalculateAssign FileInfoBlock(), BUFFER, counter
                CALL setdta(BUFFER)
```

```
        LOOP WHILE (nextfm = 0)
END IF
GET (215, 52)-(439, 255), MENU
LINE (215, 52)-(439, 74), 15, B
LOCATE 5, 30: COLOR 1, 0: PRINT path$
COLOR 15, 0
LINE (215, 75)-(439, 255), 15, B
LOCATE 8, 30
PrintDirList FileInfoBlock(), 1
IF counter < 10 THEN maxcounter = counter ELSE maxcounter = 10
FOR i = 2 TO maxcounter
        LOCATE 7 + i, 30
        COLOR 1, 0
        PrintDirList FileInfoBlock(), i
NEXT i
i = maxcounter
J% = 1
DO
        KBD$ = "": FK% = 0
        KBD$ = INKEY$
        IF LEN(KBD$) = 2 THEN FK% = ASC(RIGHT$(KBD$, 1))
        SELECT CASE FK%
                CASE 80
                        IF J% = maxcounter THEN
                                IF i < counter THEN
                                        COLOR 1, 0
                                        i = i + 1
                                        FOR K = i - 9 TO i
                                                LOCATE 8 + (K - i + 9), 30
                                                PrintDirList FileInfoBlock(), K
                                        NEXT K
                                        COLOR 15, 0
                                        LOCATE 17, 30
                                        PrintDirList FileInfoBlock(), i
                                ELSE BEEP
                                END IF
                        ELSE
                                LOCATE 7 + J%, 30
                                COLOR 1, 0
                                PrintDirList FileInfoBlock(), i + J% - maxcounter
                                J% = J% + 1
                                LOCATE 7 + J%, 30
                                COLOR 15, 0
                                PrintDirList FileInfoBlock(), i + J% - maxcounter
                        END IF
```

```
                CASE 72
                        IF J% <> 1 THEN
                                COLOR 1, 0
                                LOCATE 7 + J%, 30
                                PrintDirList FileInfoBlock(), i + J% - maxcounter
                                J% = J% - 1
                                LOCATE 7 + J%, 30
                                COLOR 15, 0
                                PrintDirList FileInfoBlock(), i + J% - maxcounter
                        ELSE
                                IF i > 10 THEN
                                        COLOR 15, 0
                                        LOCATE 8, 30
                                        PrintDirList FileInfoBlock(), i - maxcounter
                                        COLOR 1, 0
                                        LOCATE 9, 30
                                        FOR K = 2 TO 10
                                                LOCATE 9 + (K - 2), 30
                                                PrintDirList FileInfoBlock(), i + K -
maxcounter - 1
                                        NEXT K
                                        i = i - 1
                                ELSE BEEP
                                END IF
                        END IF
                CASE 81
                        IF counter > 10 THEN
                                IF counter - i >= 10 THEN
                                        COLOR 1, 0
                                        FOR K = i TO i + 9
                                                LOCATE 8 + (K - i), 30
                                                PrintDirList FileInfoBlock(), K
                                        NEXT K
                                        i = i + 9
                                        COLOR 15, 0
                                        LOCATE 7 + J%, 30
                                        PrintDirList FileInfoBlock(), i + J% - maxcounter
                                ELSE
                                        COLOR 1, 0
                                        FOR K = counter - 9 TO counter
                                                LOCATE 8 + (K - counter + 9), 30
                                                PrintDirList FileInfoBlock(), K
                                        NEXT K
```

```
                i = counter: J% = 10
                COLOR 15, 0
                LOCATE 7 + J%, 30
                PrintDirList FileInfoBlock(), i
            END IF
        ELSE
            COLOR 1, 0
            LOCATE 7 + J%, 30
            PrintDirList FileInfoBlock(), i + J% - maxcounter
            COLOR 15, 0
            J% = counter
            LOCATE 7 + J%, 30
            PrintDirList FileInfoBlock(), i + J% - maxcounter
        END IF
CASE 73
        IF i > 10 THEN
            IF i > 18 THEN
                COLOR 1, 0
                i = i - 9
                FOR K = i - 9 TO i
                    LOCATE 8 + (K - i + 9), 30
                    PrintDirList FileInfoBlock(), K
                NEXT K
                COLOR 15, 0
                LOCATE 7 + J%, 30
                PrintDirList FileInfoBlock(), i + J% - maxcounter
            ELSE
                COLOR 1, 0
                i = 10
                FOR K = i - 9 TO i
                    LOCATE 8 + (K - i + 9), 30
                    PrintDirList FileInfoBlock(), K
                NEXT K
                COLOR 15, 0
                J% = 1
                LOCATE 8, 30
                PrintDirList FileInfoBlock(), 1
            END IF
        ELSE
            COLOR 1, 0
            FOR K = i - maxcounter + 1 TO i
                LOCATE 8 + (K - i + maxcounter - 1), 30
                PrintDirList FileInfoBlock(), K
            NEXT K
            COLOR 15, 0
```

```
                        LOCATE 8, 30
                        J% = 1
                        PrintDirList FileInfoBlock(), i - maxcounter + 1
                    END IF
                END SELECT
            IF KBD$ = CHR$(13) THEN
                FILE$ = FileInfoBlock(i + J% - maxcounter).FILENAME
                EXIT DO
            END IF
            IF KBD$ = CHR$(27) THEN
                FILE$ = "ESC"
            END IF
LOOP UNTIL KBD$ = CHR$(27)
PUT (215, 52), MENU, PSET
ERASE MENU
END SUB

FUNCTION firstfm (path$, fa%)
        DIM inreg AS RegType, outreg AS RegType
        inreg.ax = &H4E00
        inreg.cx = fa%
        FILE$ = path$ + CHR$(0)
        inreg.dx = SADD(FILE$)
        CALL INTERRUPT(&H21, inreg, outreg)
        firstfm = (outreg.ax AND &HF)
END FUNCTION

SUB intbuf (BUFFER AS FileFindBuf) STATIC
' The first 20 bytes are reserved for DOS and are unchanged
        BUFFER.CreateTime = 0
        BUFFER.Attributes = ""
        BUFFER.AccessDate = 0
        BUFFER.FileSize = 0
        BUFFER.FILENAME = STRING$(13, 32)
END SUB

FUNCTION nextfm
        DIM inreg AS RegType, outreg AS RegType
        inreg.ax = &H4F00
        CALL INTERRUPT(&H21, inreg, outreg)
        nextfm = outreg.ax AND &HF
END FUNCTION

SUB PrintDirList (FileInfoBlock() AS FileInfo, i)
        PRINT TAB(30); FileInfoBlock(i).FILENAME;
```

```
        PRINT TAB(45); RTRIM$(LTRIM$(FileInfoBlock(i).Month)) + "-";
        IF LEN(RTRIM$(LTRIM$(FileInfoBlock(i).Day))) = 1 THEN
                FileInfoBlock(i).Day = "0" + LTRIM$(FileInfoBlock(i).Day)
        END IF
        PRINT RTRIM$(LTRIM$(FileInfoBlock(i).Day)) + "-";
        PRINT RTRIM$(LTRIM$(FileInfoBlock(i).Year));
        IF LEN(RTRIM$(LTRIM$(FileInfoBlock(i).Month))) = 1 THEN
                PRINT " ";
        END IF
END SUB

SUB setdta (BUFFER AS FileFindBuf) STATIC
        DIM inreg AS RegTypeX, outreg AS RegTypeX
        CALL intbuf(BUFFER)
        inreg.ax = &H1A00
        inreg.ds = VARSEG(BUFFER)
        inreg.dx = VARPTR(BUFFER)
        CALL INTERRUPTX(&H21, inreg, outreg)
END SUB
```

QB.BI Include File

```
'*****************************************************************
*                Subroutine declarations for those used in these subroutines      *
'*****************************************************************

'This file is necessary in order to make interrupt calls (these are used only in the directory
routines).  No comments are made since this file is provided by microsoft with
QuickBasic.

'***
' QB.BI - Assembly Support Include File
'
'     Copyright <C> 1987 Microsoft Corporation
'
' Purpose:
'     This include file defines the types and gives the DECLARE
'      statements for the assembly language routines ABSOLUTE,
'      INTERRUPT, INTERRUPTX, INT86OLD, and INT86XOLD.
'
'*****************************************************************************
****
'
' Define the type needed for INTERRUPT
'
TYPE RegType
   ax   AS INTEGER
   bx   AS INTEGER
   cx   AS INTEGER
   dx   AS INTEGER
   bp   AS INTEGER
   si   AS INTEGER
   di   AS INTEGER
   flags AS INTEGER
END TYPE
'
' Define the type needed for INTERUPTX
'
TYPE RegTypeX
   ax   AS INTEGER
   bx   AS INTEGER
   cx   AS INTEGER
   dx   AS INTEGER
   bp   AS INTEGER
   si   AS INTEGER
```

```
   di    AS INTEGER
   flags AS INTEGER
   ds    AS INTEGER
   es    AS INTEGER
END TYPE
'
'            DECLARE statements for the 5 routines
'            -------------------------------------
'
' Generate a software interrupt, loading all but the segment registers
'
DECLARE SUB INTERRUPT (intnum AS INTEGER, inreg AS RegType, outreg AS
RegType)
'
' Generate a software interrupt, loading all registers
'
DECLARE SUB INTERRUPTX (intnum AS INTEGER, inreg AS RegTypeX, outreg AS
RegTypeX)
'
' Call a routine at an absolute address.
' NOTE: If the routine called takes parameters, then they will have to
'      be added to this declare statement before the parameter given.
'
DECLARE SUB ABSOLUTE (address AS INTEGER)
'
' Generate a software interrupt, loading all but the segment registers
'      (old version)
'
DECLARE SUB INT86OLD (intnum AS INTEGER, inarray() AS INTEGER, outarray()
AS INTEGER)
'
' Gemerate a software interrupt, loading all the registers
'      (old version)
'
DECLARE SUB INT86XOLD (intnum AS INTEGER, inarray() AS INTEGER,
outarray() AS INTEGER)
'
```

User Include File

```
*****************************************************************
*                Subroutine declarations for those used in these subroutines          *
*****************************************************************



'*****************************************************************************
'*                                                                           *
'* The following subroutines deal with the directory routines.  They         *
'* come directly from Microsoft.  The only modification has been to          *
'* reduce the amount of information sent to the program about each           *
'* file.  All SUB and FUNCTION names have been left as written by            *
'* Microsoft.                                                                *
'*                                                                           *
'*****************************************************************************
'
DECLARE SUB intbuf (BUFFER AS ANY)
DECLARE SUB setdta (BUFFER AS ANY)
DECLARE FUNCTION firstfm! (path$, fa%)
DECLARE FUNCTION nextfm! ()
DECLARE SUB CalculateAssign (FileInfoBlock() AS ANY, BUFFER AS ANY,
counter!)
DECLARE SUB PrintDirList (FileInfoBlock() AS ANY, i!)
TYPE FileFindBuf
     dos   AS STRING * 21
     Attributes AS STRING * 1
     CreateTime AS INTEGER
     AccessDate AS INTEGER
     FileSize AS LONG
     FILENAME AS STRING * 13
END TYPE
TYPE FileInfo
     FILENAME  AS STRING * 13
     Size AS STRING * 8
     Seconds AS STRING * 4
     Minutes AS STRING * 4
     Hours AS STRING * 4
     Day  AS STRING * 4
     Month AS STRING * 4
     Year AS STRING * 5
END TYPE
```

```
DECLARE SUB intbuf (BUFFER AS FileFindBuf)
DECLARE SUB setdta (BUFFER AS FileFindBuf)
DECLARE FUNCTION firstfm! (path$, fa%)
DECLARE FUNCTION nextfm ()
DECLARE SUB CalculateAssign (FileInfoBlock() AS ANY, BUFFER AS ANY,
counter!)
DECLARE SUB PrintDirList (FileInfoBlock() AS ANY, i!)
DECLARE SUB DIRECTORY (path$, F$)       'EDP wrote this to use above routines
'
'*********************************************************************
```